SPECTROSCOPIC, MOLECULAR STRUCTURAL, OPTICAL ANALYSIS, QUANTUM MECHANICAL AND MOLECULAR DOCKING ANALYSIS ON SOME PYRIDINE DERIVATIVES

Thesis Submitted To Bharathidasan University

Tiruchirappalli

FOR THE AWARD OF THE DEGREE OF DOCTOR OF PHILOSOPHY IN PHYSICS

 \boldsymbol{B} v

S. SELVAKUMARI, M.Sc., M.Phil.,

(Ref. No: 03683/Ph.D-K3/Physics /Part Time/Nov 2018/Date:26.11.2018)

Under the Supervision and guidance of

Dr.C.VENKATARAJU, M.Sc., M.Phil., Ph.D.,
Assistant Professor of Physics



PG AND RESEARCH DEPARTMENT OF PHYSICS

THIRU. VI. KA. GOVERNMENT ARTS COLLEGE

 $(Affiliated\ to\ Bharathidas an\ University,\ Tiruchirap palli-24)$

THIRUVARUR -610 003, TAMILNADU, INDIA



Dr. C. VENKATARAJU, M.Sc., M.Phil., Ph.D.,

Research Supervisor & Convener, Assistant Professor, PG and Research Department of Physics, Thiru.Vi.Ka. Government Arts College, Thiruvarur -610 003, Tamil Nadu, India. Email ID: venkatarajuc40@gmail.com

CERTIFICATE

This is to certify that the thesis entitled "SPECTROSCOPIC, MOLECULAR STRUCTURAL, OPTICAL ANALYSIS, QUANTUM MECHANICAL AND MOLECULAR DOCKING ANALYSIS ON SOME PYRIDINE DERIVATIVES" submitted by Mrs.S.SELVAKUMARI, M.Sc., M.Phil., (Ref. No: 03683/Ph.D-K3/Physics /Part Time/Nov 2018/Date:26.11.2018) to Bharathidasan University, Thiruchirappalli-24, for the award of the Degree of DOCTOR OF PHILOSOPHY IN PHYSICS during 2018-2022 is based on the results of experiments carried out by her under my supervision. The thesis has not previously formed the basis for the award of any degree, diploma or associateship. This is also to certify that the thesis represents the independent work of the candidate.

Date: Signature of Guide

Place: Thiruvarur Dr. C.VENKATARAJU

HOD Principal

CERTIFICATE OF PLAGIARISM CHECK

From

Dr.C.VENKATARAJU, M.Sc., M.Phil., Ph.D.,

Research Supervisor & Convener,

Assistant Professor.

PG and Research Department of Physics,

Thiru. Vi. Ka. Government Arts College,

Thiruvarur -610 003, Tamil Nadu, India.

Email ID: venkatarajuc40@gmail.com

This is to certify that the thesis to be submitted by Mrs. S.SELVAKUMARI, M.Sc.,

M.Phil., (Ref. No: 03683/Ph.D-K3/Physics/Part Time /Nov' 2018/ Date: 26.11.2018)

pursued Ph.D. under my guidance is plagiarism free and the report also has been

checked for plagiarism using Urkund and found only 4% of the content from other

sources. The Librarian and Head, Department of Library and Information Science,

Bharathidasan University, Thiruchirappalli-24, has given the certificate in this regard

which is attached here.

Place: Thiruvarur

Dr. C. VENKATARAJU

Date:

iii



PG AND RESEARCH DEPARTMENT OF PHYSICS THIRU.VI.KA. GOVERNMENT ARTS COLLEGE, THIRUVARUR -610 003, TAMIL NADU, INDIA.

CERIFICATE OF PLAGIARISM CHECK

1	Name of the Research	S.SELVAKUMARI
	Scholar	
2	Course of Study	Ph.D., PHYSICS
3	Title of the	SPECTROSCOPIC, MOLECULAR
	Thesis/Dissertation	STRUCTURAL, OPTICAL ANALYSIS,
		QUANTUM MECHANICAL AND
		MOLECULAR DOCKING ANALYSIS ON
		SOME PYRIDINE DERIVATIVES
4	Name of the Research	Dr. C. VENKATARAJU
	Supervisor	
5	Department/ Institution/	PG and Research Department of Physics,
	Research Centre	Thiru.Vi.Ka. Government Arts College,
		Thiruvarur -610 003, Tamil Nadu, India.
6	Acceptable Maximum Limit	20%
7	Percentage of Similarity of	4%
	Content Identified	
8	Software Used	URKUND
9	Date of Verification	16-05-2022

Report on Plagiarism Check, item with % of similarity is attached.

Signature of Research Supervisor

Signature of the Candidate

Curiginal

Document Information

Analyzed document Thesis_S.Selvakumari.pdf (D136680815)

Submitted 2022-05-16T07:52:00.0000000

Submitted by Srinivasa ragavan S

Submitter email bdulib@gmail.com

Similarity 4%

Analysis address bdulib.bdu@analysis.urkund.com

Sources included in the report

w	URL: https://www.primescholars.com/articles/ftir-ftraman-and-uwisible-spectral-analysis-on-enthiophen2ylmethylene-nicotinohydrazide-92480.html Fetched: 2022-03-17T22:02:13.4400000	88	1
w	URL: http://www.ijcrar.com/vol-3-3/R.K.Raj1,%20et%20al.pdf Fetched: 2021-12-14T00:58:37.6770000	88	3
w	URL: https://docksci.com/download/investigation-of-structure-vibrational-electronic-nbo-and-nmr-analyses-of-2-chlo_5a8c65c0d64ab2907b078c52.html Fetched: 2021-08-20T10:33:17.6400000	88	3
w	URL: https://core.ac.uk/download/pdf/229210724.pdf Fetched: 2021-06-22T12:34:10.7470000	88	1
w	URL: https://www.derpharmachemica.com/pharma-chemica/vibrational-spectroscopic-ftir-ftraman-nmr-and-electronic-structure-calculations-of-metaxalone.pdf Fetched: 2019-11-14T01:36:35.8030000	88	4
w	URL: https://www.degruyter.com/document/doi/10.1515/chem-2017-0026/html?lang=en Fetched: 2022-05-16T07:53:35.1730000	88	2
w	URL: https://austinpublishinggroup.com/chemical-engineering/fulltext/ace-v2-id1016.php Fetched: 2020-03-12T08:09:34.6830000	88	3
w	URL: http://www.ajchem-b.com/article_128368_c1659116e70c36ba84d32084d8e352c4.pdf Fetched: 2022-01-21T15:11:54.2100000	88	1
w	URL: https://scialert.net/fulltext/7doi=ajaps.2018.83.91 Fetched: 2022-05-16T07:53:25.6870000	88	1
w	URL: https://www.ijsrr.org/down_1213.php Fetched: 2021-11-30T19:36:59.4070000	88	1
w	URL: https://www.researchgate.net/publication/351791533_Speculative_assessment_molecular_composition_PDOS_topology_exploration_ELF_LOL_RDG_ligand-protein_interactions_on_5-bromo-3-nitropyridine-2-carbonitrile Fetched: 2021-10-29T07:51:30.4400000	88	2

S.SELVAKUMARI, M. Sc., M. Phil.,

Ph.D., Part Time Research Scholar,

PG and Research Department of Physics,

Thiru. Vi. Ka. Government Arts College,

Thiruvarur -610 003, Tamil Nadu, India.

Email ID: selvi1977@gmail.com

DECLARATION

I do hereby declare that the thesis entitled "SPECTROSCOPIC,

MOLECULAR STRUCTURAL, OPTICAL ANALYSIS, QUANTUM

MECHANICAL AND MOLECULAR DOCKING ANALYSIS ON

SOME PYRIDINE DERIVATIVES" has been originally carried out by me

under the guidance of Dr. C.VENKATARAJU, M.Sc., M.Phil., Ph.D., Assistant

Professor of Physics, Thiru. Vi. Ka. Govt. Arts College, Thiruvarur, during the year

2018-2022 and this work has not been submitted elsewhere for getting any other

degree, diploma or associate ship.

Date:

Signature of Candidate

Place: Thiruvarur

Supervisor

HOD

Principal

vi

ACKNOWLEDGEMENT

I offer modest prayers of thanks giving to My Beloved Almighty, whose unseen graces have guided me through many years of research to a successful conclusion.

I consider myself privileged to express my deep sense of gratitude and indebtedness to my supervisor, **Dr.C.Venkataraju**, **M.Sc.**, **M.Phil.**, **Ph.D.**, **Assistant Professor**, PG & Research Department of Physics, Thiru.Vi.Ka. Government Arts College, Thiruvarur, whose encouragement, goodwill and invaluable suggestions have come a long way in the completion of this thesis.

My utmost genuine gratitude and thanks to **Dr. S. Muthu, M.Sc., M.Phil., Ph.D., Assistant Professor,** Arignar Anna Government Arts College, Cheyyar for his immense support in formulating my thesis work. His dynamism, vision, and motivation have profoundly influenced the direction of my work.

I owe my heartfelt gratitude to **Dr. P. Chinnadurai, M.A., M.Phil, Ph.D., Secretary and Correspondent,** Panimalar Group of Institutions for his encouragement and support to carry out this work successfully.

I would like to express my sincere thanks to **Dr.G.Geetha**, **M.Sc.**, **M.Phil.**, **Ph.D.**, **Principal**, Thiru.Vi.Ka. Government Arts College, Thiruvarur, for her generous support in completing my thesis.

I take this opportunity to register my thanks to **Dr.S.Elangovan**, **Ph.D.**, **Head of the Department**, PG & Research Department of Physics, Thiru.Vi.Ka. Government Arts College, Thiruvarur, for his tremendous support to complete this thesis work successfully.

I extend my grateful thanks to my Doctoral Committee members Dr. S. Mullainathan, M.Sc., M.Phil., Ph.D., Assistant Professor, PG & Research Department of Physics, Thiru.Vi.Ka. Government Arts College, Thiruvarur and Dr. V. Gokulakrishnan, M.Sc., M.Phil., Ph.D., Assistant Professor, PG & Research Department of Physics, A.V.C. College, Mayiladuthurai for their insightful comments and encouragement.

I would like to acknowledge my thanks to my co-research scholars for constantly supporting and encouraging me in the successful completion of this research work.

Finally, I would also like to thank my family members for providing me with good support and motivation during this phase of life. Thank you all for your unreserved adjustments, unselfish support, and genuine prayers for the successful completion of this thesis work.

S. SELVAKUMARI

PREFACE

Spectroscopy is a discipline of science that investigates the spectra of electromagnetic radiation as a function of wavelength or frequency, as measured using spectrographic apparatus and other techniques, in order to understand more about matter's structure and properties. Spectroscopy has progressed beyond academic laboratories to real-world applications in a variety of fields, including biology, pharmacology, agriculture, industry, forensics and many more. For the best characterization of detected biological constituents, spectroscopic approaches such as FT-IR, FT-Raman, and UV-Visible spectroscopy were employed. The domain of spectroscopic technique development is computational chemistry. Theoretical calculations can surely help us better to comprehend the vibrational spectrum of molecules. The density functional theory (DFT) approach has evolved into a robust and dependable instrument for determining a variety of molecular properties.

This current work, entitled "Spectroscopic, molecular structural, optical analysis, quantum mechanical and molecular docking analysis on some pyridine derivatives." primarily focusses on the theoretical and experimental studies of certain biologically important compounds. The thesis, which is divided into seven chapters, is based on the methodologies used and the results obtained in this work.

The **first chapter** provides a brief overview of the fundamental principles governing electromagnetic radiation's interaction (absorption and scattering) with molecules. The use of spectroscopy in pharmaceutical science has been discussed. FT-IR and FT-Raman spectroscopic analytical instrumentation techniques are also dealt elaborately. The significance of DFT, spectroscopic background theory, and quantum computing has been discussed.

The second chapter reports the Spectroscopic, quantum mechanical investigation and molecular docking study of 2-Amino-5-chloro-3-nitropyridine. The vibrational analysis is carried out by using FT-IR and FT-Raman spectroscopic techniques. Quantum mechanical analysis of the compound have been carried out by DFT/B3LYP using 6-311++G (d, p) basis set. The vibrational frequencies obtained from the above said DFT method has been compared with the experimental spectral data recorded. The vibrational assignments of wave numbers have been calculated using the Potential Energy Distribution. The electronic properties such as HOMO -LUMO energies, energy gap, local softness, Fukui functions were determined. NBO analysis have been performed to analyze the stability of the molecule. The Molecular Electrostatic Potential and the NLO properties in terms of first order hyperpolarizability and dipole moment have also been accounted in the study. The thermodynamic parameters for different temperatures have been calculated. Molecular docking studies have been performed to investigate the biological activity of the title compound in preparation of new compounds to act as an antagonist and also to determine its binding energy.

The **third chapter** depicts the Spectroscopic (FT-IR, FT-Raman, UV-Visible), Quantum mechanical based computational studies and molecular docking analysis of 2-amino-3,5-dichloropyridine. Spectral investigations (FT-IR, FT-Raman) of the compound 2-Amino-3,5-dichloropyridine are documented and DFT quantum mechanical estimations exercising Gaussian software package has been expended to generate the theoretical report. B3LYP scheme with 6-311++G (d, p) source set has been commissioned to exhibit the molecular structure, wavenumbers of vibration and electronic properties of the compound. The experimental vibrational frequencies in comparison with the theoretical data obtained from the above said DFT method and the

assignments of vibrations have been estimated using the Potential Energy Distribution - PED. The UV-Visible spectrum was scrutinised using the TD-DFT system with a variety of solutions. HOMO-LUMO energies, Fukui functions, softness were also accounted. NBO analysis has also been explored to reveal the steadiness of the molecule. Molecular Electrostatic Potential-MEP inspection, Electron Localisation function-ELF and Local orbital locator-LOL has also been raised in the study. Additionally, to predict the biological activity of the heading compound, drug likeness, molinspiration, ADMET, environmental toxicity properties and docking reports have been accomplished.

The **fourth chapter** explains the evaluation of electronic properties in different solvents, Spectroscopic exposition (FT-IR, FT-Raman) and molecular docking studies of 5-Chloro-2-hydroxypyridine-insulysin inhibitor. The experimental and theoretical reports on the upgraded geometrical structure, electronic and vibrational features of 5-Chloro-2-hydroxypyridine are presented assigning B3LYP method with 6-311++G (d, p) basis set. The FT-IR and FT-Raman spectra of the compound were documented and the geometric parameters and wavenumbers were obtained and with scaled quantum mechanics, comprehensive vibrational assignments of wavenumbers using Potential Energy Distribution (PED) were evaluated. NBO studies was used to calculate the interaction energy and electron densities of donor and acceptor bonds. Various solvents were used to find HOMO-LUMO orbitals and band gap energy. Molecular Electrostatic Potential (MEP), Fukui functions, Mulliken charges, Electron Localisation Function (ELF) and Localised Orbital Locator (LOL) of the heading molecule were also inspected. Using the TD-DFT method and a number of solutions, the UV-Visible spectrum was explored. Additionally, drug likeness, environmental toxicity properties

were analysed and molecular docking was accomplished so as to recognize the hydrogen bond lengths and minimum binding energy was determined.

The **fifth chapter** describes the Donor acceptor groups effect, polar protic solvents influence on electronic properties and reactivity of 2-Chloropyridine-4carboxylic acid. The computational reckoning of 2-Chloropyridine-4-carboxylic acid was accomplished employing DFT / B3LYP with the root set as 6–311++G(d, p). The impact of polar protic solvents which are eco-friendly solvents (water, methanol, ethanol, 1-propanol) on the compound were analyzed. To examine the solvent effect, vibrational investigations and NLO reports in dissimilar solvents were executed. Geometrical properties were also established in gas phase. Exercising VEDA program, the entire vibrational assignment was accomplished. Donor-acceptor exchanges were ascertained utilizing NBO scrutiny technique. Thermodynamic properties of the compound were analyzed at different temperatures. By applying TD - DFT approach, theoretic UV - Visible absorption spectrum was procured in different solvents. In order to evaluate the complete electron concentration and sensitive spots of the compound, MEP coupled with FMO analyses were employed. HOMO along with LUMO orbitals and energy band gap were acquired for the compound employing dissimilar polar protic solvents. Additionally, ELF, LOL and charge transfer studies were also executed. RDG analysis has been exercised for revealing non-covalent interactions.

The **sixth chapter** gives the Vibrational, electronic influences and reactivity using IEFPCM solvation standard and molecular docking scrutiny of 2-Fluoro-4-iodo-5-methylpyridine - Pseudolysin inhibitor and complement factor D inhibitor proteins. Geometrical optimization along with spectroscopic survey and electronic scrutiny of 2-Fluoro-4-iodo-5-methylpyridine were carried out by exercising DFT(B3LYP) using

LANL2DZ as source set. The influence of few polar protic liquids (water,2-propanol) and polar aprotic liquids (acetone, acetonitrile) on the compound were scrutinized using IEFPCM solvation standard. Geometrical properties were reckoned and compared with the experimental values in gas phase. The entire vibrational assignments were accomplished employing VEDA program. Intramolecular hydrogen bonding interaction was investigated by means of the NBO analysis. The HOMO & LUMO energies, thermodynamic parameters, mulliken charges and NLO properties were procured for in dissimilar polar protic and aprotic liquids to analyse the solvent influence. Theoretic UV-Visible spectrum of the investigation compound has been accomplished using TD-DFT in different solvents chosen. MEP study has been achieved and conferred in terms of colour distribution. Additionally, ELF, LOL, charge transfer analysis & RDG analysis were also studied. Furthermore, to reveal the biological importance of the compound, drug likeness parameters have been computed and docking of the heading compound into the energetic site of the target proteins, 2OL2 and 5DUQ associated with pseudolysin inhibitor property and complement factor D inhibitor property respectively were carried out and Ramachandran plots were used to illustrate the stereochemistry of designated proteins.

The **seventh chapter** summarizes the conclusions drawn from this research.

TABLE OF CONTENTS

CHAPTER NO.			TITLE		
	LIST	IST OF TABLES			
		OF FIG		xxi	
	LIST	OF SYN	MBOLS AND ABBREVIATIONS	XXV	
I	INTI	RODUC	TION		
	1.1	ABST	RACT	1	
	1.2	AIM A	AND OBJECTIVES	1	
	1.3	REVI	EW OF LITERATURE	3	
	1.4	INSTI	RUMENTATION TECHNIQUES	4	
		1.4.1	Fourier Transform Infra Red Spectroscopy	4	
		1.4.2	Fourier Transform Raman Spectroscopy	6	
	1.5	METH	HODOLOGY EXERCISED	8	
		1.5.1	Experimental Particulars	8	
		1.5.2	Computational Techniques	8	
	REFI	ERENCE	ES	10	
II	SPE	CTROS	COPIC, QUANTUM		
	MEC	CHANIC	CAL INVESTIGATION AND		
	MOI	LECUL	AR DOCKING STUDY OF		
	2-AN	IINO-5-	CHLORO-3-NITROPYRIDINE	15	
	2.1	INTR	ODUCTION	15	
	2.2	RESU	LTS AND DISCUSSION	16	
		2.2.1	Molecular Geometry	16	
		2.2.2	Vibrational Spectral Analysis	18	
		2.2.3	Natural Bond Orbital	24	
		2.2.4	Electronic Properties	26	
		2.2.5	Molecular Electrostatic Potential (MEP)	27	
		2.2.6	Hyperpolarizability	28	
		2.2.7	Mulliken Atomic Charges & Fukui Functions	s 29	
		2.2.8	Molecular Docking	32	
	2.3	CONC	CLUSION	33	
	REFI	ERENCE	ES	34	

III	SPEC	CTROS	COPIC					
	(FT-IR, FT-RAMAN, UV-VISIBLE),							
	QUANTUM MECHANICAL BASED							
	COMPUTATIONAL STUDIES AND							
	MOLECULAR DOCKING ANALYSIS OF							
	2-AM	IINO-3,	5-DICHLOROPYRIDINE	38				
	3.1	INTR	ODUCTION	38				
	3.2	RESU	LTS AND DISCUSSION	40				
		3.2.1	Geometrical Parameters	40				
		3.2.2	Spectral Investigation	41				
		3.2.3	Molecular Reactivity and UV - Visible Analyses	46				
		3.2.4	Molecular Electrostatic Potential	50				
		3.2.5	Natural Bond Orbital Investigation	51				
		3.2.6	Fukui Function Descriptors Analysis	53				
	3.2.7 ELF and LOL Studies							
	3.2.8 Biological Assessment							
			3.2.8.1 Pharmacological analyses	57				
			3.2.8.2 Ramachandran plot	58				
			3.2.8.3 Molecular docking	60				
	3.3	CONC	CLUSION	62				
	REFE	ERENCE	ES	63				
T T 7	CDE							
IV			COPIC EXPOSITION					
	•	•	RAMAN), EVALUATION OF					
			IIC PROPERTIES IN DIFFERENT					
			AND MOLECULAR DOCKING					
			F 5-CHLORO-2-HYDROXYPYRIDINE	(0				
			N INHIBITOR	68				
	4.1		ODUCTION THE AND DISCUSSION	68				
	4.2		LTS AND DISCUSSION	69				
		4.2.1	Geometrical Parameters	69 71				
	4.2.2 Vibrational Investigation 71							

TITLE

PAGE NO.

CHAPTER NO.

CHAPTER NO.			TITLE	PAGE NO.		
		4.2.3	Donor – Acceptor Interaction	76		
		4.2.4	FMO Analysis	78		
		4.2.5	Electronic Analysis	79		
		4.2.6	Reactive Site Analysis	81		
		4.2.7	Population and Molecular Reactivity Study	82		
		4.2.8	ELF and LOL Studies	85		
		4.2.9	Biological Assessment	87		
			4.2.9.1 Pharmacological analyses	87		
			4.2.9.2 Docking studies	88		
	4.3	CONC	CLUSION	91		
	REFE	RENCE	ES	93		
V	DONG	OR AC	CEPTOR GROUPS EFFECT,			
	POLA	AR PRO	OTIC SOLVENTS INFLUENCE ON			
	ELECTRONIC PROPERTIES AND REACTIVITY					
	OF 2-	CHLO	ROPYRIDINE-4-CARBOXYLIC ACID	97		
	5.1	INTR	ODUCTION	97		
	5.2	OUTC	COMES AND DISCUSSION	98		
		5.2.1	Geometrical Factors	98		
		5.2.2	Assignments of Vibrational bands	100		
		5.2.3	NLO Analysis	104		
		5.2.4	Donor – Acceptor interaction	107		
		5.2.5	Thermodynamical properties	109		
		5.2.6	Electronic analysis	111		
		5.2.7	Reactive site analysis	113		
		5.2.8	FMO investigation	115		
		5.2.9	Molecular reactivity and population analyses	117		
		5.2.10	ELF, LOL & Charge transfer studies	121		
		5.2.11	RDG analysis	123		
	5.3	CONC	CLUSION	124		
	REFE	RENCE	ES	126		

VI	EXP	LORAT	ION OF	FEW POLAR PROTIC AND			
	APROTIC LIQUIDS EFFECT ON VIBRATIONAL,						
	ELECTRONIC INFLUENCES AND REACTIVITY						
	USIN	IG IEFP	CM SOL	VATION STANDARD AND			
	MOL	LECULA	AR DOCI	KING SCRUTINY OF			
	2-FLUORO-4-IODO-5-METHYLPYRIDINE						
	6.1 INTRODUCTION				132		
	6.2	OUTC	COMES AND DISCUSSION		133		
		6.2.1	Geometr	rical Factors	133		
		6.2.2	Vibratio	nal Description	135		
		6.2.3	Electron	ic Properties	139		
		6.2.4	MEP An	alysis	141		
		6.2.5	NLO Inv	vestigation	142		
		6.2.6	Thermoo	lynamical Properties	143		
		6.2.7	FMO, N	BO and Topology Analyses	146		
			6.2.7.1	FMO investigation	146		
			6.2.7.2	NBO studies	147		
			6.2.7.3	Topology studies	148		
		6.2.8	Molecul	ar Reactivity and Population Analyses	150		
		6.2.9	Drug lik	eness and Molecular Docking Approach	154		
	6.3	CONCLUSION		157			
	REFE	ERENCE	ES		159		
VII	SUM	MARY	AND CO	NCLUSIONS	164		
LIST	OF PU	JBLICA	TIONS		167		

TITLE

PAGE NO.

CHAPTER NO.

LIST OF TABLES

TABLE NO.	TITLE	PAGE NO
2.1	Geometrical parameters of 2-Amino-5-chloro-3-	10
	nitropyridine: bond length(\mathring{A}) and bond angle (0).	18
2.2	Observed and calculated vibrational frequency of	22
	2A5C3NP.	22
2.3	Second order perturbation theory analysis of Fock matrix	25
	in NBO of 2A5C3NP.	25
2.4	Calculated energy values of 2-Amino-5-chloro-3-	27
	nitropyridine.	27
2.5	The calculated values of dipole moment, polarizability and	
	the first order polarizability of 2-Amino-5-chloro-3-	29
	nitropyridine.	
2.6	Mulliken charge distribution, Fukui function and local	
	softness corresponding to (0,1), (-1,2) and (1,2) charge and	31
	multiplicity of 2A5C3NP	
2.7	Molecular docking parameters of 2A5C3NP with the	33
	protein 3d6d.	33
3.1	Geometrical parameters of 2-Amino-3,5-dichloropyridine:	41
	bond length(\mathring{A}) and bond angles(0).	41
3.2	Observed and calculated vibrational frequency of 2ADCP.	44
3.3	Calculated energy values of 2-Amino-3,5-	47
	dichloropyridine with solvation effect.	47
3.4	Simulated UV-Vis spectrum with absorption maxima(nm),	
	energy (cm ⁻¹) and oscillator strength(f) of 2ADCP with	48
	different solvents.	
3.5	Second order perturbation theory analysis of Fock matrix	52
	in NBO for 2ADCP.	32
3.6	Mulliken charge distribution, Fukui function and local	
	softness corresponding to (0,1), (-1,2) and (1,2) charge and	54
	multiplicity for 2ADCP.	

TABLE NO.	TITLE	PAGE NO.
3.7	Drug likeness parameters of 2ADCP	58
3.8	Molecular docking parameters of 2ADCP with proteins 6QHB and 6Y92.	60
4.1	Geometrical parameters of 5-Chloro-2-hydroxypyridine: bond length(Å) and bond angles(⁰).	70
4.2	Theoretical comparison of vibrational frequency 5C2HOP in gas and in different solvents.	74
4.3	Second order perturbation theory analysis of Fock matrix in NBO for 5C2HOP.	77
4.4	Calculated energy values of 5-Chloro-2-hydroxypyridine with solvation effect.	79
4.5	Theoretical electronic transition parameters of 5C2HOP in different solvents.	81
4.6	Mulliken charge distribution of 5C2HOP in gas and other solvents.	83
4.7	Mulliken charge distribution, Fukui function and local softness corresponding to (0,1), (-1,2) and (1,2) charge and multiplicity of 5C2HOP.	84
4.8	Drug likeness parameters of 5C2HOP.	87
4.9	Molecular docking parameters of 5C2HOP with the proteins 4DM3 and 5DU3.	90
5.1	Geometric parameters of 2CP4CA in gas phase.	99
5.2	Theoretical comparison of vibrational frequency of 2CP4CA in gas and in different solvents.	102
5.3	The values of calculated dipole moment $\mu(D)$, polarizability(α) and first order hyperpolarizability(β) of 2CP4CA in different solvents.	105
5.4	Second order perturbation theory analysis of Fock matrix in NBO for 2CP4CA.	108
5.5	Thermodynamical parameters of 2CP4CA in different phases.	110

TABLE NO.	TITLE	PAGE NO.
5.6	Simulated UV-Vis spectrum with absorption maxima(nm),	
	energy (cm ⁻¹) and oscillator strength(f) for 2CP4CA with	112
	different solvents.	
5.7	Calculated energy values of 2CP4CA with solvation	
	effect.	116
5.8	Fukui functions, local softness and dual descriptor of	
	2CP4CA.	119
5.9	Mulliken charge distribution of 2CP4CA in gas phase and	
	in other solvents.	120
5.10	Electron - hole interaction parameters of 2CP4CA.	123
6.1	Geometric parameters of 2FIMP in gas phase at B3LYP/	
	LANL2DZ.	135
6.2	Theoretical comparison of vibrational frequency of 2FIMP	
	at B3LYP method with LANL2DZ basis set in gas and in	137
	different solvents.	
6.3	Theoretical electronic transition parameters of 2FIMP in	1.40
	gas and other solvents.	140
6.4	The values of calculated dipole moment $\mu(D)$,	
	polarizability(α)and first order hyperpolarizability(β) of	143
	2FIMP.	
6.5	Thermodynamical parameters of 2FIMP in different	1 45
	phases.	145
6.6	Calculated energy values of 2FIMP with solvation effect.	147
6.7	Second order perturbation theory analysis of Fock matrix	140
	in NBO for 2FIMP.	148
6.8	Fukui functions, local softness and dual descriptor of	150
	2FIMP.	152
6.9	Mulliken charge distribution of 2FIMP in gas phase and	152
	in other solvents.	153
6.10	Drug likeness parameters for 2FIMP.	155
6.11	Docking of 2FIMP with different proteins.	156

LIST OF FIGURES

FIGURE NO.	TITLE	PAGE NO
1.1	The schematic set-up of FT-IR Spectroscopy	5
1.2	Energy levels involved in Raman spectra	6
1.3	Schematic figure of FT-Raman Spectrometer	7
2.1	Optimised geometric structure with atom numbering of	
	2-Amino-5-chloro-3-nitropyridine	17
2.2	Compared theoretical and Experimental FT-IR spectrum	
	of 2A5C3NP.	21
2.3	Compared theoretical and Experimental FT-Raman	
	spectrum of 2A5C3NP.	21
2.4	Atomic orbital HOMO - LUMO composition of the	
	frontier molecular orbital of 2A5C3NP.	26
2.5	Molecular Electrostatic Potential of 2-Amino-5-chloro-	
	3-nitropyridine.	28
2.6	The histogram of calculated Mulliken Charges of	
	2A5C3NP.	30
2.7	Docking and hydrogen bond interaction of 2A5C3NP	
	with the protein 3d6d.	32
3.1	Optimised geometric structure with atom numbering of	
	2-Amino-3,5-dichloropyridine.	40
3.2	Compared theoretical and Experimental FT-IR spectrum	
	of 2ADCP	43
3.3	Compared theoretical and Experimental FT-Raman	
	spectrum of 2ADCP.	43
3.4	Atomic orbital HOMO - LUMO composition of the	
	frontier molecular orbital of 2-Amino-3,5-	
	dichloropyridine.	48
3.5	Theoretical UV-Visible spectra of 2ADCP in water as	
	solvent.	49
3.6	Theoretical UV-Visible spectra of 2ADCP in DMSO as	
	solvent	49

FIGURE NO.	TITLE	PAGE NO.
3.7	Theoretical UV-Visible spectra of 2ADCP in benzene as	
	solvent.	50
3.8	Molecular Electrostatic Potential of 2ADCP.	51
3.9	ELF, colour filled map of 2ADCP.	55
3.10	ELF, contour map of 2ADCP.	56
3.11	LOL, colour filled map of 2ADCP.	56
3.12	LOL, contour map of 2ADCP.	56
3.13	Ramachandran plot for receptor protein 6QHB.	59
3.14	Ramachandran plot for receptor protein 6Y92.	59
3.15	Docking and hydrogen bond interaction of 2ADCP with	
	6QHB.	61
3.16	Docking and hydrogen bond interaction of 2ADCP with	
	6Y92.	61
4.1	Optimised geometric structure with atom numbering of	
	5-Chloro-2- hydroxypyridine.	70
4.2	Compared theoretical and Experimental FT-IR spectrum	
	of 5C2HOP.	73
4.3	Compared theoretical and Experimental FT-Raman	
	spectrum of 5C2HOP.	73
4.4	Atomic orbital HOMO - LUMO composition of the	
	frontier molecular orbital of 5C2HOP.	78
4.5a	Theoretical UV spectra of 5C2HOP in Water.	80
4.5b	Theoretical UV spectra of 5C2HOP in DMSO.	80
4.5c	Theoretical UV spectra of 5C2HOP in Ethanol.	80
4.5d	Theoretical UV spectra of 5C2HOP in Acetone.	81
4.6	Molecular Electrostatic Potential of 5-Chloro-2-	
	hydroxypyridine.	82
4.7	The histogram of calculated Mulliken Charges of	
	5C2HOP.	83
4.8a	ELF, Colour filled map of 5C2HOP.	85
4.8b	ELF, Contour map of 5C2HOP.	86

FIGURE NO.	TITLE	PAGE NO.
4.9a	LOL, Colour filled map of 5C2HOP.	86
4.9b	LOL, Contour map of 5C2HOP.	86
4.10a	2D Ramachandran plot for receptor protein 4dm3.	89
4.10b	2D Ramachandran plot for receptor protein 5du3.	89
4.11	Docking and hydrogen bond interaction of 5C2HOP	
	with 4DM3.	90
4.12	Docking and hydrogen bond interaction of 5C2HOP	
	with 5DU3.	91
5.1	Optimized picture of 2CP4CA with atom numbering .	99
5.2	Graph representing dependence of entropy, specific heat	
	capacity and enthalpy on temperature of 2CP4CA in	
	gas phase.	109
5.3	Theoretical comparative UV spectra of 2CP4CA in	
	different solvents.	111
5.4	Molecular Electrostatic Potential of 2CP4CA in	
	different solvents.	114
5.5	Atomic orbital HOMO - LUMO composition of the	
	frontier molecular orbital of 2CP4CA in gas phase.	116
5.6	Fukui function graph for natural charges of 2CP4CA.	118
5.7	The histogram of calculated Mulliken Charges of	
	2CP4CA in different phases.	120
5.8	ELF, vector - colour filled map of 2CP4CA in gas	
	phase.	122
5.9	LOL, vector - colour filled map of 2CP4CA in gas phase.	122
5.10	Iso surface of hole and electron distribution of 2CP4CA.	122
5.11	RDG-colour filled map of 2CP4CA in gas phase.	124
6.1	Optimized picture of 2FIMP with atom numbering.	134
6.2	Theoretical comparative UV spectra of 2FIMP in	
	different solvents.	139
6.3	Molecular Electrostatic Potential of 2FIMP by	
	B3LYP/LANL2DZ in gas phase.	141

FIGURE NO.	TITLE	PAGE NO
6.4	Graph representing thermodynamical parameters on	
	temperature of 2FIMP in gas phase.	144
6.5	Atomic orbital HOMO - LUMO composition of the	
	frontier molecular orbital of 2FIMP in gas phase.	146
6.6a	ELF - Colour filled map of 2FIMP	149
6.6b	ELF - Contour map of 2FIMP	149
6.7a	LOL - Colour filled map of 2FIMP	150
6.7b	LOL - Contour map of 2FIMP	150
6.8	Fukui function graph for natural charges of 2FIMP.	151
6.9	The histogram of calculated Mulliken Charges of	
	2FIMP in different phases.	153
6.10a	Ramachandran plot of 2OL2 protein.	155
6.10b	Ramachandran plot of 5DUQ protein.	156
6.11	Molecular docking of active site of 2FIMP with 2OL2	
	protein.	156
6.12	Molecular docking of active site of 2FIMP with 5DUQ	
	protein.	157

LIST OF SYMBOLS AND ABBREVIATIONS

 ΔE - Band gap energy

B3LYP - Becke's 3 parameter Lee Yang and Parr

CT - Charge transfer

η - Chemical hardnessμ - Chemical potential

μ - Chemical potentiaδ - Chemical shift

S - Chemical softness

DFT - Density Functional Theory

DMSO - Dimethyl sulfoxideEA - Electron Affinity

ELF - Electron Localisation Function

χ - Electronegativity

ω - Electrophilicity index

FT - Fourier Transform

FT-IR - Fourier Transform – Infrared FT-Raman - Fourier Transform – Raman

FMOs - Frontier molecular orbitals

HOMO - Highest-Occupied Molecular Orbital

IR - Infrared

IEFPCM - Integral Equation Formalism Polarizable Continuum Model

IP - Ionization Potential

LOL - Local Orbital Localisation

LUMO - Lowest Unoccupied Molecular Orbital

MEP - Molecular electrostatic potential

MO - Molecular Orbital

NBO - Natural Bonding Orbitals

NIR - Near Infra-RedNLO - Non Linear Opticsf - Oscillator strength

PED - Potential Energy Distribution

TD-DFT - Time Dependent-Density Functional Theory

UV – Vis. - Ultraviolet-Visible

 λ - Wavelength

CHAPTER I

INTRODUCTION

1.1 ABSTRACT

The focus of the current research is on the molecular structure, vibrational spectra, electronic characteristics and molecular docking of particular pyridine derivatives which have beneficial applications in pharmaceutical field. The fundamental goal of this research is to use quantum mechanics to support and complement experimental evidence, as well as to uncover information on the geometry, chemical stability and bioactivity of the chosen compounds. The computational reckoning was accomplished employing Density Functional Theory (DFT) which has been an efficient tool in the prediction of molecular structure, vibrational wave numbers, etc. A substantial segment is devoted to molecular docking analysis, which is a common technique for predicting the binding-conformation of small molecule ligands to the proper target binding site. The goal and objectives of the five chosen compounds, along with the concept and instrumentation techniques of FT-IR, FT-Raman, and UV-Visible and various quantum computational approaches are all covered in this introductory chapter.

1.2 AIM AND OBJECTIVES

Identifying the sorts of interactions that exist and the structure of activity correlations is substantial for certain Pyridine derivatives which have remarkable biological applications [1]. The core principles of DFT can be used to better

comprehend numerous theoretical tools for modelling chemical reactivity [2]. Using vibrational spectroscopy approaches and quantum chemical simulations, elucidating their structural properties are of recent origin. The primary aspiration of this research is to examine certain pyridine derivatives with the hope that the results will be beneficial to drug producers and other researchers in the future, as well as to see if there is any physical basis for exercising electronic structure theory to enhance the bioactivity, selectivity, and stability of those compounds. The purpose of this study was to look into the characterization, structural investigations and docking locations of the chosen pyridine derivatives.

The chief objective of this work is:

- FT-IR, FT-Raman, and UV-Vis spectral techniques were used to characterize the numerous pyridine derivatives listed below, and they were compared with computational (DFT) approaches.
 - ❖ 2-Amino-5-chloro-3-nitropyridine (C₅H₄ClN₃O₂)
 - ❖ 2-Amino-3,5-dichloropyridine (C₅H₄Cl₂N₂₎
 - **♦** 5-Chloro-2-hydroxypyridine (C₅H₄ClNO)
 - ❖ 2-Chloropyridine-4-carboxylic acid (C₆H₄ClNO₂)
 - ❖ 2-Fluoro-4-iodo-5-methylpyridine (C₆H₅FIN)
- Molecular docking explorations were carried out on few above mentioned pyridine derivatives.

1.3 REVIEW OF LITERATURE

Spectroscopy has made its way from academic labs to real-world applications in a variety of sectors, including biological, pharmacological, agricultural, industrial, forensic and many more. Spectroscopic techniques are most important tools for the study of the molecular structure as well as the qualitative and quantitative determination of both inorganic and organic compounds. Some of the important applications of spectroscopy are molecular structural determinations, estimation of intra-molecular & inter- molecular forces, exposition of molecular symmetries, identification and characterization of new molecules, construing thermodynamical properties of molecular systems, etc. The most extensively utilized characterization techniques for observed biological compounds are Infrared spectroscopy (FT-IR), Raman spectroscopy (FT-Raman) and Ultraviolet-Visible spectroscopy. The use of FT-Raman and FT-IR spectra, as well as quantum chemical calculations, to study vibrational spectral analyses of bioactive compounds has piqued researchers' curiosity. FT-IR, FT-Raman, and UV-visible spectra of numerous pharmacological compounds have been used in a number of studies to establish the structure-activity relationship. DFT simulations have been used in a number of investigations to demonstrate structure-activity relationships [3-6]. Certain pyridine derivatives exhibit anti-bacterial, anti -microbial, pesticide, antitumor, anti -allergic, anti -fungal, analgesic or antihypertensive properties [7-9]. The DFT computational approach is commonly used to characterise the quantum states of multi molecule electron systems [10]. So far, no single inquiry has been conducted to determine the structure-activity link using FT-IR and FT-Raman techniques, followed by quantum chemical computations, in order to determine the bioactivity of significant pyridine derivates chosen for study. The current

work expands the function of vibrational spectroscopy in drug manufacture, stability, and activity, as addressed in the following chapters.

1.4 INSTRUMENTATION TECHNIQUES

Spectroscopic techniques use light to interact with matter, allowing them to probe specific characteristics of a sample in order to learn more about its consistency or structure. An appreciation for the variety of forms of spectra and, as a result, diverse spectroscopic techniques and their applications to the solution of biological problems stems from a comprehension of the properties of electromagnetic radiation and its interaction with matter. In the pharmaceutical sector, vibrational spectroscopic techniques like as FT-IR and FT-Raman play a critical role in understanding the solid-state characteristics such as stability and activity of various drug molecules. UV-Vis spectroscopy is commonly employed in analytical chemistry to quantify various analytes or samples.

1.4.1 Fourier Transform Infra-Red Spectroscopy

Infrared spectroscopy is one of the most powerful analytical techniques for structural elucidation and compound identification. It is employed to reveal the functional groups in the sample. The benefits of IR over other structural analysis techniques are that it instantly delivers useful information about a molecule's structure without the need for time-consuming examination. This technique is based on the simple fact that a chemical substance shows marked selective absorption in the IR region [11]. Molecules can absorb IR radiation only if their absorption instigates a change in the electric dipole. The mid-IR range (4000 – 400cm⁻¹) is the most widely used since it encompasses the majority of vibrational transitions [12, 13].

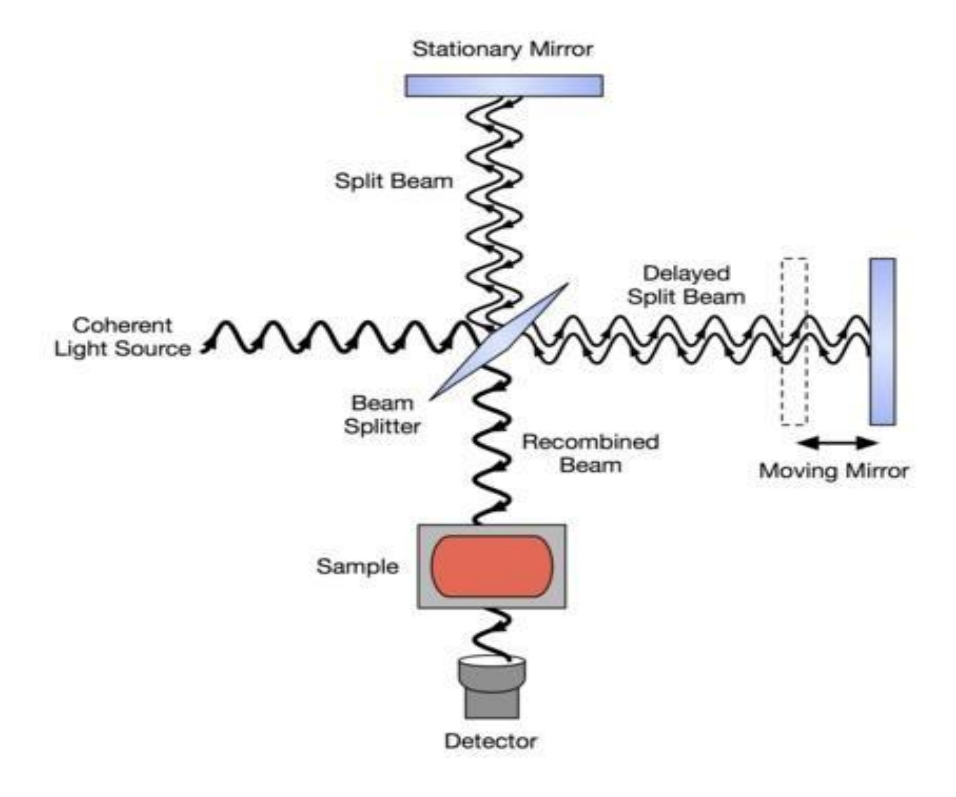


Fig 1.1 The schematic set-up of FT-IR Spectroscopy

The FT-IR technique is a simple mathematical technique to resolve a complex wave into its frequency components. It has made significant impact with regard to rapid scanning, signal to noise ratio, high sensitivity, high resolution and data processing [14, 15]. The FT-IR spectrometer comprises of an optical equipment (interferometer) and a computer (accumulates data). A beam splitter, a fixed mirror, and a moveable mirror make up the interferometer system. The beam splitter divides the incoming infrared beam into two optical beams and transmits half the arriving radiation of two mirrors. The beams recombine when they meet back at the beam splitter after reflection from the mirrors and are directed to the detector through the sample. The resulting signal is known as an interferogram, and it has the unique virtue of containing information about each IR frequency that comes from the source. Constructive interference occurs when the difference in path lengths is integral number including zero of wavelength whereas if it is half odd integral number of wavelengths, destructive interference occurs [16, 17]. Finally,

the signal captured in the detector is sent to a multichannel computer, which performs a Fourier transform on the recorded data and presents the user with the essential spectral report for analysis. Fig 1.1 depicts the schematic diagram of FT- IR spectrometer.

1.4.2 Fourier Transform Raman Spectroscopy

Raman spectroscopy has been recognized as a valuable research technique and an important analytical tool for investigating molecular vibrations. Here, when a powerful beam of light passes through a substance, the dispersed light observed perpendicular to the incident beam has a little different frequency than the incident light [18]. The Raman spectrum is a dispersed spectrum that shows a number of lines that are offset from the original frequency [19]. A change in polarizability during the vibration or rotation of the molecule is the most basic prerequisite or condition for the molecule to be Raman active. Fig 1.2 shows the energy levels involved in Raman and Rayleigh scattering.

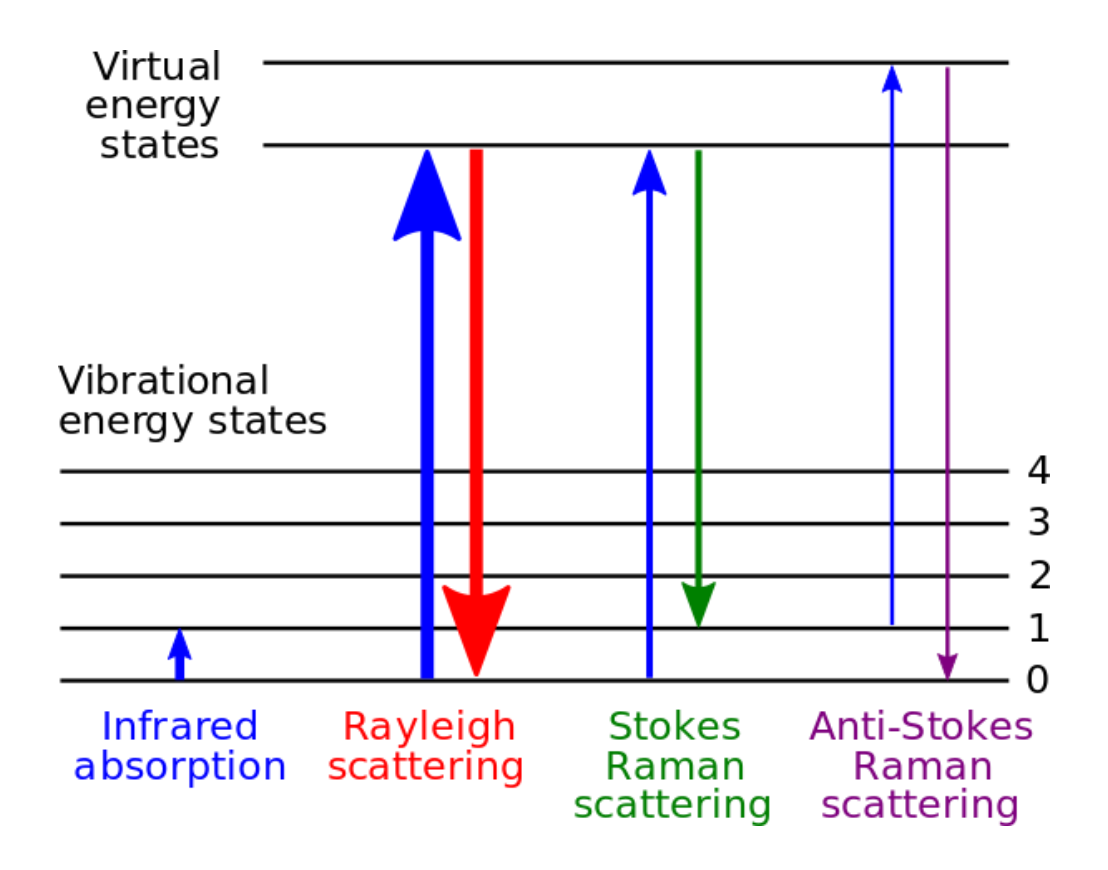


Fig 1.2 Energy levels involved in Raman spectra

FT – Raman spectroscopy is utilized for non-destructive study of a wide range of samples and has the added benefit of providing high-accuracy wavenumber values in a spectrum. The FT-Raman spectrometer uses a NIR laser for excitation and an interferometer-based system followed by an FT program to produce the spectrum. The main constituents of FT-Raman spectrometer include a laser source, a FT-Interferometer, filters, a sample chamber and a detector. The FT technique uses an Nd:YAG laser at 1.064μm to measure the Raman effect. The use of appropriate absorption filters reduces fluorescence. The final filter is placed in front of the detector [20, 21]. The FT interferometer directs all scattered energy to the detector at the same time. Fig 1.3 displays a typical FT-Raman Spectrometer. FT-Raman has revolutionized Raman spectroscopy and broadened the user base in both industry and scientific research.

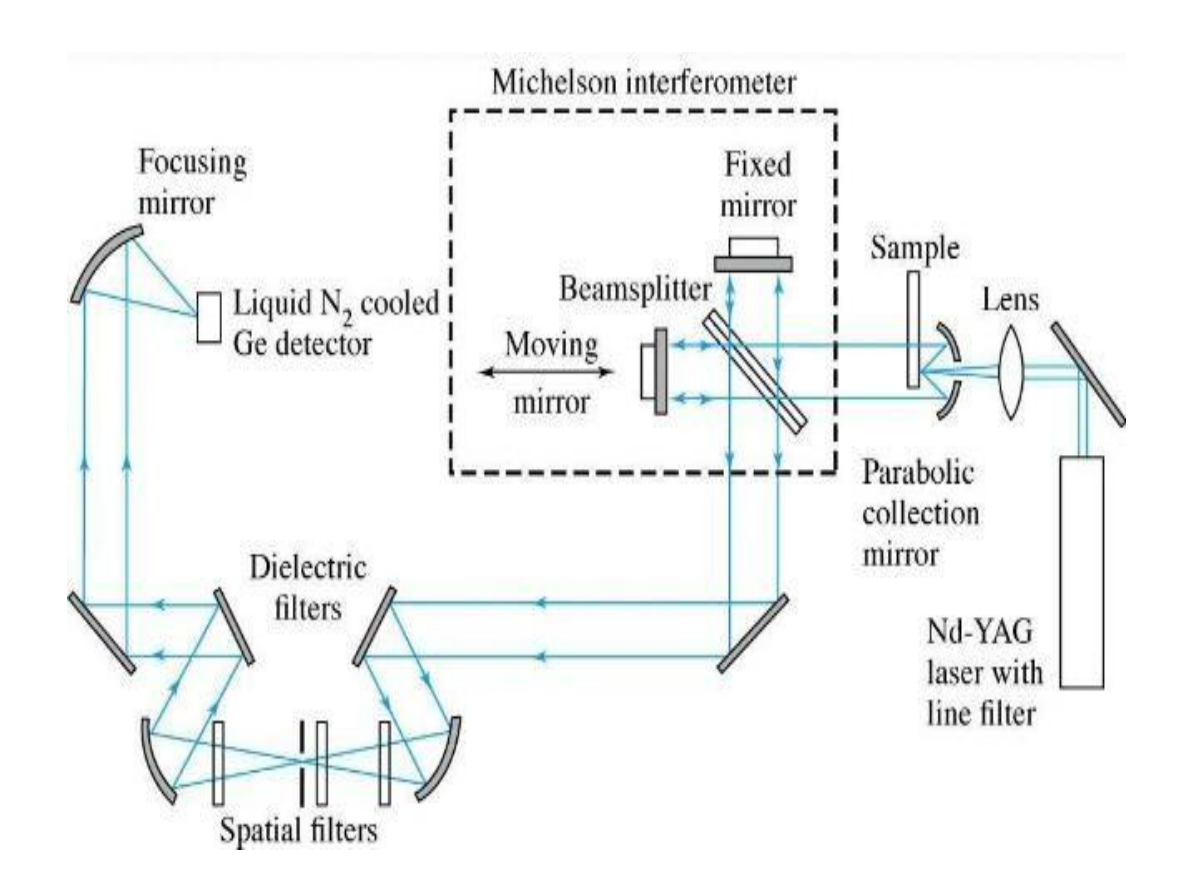


Fig 1.3 Schematic figure of FT-Raman Spectrometer.

1.5 METHODOLOGY EXERCISED

1.5.1 Experimental particulars

The FT-IR spectrum in the region 4000 cm⁻¹ to 400 cm⁻¹ using KBr pellet method on Perkin Elmer Spectrum-1 spectrometer and FT-Raman spectrum exercising Nd-Yag 1064 nm laser on Bruker RFS27 spectrophotometer in the region of 4000 cm⁻¹ to 100 cm⁻¹ were documented at SAIF, IIT, Chennai, India.

1.5.2 Computational Techniques

Quantum chemical computation is a method which uses the principle of Quantum Mechanics for simulating chemical structures and envisaging the activities of individual molecules within a chemical system. It has evolved into a valuable tool for modelling, solving fascinating chemical issues, and understanding reaction mechanisms with the use of powerful computer software. Molecular orbitals are the essential building blocks for comprehending many scientific phenomena. They are shown up as a cloud of electrical charge across a region in studies. Quantum chemistry is used to examine molecules at the quantum level and is based on these molecular orbitals. It can be utilised on its own in theory calculations or as a supplement to experimental findings. In the last ten years, technological advancements have ushered in a new era in computational studies. The electronic structure of atoms, molecules and solids is calculated using density functional theory (DFT), a quantum-mechanical approach used in chemistry and physics [22, 23]. It has become extremely important in the study of vibrational spectra and molecular structures. Gaussian software [24-27], a widely used programme in Computational Chemistry, is used to calculate theoretical vibrational modes, which entails numerical calculations of molecule electronic structures. With the use of various methodologies and basis sets, Gaussian can forecast a better level of accuracy in chemical property computations [28,29]. For most cases, the 6-311++G(d,p) basis set was utilised to evaluate chemical natures using the DFT/B3LYP approach due to the fact that this method has higher quality of theoretical style [30-32].

The current study discloses, the above approach is used to calculate Potential Energy Surface (PES) which is a conceptual tool for aiding the analysis of molecular geometry and chemical reaction dynamics. MEP, UV studies, donor- acceptor connections, HOMO-LUMO examinations, ELF and LOL analyses were accounted. NLO studies [33, 34] have been computed as their expanding applicability in electronic devices are receiving a lot of interest and are very important. The Fukui functions [35-37] analysis has also been carried out which aids one to envisage the most responsive locations for electrophilic and nucleophilic occurrence within the molecule. Molecular docking is an influential computational tool used to examine the ligand confirmation within the binding site of protein targets [38,39]. Auto Dock set 4.2.6 software package [40,41] has been used to investigate the molecular activity of protein-ligand connections.

REFERENCES

- [1] S. Sivaprakash, S. Prakash, S. Mohan, Sujin. P. Jose, Heliyon (2019) 2405-8440.
- [2] P. W. Ayers and Robert G. Parr, Variational Principles for Describing Chemical Reactions: The Fukui Function and Chemical Hardness Revisited, J. Am. Chem. Soc. 122 (2000) 2010-2018.
- [3] D. Simoni, R. Romagnoli, R. Baruchello, R. Rondanin, M. Rizzi, M. G. Pavani, D. Alloatti, G. Giannini, M. Marcellini, T. Riccioni, M. Castorina, Mario B. Guglielmi, F. Bucci, P. Carminati, C. Pisano, Novel Combretastatin Analogues Endowed with Antitumor Activity, J. Med. Chem., 49 (2006) 3143-3152.
- [4] K. Ohsumi, R. Nakagawa, Y. Fukuda, T. Hatanaka, Y. Morinaga, Y. Nihei, K. Ohishi, Y. Suga, Y. Akiyama, T. Tsuji, Novel combretastatin analogues effective against murine solid tumors: design and structure-activity relationships, J. Med. Chem., 41 (1998) 3022-3032.
- [5] K. Gaukroger, John A. Hadfield, Lucy A. Hepworth, Nicholas J. Lawrence, Alan T. McGown, Novel Syntheses of Cis and Trans Isomers of Combretastatin A-4, J. Org. Chem., 66 (2001) 8135-8138.
- [6] J. Binoy, Jose P. Abraham, I. Hubert Joe, V. S. Jayakumar, G. R. Pettit and O. F. Nielsen, NIR-FT Raman and FT-IR spectral studies and ab initio calculations of the anti-cancer drug combretastatin-A4, J. Raman Spectrosc., 35(11), (2004) 939-946.
- [7] Cocco, M.T., C. Congiu, and V. Onnis, Synthesis and antitumour activity of 4-hydroxy-2-pyridone derivatives. European Journal of Medicinal Chemistry, 35 (2000) 545-552.
- [8] Al-Otaibi, J.S., Experimental (FT-IR and FT-Raman spectra) and Theoretical (Ab initio/HF, DFT/B3LYP) Study of 2-Amino-5-Chloropyridine and 2-Amino-6- Chloropyridine Chemistry and Materials Research 7 (2015).

- [9] M. M. Krayushkin, I. P. Sedishev, V. N. Yarovenko, I. V. Zavarzin, S. K. Kotovskaya, D. N. Kozhevnikov, Synthesis of Pyridines from 1,2,4-Triazines under High Pressure Russian Journal of Organic Chemistry, 44 (2008) 407-411.
- [10] Issa, T.B., Sagaama, A., Noureddine, I. (2020). Computational study of 3-thiophene acetic acid: Molecular docking, electronic and intermolecular interactions investigations. Computational Biology and Chemistry. 86: 107268.
- [11] Yang Leng, Materials Characterization: Introduction to Microscopic and Spectroscopic Methods, JohnWiley& Sons (Asia) Pte Ltd, Singapore, 2008.
- [12] F.R. Dollish, W.G. Fateley, F.F. Bentley, Characteristic Raman Frequencies of Organic Compounds, John Wiley & Sons, New York, (1990).
- [13] S. Wartewig, IR and Raman Spectroscopy Fundamental Processing, Wiley VCH, (2003).
- [14] R.G.J. Miller, B.C. Stace, Laboratory Methods in Infrared Spectroscopy, Heyden and Sons Ltd, London, (1972).
- [15] D.C. Harries, Qualitative Chemical Analysis, Freeman and Company, New York, (1995).
- [16] G. Aruldhas, Molecular Structure and Spectroscopy, Prentice Hall, India, (2001).
- [17] Mink J, Pápai I, Gál M, Goggin P.L, "Recent developments of FT-IR and Raman spectroscopy in coordination chemistry", Pure and Appl. Chem., 61, (1989) 973- 978.
- [18] S.F. Parker, K. Williams, A.J. Turner & P.J. Hendra, Fourier Transform Raman Spectroscopy Using a Bench-Top FT-IR Spectrometer, Appl. Spectrosc., 42 (1988) 796-800.

- [19] Gi Xue, 1997, "Fourier transform Raman spectroscopy and its application for the analysis of polymeric materials", Progress in Polymer Science, vol. 22, no. 2, pp. 313-406.
- [20] P. J. Hendra, C. Jones, G. Warnes, Fourier Transform Raman Spectroscopy, Ellis Horwood, Chichester, England, 1991.
- [21] D. N. Sathyanarayana, Vibrational Spectroscopy Theory and Applications, New Age International (P) Limited, New Delhi, 2004.
- [22] J. Seminario, Recent Developments and Applications of Modern Density Functional Theory, Elsevier, Amsterdam, 4 (1996).
- [23] M. Raja, R. Raj Muhamed, S. Muthu, M. Suresh, J. Mol. Struct., 1141 (2017) 284-298.
- [24] Sir John A. Pople, J. Comput. Chem. 25 (9) (2004) 1925.
- [25] J. A. Pople and Sir John Lennard-Jones, The Molecular Orbital Theory of Chemical Valency: IV. The Significance of Equivalent Orbitals, Proc. Roy. Soc.A 202 (1950) 166-180.
- [26] J. A. Pople, A. C. Hurley, and Sir J. Lennard-Jones, The Molecular Orbital Theory of Chemical Valency: XVI. A Theory of Paired-electrons in Polyatomic Molecules, Proc. Roy. Soc.A 220 (1953) 446-455.
- [27] M. J. Frisch, G. W. Trucks, H. B. Schlegel, G. E. Scuseria, M. A. Robb, J. R. Cheeseman, Jr. J. A. Montgomery, T. Vreven, K. N. Kudin, J. C. Burant, J.M. Millam, Iyengar, J. Tomasi, V. Barone, B. Mennucci, M. Cossi, G. Scalmani, N. Rega, G. A. Petersson, H. Nakatsuji, M. Hada, M. Ehara, K. Toyota, R. Fukuda, J. Hasegawa, M. Ishida, T. Nakajima, Y. Honda, O. Kitao, H. Nakai, M. Klene, X. Li, J. E. Knox, H. P. Hratchian, J. B. Cross, V. Bakken, C. Adamo, J. Jaramillo, R. Gomperts, R. E. Stratmann, O. Yazyev, A. J. Austin, R. Cammi, C. Pomelli, J. W. Ochterski, P. Y. Ayala, K. Morokuma, G.A. Voth, P. Salvador, J. J. Dannenberg, V. G. Zakrzewski, S. Dapprich, A. D. Daniels, M.

- C. Strain, O. Farkas, D. K. Malick, A. D. Rabuck, K. Raghavachari, J. B. Foresman, J. V. Ortiz, Q. Cui, A. G. Baboul, S. Clifford, J. Cioslowski, B. B. Stefanov, G. Liu, A. Liashenko, P. Piskorz, I. Komaromi, R. L. Martin, D. J. Fox, T. Keith, M. A. Al-Laham, C. Y. Peng, A. Nanayakkara, M. Challacombe, P. M. W. Gill, B. Johnson, W. Chen, M. W. Wong, C. Gonzalez, J. A. Pople, Gaussian 09, Revision B.0, Gaussian, Inc., Wallingford, C.T. (2010).
- [28] Krishnakumar V, Surumbarkuzhali N, Analysis of structure and vibrational spectra of 2,5-dihydroxybenzoicacid based on density functional theory calculations, Journal of Raman Spectroscopy, 41, (2010) 473-478.
- [29] Tonannavar J, Yenagi J, Sortur V, Jadhav V.B, Kulkarni M.V, Vibrational spectra, normal modes, ab initio and DFT calculations for 6-Chloro- and 7-Chloro-4- bromomethylcoumarins, Spectrochimica Acta Part A:Molecular and Biomolecular Spectroscopy, 77,.(2010).351-358.
- [30] Casida M E, Jamorski C, Casida K C, Salahub D R., J.Chem. Phys. 108 (11) (1998) 4439-4449.
- [31] Stratmann R E, Scuseria G E, Frisch M J., J.Chem. Phys. 109 (19) (1998) 8218-8224.
- [32] Kone M, Illien B, Graton J, Laurence C., J. Phys. Chem.109 (51) (2005) 11907-11913.
- [33] Ben Ahmed, A, Elleuch, N, Feki, H, Abid, Y & Minot, C 2011, Vibrational spectra and non linear optical properties of I- histidine oxalate: DFT studies, Spectrochimica Acta A, vol. 79, pp. 554-561.
- [34] Sajan, D, Ravindra, HJ, Mishra, N & Joe, IH 2010, Intramolecular charge transfer and hydrogen bonding interactions of nonlinear optical material N-benzoyl glycine: Vibrational spectral study, Vib. Spectrosc., vol. 54, pp. 72-80.
- [35] K. Fukui, Y. Teijiro, S. Haruo, J Chem. Phys., 20 (1952) 722-725.

- [36] R.G. Parr, W. Yang, DFT approach to the frontier-electron theory of chemical reactivity, J. Am. Chem. Soc., 106 (1984) 4049 4050.
- [37] R.G. Parr, L.V. Szentpaly, S. Liu, Electrophilicity index. J Am. Chem.Soc.1999;121(9):1922-1924.
- [38] K.B. Benzon, M.Y. Sheenaa, C. Yohannan Panicker, S. Armakovic, S.J. Armakovic, K. Pradhan, A. Nanda, C. Van Alsenoy, J. Mol. Struc., 1130 (2017) 644-658.
- [39] K. Chandrasekaran, R. Thilak Kumar, J. Chem. Pharm. Res., 8 (2016) 849-861.
- [40] O. Trott, A.J. Olson, J. Comput. Chem., 31 (2010) 455-461.
- [41] Morris G M, Huey R, Olson A J., Using AutoDock for ligand-receptor docking, Curr. Protoc. Bioinf. 24 (8.14) (2008) 1-40.

CHAPTER II

SPECTROSCOPIC, QUANTUM MECHANICAL INVESTIGATION AND MOLECULAR DOCKING STUDY OF 2-AMINO-5-CHLORO3-NITROPYRIDINE

2.1 INTRODUCTION

Pyridine is a basic heterocyclic compound with the chemical formula C₅H₅N. Pyridine derivatives are very important chemicals with remarkable biological applications.[1]. It plays a key role in catalyzing both biological and chemical systems. Pyridine forms the nucleus over 7000 existing drugs in pharmaceutical industries. Many synthetic methods have been developed for the construction of the pyridine ring and for its substitution [2] due to its applications in many pharmaceutical, agrochemical and research fields. Researches carried out on nitropyridine and its derivatives show antimicrobial, anti-fungal, anti-bacterial, pesticide, anti-allergic, antihypertensive, antitumour, antagonist or analgesic properties[3-5].2-Amino-5-chloro-3-nitropyridine (2A5C3NP) with molecular formula C₅H₄ClN₃O₂ has a molecular weight of 173.56g/mol. Direct nitration of 2-amino-5-chloropyridine gave 2-amino-5-chloro-3-nitropyridine which was reduced and further made to undergo chemical reactions to yield various heterocyclic compounds which plays a vital role in pharmaceutical industry.

Many problems in different areas of research could be solved by combined studies of theoretical and experimental work [6,7]. Density functional investigations and spectroscopic analysis of the title compound were carried out. Molecular docking studies was conducted to study the antagonist activity of the title compound.

Geometrical structure, spectral analysis along with molecular electrostatic potential surfaces may lead to the better understanding of structural and spectral characteristics of the compound. The FT -IR and FT- Raman spectra of 2-Amino-5-chloro-3-nitropyridine have been recorded.

The DFT investigation helps in revealing molecular electronic structure. Vibrational spectral analyses have been done on the basis of Potential Energy Distribution (PED). The HOMO-LUMO investigations have been performed to find the bio-active property of the molecule. As NLO materials has remarkable applications in optoelectronic technology that includes optical computing and communications [8-11], attention has been paid in the present study. Fukui function, molecular electrostatic potential and NBO studies have been performed with GUASSIAN'09 software [12]. Therefore, the present study provides a complete vibrational and electronic analysis under both theoretical and experimental background.

2.2 RESULTS AND DISCUSSION

2.2.1 Molecular Geometry

The optimized molecular structure of the title compound with the numbering scheme of the atoms is shown in Fig 2.1. The parameters like bond lengths and bond angles were obtained from Gaussian 09 W. This molecule has four C-C bonds, four C-N bonds, two C-H bonds, one C-Cl bond, two N-O bond and two N-H bonds. The crystal data of a closely related molecule [13] is compared with that of the title molecule. The theoretical values variation when compared to the experimental values is because isolated molecule in the gaseous phase is considered in theoretical calculations and the experimental results belong to the molecule in the solid state.

The average bond distance of C-C and C-N as calculated by DFT method using B3LYP/6-311++G(d,p) basis sets are 1.39975Å and 1.368Å respectively. All bonds are single except N7 - O8 which has a double bond. The C-C bonds had a range of 1.378 - 1.424Å. The carbon atoms are bonded to hydrogen atoms with σ bond in the benzene ring. The bond length of C-Cl shows a comparatively higher value (1.75Å). This is due to the repulsion between the electron of the carbon atom in the ring and lone pair of electrons on the chlorine atom. The maximum bond angle was observed at O8-N7-O9 (123.5°). This is attributed to the fact that the nitrogen atom present at the centre is less electronegative and smaller when compared to the electronegative oxygen. The repulsive forces arising due to the lesser distance between the two oxygen atoms lead to increment in the angle in order to decrease the repulsion. The bond angles and bond length of the title compound are presented in Table 2.1.

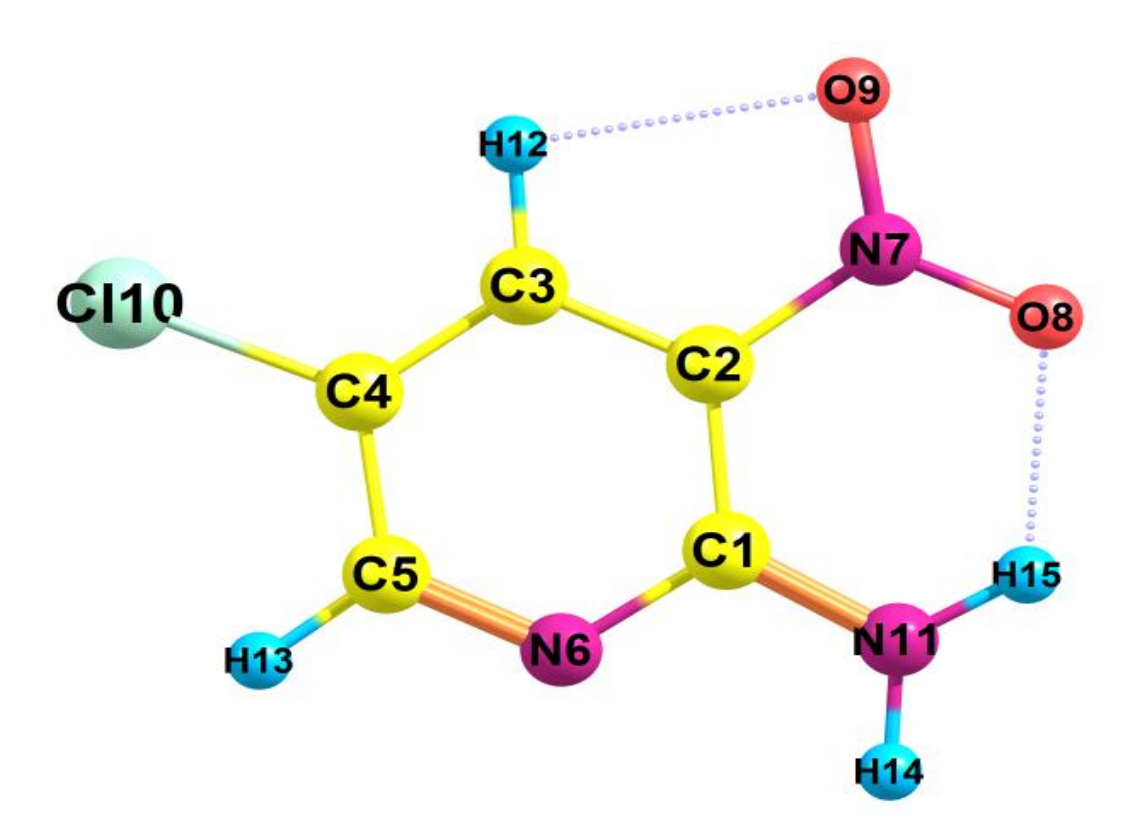


Fig 2.1 Optimised geometric structure with atom numbering of 2-Amino-5-chloro-3-nitropyridine.

Table 2.1 Geometrical parameters of 2-Amino-5-chloro-3-nitropyridine: bond length(\mathring{A}) and bond angle (0).

PARAMETER	B3LYP/6311++G(d,p)	Experimental	PARAMETER	B3LYP/6-311++G(d,p)	PARAMETER	B3LYP/6311++G(d,p)	
BOND LENGT	H(Å)		BOND ANGLE	E(0)	BOND ANGLE (⁰)		
C1-C2	1.424	1.423	C2-C1-N6	119.6	C5-C4-C110	120.1	
C1-N6	1.352	1.344	C2-C1-N11	124.8	C4-C5-N6	123.3	
C1-N11	1.346	1.355	C1-C2-C3	119.8	C4-C5-H13	120	
C2-C3	1.396	1.381	C1-C2-N7	122.7	N6-C5-H13	116.7	
C2-N7	1.454		N6-C1-N11	115.6	O8-N7-O9	123.5	
C3-C4	1.378	1.375	C1-N6-C5	120.1	N7-O8-H15	110.9	
C3-H12	1.081	1.084	C1-N11-H14	117.3	N7-O9-H12	88.6	
C4-C5	1.401	1.375	C1-N11-H15	120.3	H14-N11-H15	122.4	
C4-C110	1.75		C3-C2-N7	117.5	N11-H15-O8	123.2	
C5-N6	1.32	1.316	C2-C3-C4	118.7			
C5-H13	1.086	1.084	C2-C3-H12	119			
N7-O8	1.238	1.236	C2-N7-O8	118.1			
N7-O9	1.225	1.011	C2-N7-O9	118.4			
N11-H14	1.007	1.009	C4-C3-H12	122.2			
N11-H15	1.008		C3-C4-C5	118.5			
O8-H15	1.97		C3-C4-C110	121.4			
O9-H12	2.34		C3-H12-O9	96.5			

2.2.2 Vibrational Spectral Analysis

The non-linear molecule contains N number of atoms has a maximum number of potentially active observable fundamentals is equal to (3N-6) excluding the translational and three rotational degrees of freedom. The title compound consists of 15 atoms, which has 39 normal modes of vibration. In order to check whether the chosen set of vibrational frequencies contribute the maximum to the potential energy associated with the normal coordinates of the molecule, the potential energy distribution has been evaluated. The comparative observed and simulated FT-IR and FT-Raman spectra are shown in Figs.2.2 and 2.3. The resultant scaled frequencies, measured infrared and Raman band positions and PED are presented in Table 2.2.

N-H vibrations

The N-H stretching vibrations arise in the region 3450 – 3250cm⁻¹ for primary amines and in region 3400 – 3000cm⁻¹ for secondary amines. The frequencies of the amino group appear at 3500-3300 cm⁻¹ for N-H stretching,1700 -1600 cm⁻¹ for scissoring and 1150-900 cm⁻¹ for rocking deformations [14]. In the present study the N-H stretching vibrations have shifted to higher region clearly indicating that this stretching depends on protonation. The experimental N-H vibration for the title compound is observed at 3466cm⁻¹ in FT-IR spectrum with a PED contribution of 99%.

C-H vibrations

The aromatic compounds have C-H stretching vibration in the region 3100 – 3000cm⁻¹ which is the characteristic region for the identification of C-H stretching vibrations [15]. The C-H stretching modes of vibration usually appear in the strong Raman intensity regions and are highly polarised. The C-H stretching vibration in the title molecule were observed at 3075cm⁻¹ and 3045cm⁻¹ in FT-Raman spectrum. The peak corresponding to C-H stretching vibration is observed in the range 3102 and 3045cm⁻¹ by B3LYP/6-311++G(d,p) method shows good results with the recorded FT-Raman spectral values.

C-C vibrations

The C-C vibrations are observed within the region 1650-1200 cm⁻¹[16-18]. In the present study, the bands were identified at 1594,1511,1452,1392,1223,1140cm⁻¹ in FT-IR spectrum and at 1563,1457,1261,1228,1133 cm⁻¹ at FT-Raman spectrum. Theoretically, the calculated values of C-C stretching vibrations are observed between 1592 and 637cm⁻¹. It shows that the theoretical values are in good agreement with the experimental values obtained.

C-N vibrations

The C-N stretching frequency is observed in a composite region where mixing of several bands of the vibrational spectrum are possible [19]. The vibration corresponding to this stretching is in the range 1386 - 1266 cm⁻¹region for an aromatic compound. The band observed at 1337cm⁻¹ in FT-IR and 1330 cm⁻¹ in FT-Raman are assigned as CN stretching vibrations. The theoretically scaled wavenumbers are calculated at 1592 cm⁻¹ to 361cm⁻¹ with a maximum PED contribution of 41%.

N-O vibrations

In nitro compounds the NO_2 stretching vibrations are responsible for the most characteristic bands, which are the two most important group wavenumbers, not only because of the spectral position but also for the strong intensity [20]. In nitro compounds the anti-symmetric NO_2 stretching vibrations are observed in the region $1551 \pm 70 \text{ cm}^{-1}$. The symmetric NO_2 stretching vibrations are located in the region $1380 \pm 20 \text{ cm}^{-1}$. In the present study bands are observed at 1511,1452 and 1223cm^{-1} in the FT-IR spectrum and at 1457and 1261cm^{-1} in the FT-Raman spectrum. The theoretical values were obtained at $1527,1488,1302,124 \text{ cm}^{-1}$ which has good agreement with the experimental data having a maximum PED contribution of 37%.

C -Cl vibrations

The C-Cl stretching vibrations of most aromatic chloro compounds occur in the region 850 – 550 cm⁻¹[21]. For the title compound the C-Cl stretching vibrations is assigned at 707 and 637cm⁻¹in B3LYP/6-311++G(d,p) method. Experimentally the peak is observed at 615cm⁻¹in FT-IR spectrum. Owing to longer bond length, C-Cl stretching lies in the lower frequency region.

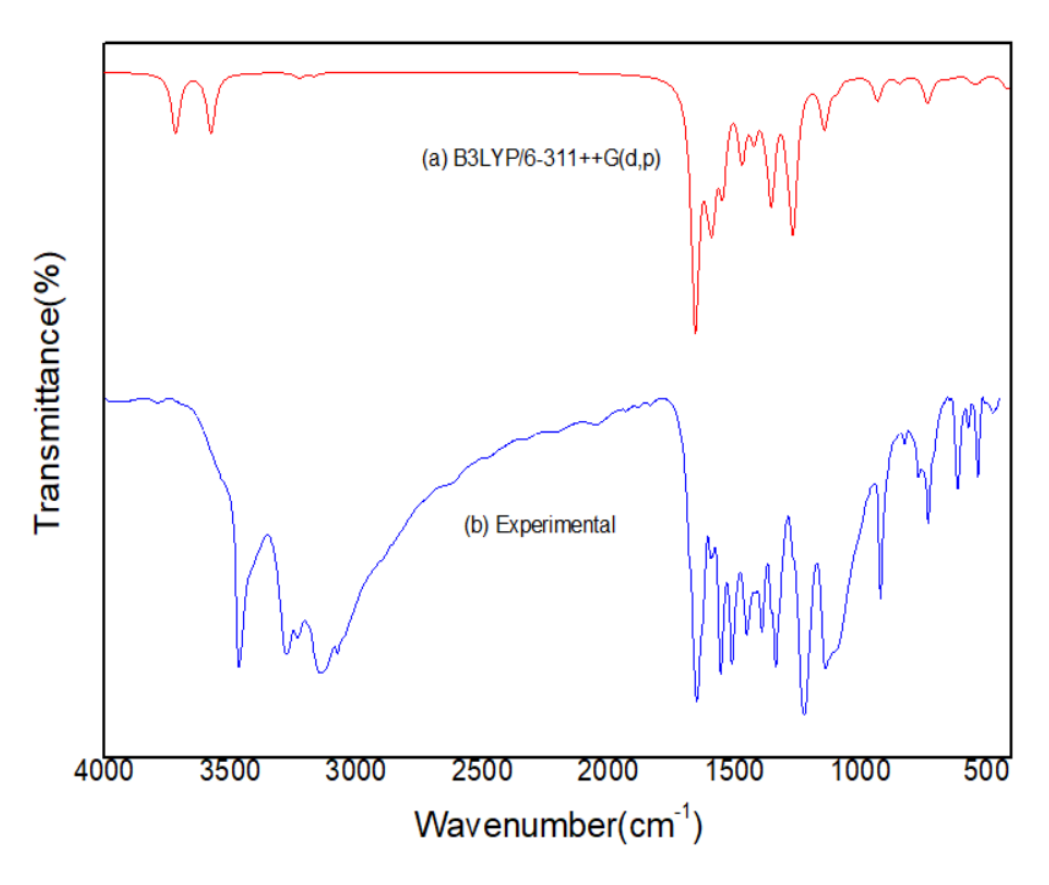


Fig 2.2 Compared theoretical and Experimental FT-IR spectrum of 2A5C3NP.

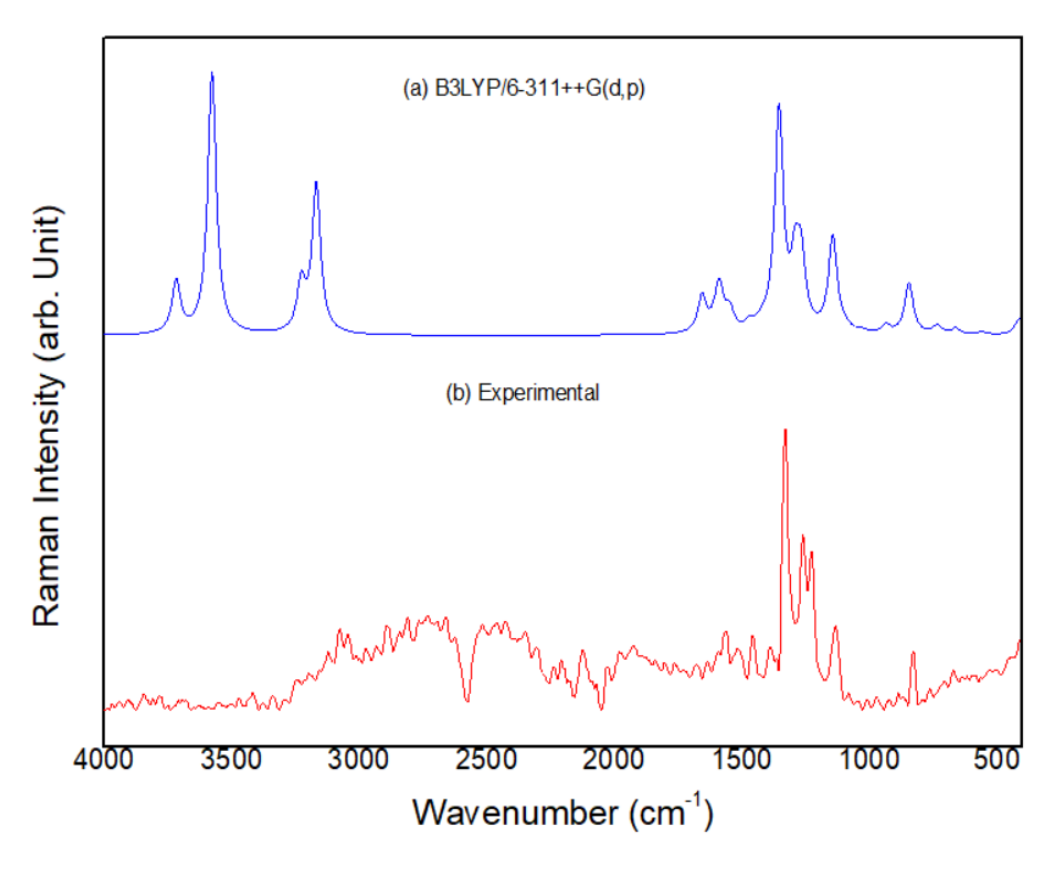


Fig 2.3 Compared theoretical and Experimental FT-Raman spectrum of 2A5C3NP

Table 2.2 Observed and calculated vibrational frequency of 2A5C3NP.

S. No.	_	rimental ency(cm ⁻¹)	Theore Frequence		IR Int	ensity	Raman	Intensity	A spirmm and (DED)
	FT -IR	FT - RAMAN	Unscaled	Scaled	Relative	Absolute	Relative	Absolute	Assignment (PED)
1			3718	3573	107	25	39	20	YNH (99)
2	3466		3577	3438	107	25	198	100	YNH (99)
3	3142	3075	3227	3102	10	2	37	19	YCH (99)
4	3076	3045	3169	3045	6	1	112	57	YCH (100)
5	1594	1563	1656	1592	428	100	28	14	ΥCC (20) + ΥNC (13) + βCNC (10)
6	1555		1609	1546	81	19	4	2	βHNC (53)
7	1511		1589	1527	177	41	35	18	$\Upsilon CC (13) + \Upsilon ON(15)$
8	1452	1457	1548	1488	157	37	15	8	$YON (32) + YCC(18) + \beta HCN(10)$
9			1471	1414	122	29	6	3	ΥON(19) + ΥNC(14) + βHNH(20) + βHCN(19)
10	1392		1424	1369	76	18	5	2	$\Upsilon NC(25) + \Upsilon CC(29) + \beta HCC(12)$
11	1337	1330	1380	1326	31	7	2	1	$YNC(41) + \beta HCN(33)$
12			1355	1302	194	45	166	84	Υ ON(37) + Υ CC(12)+ β HNC(10)
13	1223	1261	1291	1241	52	12	46	23	YCC(10)+ YON(15)+ YNC (12)+ βHCN(21)
14		1228	1268	1219	249	58	49	25	$\Upsilon CC(23) + \beta HCC(20)$
15	1140	1133	1144	1100	88	20	72	36	$\Upsilon CC(37) + \Upsilon NC(10) + \Upsilon ClC(10)$
16			1096	1053	19	4	3	2	ΥNC(16) + βHCC(21)+βNCC(11)+βCCC(24)
17			1032	992	2	0	2	1	ΥNC(29) + βHNC(40)
18	921		970	932	0	0	0	0	τ HCCN(28) + τ HCNC(61)
19			935	899	29	7	6	3	YNC(12) + YClC (10)+βCNC(15)+ βONO(10)+ βCCC(14)
20	826		931	895	18	4	0	0	τHCCN(56)+ τHCNC(15)

S.	Experi frequen		Theore Frequenc		IR Int	ensity	Raman I	ntensity	Aggigmment (DED)
No.	FT -IR	FT - RAMAN	Unscaled	Scaled	Relative	Absolute	Relative	Absolute	- Assignment (PED)
21	771		846	813	13	3	39	19	βONO(38)+ βCCC(14)
22	732		736	708	8	2	0	0	YCNCC(23)+ωNCNC(53)
23			735	707	41	9	6	3	YCIC (16)+βNCC(17)+ βONO(20)+ βONC(10)
24			717	689	5	1	0	0	OUT OCON(85)
25	615		663	637	5	1	5	2	$\Upsilon CC(18) + \Upsilon CIC (16) + \beta NCC(21) + \beta CCC(11) + \beta NCN(16)$
26	573		634	610	4	1	0	0	τHNCC(79)
27	535		560	538	10	2	2	1	βONC(27)+ βNCN(18)
28	475		536	515	13	3	0	0	τHCNC(14)+ τCCCC(18) + τCNCC(13)+OUTClCCC(15)+OUT NCNC(21)
29		410	423	407	13	3	0	0	τ CCCC(19) + τ CNCC(33)+OUT NCCC(27)
30		379	415	399	5	1	8	4	βCNC(25)+ βONC(21)+ βNCN(24)
31			399	383	1	0	3	2	YNC(23)+ βCCC(30)+ βNCN(10)
32			376	361	3	1	11	6	YNC(10)+ YCIC (40)
33			331	318	125	29	0	0	τHNCC(60)+OUT ClCCC(20)
34			327	315	3	1	0	0	βONC(10)+ βNCC(43)+ βCICC(24)
35		305	321	308	71	17	0	0	τHNCC(43)+OUT ClCCC(28)
36		189	187	180	2	0	3	1	βNCC(27)+ βCICC(48)
37			150		0	0	0	0	τCCCC(11)+OUT CICCC(29)+OUT NCCC(42)
38		100	105	100	0	0	1	0	τCCCN(58)+τCCCC(20)+
39		80	61	59	1	0	1	0	τONCC(85)

Υ-stretching, β- in plane bending, ω – out plane bending, τ – torsion.

2.2.3 Natural bond orbital

The inter and intramolecular interactions within the molecules can be obtained from natural bond orbital analysis [22,23]. The interaction leads to the donation of occupancy from the localized orbitals of the idealized Lewis structure into the empty non-Lewis orbitals. NBO analysis is a highly effective tool for chemical interpretation of hyper conjugative interaction and electron density from filled lone electron pairs of Lewis base into the unfilled anti-bond of Lewis acid. For each donor (i) and acceptor(j), the stabilization energy E(2) associated with the delocalization $i \rightarrow j$ is obtained as

$$E(2) = \Delta E_{ij} = q_i (F_{ij})^2 / (\varepsilon_i - \varepsilon_i)$$
 -----(1)

where q_i is the donor orbital occupancy, ϵ_j and ϵ_i are diagonal elements, F_{ij} is the off-diagonal NBO Fock matrix element [24,25]. The possible donor – acceptor pairs, the donor acceptor stabilization energy value calculated using the above relation (1) are tabulated in Table 2.3. The delocalization of electron from $\sigma(C1\text{-}C2)$ distribute to antibonding $\sigma^*(C1\text{-}N6)$ and $\pi^*(N7\text{-}O8)$ lead to the stabilization energy of 1.07 kcal/mol and 0.55kcal/mol respectively due to conjugate interactions. The delocalization of electron from $\pi(C1\text{-}N6)$ distribute to antibonding $\pi^*(C2\text{-}C3)$ and $\sigma^*(N11\text{-}H14)$ lead to the stabilization energy of 12.23kcal/mol and 1.42kcal/mol respectively. It has been observed that a strong interaction due to electron density transfer occur from the lone pair LP(3) of Oxygen atom(O9) to the antibonding acceptor $\pi^*(N7\text{-}O8)$ with a large stabilization energy of 94.59kcal/mol.

Table 2.3 Second order perturbation theory analysis of Fock matrix in NBO of 2A5C3NP

Donor	Type	ED/e	Acceptor	Type	ED/e	E(2)kcal/mol	E(j)-E(i) a.u.	F(i,j)a.u.
C 1-C 2	σ	1.97701	C 1-N 6	σ^*	0.0319	1.07	1.22	0.032
			N 7-O 8	π*	0.51648	0.55	0.65	0.019
C 1-N 6	σ	1.98287	C 1-C 2	σ*	0.04301	1.75	1.33	0.043
C 1-N 6	π	1.71248	C 2-C 3	π*	0.32569	12.23	0.3	0.055
			N 11 - H 14	σ*	0.00683	1.42	0.69	0.03
C 1-N 11	σ	1.9902	C 1-C 2	σ*	0.04301	0.69	1.26	0.027
C 2-C 3	σ	1.97044	C 1-C 2	σ*	0.04301	3.4	1.23	0.058
C 2-C 3	π	1.68322	N 7-O 8	π*	0.51648	13.42	0.2	0.048
			N 7-O 9	σ*	0.09158	1.48	0.58	0.028
C 2-N 7	σ	1.98702	C 1-N 6	σ*	0.0319	1.76	1.29	0.043
C 3-C 4	σ	1.97523	C 2-C 3	σ*	0.01838	1.92	1.22	0.043
C 3-H 12	σ	1.97916	C 1-C 2	σ*	0.04301	3.74	1.04	0.056
C 4-C 5	σ	1.98229	C 3-C 4	σ*	0.03237	3.82	1.29	0.063
C 4-C 5	π	1.67854	C 1-N 6	π*	0.38301	11.62	0.29	0.052
C 4-Cl 10	σ	1.98799	C 2-C 3	σ*	0.01838	1.52	1.25	0.039
C 5-N 6	σ	1.97501	C 1-N 6	σ*	0.0319	0.66	1.3	0.026
C 5-H 13	σ	1.97473	C 1 - N 6	σ*	0.0319	4.37	0.99	0.059
N 7-O 8	σ	1.99611	C 2 - N 7	σ*	0.11148	1.16	1.5	0.038
N 7-O 8	π	1.99111	C 2-C 3	π*	0.32569	2.08	0.5	0.031
N 7-O 9	σ	1.99398	C 1 - C 2	σ*	0.04301	0.53	1.44	0.025
N 11 - H 14	σ	1.98559	C 1 - C 2	σ* π*	0.04301	1.49	1.13	0.037
N 11 - H 15		1.95449	C 1-N 6	σ*	0.38301 0.0319	2.32 1.63	0.62 1.12	0.037 0.038
N 11 - 11 13	σ	1.73447		π*	0.38301			
N 6	I D (1)	1.90985		σ*	0.04301		0.62 0.88	0.038
						8.76		0.079
0 8	` ′	1.97869	C 2-N 7	σ*	0.11148		1.02	0.062
0 8	, ,	1.84602	C 2-N 7	σ*	0.11148		0.55	0.097
0 9	` '	1.98561	C 2-N 7	σ*	0.11148		1.06	0.053
0 9		1.93072	C 2-N 7	σ*	0.11148		0.51	0.064
0 9	. ,	1.51782	N 7-O 8	π*	0.51648		0.16	0.112
		1.99169		σ*	0.03237		1.44	0.047
Cl 10	LP (2)	1.9629	C 3-C 4	σ^*	0.03237	5.6	0.83	0.061
Cl 10	LP (3)	1.92022	C 4-C 5	π*	0.32149	14.17	0.34	0.066
N 11	LP (1)	1.89697	C 1-C 2	σ^*	0.04301	5.6	0.74	0.058
			C 1-N 6	π^*	0.38301	9.56	0.22	0.044
C 1-N 6	π*	0.38301	C 4-C 5	π*	0.32149	87.58	0.03	0.077
			N 11 - H 15	σ*	0.00675	1.21	0.39	0.044
C 2-C 3	π*	0.32569	C 4-C 5	π*	0.32149	95.56	0.02	0.076
			N 7-O 9	σ*	0.09158	0.71	0.3	0.029
C 2-N 7	σ*	0.11148		σ*	0.0319	1.58	0.24	0.065
N 7-O 8	π*	0.51648		σ*	0.04301		0.59	0.03
		1.2 20 .0	C 2-C 3	π*	0.32569		0.08	0.045
					0.02007	15.11	0.00	0.015

2.2.4 Electronic properties

The concept of HOMO and LUMO plays an important role in understanding the chemical stability and reactivity of a given molecule. The HOMO is outermost electron containing orbital that give away these electrons as electron donor whereas the LUMO is outermost orbital having free sites to accept electrons [26,27]. From the HOMO and LUMO orbitals of a compound, information regarding the electron density and thereby the active participation of the molecule in energy transfer event can be determined. The HOMO and LUMO energies, electron affinity, ionisation potential, electronegativity, global hardness and the softness of the title molecule have been computed at B3LYP/6-311++G(d,p) basis set and the resulted is presented in Table 2.4. The pictorial representation of HOMO and LUMO for the title compound is shown in Fig.2.4. The title compound has a softness value = 0.269086. This when compared with the softness value of a related compound which has got a softness value of 0.239[28] reveals that pyridine derivatives have high degree of chemical reactivity. Higher hardness and lower softness values confirm the higher molecular hardness associated with the molecule. The calculated electrophilicity index (6.905495) describes the biological activity. The value of energy band gap is 3.716288 eV.

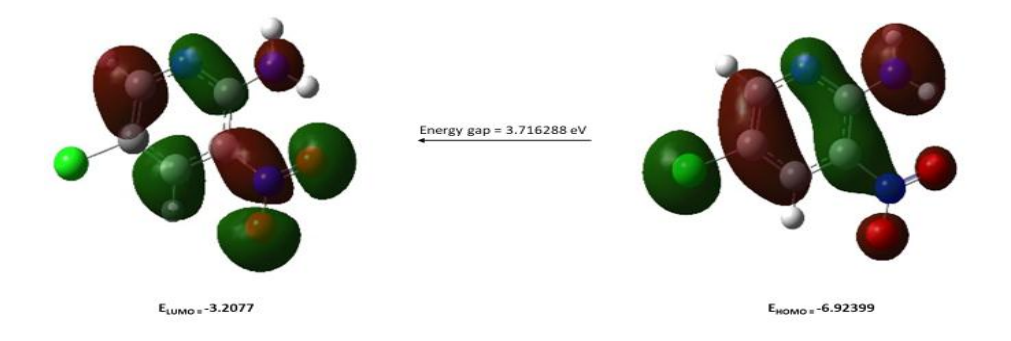


Fig 2.4 Atomic orbital HOMO - LUMO composition of the frontier molecular orbital of 2A5C3NP

Table 2.4 Calculated energy values of 2-Amino-5-chloro-3-nitropyridine

HOMO(eV)	-6.92399
LUMO(eV)	-3.2077
Ionization potential	6.923992
Electron affinity	3.207703
Energy gap(eV)	3.716288
Electronegativity	5.065848
Chemical potential	-5.06585
Chemical hardness	1.858144
Chemical softness	0.269086
Electrophilicity index	6.905495

2.2.5 Molecular Electrostatic Potential (MEP)

The molecular electrostatic potential is the potential energy of a proton at a particular location near a molecule. These maps allow us to visualize variably charged regions of a molecule. Electrostatic potential correlates with dipole moment, electronegativity and partial charges. MEP was obtained at the B3LYP/6-311++G(d,p) optimized geometry using Argus Lab software. Negative electrostatic potential corresponds to the attraction of proton by concentrated electron density in the molecule (red) and positive electrostatic potential corresponds to the repulsion of a proton by atomic nuclei in the regions of low electron density (blue). The oxygen atoms are electrophilic, while hydrogen atoms constitute the nucleophilic centers. Fig 2.5 gives colour code ranging from -5.547e V to 5.547eV.

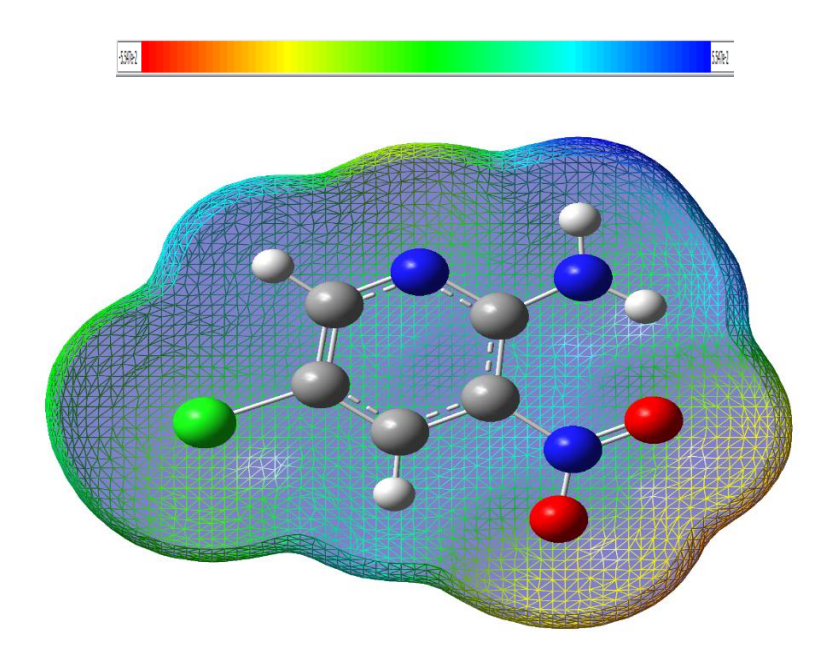


Fig 2.5 Molecular Electrostatic Potential of 2-Amino-5-chloro-3-nitropyridine.

2.2.6 Hyperpolarizability

Study of NLO effects in recent days are of most important since many optical properties which act as key functions for the developing technologies in the fields such as telecommunication, signal processing, optical interconnections can be analysed [29,30]. The NLO activities of the title compound were obtained by using the Gaussian software with the same basis set as used earlier. Urea is used as a reference for the characterization of organic NLO materials. The calculated values of dipole moment and hyperpolarizability for the title compound are tabulated in Table 2.5. The obtained value of hyperpolarizability of the title molecule is 6.5492×10^{-31} which is more than urea which shows that the title molecule is a potential for NLO properties [31]. The total dipole moment of the title compound $\mu(D)$ is 0.962037442 Debye.

Table 2.5 The calculated values of dipole moment, polarizability and the first order polarizability of 2-Amino-5-chloro-3-nitropyridine.

Parameter	B3LYP/6-311++G(d,p)	parameter	B3LYP/6-311++G(d,p)
Bxxx	-188.503	α_{xy}	19.413
Bxxy	7.040	$lpha_{ m yy}$	128.336
Bxyy	91.167	α_{xz}	2.498
Вууу	1.082	α_{yz}	-6.195
Bzxx	-1.233	α_{zz}	61.709
Bxyz	-0.215	α (a.u)	106.424
Bzyy	-0.008	α (e.s.u)	0.000
Bxzz	23.094	$\Delta\alpha$ (a.u)	233.662
Byzz	-19.053	$\Delta\alpha$ (e.s.u)	0.000
Bzzz	-9.502	μ_{x}	0.879
βtot (a.u)	75.807	μ_{y}	-0.274
βtot (e.s.u)	6.5491×10^{-31}	μ_{z}	0.281
$lpha_{xx}$	129.227	μ(D)	0.962

2.2.7 Mulliken atomic charges & Fukui functions

There are a number of methods for calculating the atomic charges from chemical wave functions [32]. Mulliken population is one of the widely used charge partitioning schemes. This distribution of charges reveals that all the hydrogen atoms present in the title compound are positively charged and the magnitude of atomic charges on carbon atoms were found to be both positive and negative ranging from 0.325889 to -0.70485. It is also clear from Fig 2.6 that the C3 atom possess the maximum atomic charge.

The chemical selectivity or reactivity at a particular site of a chemical system can be explained using electron density based local reactivity descriptors like Fukui functions [33]. Fukui functions are defined as the derivative of the density of electrons

with respect to the number of electrons at a constant potential. In other words, it is evident that Fukui function helps us to predict the most reactive sites for electrophilic and nucleophilic attack within a molecule. It is found that the Nitrogen (N) atoms are the most preferable site for protonation because of the intramolecular hydrogen bonding interaction between the N – H groups. It is clear from the Mulliken population analysis that N11 attached to the carbon atom acts as the most reactive sites during an electrophilic attack (-0.006771) and the atom C4 attached to the C110 acts as the most reactive sites during an nucleophilic attack because the atom C110 is more electronegative than carbon. Local softness of a system can determined using Fukui function. Local softness is measured as the product of condensed fukui function and global softness [34]. The results of the title compound are listed in Table 2.6. The largest descriptor value corresponding to the softness being maximum is found at the site C4 (0.020791).

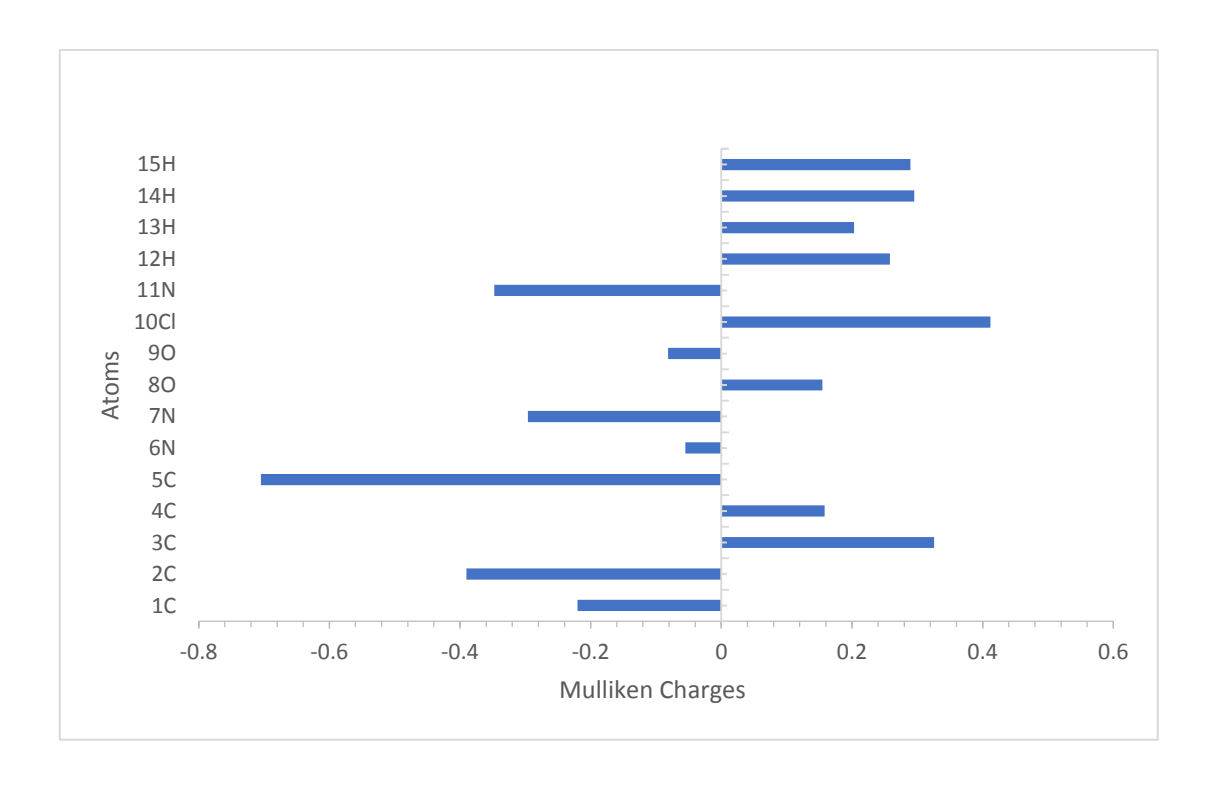


Fig 2.6 The histogram of calculated Mulliken Charges of 2A5C3NP.

Table 2.6 Mulliken charge distribution, Fukui function and local softness corresponding to (0,1), (-1,2) and (1,2) charge and multiplicity of 2A5C3NP.

Atom	Mu	lliken atomic cha	arges	F	ukui function	ıs	local softness			
Atom	0, 1 (N)	N+1 (-1, 2)	N -1 (1, 2)	f_r^+	f_r^-	f_r^{0}	$s_r^+ f_r^+$	$s_r^- f_r^-$	$s_r^0 f_r^0$	
1C	-0.22018	-0.249948	-0.245071	-0.029771	0.024894	-0.00244	-0.00801	0.006699	-0.00066	
2C	-0.39015	-0.456194	-0.341004	-0.066046	-0.04914	-0.0576	-0.01777	-0.013224	-0.0155	
3C	0.325889	0.23221	0.362286	-0.093679	-0.0364	-0.06504	-0.02521	-0.009794	-0.0175	
4C	0.15786	0.235126	0.148311	0.077266	0.009549	0.043408	0.020791	0.00257	0.01168	
5C	-0.70485	-0.769451	-0.714588	-0.064606	0.009743	-0.02743	-0.01738	0.002622	-0.00738	
6N	-0.05496	-0.127233	0.014965	-0.072273	-0.06993	-0.0711	-0.01945	-0.018816	-0.01913	
7N	-0.29628	-0.347483	-0.253362	-0.051205	-0.04292	-0.04706	-0.01378	-0.011548	-0.01266	
8O	0.154536	-0.003226	0.144058	-0.157762	0.010478	-0.07364	-0.04245	0.002819	-0.01982	
90	-0.08167	-0.259613	0.008962	-0.177942	-0.09063	-0.13429	-0.04788	-0.024388	-0.03613	
10Cl	0.411777	0.26916	0.635862	-0.142617	-0.22409	-0.18335	-0.03838	-0.060298	-0.04934	
11N	-0.34781	-0.354583	-0.06977	-0.006771	-0.27804	-0.14241	-0.00182	-0.074817	-0.03832	
12H	0.258146	0.194422	0.310015	-0.063724	-0.05187	-0.0578	-0.01715	-0.013957	-0.01555	
13H	0.203016	0.129447	0.26547	-0.073569	-0.06245	-0.06801	-0.0198	-0.016805	-0.0183	
14H	0.295412	0.251357	0.370606	-0.044055	-0.07519	-0.05962	-0.01185	-0.020234	-0.01604	
15H	0.289254	0.25601	0.363261	-0.033244	-0.07401	-0.05363	-0.00895	-0.019914	-0.01443	

2.2.8 Molecular docking

Molecular docking is used to investigate the binding orientation, affinity and activity of drug molecules and their protein targets. Auto dock suite 4.2.6 is helpful in obtaining the protein-ligand interactions. The structure of the targeted protein was downloaded from the RCSB in PDB format [35,36]. The title molecule was selected to be docked into the active site of the protein 3d6d which belongs to the property of antagonist. The docking parameters of binding energy, inhibition constant and intermolecular energy of the molecule with respect to the targeted protein is obtained and listed in Table 2.7. The affinity of ligand-protein complex can be measured using the binding energy and the energy between the non-bounded atoms is obtained as intermolecular energy. The binding orientation of the title compound with the targeted proteins are shown in Fig 2.7. In the interaction, the minimum binding energy of - 4.50 kcal/mol and the intermolecular energy of - 5.10 kcal/mol were observed for docking with 3d6d protein.

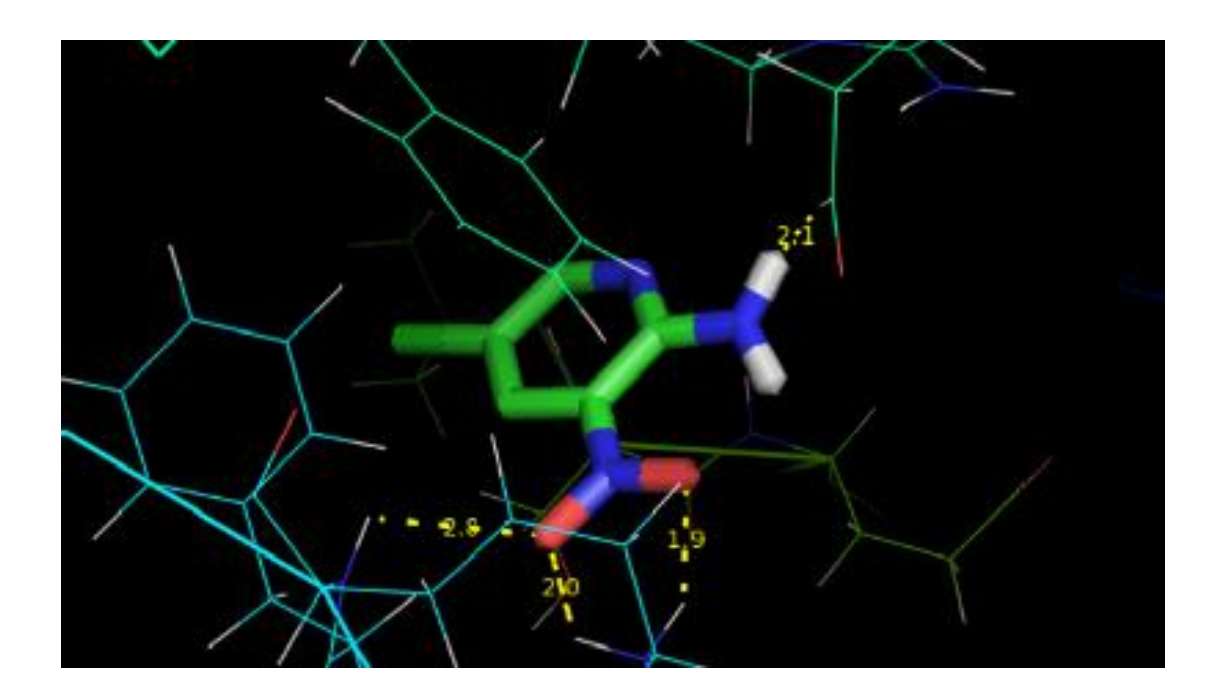


Fig 2.7 Docking and hydrogen bond interaction of 2A5C3NP with the protein 3d6d.

Table 2.7 Molecular docking parameters of 2A5C3NP with the protein 3d6d.

Protein	Bonded residues	Bond distance (Å)	Intermolecular Energy (Kcal/mol)	Inhibition Constant (µmol)	Binding Energy (Kcal/mol)	Reference RMSD (Å)
3d6d	LYS 265	2.0	-5.10	499.50	-4.50	64.41
	LYS 265	1.9				
	LYS 265	2.8				
	GLU291	2.1				

2.3 CONCLUSION

In the present work, the experimental and theoretical spectroscopic analyses of 2-Amino-5-chloro-3-nitropyridine using FT-IR, FT Raman and tools derived from the DFT has been obtained. The optimized parameters such as bond length and bond angles were theoretically determined by B3LYP/6-311++G(d,p) basis set. The vibrational FT-IR, FT Raman spectra of the title compound were recorded and computed vibrational wavenumbers of all the fundamental vibrational modes of the compound were obtained in this analysis and their PED is evaluated. The possible electrophilic and nucleophilic reactive sites of the molecule were predicted and the intramolecular interactions of the molecule were also analysed using NBO analysis. The band gap energy of HOMO – LUMO is 3.716288eV. MEP diagram of the title molecule shows the negative and positive region. The first order hyperpolarizability calculations reveals the possibility of the molecule to have non-linear optical properties. Molecular docking shows that the title compound acts as an antagonist with binding energy of - 4.50 kcal/mol and for phobic disorder treatment with binding energy of -4.64 kcal/mol.

REFERENCES

- [1] S. Sivaprakash, S. Prakash, S. Mohan, Sujin. P. Jose, Heliyon 5 (2019) 2405-8440.
- [2] A.McKillop,in: D.L. Commins, S.P. Joseph, G.Jones ,Comprehensive Heterocyclic Chemistry II, Vol.5, 1984 Pergamon,Oxford. A. McKillop,Pergamon,Oxford(1996).
- [3] M.T. Cocco, C. Congiu, V. Onnis, Synthesis and antitumour activity of 4-hydroxy-2-pyridone derivatives, Eur. J. Med. Chem. 35 (2000) 545–552.
- [4] J.S. Al-Otaibi, Experimental (FT-IR and FT-Raman spectra) and theoretical (Ab initio/HF, DFT/B3LYP) study of 2-Amino-5-Chloropyridine and 2-Amino-6-Chloropyridine, Chem. Mater. Res. 7 (2015) 1–13.
- [5] M.M. Krayushkin, I.P. Sedishev, V.N. Yarovenko, I.V. Zavarzin, S.K. Kotovskaya, D.N. Kozhevnikov, Synthesis of pyridines from 1,2,4-Triazines under highpressure, Rus. J. Org. Chem. 44 (2008) 407–411.
- [6] D.R.Kanis, M.A. Ratner, T.J.Marks, Chem. Rev. 94 (1994) 195-242.
- [7] H.S. Nalwa, S.Miyata, Nonlinear Optical Properties of Organic Molecules and Poly-mers, CRC Press, Boca Raton, FL, 1996.
- [8] Ping Wang, Qi Wang, Yonghong Yang, James K. Coward, Alexis Nzila, Paul F.G. Sims, John E. Hyde, Mol. Biochem. Parasitol. 172 (2010) 41-51.
- [9] http://www.yeastgenome.org/go/GO:0008841/overview.
- [10] M.Ibrahim, Spectrochim. Acta A 77 (2010) 1034-1038.
- [11] M.Ibrahim, A.Aziz Muhmouda, O.Osmana, A.Refaata, M. El-Sayed, Spectrochim. Acta A 77 (2010) 802-806.

- [12] M.J. Frisch, G.W. Trucks, H.B. Schlegel, G.E. Scuseria, M.A. Robb, J.R. G. Scalmani, V. В. Cheeseman, Barone, G.A. Petersson, H. Nakatsuji, M. Caricato, X. Li, H.P. Mennucci. A.F. Izmaylov, J. Bloino, G. J.L. Hratchian, Zheng, Sonnenberg, M. Toyota, K. Vreven, T. Montgomery, J.A. Hada M. Ehara. Perlta, J.E. Ogliaro, F. Bearpark, M. Heyd, J.J. Brothers, E. Kudin, K.N. Staroverov, V.N. Kobayashi, R. Normand, J. Raghavachari, K. Rendell, A. Burant, J.C. Iyengar, S.S. Tomasi, J. Cossi, M. Rega, N. Millam, J.M. Klene, M. Knox, J.E. Cross, J.B. Bakken, V. Adamo, C. Jaramillo, J. Gomperts, R. Stratmann, R.E. Yazyev, O. Austin, A.J. Cammi, R. Pomelli, C. Ochterski, J.W. Martin, R.J. Morokuma, Zakrzewski, V.G. Voth, G.A. Salvador, P. Dannenberg, J.J. Dapprich, S. Daniels, A.D. Farkas, O. Foresman, J.B. Ortiz, J.V. Ciolslowski, J. Fox, D J, Gaussian 09, Revision E.01, Gaussian, Inc, Wall-ingford CT, 2009.
- [13] C.B. Aakeroey, A.M. Beatty, M. Nievwenhuyzen, M. Zou, J. Mater. Chem. 8 (1988) 1385.
- [14] G. Socrates, Infrared and Raman Characteristics Group Frequencies, Tables and Charts, third ed. Wiley, Chichester, 2001.
- [15] G. Varsanyi, Assignment for Vibrational Spectra of Seven Hundred Benzene Derivatives, Academic Kiaclo, Budapest,1-2,(1973).
- [16] M. Karabacak, C. Karaca, A. Atac, M.Eskici, A. Karanfil Spectrochim. Acta A 97 (2012)556-567.
- [17] C.Surisseau, P. Marvell, J. Raman Spectrosc. 25 (1994) 447-455.
- [18] A.J. Barnes, M.A. Majid, M.A. Stuckey, P. Gregory, C.V. Stead, Spectrochim. Acta A (1985) 629-635.
- [19] M.Silverstein, G.C.Basseler, C. Morill. Spectrometric Identification of Organic compounds, Wiley. New York. 1981.
- [20] N.P.G. Roeges, A Guide to the Complete Interpretation of Infrared Spectra of Organic Structures, Wiley, New York, 1994.

- [21] G. Varsanyi, Assignments for Vibrational Spectra of Seven Hundred Benzene Derivatives, Vol. 1, Adam Hilger, London, 1974.
- [22] F. Weinhold, C.R. Landis, Valency and Bonding: a Natural Bond Orbital Donor-acceptor Perspective, Cambridge University Press, C2mbridge, 2005.
- [23] I. Sidir, Y.G. Sidir. M. Kumalar, E. Tasal. J. Mol.Struct. 964 (2010) 134-151.
- [24] J. Jayabharathi. V. Thanikachalam, K. Jayamoorthy, M.V. Perumal, Spectrochim. Acta Mol. Biomol. Spectrosc. 97(2012) 131-136.
- [25] N.R. Rajagopalan, P. Krishnamoorthy, K. Jayamoorthy. M. Austeria, Karbala Inter.J. Mod. Sci. 2 (2016) 219-225.
- [26] N. Subramanian, N. Sundaraganesan, J. Jayabharathi, Spectrochim. Acta A 76 (2010) 259-269.
- [27] S. Muthu, S. Renuga, Spectrochim. Acta 132 (2014) 313-325.
- [28] Christina Susan Abraham, Johanan Christian Prasana, S. Muthu, Spectrochimica Acta Part A: Molecular and Biomolecular Spectroscopy 181 (2017) 153–163.
- [29] Y.X. Sun, Q.L. Hao, W.X. Wei, Z.X. Yu, D.D. Lu, X. Wang, Y.S. Wang, J. Mol. Struct. Theochem. 904 (2009) 74-82.
- [30] M. Nakano, H. Fujita. M. Takcathata, K. Yamaguchi, J. Am. Chem. Soc. 124 (2002) 9648-9655.
- [31] Christina Susan Abraham, Johanan Christian Prasana, S. Muthu, B. Fathima Rizwana, M. Raja, J. Mol. Struct. 1160 (2018) 393-405.
- [32] K. Jug. Z.B. Maksic, in: Z.B. Maksic, Theoretical Model of Chemical Bonding. Springer, Berlin, 3, 1991,9-233.
- [33] W. Yang, R.G. Parr, Proc. Natl. Acad. Sci. U. S. A. 82 (1985) 6723-6726.
- [34] Jacob George, Johanan Christian Prasana, S.Muthu. Tintu K. Kuruvilla. Int. J. Mater. Sci. 12 (2017) 302-320.

- [35] T.Joselin Beaula. I. Hubert Joe. V.K. Rastogi, V. Bena Jothy. Che.Phy. Lett.624 (2015) 93-101.
- [36] H.M. Berman, J.Westbrook, Z. Feng, G. Gilliland, T.N. Bhat, H. Weissig, I.N. Shindyalov, P.E. Bourne, The protein data, Nucleic Acids Res. 28 (2000) 235-242.

CHAPTER III

SPECTROSCOPIC (FT-IR, FT-RAMAN, UV-VISIBLE), QUANTUM MECHANICAL BASED COMPUTATIONAL STUDIES AND MOLECULAR DOCKING ANALYSIS OF 2-AMINO-3,5DICHLOROPYRIDINE

3.1 INTRODUCTION

Pyridine derivatives are a complex group of heterocyclic-containing compounds with a wide range of therapeutic applications, making them attractive targets for pharmacological and industrial applications [1,2]. Because of the numerous pharmaceutical research activities associated with the presence of 2-aminopyridines in targeted molecules, they have got a lot of attention. Researchers discovered that the presence of a small molecule of 2-aminopyridine increases the therapeutic properties of the target molecule, regardless of whether it is a simple molecule with just a few groups or a complex one with more heterocycles. In the field of biology, they show a lot of potential owing to their noteworthy antitumoral, antidiabetic, antimicrobial, analgesic, anti-inflammatory properties. They have also been reported as glucokinase activators or selective inhibitors of neuronal nitric oxide synthase [3]. One of the essential industrial chemicals and most important primary ingredients in medications to treat a variety of diseases is chlorine, such as respiratory, nervous system problems, etc whose insertion into one or more unique positions of a biologically dynamic molecule has also been found to greatly increase the essential biological activity. Taking into account the various high-tech purposes of pyridine and its derivatives, an attempt has been developed to conduct a quantum mechanical analysis of the heading compound.

Computational methods have evidenced to be a vital tool for rendering and envisaging the spectra of vibration. The DFT computational approach is commonly used to characterise the quantum states of multi molecule electron systems [4]. Docking studies are employed at several stages in the drug development process, including predicting the docked structure of a ligand–receptor complex and ranking ligand compounds based on their binding energy [5]. The title compound, 2ADCP having the chemical formula $C_5H_4Cl_2N_2$ has a molecular weight of 163.01 with boiling point of 235.2°C at 760mm of Hg is a derivative of pyridine and to our finest familiarity, this compound has not been subjected to any quantum chemical research.

The current research deals with wide-ranging examination on molecular geometry of the enhanced molecule, infrared, Raman scattering activities and harmonic frequencies of vibration of the heading compound. The B3LYP method has been used in the execution of the aforesaid, with 6–311++G(d,p) source set. Various molecular characteristics have been calculated and stated, which includes MEP, ELF, HOMO, LUMO and Fukui functions. The NBO study has been beneficial to understand the constancy of the molecule as a result of delocalization of charges. Time dependant DFT with IEFPCM solvation models in water, DMSO, benzene solutions were used to explore the UV – Visible spectrum. To comprehend the molecule's biological activity, docking studies along with drug likeness, ADMET, toxicity, molinspiration and environmental toxicity have been reported. As a significance, the current work offers a comprehensive description of the caption compound's spectroscopic and computational analyses.

3.2 RESULTS AND DISCUSSION

3.2.1 Geometrical parameters

Fig.3.1 displays the optimised structure of the title molecule, along with the atom numbering scheme. The optimized structure parameters (bond lengths & bond angles) were procured and tabulated in Table 3.1. Four C - C bonds, three C - N bonds, two N - H bonds, two C - H bonds and two C - Cl bonds are observed in 2ADCP. The crystal statistics of a very closely correlated molecule [6,7] is compared with that of the heading molecule. The mean bond distance of C - C and C - N as calculated by DFT method are 1.394Å and 1.346Å respectively. The C2 – Cl8 and N9 – H12 bond lengths display a relatively greater value of 1.732Å and lower value of 1.007Å respectively. The greatest bond angle was observed at C4-C5-N6 (122.6°) and lowest at C1-N9-H13(115.9°).

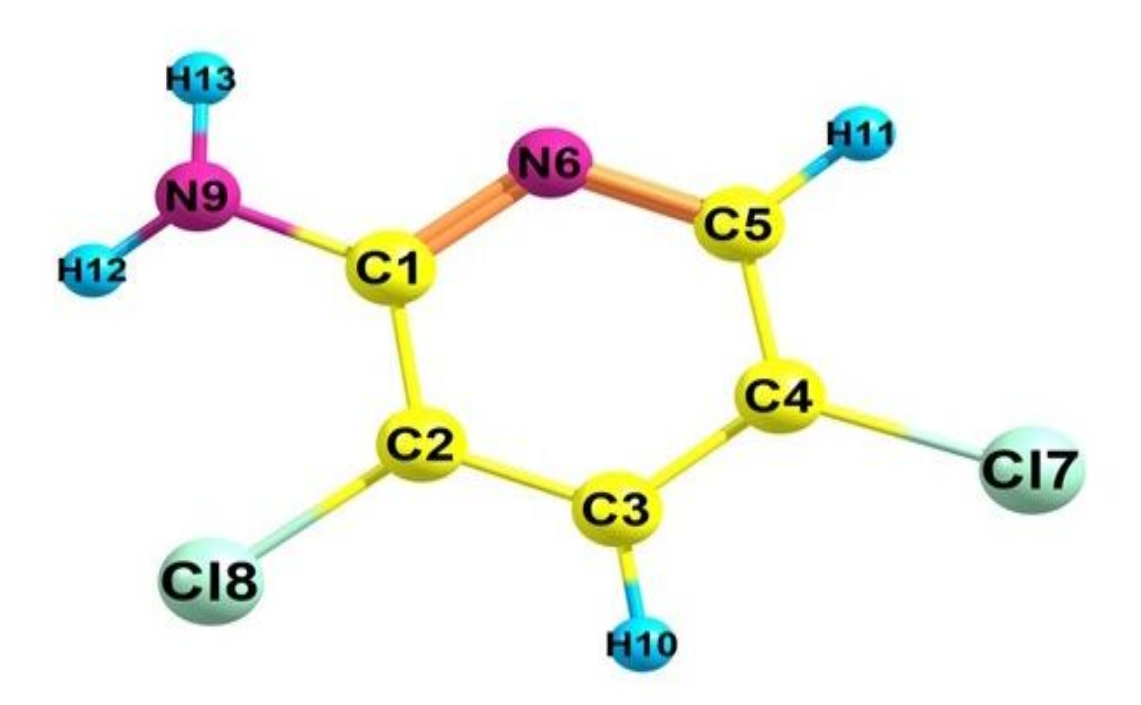


Fig 3.1 Optimised geometric structure with atom numbering of 2-Amino-3,5-dichloropyridine.

Table 3.1 Geometrical parameters of 2-Amino-3,5-dichloropyridine: bond length(\mathring{A}) and bond angles(0).

PARAMETER	B3LYP/6- 311++G(d,p)	Experimental*	PARAMETER	B3LYP/6- 311++G(d,p)	Experimental*
BOND LENGTH(Å)			BOND ANGLE (0)		
C1-C2	1.413	1.419	C2-C1-N6	120.4	116.17
C1-N6	1.338	1.342	C2-C1-N9	122.3	124.9
C1-N9	1.369	1.328	C1-C2-C3	120.1	121
C2-C3	1.381	1.357	C1-C2-C18	120	117.77
C2-C18	1.758	1.721	N6-C1-N9	117.2	118.9
C3-C4	1.393	1.401	C1-N6-C5	119.8	124.58
C3-H10	1.082	1.084	C1-N9-H12	119.3	
C4-C5	1.389	1.349	C1-N9-H13	115.9	
C4-C17	1.754	1.732	C3-C2-C18	119.9	121.26
C5-N6	1.332	1.357	C2-C3-C4	118.1	119.2
C5-H11	1.085	1.084	C2-C3-H10	120.6	
N9-H12	1.007	1.011	C4-C3-H10	121.2	
N9-H13	1.008	1.009	C3-C4-C5	118.9	120.3
			C3-C4-C17	120.4	119.84
			C5-C4-C17	120.6	119.84
			C4-C5-N6	122.6	118.8
			C4-C5-H11	120.6	
			N6-C5-H11	116.8	
			H12-N9-H13	117.5	

^{*}Experimental data taken from [6,7]

3.2.2 Spectral Investigation

The intention of vibrational study is to determine which vibrational modes are responsible for each of the bands detected [8]. For a nonlinear molecule with N atoms, the extreme number of probably working noticeable fundamentals is equal to 3N-6. The heading compound comprises of 13 atoms, having 33 normal modes of vibration. Complete assignments are projected after evaluating the potential energy dispersal for each normal mode amongst the compound's symmetry coordinates. Figs. 3.2 and 3.3 shows the relative representation of theoretically forecasted and experimental FT - IR and FT - Raman correspondingly. Table 3.2 displays the resulting scaled frequencies, estimated infrared and Raman band locations, and PED.

Primary amines have N- H vibrations of stretching in the range 3450 – 3250cm⁻¹ and in 3400 – 3000 cm⁻¹ for secondary amines. The frequencies of the amino group exist at 3500-3300 cm⁻¹ for N - H stretching deformations [9]. The experimental N - H vibration for the caption compound is noticed at 3467 cm⁻¹ in FT-IR spectrum with 100% PED influence.

The C-H stretching vibration are obtained in the range 3100–3000 cm⁻¹ as numerous strong and weak bands. Experimentally, the C-H vibrations for the caption molecule were noted at 3154 cm⁻¹ in FT-IR spectra and 3146 cm⁻¹, 3065 cm⁻¹ in FT-Raman spectrum. Theoretically, C-H stretching bands are spotted in the range 3086 cm⁻¹ and 3052 cm⁻¹.

The ring stretching vibrations (C-C) are noticed in the range 1650-800 cm⁻¹ [10]. In the existing study, the bands were detected at 1631,1546,1321,1238,1098 cm⁻¹ in FT-IR spectrum and at 1584,1543,1396,1239,1075 cm⁻¹ in FT-Raman spectrum. Theoretically, the forecasted values were detected between 1582 and 633 cm⁻¹.

The vibration equivalent to the C-N stretching probably occur in the range 1400 – 1200 cm⁻¹ region for an aromatic compound. In the existing study, the bands are spotted at 1631,1473,1321,1280,1238 cm⁻¹ in FT-IR and 1584,1467,1396,1320,1239 cm⁻¹ in FT-Raman. The theoretically ascended wavenumbers are assessed from 1582 to 707 cm⁻¹ with highest PED influence of 51%.

Most aromatic chloro compounds have intense vibrations in the 850–550 cm⁻¹ range due to C-Cl stretching. Because of the asymmetric and symmetric stretching modes, very strong bands can be found in compounds containing more than one atom of chlorine [11]. For the inspecting compound the C-Cl stretching vibrations is ascribed at 707 cm⁻¹. Experimentally, the peak is detected at 740 cm⁻¹ in FT-IR spectrum.

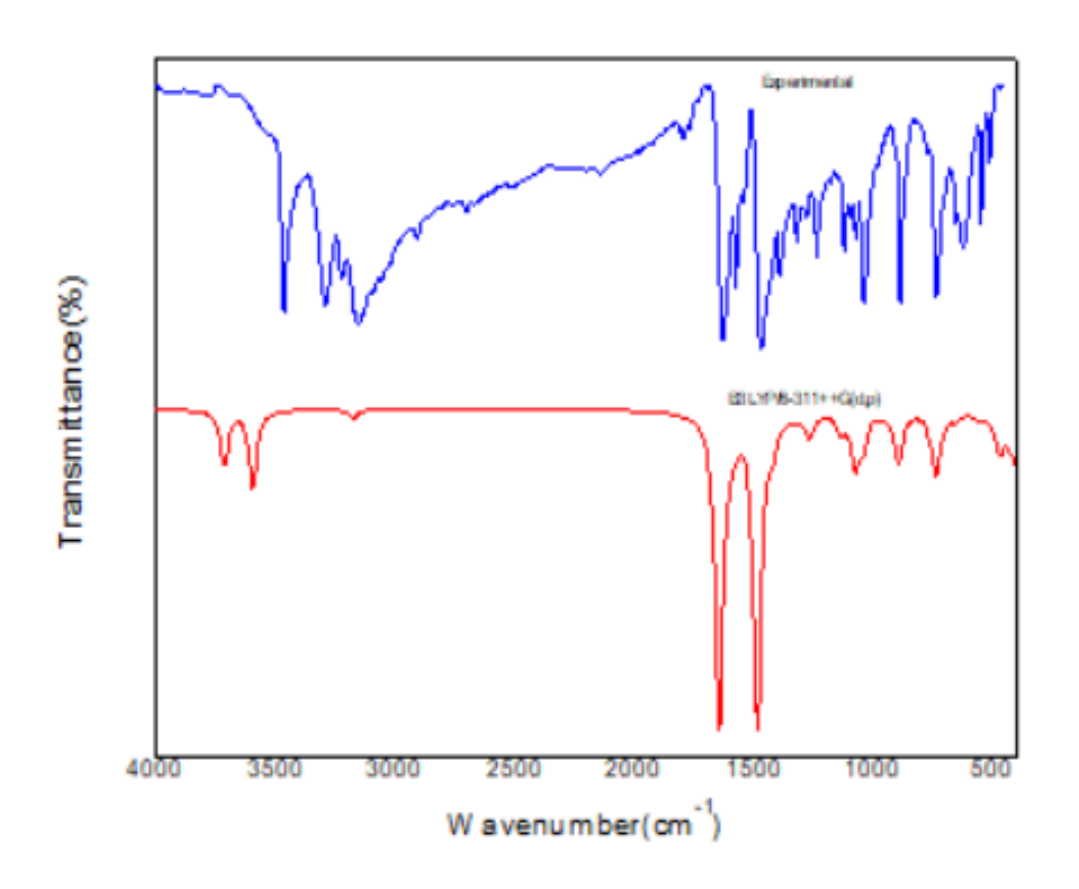


Fig 3.2 Compared theoretical and Experimental FT-IR spectrum of 2ADCP

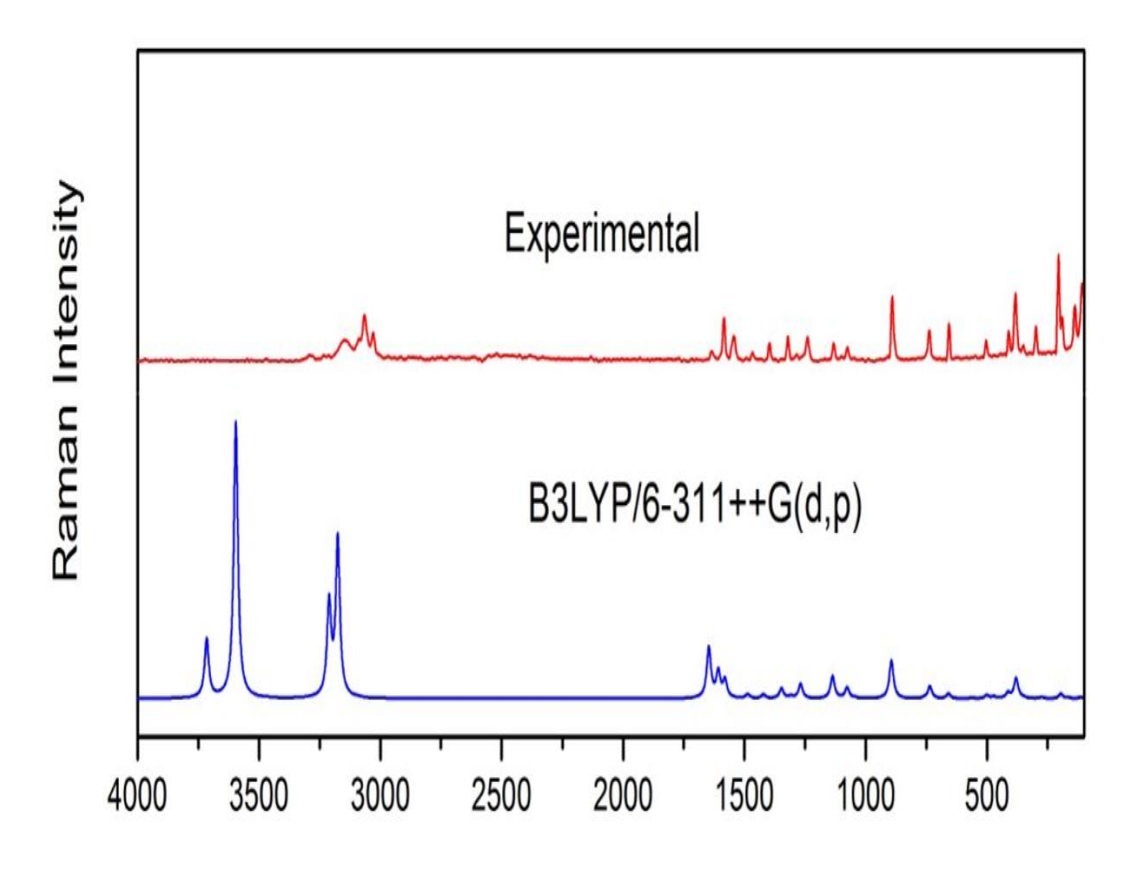


Fig 3.3 Compared theoretical and Experimental FT-Raman spectrum of 2ADCP.

Table 3.2 Observed and calculated vibrational frequency of 2ADCP.

S.	Expe	erimental	Frequ	ency	IR Int	ensity	Raman	Intensity	Assignment
No	FT- IR	FT- RAMAN	Unscaled	Scaled	Relative	Absolute	Relative	Absolute	Assignment
1			3716	3571	50	17	39	21	YNH (100)
2	3467		3596	3455	72	25	182	100	YNH (100)
3	3154	3146	3211	3086	0	0	61	34	YCH (100)
4		3065	3175	3052	7	2	104	57	YCH (100)
5	1631	1584	1647	1582	291	100	33	18	YCC (12) + YNC (11) +βHNH (47)
6	1546	1543	1608	1545	12	4	17	9	YCC (32) +βHNH (31)
7			1580	1518	11	4	11	6	YCC (35) + YNC (21) +βCCC (10)
8	1473	1467	1487	1429	292	100	3	1	ΥNC (37) +βHCC (10) +βHCN (23) +βCCC (10)
9	1321	1396	1422	1366	26	9	2	1	YCC (36) + YNC (21)
10	1280	1320	1347	1295	3	1	7	4	YNC (51) +βHCN (27)
11	1238	1239	1308	1257	4	1	1	1	ΥNC (21) + ΥCC (20) +βHNC (18+βHCC (13)
12			1268	1219	22	7	9	5	YCC (34) + YNC (10) +βHCC (27) +βHCN (14)
13	1098	1075	1137	1092	18	6	15	8	YCC (47) + YClC (11) +βHCC (10)
14	1075		1077	1035	49	17	7	4	βCCC (17) +βHNC (20) +βHCC (16) +βNCC (15)
15	1040		1044	1003	27	9	1	0	YNC (26) +βCCC (10) +βHNC (33) +βCNC (11)
16		890	938	901	2	1	0	0	τHCCC(12)+ τHCNC(73)+ τCNCC(11)
17	888		902	867	19	7	0	0	τHCCC(70)+ τHCNC(11)
18			894	859	30	10	25	14	YNC (12) +βNCC (14) +βCCC (30) +βCNC (10)
19		738	757	728	14	5	0	0	τ CCCC(12)+ τ CNCC(24)+ ω NCNC(43)
20	740		736	707	52	18	8	4	YNC (14) + YClC (36) +βNCC (23)
21	658	656	659	633	7	2	3	2	ΥCC (15) + ΥCIC (17) + βCCC (23) + βNCC (19) + βNCN (10)
22	550	503	563	541	4	1	1	0	$\tau CCCC(18) + \tau NCCC(14) + \tau CNCC(16) + \omega CICCC(12) + \omega NCNC(17)$

S.	Expo	erimental	Freque	ency	IR Int	ensity	Raman	Intensity	A
No	FT- IR	FT- RAMAN	Unscaled	Scaled	Relative	Absolute	Relative	Absolute	Assignment
23	516		501	482	4	1	2	1	βNCN (36) +βCICC (11) +τHNCC(16)
24		442	472	454	31	11	1	1	τHNCC(35)+ ωClCCC(15)
25		410	435	418	9	3	0	0	τHNCC(25)+ τCCCC(23)+ τCNCC(12)
26			413	397	10	3	4	2	ΥCIC (30) +βCCC (13) +βCICC (12)
27			380	365	4	2	13	7	YCIC (51) +βCNC (13)
28			358	344	234	80	1	0	τHNCC(86)
29			343	329	13	5	0	0	τCNCC(15)+ωClCCC(54)+ωNCNC(21)
30			275	264	4	1	1	1	βNCN (26) +βCICC (48)
31			196	188	0	0	3	2	βCICC (81)
32			167	160	0	0	1	0	τ CCCC(14)+ τ NCCC(10)+ τ CNCC(13)+ ω ClCCC(60)
33			113	109	1	0	1	1	τ CCCC(21)+ τ NCCC(56)+ωClCCC(12)

 $[\]Upsilon$ -stretching, β- in plane bending, ω – out plane bending, τ - torsion

3.2.3 Molecular reactivity and UV - Visible analyses

The concept of HOMO and LUMO plays a vital role in understanding the kinetic firmness and chemical reactivity of a molecule. The transition of electrons is caused by the interaction of HOMO & LUMO [12]. The various parameters like electron affinity, electronegativity, chemical ability, electrophilicity index, global hardness, softness, electronic charge, electron donating capability and electron accepting capability of the heading molecule have been assessed. Additionally, to investigate the electronic solvation properties, IEFPCM solvation model has been employed and the results are presented in Table 3.3. In order to visualize the chemical behaviour of title compound, solvent effect has been instigated in the present study. Fig.3.4 depicts the pictographic illustration of HOMO-LUMO for the heading molecule. The bandgap energy value of the heading molecule in gas phase is noticed to be 4.882305 eV whereas in solvents water, DMSO and benzene were computed to be 4.796589 eV, 4.797133 eV and 4.809922 eV respectively, validating that the molecule has a steady structure and a bandgap energy value that is close to that of bioactive molecules [13]. The measure of Ionization Potential and Electron Attraction are found to be 6.387eV and 1.505 eV respectively in gas phase. The elevated values of chemical hardness (2.441,2.3982, 2.3985,2.4049) in gas and various solvents reveal that 2ADCP is chemically stable, and on the other hand the value of softness being low, signifies non-toxic nature of the compound.

By using the TDDFT M062X/6–311++G(d,p) origin for each transitions, the UV- Visible explorations can be done theoretically. In this current study, exclusive M062X method [14] has been employed with polar and nonpolar solvents like water, DMSO and benzene to investigate the transformation of electronic charges for the

caption compound. IEFPCM pattern [15] is instigated to study the correlations of the system. Figures 3.5, 3.6, 3.7 depicts the theoretical UV spectrum with different solvent phases. The calculated theoretical values of λ max, energy, oscillator strength, symmetry and major contributions are tabularized in Table 3.4. It is observed that no major differences emerged in assessed wavelength and band gap for the different solvents used.

Table 3.3 Calculated energy values of 2-Amino-3,5-dichloropyridine with solvation effect.

Parameters	Gas	Water	DMSO	Benzene
HOMO(eV)	-6.38738	-6.46493	-6.46466	-6.46276
LUMO(eV)	-1.50507	-1.66834	-1.667527	-1.65283
Ionization potential	6.387378	6.464932	6.4646598	6.462755
Electron affinity	1.505073	1.668343	1.6675268	1.652833
Energy gap(eV)	4.882305	4.796589	4.797133	4.809922
Electronegativity	3.946226	4.066638	4.0660933	4.057794
Chemical potential	-3.94623	-4.06664	-4.066093	-4.05779
Chemical hardness	2.441153	2.398294	2.3985665	2.404961
Chemical softness	0.204821	0.208481	0.2084578	0.207904
Electrophilicity index	3.18962	3.447771	3.4464575	3.423276
Electronic charge	1.616542	1.695637	1.6952181	1.68726
Electron donating capability (w-)	5.467876	5.780877	5.779325	5.752793
Electron accepting capability (w+)	1.521651	1.714239	1.7132317	1.694999

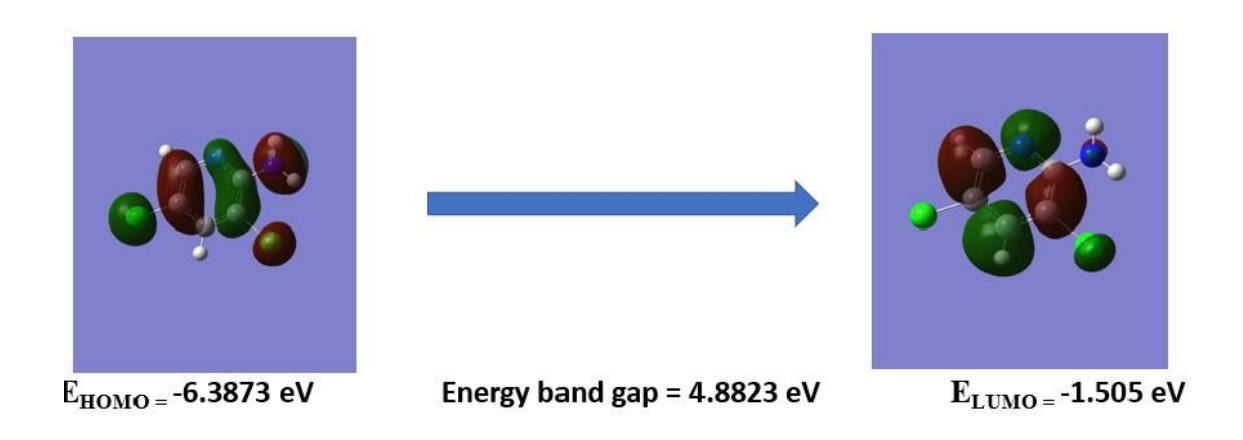


Fig 3.4 Atomic orbital HOMO - LUMO composition of the frontier molecular orbital of 2-Amino-3,5-dichloropyridine.

Table 3.4 Simulated UV-Vis spectrum with absorption maxima(nm), energy (cm⁻¹) and oscillator strength(f) of 2ADCP with different solvents.

Solvents	Wavelength (nm)	Band gap (ev)	Energy (cm ⁻¹)	Osc. Strength(f)	Symmetry	Major contributions
WATER	228.8291185	5.42	43700.73207	0.0881	Singlet-A	HOMO->LUMO (91%)
	226.4427392	5.48	44161.27465	0.0049	Singlet-A	H-1->LUMO (95%)
DMSO	228.9601171	5.42	43675.72888	0.0912	Singlet-A	HOMO->LUMO (91%)
	226.5668787	5.47	44137.07802	0.005	Singlet-A	H-1->LUMO (95%)
BENZENE	228.985489 228.2813982	5.41 5.43	43670.88956 43805.58415	0.0052 0.0939	Singlet-A Singlet-A	H-1->LUMO (95%) H-1->LUMO (95%)

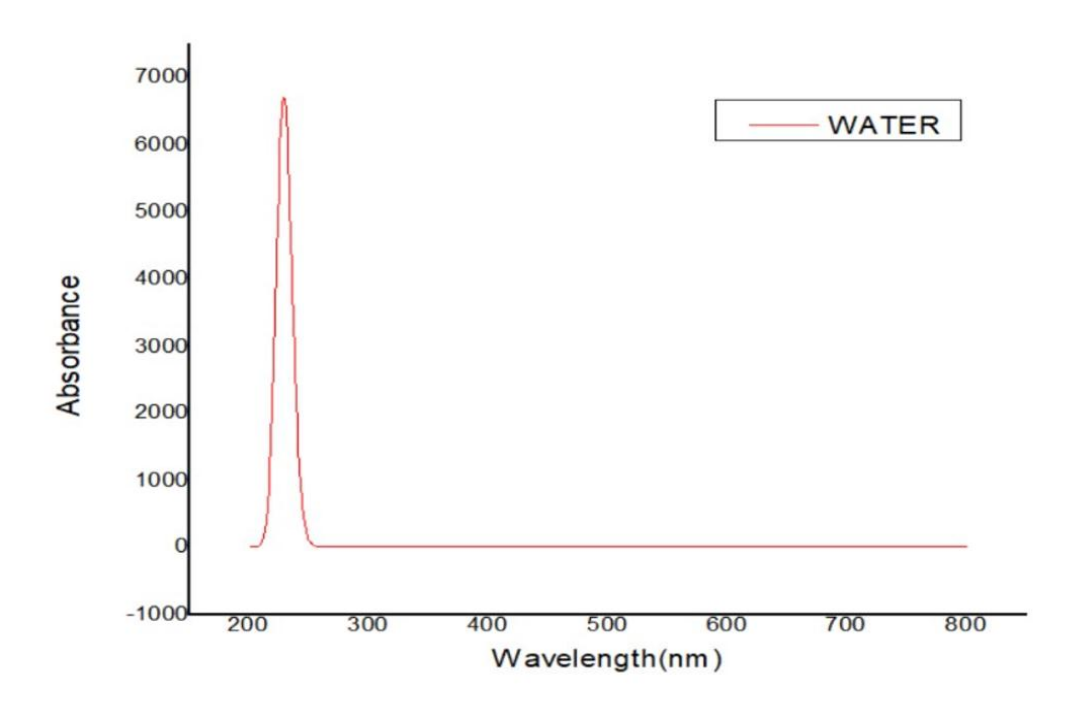


Fig 3.5 Theoretical UV-Visible spectra of 2ADCP in water as solvent.

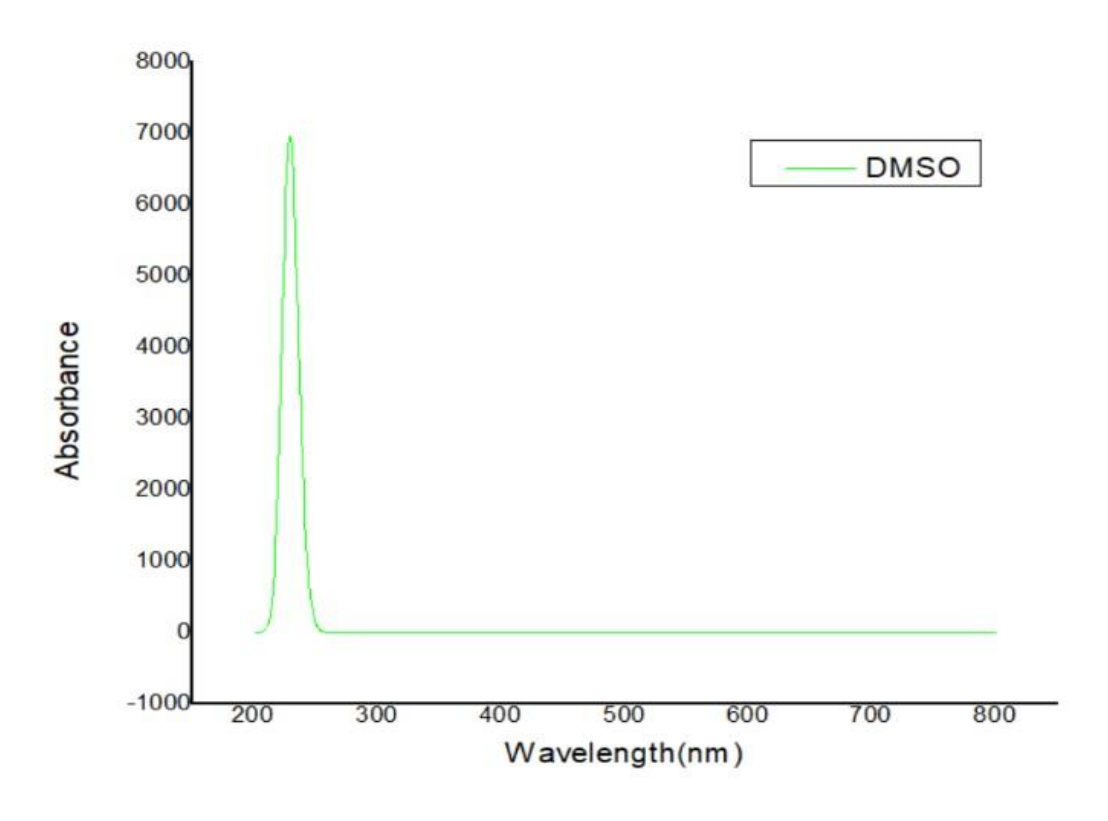


Fig 3.6 Theoretical UV-Visible spectra of 2ADCP in DMSO as solvent.

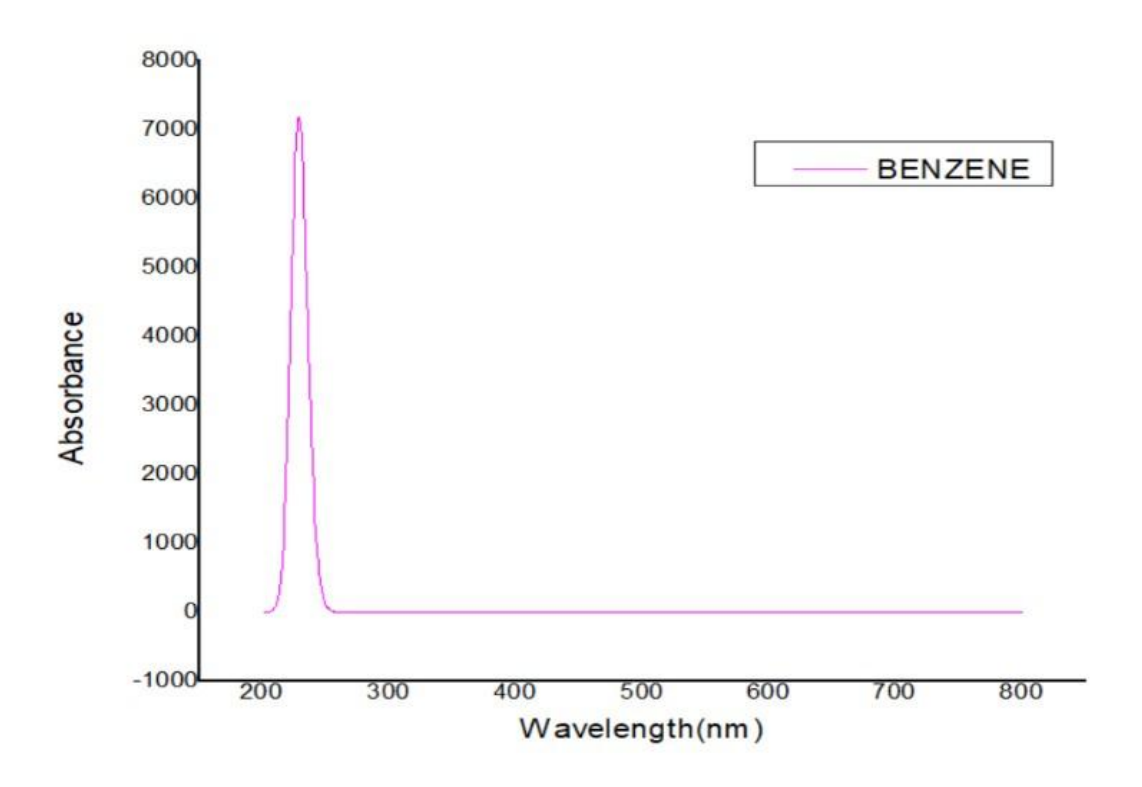


Fig 3.7 Theoretical UV-Visible spectra of 2ADCP in benzene as solvent.

3.2.4 Molecular Electrostatic Potential

The MEP is envisioned through charting to explain the charge dispersals of molecules three dimensionally and potential energy of a proton at a specific location near a molecule. It is a useful feature for determining a molecule's reactivity [16]. MEP map of 2ADCP is shown in Fig 3.8 having colour code ranging from -0.172e0 eV to 0.172e0 eV. Different colours, ranging from red to blue, reflect different electrostatic potential values. Red and blue colour signify the areas of the most negative and positive electrostatic capacity. It can be observed from the MEP that for the caption molecule, chlorine and nitrogen atoms are in negative potentials region and hydrogen atoms are in positive potentials region.

-0.172e0 0.172e0

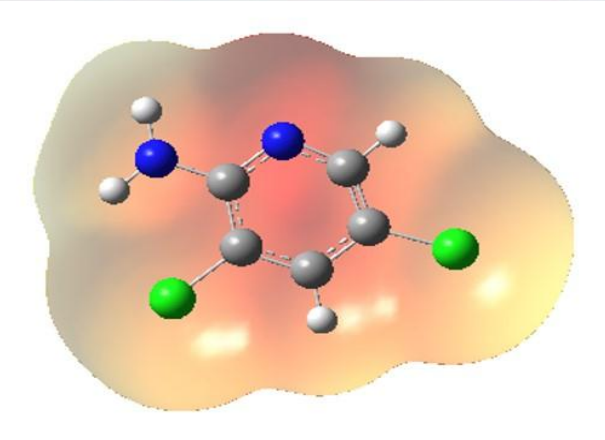


Fig 3.8 Molecular Electrostatic Potential of 2ADCP.

3.2.5 Natural Bond Orbital Investigation

The NBO study can be used to examine the inter and intramolecular connections within the molecules [17,18]. The stabilization energy linked with the delocalization can be obtained using orbital occupancy and Fock matrix element [19,20]. In order to investigate the intermolecular hydrogen bonding and transfer of charges, NBO analysis was exhibited on the heading molecule using B3LYP/6-311G(d,p) Pop = NBO test origin[21]. Table 3.5 shows the corresponding data. The interaction between $\sigma(\text{C1-C2})$ to $\sigma^*(\text{C1-N6})$ and $\pi(\text{C1-N6})$ to $\pi^*(\text{C2-C3})$ led to the stabilization energy of 1.66 kcal/mol and 11.1kcal/mol respectively. For 2ADCP, the strong intra-molecular interaction is 25.28 kJ/mol via $\pi(\text{C2-C3})$ to $\pi^*(\text{C1-N6})$ and from the LP(1) of Nitrogen atom(N9) to $\pi^*(\text{C1-N6})$ with an energy of 37.39 kJ/mol.

Table 3.5 Second order perturbation theory analysis of Fock matrix in NBO for 2ADCP.

Donor	Туре	ED/e(qi)	Acceptor	Туре	ED/e(qi)	E(2) kcal/mol	E(j)-E(i) a.u.	F(i,j) a.u.
C 1-C 2	σ	1.98088	C 1-N 6	σ*	0.0208	1.66	1.23	0.04
C 1-N 6	σ	1.98058	C 1-C 2	σ*	0.0424	2.34	1.32	0.05
C 1-N 6	π	1.71896	C 2-C 3	π*	0.35043	11.1	0.29	0.052
C 1-N 9	σ	1.99193	C 1-C 2	σ*	0.0424	0.78	1.27	0.028
C 2-C 3	σ	1.97485	C 1-C 2	σ*	0.042	3.19	1.23	0.056
C 2-C 3	π	1.74093	C 1-N 6	π*	0.44344	25.28	0.27	0.078
C 2-Cl 8	σ	1.98916	C 1-N 6	σ*	0.0208	2.66	1.24	0.052
C 3-C 4	σ	1.97278	C 2-C 3	σ*	0.0245	2.34	1.22	0.048
C 3-H 10	σ	1.98126	C 1-C 2	σ*	0.0424	3.73	1.04	0.056
C 4-C 5	σ	1.98138	C 3-C 4	σ*	0.03336	4.02	1.29	0.065
C 4-C 5	π	1.71264	C 1-N 6	π*	0.44334	10.27	0.28	0.05
C 4-Cl 7	σ	1.98823	C 2-C 3	σ*	0.0245	1.37	1.26	0.037
C 5-N 6	σ	1.97472	C 1-N 6	σ*	0.0208	0.82	1.3	0.029
C 5-H 11	σ	1.97465	C 1-N 6	σ*	0.0208	4.41	0.99	0.059
N 9-H 12	σ	1.9912	C 1-N 6	σ*	0.0208	3.68	1.14	0.058
N 9-H 13	σ	1.99255	C 1-C 2	σ*	0.0424	2.76	1.15	0.051
N 6	LP (1)	1.90771	C 1-C 2	σ*	0.0424	8.15	0.87	0.076
Cl 7	LP (1)	1.99179	C 3-C 4	σ*	0.03336	1.86	1.44	0.047
Cl 7	LP (2)	1.96394	C 3-C 4	σ*	0.03336	5.5	0.84	0.061
Cl 7	LP (3)	1.9297	C 4-C 5	π*	0.3388	13.58	0.35	0.066
Cl 8	LP (1)	1.99251	C 1-C 2	σ*	0.0424	1.38	1.44	0.04
Cl 8	LP (2)	1.96046	C 1-C 2	σ*	0.0424	4.96	0.84	0.058
Cl 8	LP (3)	1.9255	C 2-C 3	π*	0.35043	13.75	0.32	0.064
N 9	LP (1)	1.81018	C 1-N 6	π*	0.44334	37.39	0.24	0.091
C 1-N 6	π*	0.44334	C 4-C 5	π*	0.3388	80.32	0.03	0.076
C 2-C 3	π*	0.35043	C 4-C 5	π*	0.3388	70.08	0.04	0.075

3.2.6 Fukui Function Descriptors Analysis

Local reactivity signifiers such as Fukui functions, may be predicted to reveal chemical selectivity or reactivity at a specific location in a chemical system. It can be used to predict which atoms in a molecule are more likely to lose or accept electrons. [22]. During an electrophilic strike, it is obvious that N9 attached to the carbon atom is the most reactive site (-0.0289) whereas nucleophilic strike, the atoms C2 and C4 are discovered to be the chosen locations as they are attached to chlorine atoms C18 and C17 respectively which are highly electronegative than carbon.

The site C4 has the highest descriptor value, showing the greatest softness (0.033441). Interpreting the dual descriptor conditions from Table 3.6, the electrophilic locations are C5, C1, C3, N6, C18, H10 and H11. Similarly the nucleophilic locations are C2, C4, C17, N9, H12 and H13. These results exhibit the reactive sites of the heading molecule.

Table 3.6 Mulliken charge distribution, Fukui function and local softness corresponding to (0,1), (-1,2) and (1,2) charge and multiplicity for 2ADCP.

Atom	Mulli	iken atomic ch	arges		Fukui fu	inctions			local so	oftness
	0, 1 (N)	N+1 (-1, 2)	N-1 (1,2)	f_r^+	f_r^-	f_r^{0}	Δf(r)	$s_r^+ f_r^+$	$s_r^- f_r^-$	$s_r^0 f_r^0$
1 C	-0.64784	-0.652219	-0.71038	-0.00438	0.06254	0.029081	-0.06692	-0.0009	0.01281	0.005956
2 C	0.631578	0.730535	0.684839	0.098957	-0.05326	0.022848	0.152218	0.020268	-0.01091	0.00468
3 C	-0.82751	-1.25491	-0.74852	-0.4274	-0.07899	-0.2532	-0.34841	-0.08754	-0.01618	-0.05186
4 C	0.362579	0.525849	0.333132	0.16327	0.029447	0.096359	0.133823	0.033441	0.006031	0.019736
5 C	-0.65019	-0.707098	-0.63666	-0.05691	-0.01353	-0.03522	-0.04337	-0.01166	-0.00277	-0.00721
6 N	-0.08721	-0.230565	0.006867	-0.14336	-0.09408	-0.11872	-0.04928	-0.02936	-0.01927	-0.02432
7 Cl	0.347347	0.18337	0.58092	-0.16398	-0.23357	-0.19878	0.069596	-0.03359	-0.04784	-0.04071
8 Cl	0.311001	0.133483	0.486842	-0.17752	-0.17584	-0.17668	-0.00168	-0.03636	-0.03602	-0.03619
9 N	-0.36667	-0.395573	-0.17478	-0.0289	-0.19189	-0.11039	0.162991	-0.00592	-0.0393	-0.02261
10 H	0.193356	0.111625	0.256633	-0.08173	-0.06328	-0.0725	-0.01845	-0.01674	-0.01296	-0.01485
11 H	0.178617	0.094192	0.24946	-0.08443	-0.07084	-0.07763	-0.01358	-0.01729	-0.01451	-0.0159
12 H	0.255661	0.219077	0.305945	-0.03658	-0.05028	-0.04343	0.0137	-0.00749	-0.0103	-0.0089
13 H	0.299289	0.242235	0.365702	-0.05705	-0.06641	-0.06173	0.009359	-0.01169	-0.0136	-0.01264

3.2.7 ELF and LOL studies

ELF is a metric for locating an electron in the same spin as a reference electron located at a specific point [23]. The numerical stability of the ELF with respect to the theoretical level at which the electron density and molecular orbitals are measured is one of its most important features. For 2ADCP, colour and contour filled maps of ELF are displayed in Figs. 3.9 and 3.10. The Bond Critical Point 's, hydrogen, nitrogen, Chlorine, and carbon atoms with the electronic dispersal and depletion layer of electron between the outer and inner shells, as well as the lone pair at the N and Cl atoms are evidently revealed in the figure.

LOL is one among the exclusive signifiers to study atom-to-atom bonding in the molecule. LOL contributed by atoms [24] can be explicated through a colour filled plane map. Blue colour circle represents the benzene ring and BCP is represented by red with a yellow path where delocalization of 2ADCP electrons can be viewed. Figs.3.11 and 3.12 expresses the coloured and contour filled maps of LOL. Thus, these findings indicate that 2ADCP is chemically effective, suggesting that it may have biological applications.

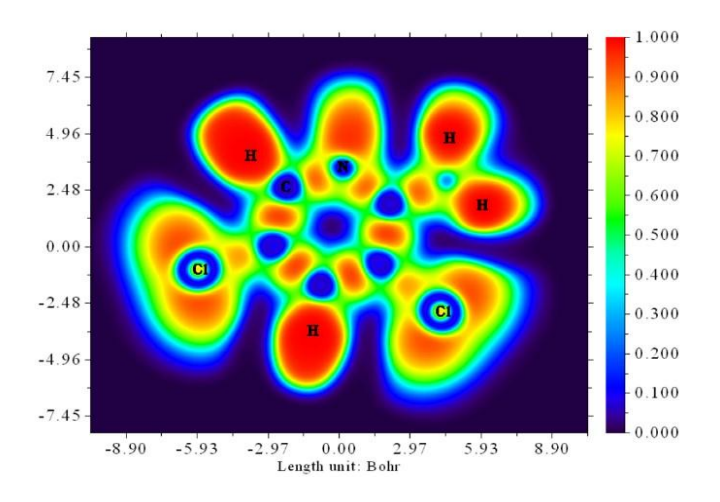


Fig. 3.9 ELF, colour filled map of 2ADCP.

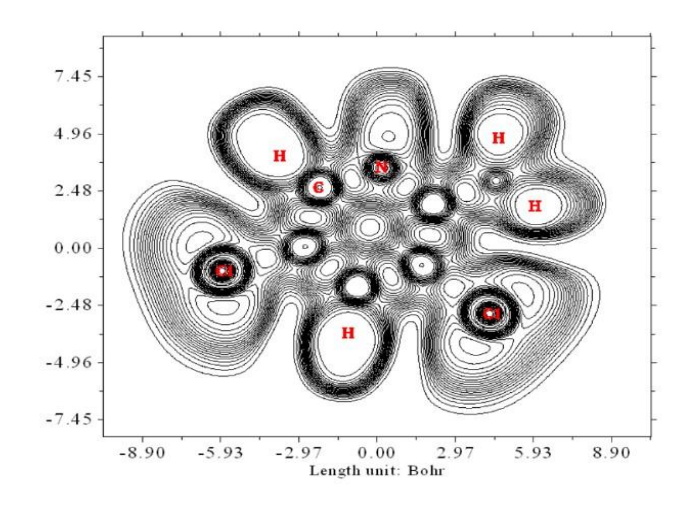


Fig. 3.10 ELF, contour map of 2ADCP.

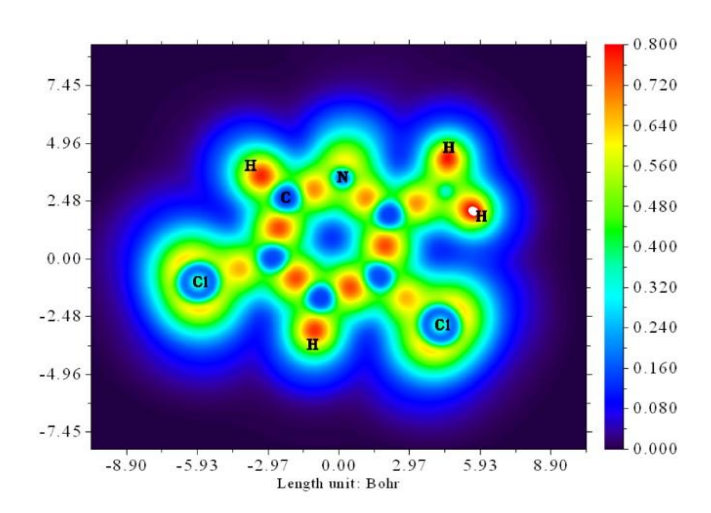


Fig. 3.11 LOL, colour filled map of 2ADCP.

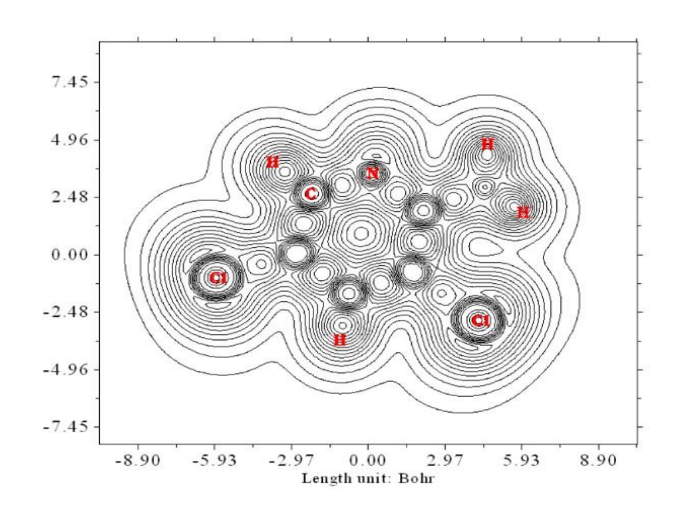


Fig. 3.12 LOL, contour map of 2ADCP.

3.2.8 Biological Assessment

3.2.8.1 Pharmacological analyses

The possible potential of 2ADCP to be exercised as an active constituent in few pharmaceutical products, can be analysed by using drug likeness. The Lipinski's rule of five reveals the value of drug likeness for a molecule to act as a possible drug [25]. The drug likeness parameters have been declared in Table 3.7, which shows that the values of HBD and HBA are 2 each, AlogP is equal to 1.98 and TPSA is found to be 38.91Å² indicating that 2ADCP can be considered as a drug. In addition to drug likeness other parameters like ADMET (Absorption Distribution Metabolism Excretion Toxicity), molinspiration values, toxicity and environmental toxicity are also explored in the existing work. There is no violation of drug resemblance properties like the CMC (Comprehensive Medicinal Chemistry) like rule. It is calculated that the MDDR (Modern Drug Data Report) like rule has two violations: no rings and no rotatable bonds whereas WDI (World Drug Index) like rule has a 90% cut off, suggesting no violations. To conclude, the significant Lipinski rule of five is appropriate and has zero violation. By examining dissimilar drug likeness results, the major results predict the compound to be a drug. The additional parameters like BBB penetration, Buffer solubility, Caco2, HIA and MDCK are 0.654546, 1368.02, 18.2762, 96.62643, and 53.5047 respectively. The CYP 2C19,2C9,3A4 inhibition reveal inhibition nature whereas CY2D6 inhibition, CYP 2D6,3A4 substrate, Pgp inhibition for frontpage compound reveal non inhibiting nature. The estimates of water solubility, plasma protein binding, skin permeability, SKlog for D and S(pure) are 360.706 mg/L, 8.578176, - 2.44836, 2.02654, - 2.65505 respectively. Then different toxicity assessments are accomplished on 2ADCP and the factors daphniaat, algaeat, minnowat, medakaat show values 0.381412, 0.0721276, 0.127493, 0.188662, respectively. The bio

action projections from environmental toxicity like GPCR ligand, kinase inhibitor, nuclear receptor ligand, and enzyme inhibitor possess values -2.02, -1.62, -3.47, and -1.56 respectively. On the whole, investigations of the pharmacological properties reveal that the heading compound possess drug feature.

Table 3.7 Drug likeness parameters for 2ADCP.

Descriptor	Value
Hydrogen Bond Donor (HBD)	2
Hydrogen Bond Acceptor (HBA)	2
AlogP	1.98
Topological polar surface area (PSA)	38.91
Molar refractivity	163.01
Number of atoms	9
Number of rotatable bonds	0

3.2.8.2 Ramachandran plot

Ramachandran plots are useful in investigating the protein quality. They are helpful in selecting the proteins for docking studies from PASS online predictor [26]. From the Figs. 3.13 and 3.14, it is evident that greater part of the residues and small amount of residues appear within the permitted red and forbidden regions correspondingly for the two designated proteins. Ramachandran plot outcome approves the preferred proteins 6QHB and 6Y92 are structurally steady.

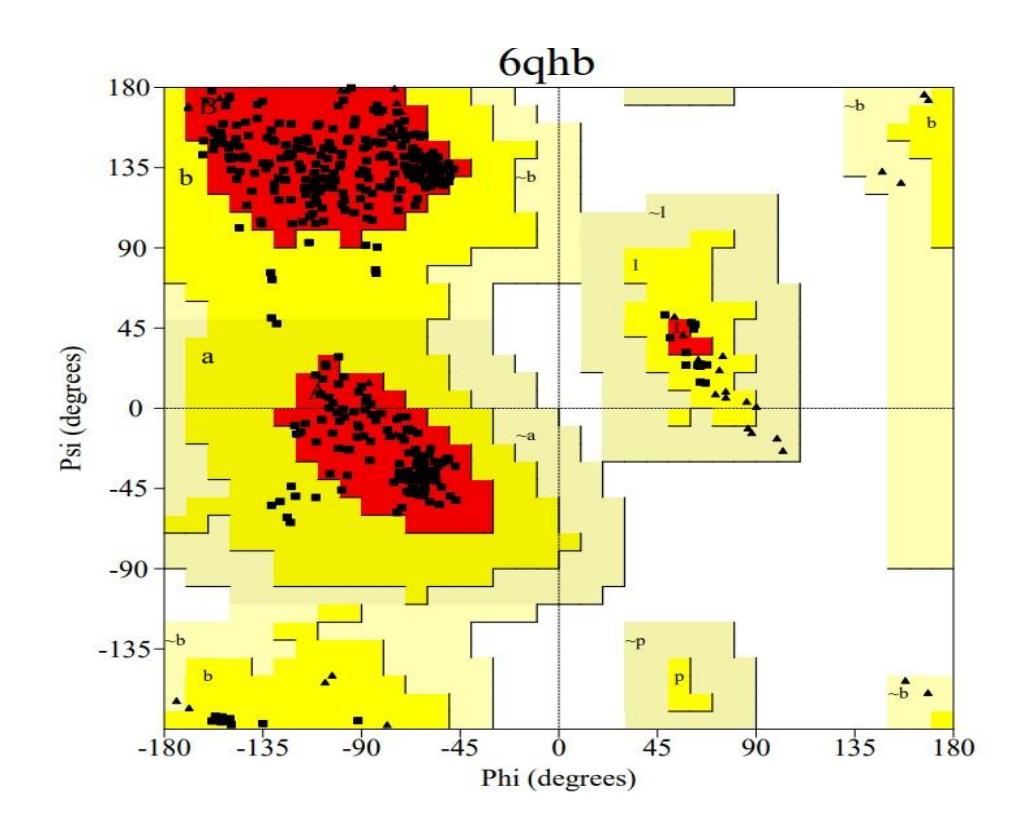


Fig. 3.13 Ramachandran plot for receptor protein 6QHB.

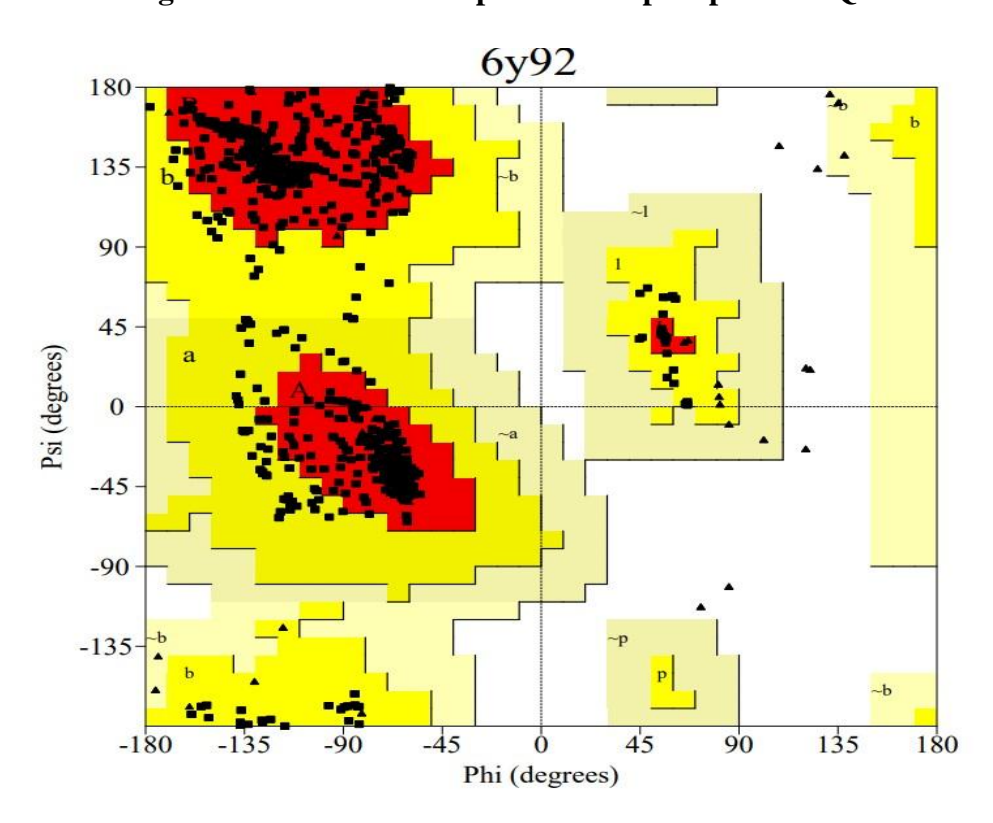


Fig. 3.14 Ramachandran plot for receptor protein 6Y92.

3.2.8.3 Molecular docking

The ligand confirmation inside the binding site of protein targets is observed using a molecular docking analysis. This is an influential computational tool to estimate the ideal binding tendency and activity of drug molecules and their targeted proteins. The target protein's structure was downloaded in PDB format from RCSB [27,28]. 2ADCP was docked into the effective location of proteins 6QHB and 6Y92 associated with diabetic neuropathy treatment. Auto Dock suite 4.2.6 was used to learn the molecular mechanism of ligand and protein interactions [29]. The docking factors of the molecule with respect to the aimed proteins were obtained and listed in Table 3.8. The binding orientation of 2ADCP with the aimed proteins are publicized in Fig 3.15 and Fig 3.16 respectively. The least binding energy of - 4.52 kcal/mol and - 4.16 kcal/mol and intermolecular energy of - 4.81 kcal/mol and - 4.45 kcal/mol were observed for docking with 6QHB and 6Y92 proteins respectively. Various bonded residues like ASP 189 and TRP 215 for 6QHB protein and SER 162 and GLU 161 for 6Y92 protein were also observed with bond length variations.

Table 3.8 Molecular docking parameters of 2ADCP with proteins 6QHB and 6Y92.

Protei n	Bonded residues	Bond distance (Å)	Intermolec ular Energy (Kcal/mol)	Inhibition Constant (μmol)	Binding Energy (Kcal/mol)	Referen ce RMSD (Å)
6QHB	ASP 189	2.2	-4.81	489.67	-4.52	32.90
	TRP 215	2.5				
6Y92	SER 162	1.9	-4.45	899.31	-4.16	263.60
	SER 162	2.3				
	GLU161	2.0				

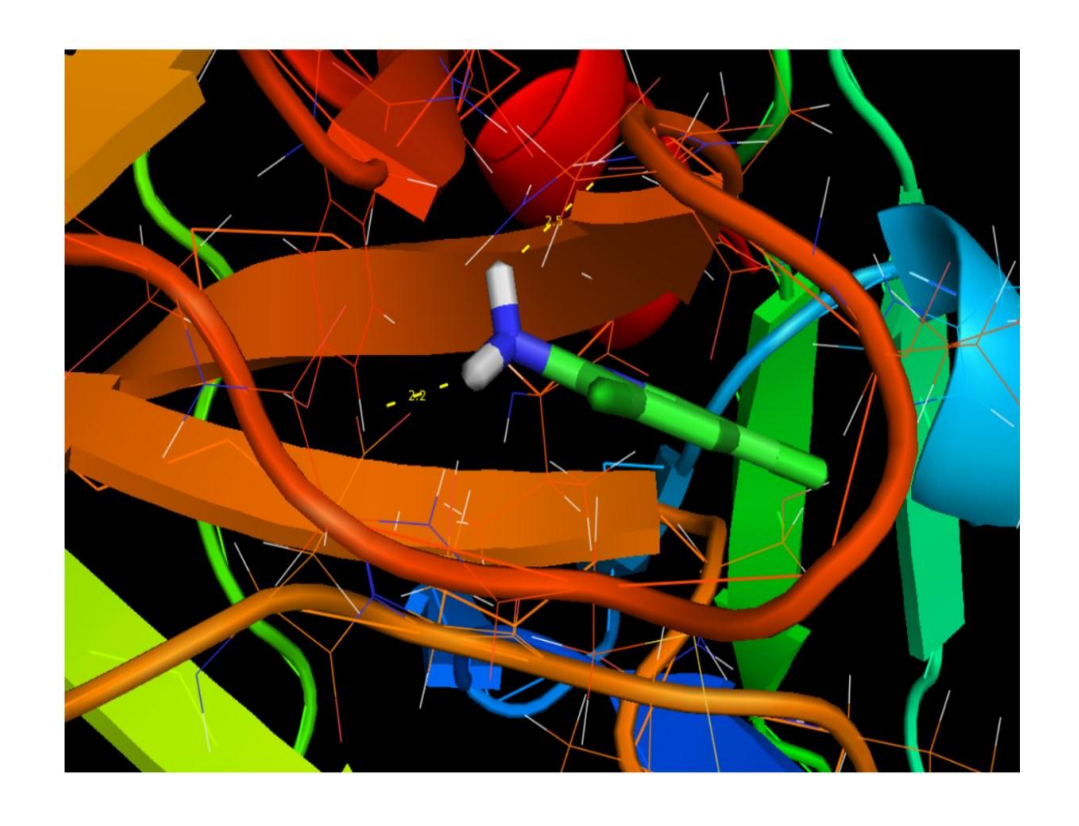


Fig 3.15 Docking and hydrogen bond interaction of 2ADCP with 6QHB.

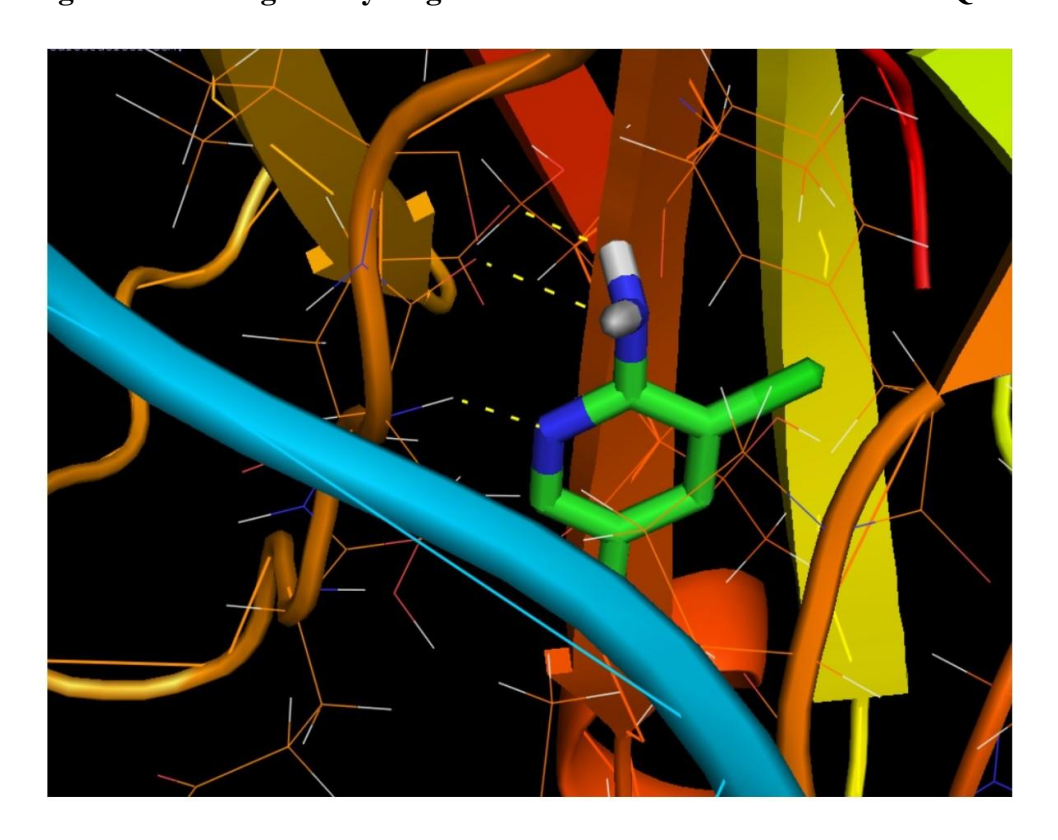


Fig 3.16 Docking and hydrogen bond interaction of 2ADCP with 6Y92.

3.3 CONCLUSION

A comprehensive vibrational spectral analysis as well as quantum mechanical evaluations were achieved for the heading compound. Bond length and bond angle are the optimized geometric parameters theoretically determined from DFT and related with structurally alike compound. The vibrational FT-IR, FT Raman spectra of the molecule were recorded and wavenumbers of vibration with their PED were evaluated. The electrophilic and nucleophilic sites were identified using the MEP diagram. The energy gap of 2ADCP was 4.882305 eV at gas phase and Fukui functions was also analysed. ELF and LOL emphasize the chemically noteworthy region of 2ADCP. UV—Vis spectral study with IEFPCM mode was accomplished to estimate the absorption maxima and band gap energies for 2ADCP in water, benzene and DMSO solvents. In order to validate the sample to be a drug, parameters like toxicity, drug likeness, ADMET and environmental toxicity studies were also accounted. When the heading compound was docked into the functional site of the proteins 6QHB and 6Y92 associated with diabetic neuropathy treatment, minimum binding energy of -4.52 kcal/mol and -4.16 kcal/mol respectively were evaluated.

REFERENCES

- [1] Ramalingam, S., Periandy, S., Mohan, S. (2010). Vibrational spectroscopy (FTIR and FTRaman) investigation using ab initio (HF) and DFT (B3LYP and B3PW91) analysis on the structure of 2-amino pyridine. Spectrochim. Acta A Mol. Biomol. Spectrosc. 77(1): 73–81.
- [2] Borisenko, V. E., Krekov, S. A., Guzemin, A. G., Koll, A. (2003). The influence of hetero-substitution in the aromatic ring of amino pyrimidine on amino group characteristics in free and H-bonded molecules. J. Mol. Struct. 646(1-3): 125–140.
- [3] Lawton, G. R., Ranaivo, H. R., Chico, L. K., Ji, H., Xue, F., Martásek, P., Roman, L. J., Watterson, D. M., Silverman, R. B. (2009). Analogues of 2-aminopyridine-based selective inhibitors of neuronal nitric oxide synthase with increased bioavailability. Bioorg. Med. Chem. 17(6): 2371–2380.
- [4] Issa, T. B., Sagaama, A., Noureddine, I. (2020). Computational study of 3-thiophene acetic acid: Molecular docking, electronic and intermolecular interactions investigations. Computational Biology and Chemistry. 86: 107268.
- [5] Maryam Iman., Atefeh Saadabadi., Asghar Davood. (2015).Molecular docking analysis and molecular dynamics simulation study of ameltolide analogous as a sodium channel blocker. Turk J Chem. 39: 306 316.
- [6] Anagnostis, J., Turnbull, M. M. (1998). 2-Amino-3,5-dichloropyridinium Chloride Monohydrate. Acta Crystallographica Section C Crystal Structure Communication. 54(5): 681–683.
- [7] Abraham, C. S., Prasana, J. C., Muthu, S. (2017). Quantum mechanical, spectroscopic and docking studies of 2-Amino-3-bromo-5-nitropyridine by

- Density Functional Method. Spectrochim. Acta Part A Mol. Biomol. Spectrosc.181: 153–163.
- [8] Kuruvilla, T. K., Prasana, J. C., Muthu, S., George, J. (2018). Vibrational spectroscopic (FT-IR, FT-Raman) and quantum mechanical study of 4-(2-chlorophenyl)-2-ethyl-9-methyl-6H-thieno [3,2-f] [1,2,4] triazolo [4,3-a] [1,4] diazepine. J. Mol.Struct. 1157: 519–529.
- [9] Fathima Rizwana, B., Prasana, J. C., Abraham, C. S., Muthu, S. (2018). Spectroscopic investigation, hirshfeld surface analysis and molecular docking studies on anti-viral drug entecavir. J. Mol.Struct. 1164: 447–458.
- [10] Karabacak, M., Karaca, C., Atac, A., Eskici, M., Karanfil, A., Kose, E. (2012). Synthesis, analysis of spectroscopic and nonlinear optical properties of the novel compound: (S)-N-benzyl-1-phenyl-5-(thiophen-3-yl)-4-pentyn-2-amine. Spectrochim. Acta Part A Mol. Biomol. Spectrosc. 97: 556–567.
- [11] Muthu, S., Prasath, M., Isac Paulraj, E., Arun Balaji, R. (2014). FT-IR, FT-Raman spectra and ab initio HF and DFT calculations of 7-chloro-5-(2-chlorophenyl)-3-hydroxy-2,3-dihydro-1H-1,4-benzodiazepin-2-one.

 Spectrochim. Acta Part A Mol. Biomol. Spectrosc. 120: 185–194.
- [12] Subramanian, N., Sundaraganesan, N., Jayabharathi, J. (2010). Molecular structure, spectroscopic (FT-IR, FT-Raman, NMR, UV) studies and first-order molecular hyperpolarizabilities of 1,2-bis(3-methoxy-4-hydroxybenzylidene) hydrazine by density functional method. Spectrochim. Acta Part A Mol. Biomol. Spectrosc. 76(2): 259–269.
- [13] Fathima Rizwana, B., Prasana, J.C., Muthu, S. (2017). Spectroscopic investigation (FT-IR, FT-Raman, UV, NMR), Computational analysis (DFT method) and Molecular docking studies on 2-[(acetyloxy) methyl]- 4-(2-amino-9h-purin-9-yl) butyl acetate. Int. J. Mater. Sci. 12:196-216.

- [14] Walker, M., Harvey, A. J. A., Sen, A., Dessent, C. E. H. (2013). Performance of M06, M06-2X, and M06-HF Density Functionals for Conformationally Flexible Anionic Clusters: M06 Functionals Perform Better than B3LYP for a Model System with Dispersion and Ionic Hydrogen-Bonding Interactions. J. Phys. Chem. A. 117(47): 12590–12600.
- [15] Klamt, A., Moya, C., Palomar, J. (2015). A Comprehensive Comparison of the IEFPCM and SS(V)PE Continuum Solvation Methods with the COSMO Approach. J. Chem. Theory Comput. 11(9): 4220–4225.
- [16] Sagaama, A., Noureddine, O., Brandán, S. A., Jędryka, A. J., Flakus, H. T., Ghalla, H., Issaoui, N. (2020). Molecular docking studies, structural and spectroscopic properties of monomeric and dimeric species of benzofurancarboxylic acids derivatives: DFT calculations and biological activities. J. compbiolchem. 107311.
- [17] Weinhold, F., Landis, C.R., (2005). Valency and Bonding: a Natural Bond Orbital Donor-acceptor Perspective, Cambridge University Press, Cambridge.
- [18] Sıdır, İ., Sıdır, Y. G., Kumalar, M., Taşal, E. (2010). Ab initio Hartree–Fock and density functional theory investigations on the conformational stability, molecular structure and vibrational spectra of 7-acetoxy-6-(2,3-dibromopropyl)-4,8-dimethylcoumarin molecule. J. Mol.Struct. 964(1-3): 134–151.
- [19] Jayabharathi, J., Thanikachalam, V., Jayamoorthy, K., Venkatesh Perumal, M. (2012). Computational studies of 1,2-disubstituted benzimidazole derivatives. Spectrochim. Acta Part A Mol. Biomol. Spectrosc. 97:131–136.
- [20] Rajagopalan, N. R., Krishnamoorthy, P., Jayamoorthy, K., Austeria, M. (2016). Bis (thiourea) strontium chloride as promising NLO material: An experimental and theoretical study. Karbala Inter.J. Mod. Sci. 2(4): 219–225.

- [21] Issaoui, N., Ghalla, H., Muthu, S., Flakus, H. T., Oujia, B. (2015). Molecular structure, vibrational spectra, AIM, HOMO–LUMO, NBO, UV, first order hyperpolarizability, analysis of 3-thiophenecarboxylic acid monomer and dimer by Hartree–Fock and density functional theory. Spectrochim. Acta A Mol. Biomol. Spectrosc. 136 C: 1227-1242.
- [22] Ayers, P. W., Parr, R. G. (2000). Variational Principles for Describing Chemical Reactions: The Fukui Function and Chemical Hardness Revisited. J. Am. Phys. Soc. 122(9): 2010–2018.
- [23] Ramalingam, S., Karabacak, M., Periandy, S., Puviarasan, N., Tanuja, D. (2012). Spectroscopic (infrared, Raman, UV and NMR) analysis, Gaussian hybrid computational investigation (MEP maps/HOMO and LUMO) on cyclohexanone oxime. Spectrochim. Acta A Mol. Biomol. Spectrosc. 96: 207–220.
- [24] Rizwana B., F., Muthu, S., Prasana, J. C., Abraham, C. S., Raja, M. (2018). Spectroscopic (FT-IR, FT-RAMAN) Investigation, Topology (ESP, ELF, LOL) analyses, Charge Transfer Excitation and Molecular docking (DENGUE, HCV) studies on Ribavirin. Chem. Data Collections. 17–18: 236–250.
- [25] Lipinski, C. A. (2004). Lead- and drug-like compounds: the rule-of-five revolution. Drug Discov. Today Technol. 1(4): 337–341.
- [26] Thomas, R., Mary, Y. S., Resmi, K. S., Narayana, B., Sarojini, B. K., Vijayakumar, G., Van Alsenoy, C. (2019). Two neoteric pyrazole compounds as potential anti-cancer agents: Synthesis, electronic structure, physico-chemical properties and docking analysis. J. Mol. Struct. 1181: 455–466.
- [27] Beaula, T. J., Joe, I. H., Rastogi, V. K., Jothy, V. B. (2015). Spectral investigations, DFT computations and molecular docking studies of the antimicrobial 5-nitroisatin dimer. Che. Phy. Lett. 624: 93–101.

- [28] Berman, H. M., Westbrook, J., Feng, Z., Gilliland, G., Bhat, T.N., Weissig, H., Shindyalov, I.N., Bourne, P.E. (2000). The protein data, Nucleic Acids Res. 28 (1): 235-242.
- [29] Morris, G. M., Huey, R., Olson, A. J. (2008). Using AutoDock for Ligand-Receptor Docking. Curr. Protoc. Bioinf. 24 (8.14): 1-40.

CHAPTER IV

SPECTROSCOPIC EXPOSITION (FT-IR, FT-RAMAN), EVALUATION OF ELECTRONIC PROPERTIES IN DIFFERENT SOLVENTS AND MOLECULAR DOCKING STUDIES OF 5CHLORO-2-HYDROXYPYRIDINE - INSULYSIN INHIBITOR

4.1 INTRODUCTION

Heterocyclic mixtures are significant in the field of natural science and organic chemistry as they are predominant among the sorts of mixtures utilized as medications, veterinary items and agrochemicals [1]. Pyridine nucleus is present in many biologically noteworthy compounds used in drugs [2,3]. Pyridines have additionally routinely been utilized as ligands for metals in natural blend, and furthermore utilized as chiral ligands for transition metals [4,5]. Because of the biological significance of pyridine derivatives, a variety of synthetic approaches for constructing the pyridine ring and forming its derivatives have been created. [6,7]. One of the pyridine derivatives is 5-chloro-2-hydroxypyridine (5C2HOP) with molecular formula C₅H₄ClNO has molecular weight of 129.54 has been chosen here for quantum mechanical study. The DFT approach was used to investigate the structural parameters of the heading molecule, as these methods have become progressively popular for demonstrating molecular properties such as symmetry structures, frequencies of vibrations and intensities. [8]. The FT- IR and FT-Raman spectral investigations were performed for the heading compound by using B3LYP/6-311++G(d,p) set. In the existing study, the experimentally attained frequencies of vibrations were compared with the calculated wavenumbers. Full outlines of the heading molecule's geometry, motions and electronic attributes have also been computed. MEP, LOL, ELF, HOMO, LUMO and Fukui functions are among the molecular characteristics that have been determined and stated. The charge transfer and intramolecular relations within the molecule were scrutinized using NBO analysis and Mulliken atomic charges were also calculated. The eco-friendly solvents namely water, DMSO, ethanol and acetone which lies in utilisable categorizing [9] were opted to report the solvent influence of 5C2HOP. Docking studies of 5C2HOP along with drug likeness and environmental toxicity properties have also been accomplished.

4.2 RESULTS AND DISCUSSION

4.2.1 Geometrical Parameters

The optimized parameters were estimated in eco-friendly solvents and are recorded in Table 4.1. The crystal data of very closely related molecules [10,11] are compared with that of the heading molecule. The molecular skeletal of 5C2HOP with the numbering system of the atoms is exposed in Figure 4.1. This molecule has four C-C bond lengths, two C-N bond lengths, three C-H bond lengths, one C-O bond length, one C-Cl bond length and one O-H bond length. The average bond distances of C-C and C-H in the benzene ring are 1.392Å and 1.083Å respectively. The bond length of C-Cl is found to be significantly higher value (1.754Å) and the largest bond angle was detected at C2-C1-N6 (123.7°). Amongst the gas phase and the eco-friendly solvents, only minor variations in geometrical parameters were spotted. The bond length and bond angle were observed to have same values for the green solvents used. All the green solvents used are equally effective in deciding the structure parameters.

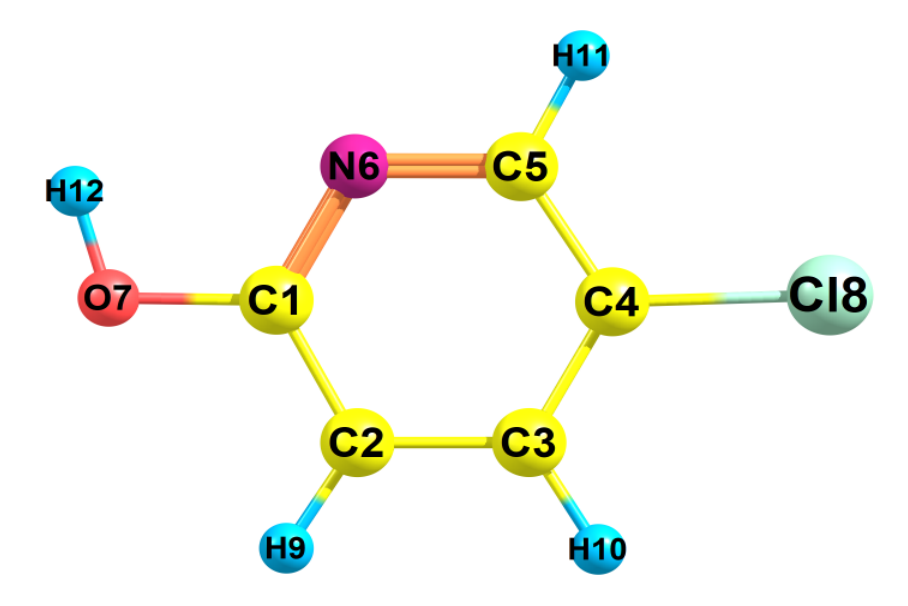


Fig 4.1 Optimised geometric structure with atom numbering of 5-Chloro-2-hydroxypyridine.

Table 4.1 Geometrical parameters of 5-Chloro-2-hydroxypyridine bond length(Å) and bond angles($^{\rm 0}$).

PARAMETER	Ermanimantal	B3LYP/6-311++G(d,p)							
BOND LENGTH(Å)	Experimental	Gas	Water	DMSO	Ethanol	Acetone			
C1-C2	1.41	1.401	1.401	1.401	1.401	1.401			
C1-N6	1.3506	1.325	1.327	1.327	1.327	1.327			
C1-O7	1.3602	1.353	1.354	1.354	1.354	1.354			
C2-C3	1.375	1.384	1.384	1.384	1.384	1.384			
С2-Н9	0.954	1.082	1.082	1.082	1.082	1.082			
C3-C4	1.397	1.396	1.396	1.396	1.396	1.396			
C3-H10	0.92	1.083	1.083	1.083	1.083	1.083			
C4-C5	1.379	1.387	1.386	1.386	1.386	1.386			
C4-C18	1.7404	1.754	1.758	1.758	1.758	1.758			
C5-N6	1.3479	1.338	1.34	1.34	1.34	1.34			
C5-H11	0.961	1.084	1.084	1.084	1.084	1.084			
O7-H12	0.903	0.967	0.968	0.968	0.968	0.968			
BOND ANGLE (0)									
C2-C1-N6	121.73	123.7	123.7	123.7	123.7	123.7			
C2-C1-O7		118.6	118.4	118.4	118.4	118.4			
C1-C2-C3	119.39	117.8	117.9	117.9	117.9	117.9			
C1-C2-H9	120.8	120.3	120.5	120.5	120.5	120.5			
N6-C1-O7		117.7	117.9	117.9	117.9	117.9			
C1-N6-C5	118.11	118.4	118.3	118.3	118.3	118.3			
C1-O7-H12		107	107.9	107.9	107.9	107.9			
С3-С2-Н9	119.8	122	121.6	121.6	121.6	121.6			

C2-C3-C4	118.55	118.7	118.5	118.5	118.5	118.5
C2-C3-H10	121.5	120.9	120.7	120.7	120.7	120.7
C4-C3-H10	119.9	120.4	120.8	120.8	120.8	120.8
C1-C2-C3	119.23	119.2	119.5	119.5	119.5	119.5
C3-C4-C18	120.45	120.6	120.5	120.5	120.5	120.5
C5-C4-C18	120.31	120.2	120	120	120	120
C4-C5-N6	122.98	122.2	122	122	122	122
C4-C5-H11	120.5	120.8	121	121	121	121
N6-C5-H11	116.5	117	117	117	117	117

^{*}Ref [10,11]

4.2.2 Vibrational Investigation

The heading compound consists of 12 atoms with 30 normal modes of vibration. The theoretical values obtained from computational methods are compared to the experimental FT-RAMAN and FT-IR results. Modes of vibration along with the reckoned frequencies in various solvents and PED assignments are represented in Table 4.2. PED calculations express the relative contributions of the redundant internal coordinates to each normal vibrational mode of the molecule and thus make it conceivable to define the character of each mode numerically. Slight variations in the frequencies were observed for the heading molecule between the gas phase and the other solvents. Figure 4.2 and Figure 4.3 shows the relative depictions of theoretically obtained and experimental FT-IR and FT-Raman spectra correspondingly.

C-C bands have a stronger effect on aromatic ring modes. The C-C vibrations due to stretching are projected within the zone 1650-1100 cm⁻¹ [12-14]. In the current analysis, the bands were identified at 1379, 1230, 1037 cm⁻¹ in FT-IR spectrum and at 1380, 1239, 1041 cm⁻¹ at FT-Raman spectrum. The determined estimates of C-C stretching vibrations are detected theoretically between 1378 and 1074 cm⁻¹.

The C-H stretching vibration lies in the zone 3100 – 3000 cm⁻¹ [15]. Experimentally, the C-H vibrations for the heading molecule were detected at 3058 cm⁻¹ and 3059 cm⁻¹ in in FT-IR and FT-Raman spectra correspondingly. Theoretical method showing peak matching to C-H stretching vibration is detected in the range 3086 cm⁻¹ and 3055 cm⁻¹. This vibration corresponds to a PED that contributes 100%.

Detection of the C-N stretching vibration in a composite area is a hectic mission [16]. The vibrations relating to this stretching possibly occur in the range 1400 – 1200 cm⁻¹ [17]. In the existing analysis, the bands are noticed at 1552, 1437, 1379, 1179, 1230 cm⁻¹ in FT-IR and 1551, 1442, 1380, 1239 cm⁻¹ in FT-Raman. With a maximum PED contribution of 35 percent, the theoretically ascended wavenumbers are measured from 1554 cm⁻¹ to 1246 cm⁻¹.

Generally aromatic chloro compounds have a C-Cl stretching provides sturdy vibration in the region 850 – 550 cm⁻¹ [18]. For the heading compound the vibrations are ascribed at 639 and 372 cm⁻¹ and experimentally the peak is detected at 673 cm⁻¹ in FT-IR spectrum.

The stretching vibrations of C-O are in the 1300–1000 cm⁻¹ range. [19]. The theoretical method detects the peaks corresponding to this vibration at 1267, 831, 639 cm⁻¹ in this sample. The peaks are spotted at 673 cm⁻¹ in FT – IR spectrum and at 882 and 678 cm⁻¹ in the FT-Raman spectrum, theoretically.

The frequency range of the O-H stretching vibrations is 3300-3600 cm⁻¹ [20]. For the heading compound, the band agreeing to O-H stretching vibration is identified at 3631 cm⁻¹ with a PED contribution of 100%.

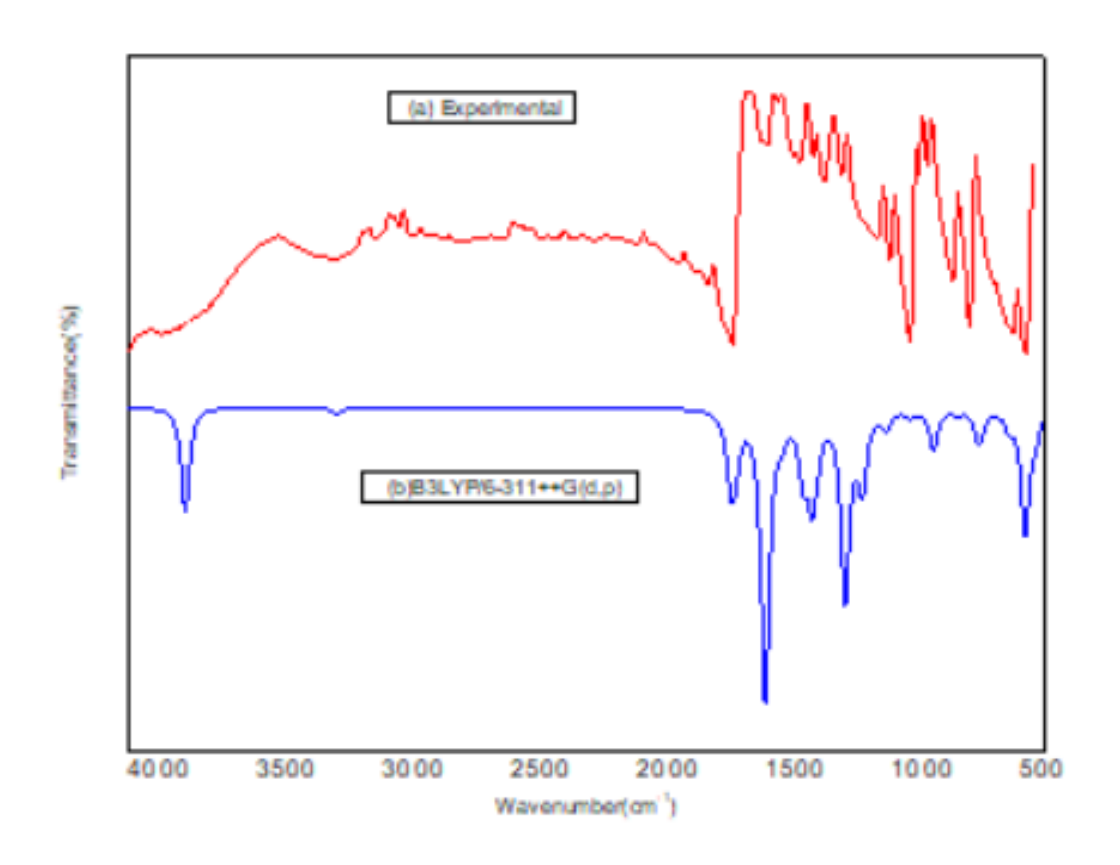


Fig 4.2 Compared theoretical and Experimental FT-IR spectrum of 5C2HOP.

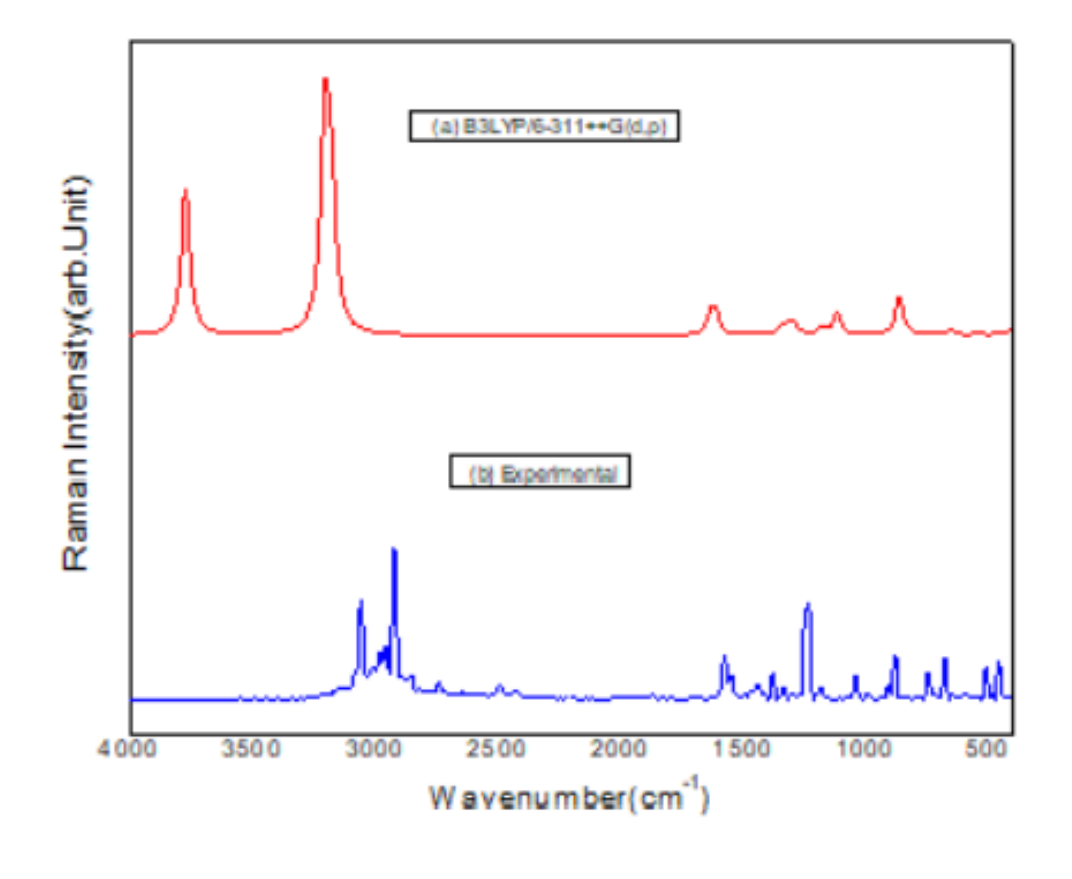


Fig 4.3 Compared theoretical and Experimental FT-Raman spectrum of 5C2HOP.

Table 4.2 Theoretical comparison of vibrational frequency of 5C2HOP in gas and in different solvents.

	Expe	rimental	I	Frequency - (Gas	Free	quency in d	ifferent sol	vents	
S.No	FT-IR	FT- RAMAN	Scaled	Intensity- IR	Intensity- RAMAN	Water	DMSO	Ethanol	Acetone	Assignment
1			3631.49	97	124	3619.30	3619.46	3619.82	3619.98	YOH (100)
2	3200	3100	3085.85	1	154	3088.48	3088.46	3088.42	3088.40	YCH (99)
3			3071.17	1	58	3076.14	3076.08	3075.95	3075.89	YCH (100)
4	3058	3059	3055.24	6	82	3057.08	3057.06	3057.02	3057.01	YCH (99)
5	1573	1577	1572.17	59	12	1567.38	1567.45	1567.61	1567.67	YCC (43)+βCNC (10)+βCCC (21)
6	1552	1551	1554.27	42	17	1546.63	1546.75	1547.01	1547.13	YNC(32)+YCC (33)
7	1437	1442	1441.71	273	1	1432.46	1432.61	1432.93	1433.07	YNC (15)+YOC (10)+βHCC (28)+βHCN(26)
8	1379	1380	1378.25	17	1	1372.25	1372.35	1372.58	1372.68	YCC (24) + YNC (17) +βHOC (16)
9	1298		1299.10	54	6	1296.70	1296.76	1296.89	1296.94	βHOC (20)+βHCC (18)+βHCN (38)
10			1266.51	74	7	1252.59	1252.82	1253.31	1253.53	YNC (25)+YOC (42)+βHCC (12)
11	1230	1239	1245.70	25	9	1244.44	1244.48	1244.57	1244.61	YNC (35)+YCC (30)+βHCC (11)+βHCN(10)
12	1179		1139.78	175	6	1129.45	1129.61	1129.96	1130.12	ΥNC (19)+βHOC (40)+βHCC(10)
13			1096.13	10	1	1094.27	1094.41	1094.71	1094.84	YCC (17)+βHCC (63)
14	1037	1041	1074.36	66	16	1068.79	1068.89	1069.09	1069.18	YCC(44)+YClC (16)
15	992		984.87	16	1	981.13	981.18	981.30	981.36	βCCC (61)+βNCC (20)
16	902	908	935.38	0	0	942.74	942.64	942.43	942.33	τHCCC(86)
17	882		895.94	6	0	896.81	896.80	896.78	896.77	τHCNC(77)+ τCNCC(14)
18		882	830.90	1	31	827.34	827.40	827.51	827.57	YOC (15) +βCCC (47)+βNCC (14)
19	847		806.59	37	0	806.88	806.93	807.02	807.06	τHCCC(72)+ ωOCNC(17)
20	742	746	719.93	5	0	720.41	720.41	720.40	720.39	τHCCC(10)+τCNCC(36)+τCCCC(15)+τNCCC(12)
	=			_	-					+ωOCNC(22)

	Expe	rimental	Frequency - Gas			Freq	quency in d	ifferent sol	vents	
S.No	FT-IR	FT- RAMAN	Scaled	Intensity- IR	Intensity- RAMAN	Water	DMSO	Ethanol	Acetone	Assignment
21	673	678	639.11	25	1	634.07	634.14	634.30	634.37	ΥΟC (16) + YCIC (28) +βCNC (23)+βOCN (10)
22			625.68	11	4	623.70	623.73	623.79	623.81	βCNC (22)+βCCC (15)+βNCC (34)
23	509	511	521.13	15	2	509.83	509.96	510.23	510.35	τHOCC(24)+ τCCCC(16)
24		459	460.50	115	1	435.12	435.65	436.79	437.29	τHOCC(73)
25			424.26	20	1	421.46	421.50	421.59	421.63	βCNC (13)+βOCN (56)
26			413.85	1	0	412.59	412.60	412.62	412.63	τHCNC(10)+ τCNCC(33)+ τCCCC(29)+ τNCCC(12)
27			372.37	1	10	371.14	371.16	371.19	371.21	YCIC (48) +βCNC (17)
28			307.27	0	0	307.02	307.01	307.00	307.00	τNCCC(15)+ωClCCC(56)+ωOCNC(17)
29			249.91	1	1	249.08	249.10	249.13	249.15	βOCN (12)+βCICC (80)
30			116.36	0	0	116.08	116.08	116.08	116.08	τCCCC(19)+ τNCCC(50)+ωClCCC(22)

Υ -stretching, β- in plane bending, ω – out plane bending, τ - torsion

4.2.3 Donor – Acceptor Interaction

The charge shift within the molecule is used to examine the molecular interactions occurring in a molecule. The donor-acceptor interactions were reckoned using second order Fock matrix [21,22]. The connections lead to the contribution of occupancy from the localized Lewis structure into the empty non-Lewis orbitals [23]. The stabilisation energy linked with the delocalization $i\rightarrow j$ is attained as E(2) for each donor(i) and acceptor(j) [24,25]. The NBO computations were achieved for 5C2HOP involving the basis set as mentioned earlier. The stabilization energy E(2), bonding and antibonding of 5C2HOP are obtained and tabulated in Table 4.3. The delocalization of electron from σ (C1- N6) deliver to σ *(C1- C2) and from π (C1-N6) deliver to π *(C2-C3) resulted in the stabilization energy of 1.86 kcal /mol and 11.89 kcal /mol correspondingly. The strong delocalization of 27.08 kJ/mol is observed from π (C2-C3) to π *(C1-N6) for the heading molecule. The other interactions involve the electron donations from lone pairs of N6, O7 and Cl8 to the σ * and π * orbitals. The LP (3) C1 \rightarrow π *(C4–C5) shows intense interactions with the electron density of 0.35e and stabilization energy of 13.93 k cal/mol in 5C2HOP molecule.

Table 4.3 Second order perturbation theory analysis of Fock matrix in NBO for 5C2HOP.

Donor	Туре	ED/e(qi)	Acceptor	Туре	ED/e(qi)	E(2) kcal/mol	E(j)- E(i) a.u.	F(i,j) a.u.
C 1-C 2	σ	1.9841	C 1-N 6	σ*	0.03605	1.57	1.21	0.039
C 1-N 6	σ	1.98568	C 1-C 2	σ*	0.03549	1.86	1.32	0.045
C 1-N 6	π	1.72282	C 2-C 3	π*	0.28812	11.89	0.31	0.055
C 1-N 6	π	1.72282	O 7-H 12	σ*	0.0085	1.01	0.69	0.025
C 1-O 7	σ	1.99411	C 1-C 2	σ*	0.03549	0.64	1.44	0.027
C 2-C 3	σ	1.97327	C 1-C 2	σ*	0.03549	1.77	1.22	0.042
C 2-C 3	π	1.7011	C 1-N 6	π*	0.4048	27.08	0.25	0.076
C 2-H 9	σ	1.97962	C 1-N 6	σ*	0.03605	4.08	1.02	0.058
C 3-C 4	σ	1.97831	C 2-C 3	σ*	0.01182	1.76	1.24	0.042
C 3-H 10	σ	1.98231	C 1-C 2	σ*	0.03549	3.19	1.04	0.052
C 4-C 5	σ	1.98159	C 3-C 4	σ*	0.0334	4.06	1.29	0.065
C 4-C 5	π	1.70028	C 1-N 6	π*	0.4048	11.72	0.28	0.053
C 4-Cl 8	σ	1.98858	C 2-C 3	σ*	0.01182	1.52	1.28	0.039
C 5-N 6	σ	1.97669	C 1-N 6	σ*	0.03605	0.53	1.3	0.024
C 5-H 11	σ	1.97503	C 1-N 6	σ*	0.03605	4.23	0.99	0.058
O 7-H 12	σ	1.97029	C 1-C 2	σ*	0.03549	2.46	1.23	0.049
O 7-H 12	σ	1.97029	C 1-N 6	π*	0.4048	4.48	0.71	0.056
N 6	LP (1)	1.9155	C 1-C 2	σ*	0.03549	7.9	0.88	0.075
O 7	LP (1)	1.9691	C 1-N 6	σ*	0.03605	6.36	1.04	0.073
O 7	LP (1)	1.9691	C 1-N 6	π*	0.4048	0.92	0.54	0.022
O 7	LP (2)	1.90929	C 1-C 2	σ*	0.03549	5.49	0.9	0.064
O 7	LP (2)	1.90929	C 1-N 6	π*	0.4048	12.9	0.38	0.068
Cl 8	LP (1)	1.99186	C 3-C 4	σ*	0.0334	2	1.44	0.048
Cl 8	LP (2)	1.96487	C 3-C 4	σ*	0.0334	5.37	0.84	0.06
Cl 8	LP (3)	1.926	C 4-C 5	π*	0.32801	13.93	0.35	0.067
C 1-N 6	π*	0.4048	C 2-C 3	π*	0.28812	156.63	0.02	0.081
C 1-N 6	π*	0.4048	O 7-H 12	σ*	0.0085	1.1	0.4	0.041
C 2-C 3	π*	0.28812	C 4-C 5	π*	0.32801	115.4	0.02	0.074

4.2.4 FMO Analysis

The difference among HOMO and LUMO which gives the excitation energy of a molecule helps in spotting the chemical steadiness of a molecule [26]. Table 4.4 indicates the calculated values of global descriptors of 5C2HOP in different solvents. Amongst the gas phase and the solvents, significant variations in the molecule's HOMO-LUMO orbitals were observed. For 5C2HOP, in gas phase, the higher value of chemical hardness (2.666873) exposes that compound is chemically stable, and the softness value being 0.187486 specifies the harmless nature of the compound. The energy gap, ionisation potential and electron affinity of 5C2HOP in gas phase are found to be 5.333746eV, 6.844534 eV and 1.510788 eV respectively. As compared to the solvents' molecular descriptors, water has the topmost energy gap (5.553891eV) with chemical hardness as 2.776946 and lowest chemical softness as 0.180054. Among the green solvents, water possess higher value of ionisation potential (7.210801) whereas acetone possess a lower value of 7.20998. The illustrative image of HOMO and LUMO for 5C2HOP is displayed in Figure 4.4.

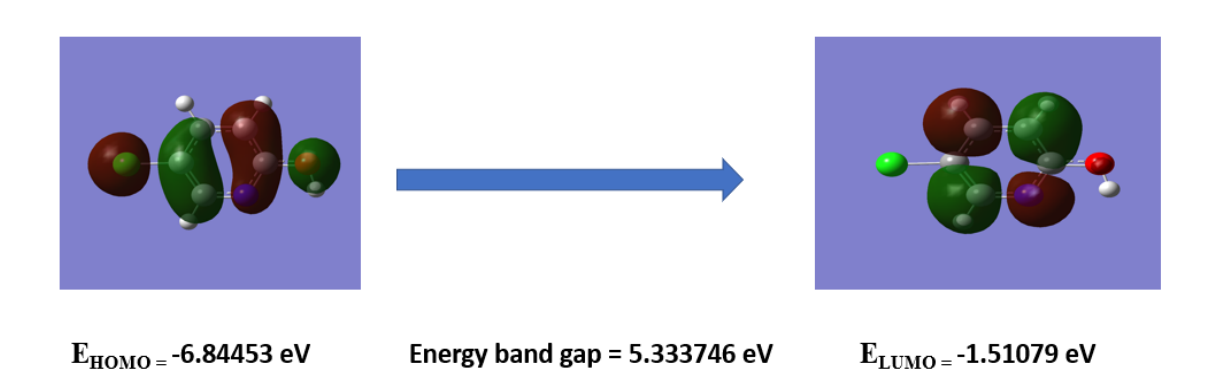


Fig 4.4 Atomic orbital HOMO - LUMO composition of the frontier molecular orbital of 5C2HOP

Table 4.4 Calculated energy values of 5-Chloro-2-hydroxypyridine with solvation effect.

Parameters	Gas	Water	DMSO	Ethanol	Acetone
HOMO(eV)	-6.84453	-7.2108	-7.21053	-7.21026	-7.20998
LUMO(eV)	-1.51079	-1.65691	-1.65718	-1.65773	-1.65773
Ionization potential	6.844534	7.210801	7.210529	7.210258	7.20998
Electron affinity	1.510788	1.65691	1.65718	1.657731	1.65773
Energy gap(eV)	5.333746	5.553891	5.553349	5.552527	5.55225
Electronegativity	4.177661	4.433856	4.433855	4.433994	4.433855
Chemical potential	-4.17766	-4.43386	-4.43385	-4.43399	-4.43386
Chemical hardness	2.666873	2.776946	2.776675	2.776263	2.776125
Chemical softness	0.187486	0.180054	0.180072	0.180098	0.180107
Electrophilicity index	3.272156	3.539694	3.540038	3.540785	3.540739
Electronic charge	1.566502	1.596666	1.596822	1.597109	1.597138
Electron donating capability (w-)	5.694346	6.10374	6.104049	6.104815	6.104682
Electron accepting capability (w+)	1.516685	1.669884	1.670195	1.670821	1.670827

4.2.5 Electronic Analysis

The energetic and standing properties of molecules in their higher states are premeditated using UV-Visible spectroscopy. [27]. TD-DFT technique was employed to calculate theoretically the electronic transition spectra of 5C2HOP for eco-friendly solvents with IEFPCM solvation mode [28]. The absorption wavelength, oscillator strength, transition contribution % and transition energy reckoned for different solvents (water, DMSO, ethanol, acetone) are presented in Table 4.5. The theoretical UV spectrums for different green solvents are depicted in Figures 4.5a, 4.5b, 4.5c, 4.5d. The highest absorption peak for water was 241.835nm with band gap energy 5.13eV whereas for DMSO, ethanol and acetone, it was 242.104nm, 242.00nm and 242.014 nm respectively with identical band gap energy of 5.12eV. Slight variations in oscillatory strength were found among the different solvents used.

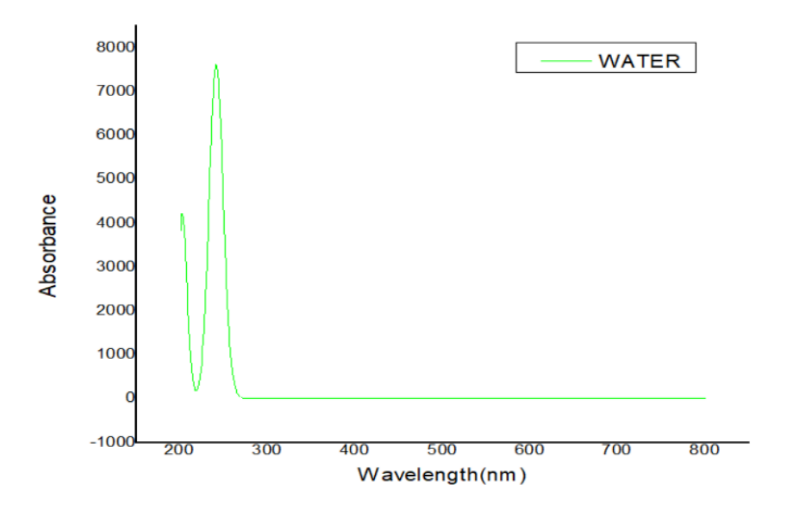


Fig 4.5a Theoretical UV spectra of 5C2HOP in Water.

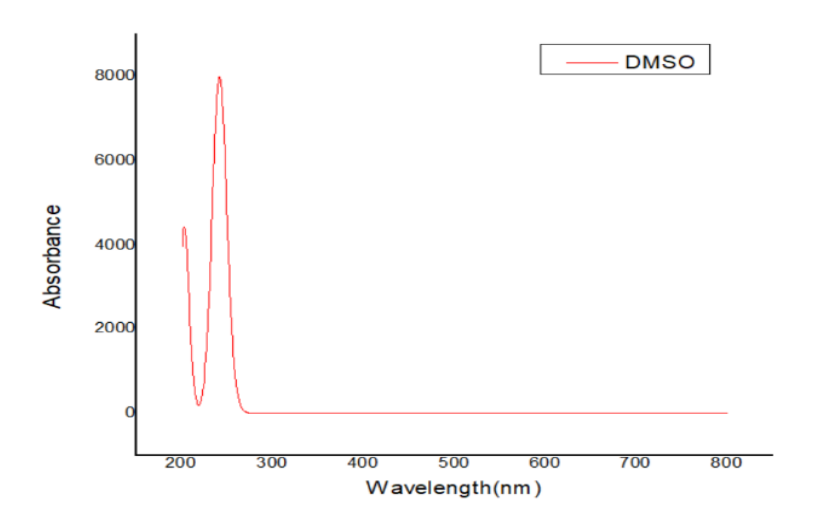


Fig 4.5b Theoretical UV spectra of 5C2HOP in DMSO.

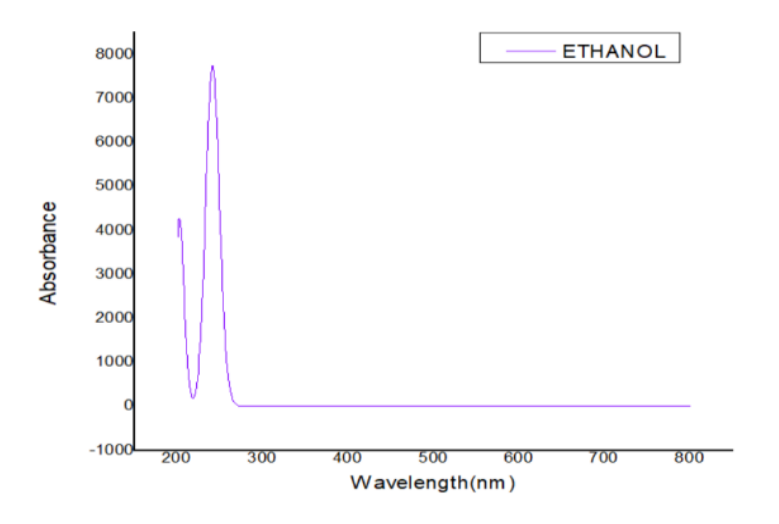


Fig 4.5c Theoretical UV spectra of 5C2HOP in Ethanol.

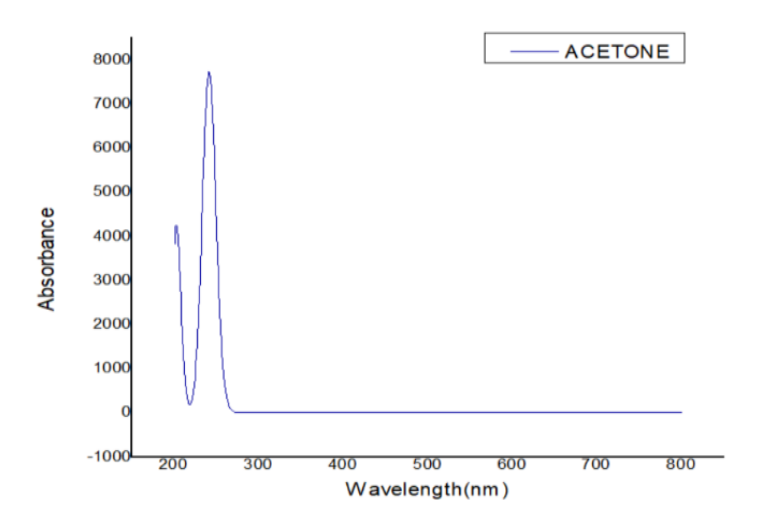


Fig 4.5d Theoretical UV spectra of 5C2HOP in Acetone.

Table 4.5 Theoretical electronic transition parameters of 5C2HOP in different solvents.

Solvents	Wavelength (nm)	Band gap (ev)	Energy (cm ⁻¹)	Osc. Strength(f)	Symmetry	Major contributions
WATER	241.8354393	5.13	41350.43247	0.095	Singlet-A	H-2->LUMO (10%), HOMO- >LUMO (79%)
	233.4039778	5.31	42844.17127	0.0188	Singlet-A	H-2->LUMO (84%)
DMSO	242.1046123	5.12	41304.45886	0.1001	Singlet-A	HOMO->LUMO (80%)
	233.5754658	5.31	42812.71565	0.0194	Singlet-A	H-2->LUMO (84%)
ETHANOL	242.00065	5.12	41322.20306	0.096	Singlet-A	H-2->LUMO (10%), HOMO- >LUMO (79%)
	233.6899312	5.31	42791.74523	0.0197	Singlet-A	H-2->LUMO (83%)
ACETONE	242.0148214	5.12	41319.7834	0.0956	Singlet-A	H-2->LUMO (10%), HOMO- >LUMO (79%)
	233.7648347	5.3	42778.03381	0.0199	Singlet-A	H-2->LUMO (83%)

4.2.6 Reactive Site Analysis

MEP denotes the force working on a proton at a given point in the locality of a molecule through the electrical charge cloud and nuclei [29]. The red area of the MEP designates electrophilic reactivity whereas the blue region specifies the nucleophilic reactivity and green region specifies neutral sites [30]. For the heading molecule, the hydrogen atoms are displayed in the region of positive potential whereas nitrogen atom is exhibited in the region of negative potential. The Figure 4.6 indicates the colour code at the region from -5.223 eV to +5.223 eV.

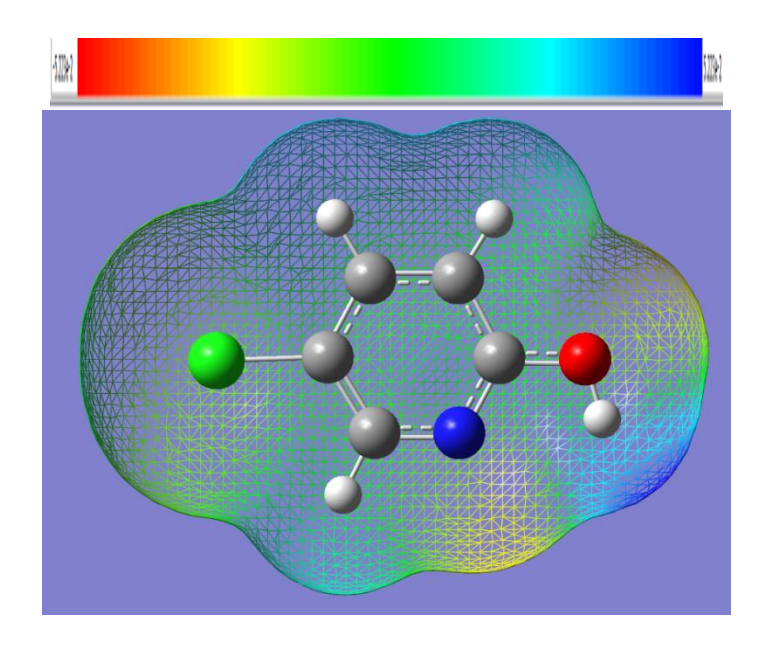


Fig 4.6 Molecular Electrostatic Potential of 5-Chloro-2-hydroxypyridine.

4.2.7 Population and molecular reactivity study

The various factors like electronic structure and molecular polarizability are affected by atomic charges [31]. The Mulliken charge distribution is estimated for 5C2HOP in gas and in different solvents (water, DMSO, ethanol and acetone) and presented in Table 4.6. The intended Mulliken atomic charge distribution for the heading compound is represented in Figure 4.7 which reveals that the atomic charges on carbon atoms were spotted to be both positive and negative while all the hydrogen atoms are positively charged in gas as well as in various solvents mentioned earlier. The different solvents show noticeable variations in the Mulliken charges when related with gas phase. Also, we can observe that in gas phase and also in other solvents used, the maximum atomic charge is attained for C4 atom.

The derivative of the electron density to the number of electrons at a continual potential is identified as Fukui function [32]. The Fukui functions on the r^{th} atomic site [33] for free radical f_r^0 , for an electrophilic f_r^- and nucleophilic f_r^+ and dual descriptor $\Delta f(r)$ are estimated along with mulliken atomic charges and local softness for all the atomic sites for 5C2HOP and have been presented in Table 4.7. It is found that C1, C2, C4 are the spots for nucleophilic occurrence and C3, C5, N6, O7, C18, H9, H10, H11,

H12 are the spots for electrophilic occurrence. The value of local softness being maximum at C2 = 0.056768.

Table 4.6 Mulliken charge distribution of 5C2HOP in gas and other solvents.

Atom	Mulliken charge distribution				
	Gas	Water	DMSO	Ethanol	Acetone
1 C	-0.37413	-0.33766	-0.33827	-0.33958	-0.34015
2 C	0.256319	0.237651	0.237861	0.23832	0.238527
3 C	-0.38978	-0.3945	-0.39448	-0.39442	-0.3944
4 C	0.362271	0.37684	0.3766	0.376088	0.375862
5 C	-0.70208	-0.69836	-0.69835	-0.69833	-0.69833
6 N	-0.11804	-0.18088	-0.1799	-0.17781	-0.17689
7 O	-0.22648	-0.2748	-0.2741	-0.27258	-0.2719
8 Cl	0.33352	0.314376	0.314597	0.315078	0.315294
9 H	0.209885	0.235184	0.234854	0.23414	0.23382
10 H	0.188628	0.220643	0.220199	0.219242	0.218815
11 H	0.177086	0.18776	0.187654	0.187421	0.187315
12 H	0.28279	0.313742	0.313329	0.312435	0.312036

12 H 11 H 10 H 9 H 8 CI Acetone 7 0 Ethanol 6 N **■** DMSO 5 C ■ Water 4 C Gas 3 C 2 C 1C -0.8 -0.6 -0.4 -0.2 0.2 0.4 0.6 Mulliken charges

Figure 4.7 The histogram of calculated Mulliken Charges of 5C2HOP.

Table 4.7 Mulliken charge distribution, Fukui function and local softness corresponding to (0,1), (-1,2) and (1,2) charge and multiplicity of 5C2HOP.

	Mu	lliken atomic ch		Fukui fu	ınctions	local softness				
Atom	0, 1 (N)	N +1 (-1, 2)	N-1 (1,2)	f_r^+	f_r^-	f_r^{0}	Δf(r)	$s_r^+ f_r^+$	$s_r^- f_r^-$	$s_r^0 f_r^0$
1 C	-0.3741	-0.113145	-0.372041	0.260984	-0.00209	0.12945	0.26307	0.04893	-0.00039	0.02427
2 C	0.25632	0.559106	0.37527	0.302787	-0.11895	0.09192	0.42174	0.05677	-0.0223	0.017233
3 C	-0.3898	-0.797471	-0.355247	-0.4077	-0.03453	-0.22111	-0.37317	-0.07644	-0.00647	-0.04146
4 C	0.36227	0.568501	0.335357	0.20623	0.02691	0.11657	0.17932	0.03867	0.005046	0.021856
5 C	-0.7021	-0.753458	-0.667185	-0.05138	-0.03489	-0.04314	-0.01649	-0.00963	-0.00654	-0.00809
6 N	-0.118	-0.231209	-0.008045	-0.11317	-0.10999	-0.11158	-0.00318	-0.02122	-0.02062	-0.02092
7 O	-0.2265	-0.23507	-0.096872	-0.00859	-0.1296	-0.0691	0.12101	-0.00161	-0.0243	-0.01296
8 Cl	0.33352	0.19697	0.646286	-0.13655	-0.31277	-0.22466	0.17622	-0.0256	-0.05864	-0.04212
9 H	0.20989	-0.002246	0.295296	-0.21213	-0.08541	-0.14877	-0.12672	-0.03977	-0.01601	-0.02789
10 H	0.18863	0.106619	0.263522	-0.08201	-0.07489	-0.07845	-0.00712	-0.01538	-0.01404	-0.01471
11 H	0.17709	0.089419	0.256284	-0.08767	-0.0792	-0.08343	-0.00847	-0.01644	-0.01485	-0.01564
12 H	0.28279	-0.388015	0.327373	-0.67081	-0.04458	-0.35769	-0.62622	-0.12577	-0.00836	-0.06706

4.2.8 ELF and LOL studies

ELF demonstrates the electron pair density and LOL just displays the utmost localized orbitals coinciding because of the orbital gradients [34,35]. Multiwfn program was exercised to generate the mapping figures of ELF & LOL in order to examine the electronic wave functions. The Figures 4.8a & 4.8b represents the colour and contour filled maps of ELF and Figures 4.9a & 4.9b symbolises the colour and contour filled maps of LOL. The existence of bonding and nonbonding electrons are evidenced from the colour shades of ELF and LOL maps. The presence of bonding and nonbonding electrons is exposed by the red colour over the hydrogen atoms with the highest value whereas blue colour over the carbon atoms specifies low electron localization values which reveals the zone of electronic exhaustion between the inner and the valance layer.

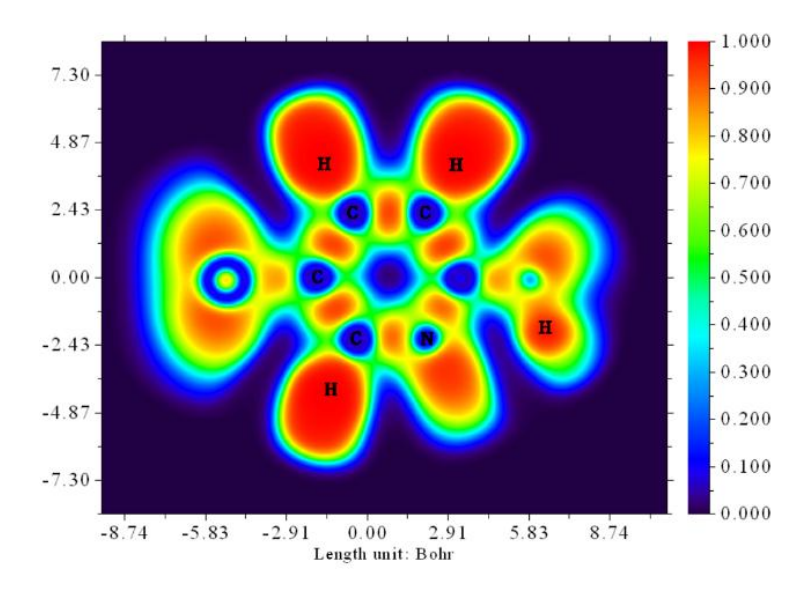


Fig 4.8a ELF, Colour filled map of 5C2HOP.

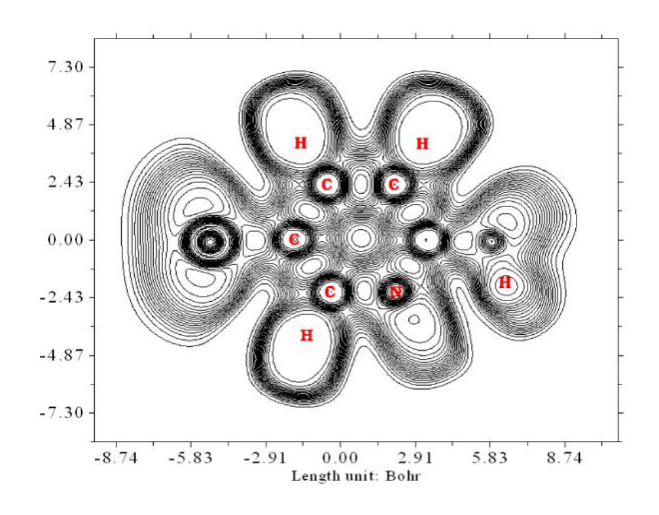


Fig 4.8b ELF, Contour map of 5C2HOP.

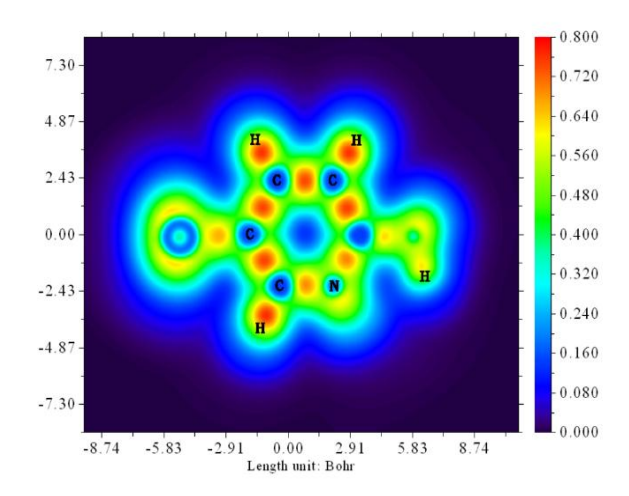


Fig 4.9a LOL, Colour filled map of 5C2HOP.

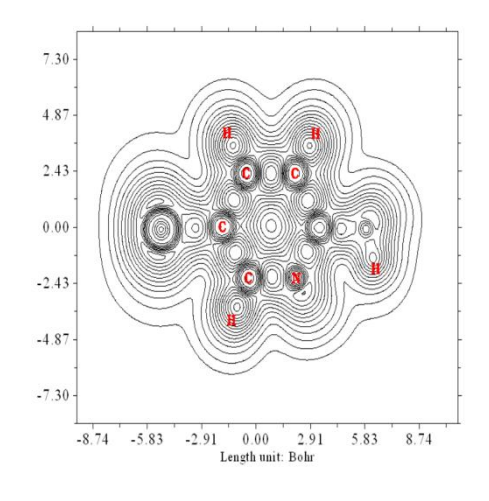


Fig 4.9b. LOL, Contour map of 5C2HOP.

4.2.9 Biological Assessment

4.2.9.1 Pharmacological analyses

Drug likeness of the heading molecule is examined in order to estimate its probable capacity to be expended as an active constituent in some new pharmacological products. The number of hydrogen bond donors and acceptors, AlogP, number of rotatable bonds, PSA and molar refractivity are the various drug likeness parameters included in this work. Table 4.8 reveals the estimates of these parameters. The drug likeness of the molecule should possess estimates in acquiescence with the Lipinski's rule of five so as to accept a molecule as a potential drug [36,37]. One of the most significant parameters, AlogP is equal to 1.67 and TPSA for the heading compound is found to be 33.12Å². Most of the criteria are contented by the heading molecule to behave as a drug. The bio activity predictions from environmental toxicity like GPCR ligand, ion channel, nuclear receptor ligand, kinase inhibitor, enzyme inhibitor and protease inhibitor possess values -2.95, -2.48, -3.29, -2.94, -2.36 and -3.21 respectively.

Table 4.8 Drug likeness parameters of 5C2HOP.

Descriptor	Value
Hydrogen Bond Donor (HBD)	1
Hydrogen Bond Acceptor (HBA)	2
AlogP	1.67
Topological polar surface area (PSA)	33.12
Molar refractivity	129.55
Number of atoms	8
Number of rotatable bonds	0

4.2.9.2 Docking studies

Molecular docking is an influential computational tool used to examine the ligand confirmation within the binding site of protein targets. AutoDock set 4.2.6 is the recently used software tool used to investigate the molecular activity of protein-ligand connections [38]. The heading compound was docked into the active spots of proteins 4DM3 and 5DU3 which are associated with Alopecia treatment and exhibiting the property as Insulysin inhibitor respectively. Using Open babel software, protein data bank output was created from the original Gaussian 09 software. The configuration of the aimed proteins were acquired from RCSB data base [39]. The pi and psi angles of the Ramachandran plot are expended to test the qualities of the chosen proteins [40,41]. Both proteins have majority of amino acid residues in the approved region as shown in Figures 4.10a & 4.10b. The molecular docking factors like inhibition constant (mmol), binding energy(kcal/mol) and intermolecular energy (kcal/mol) of the molecule pertaining to the aimed proteins were obtained and listed in Table 4.9. The binding orientations of 5C2HOP with the aimed proteins are shown in Figure 4.11 and Figure 4.12. In both interactions, minimum binding energy of -4.02 kcal/mol were spotted. The intermolecular energy of -4.32 k cal / mol and -4.31 k cal / mol correspondingly were obtained for the interactions.

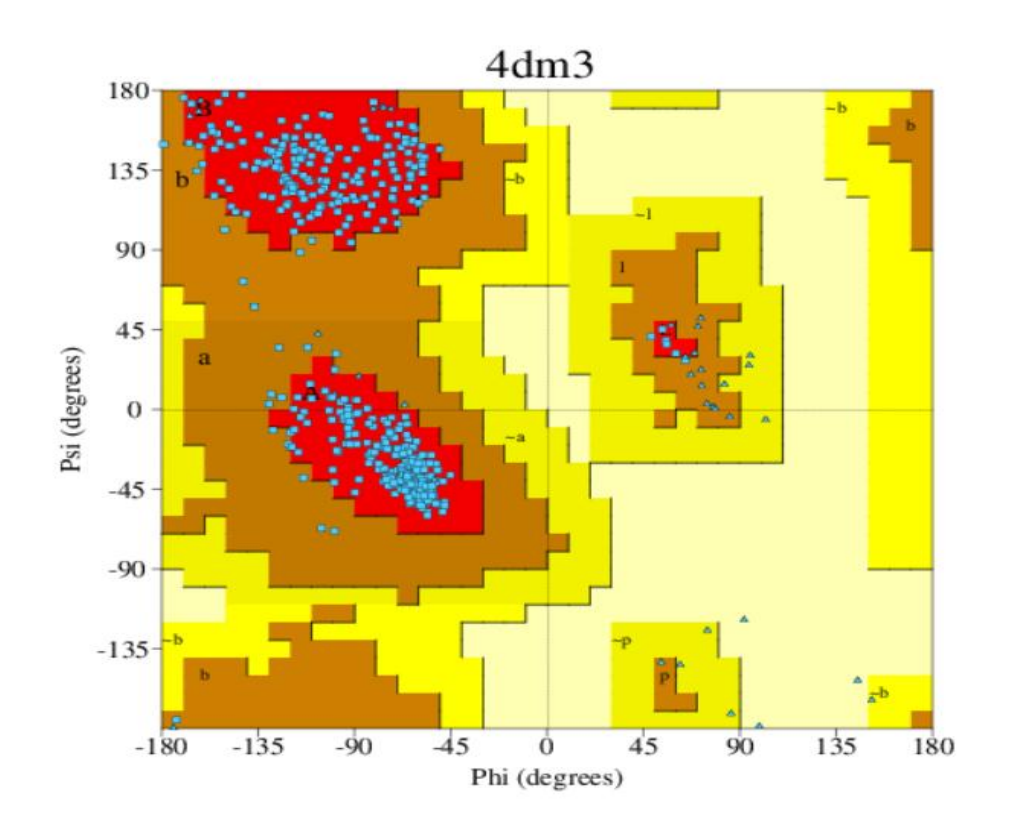


Figure 4.10a 2D Ramachandran plot for receptor protein 4dm3.

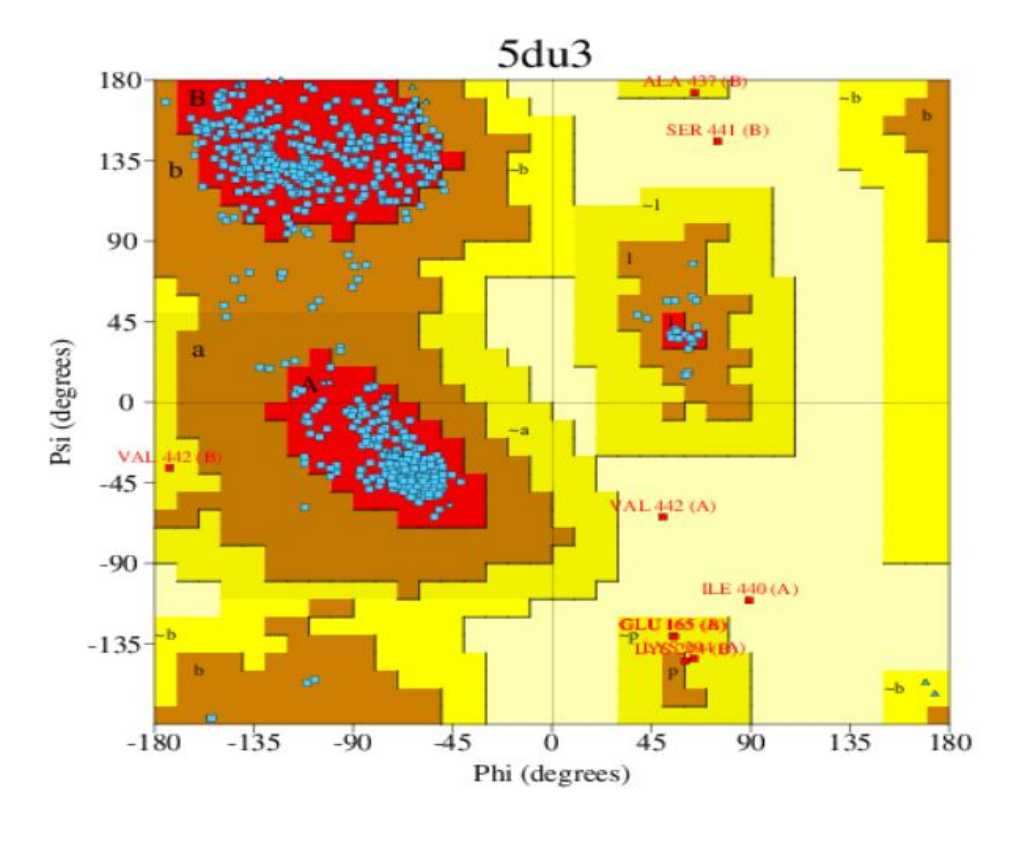


Fig 4.10b 2D Ramachandran plot for receptor protein 5du3.

Table 4.9 Molecular docking parameters of 5C2HOP with the proteins 4DM3 and 5DU3.

Protein	Bonded residues		Intermolecular Energy (Kcal/mol)	Inhibition	Binding Energy(Kcal/mol)	Reference RMSD(Å)
	VAL159	2.3	-4.32	1.12	-4.02	68.25
4DM3	ILE157	2.6				
	VAL159	2.2				
	LEU161	207	-4.31	1.14	-4.02	62.356
5DU3	VAL105	204				
	VAL105	2.1				

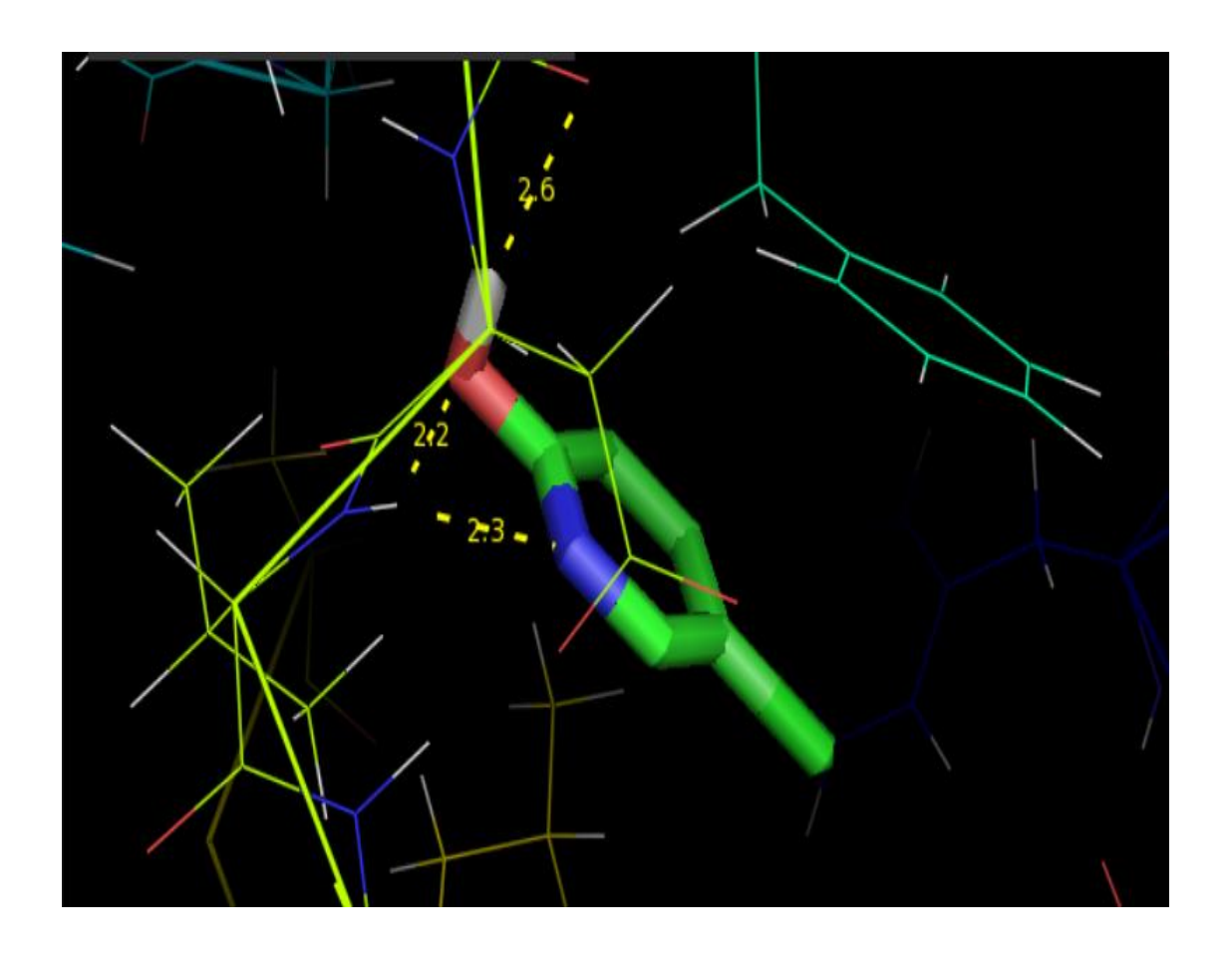


Fig 4.11 Docking and hydrogen bond interaction of 5C2HOP with 4DM3.

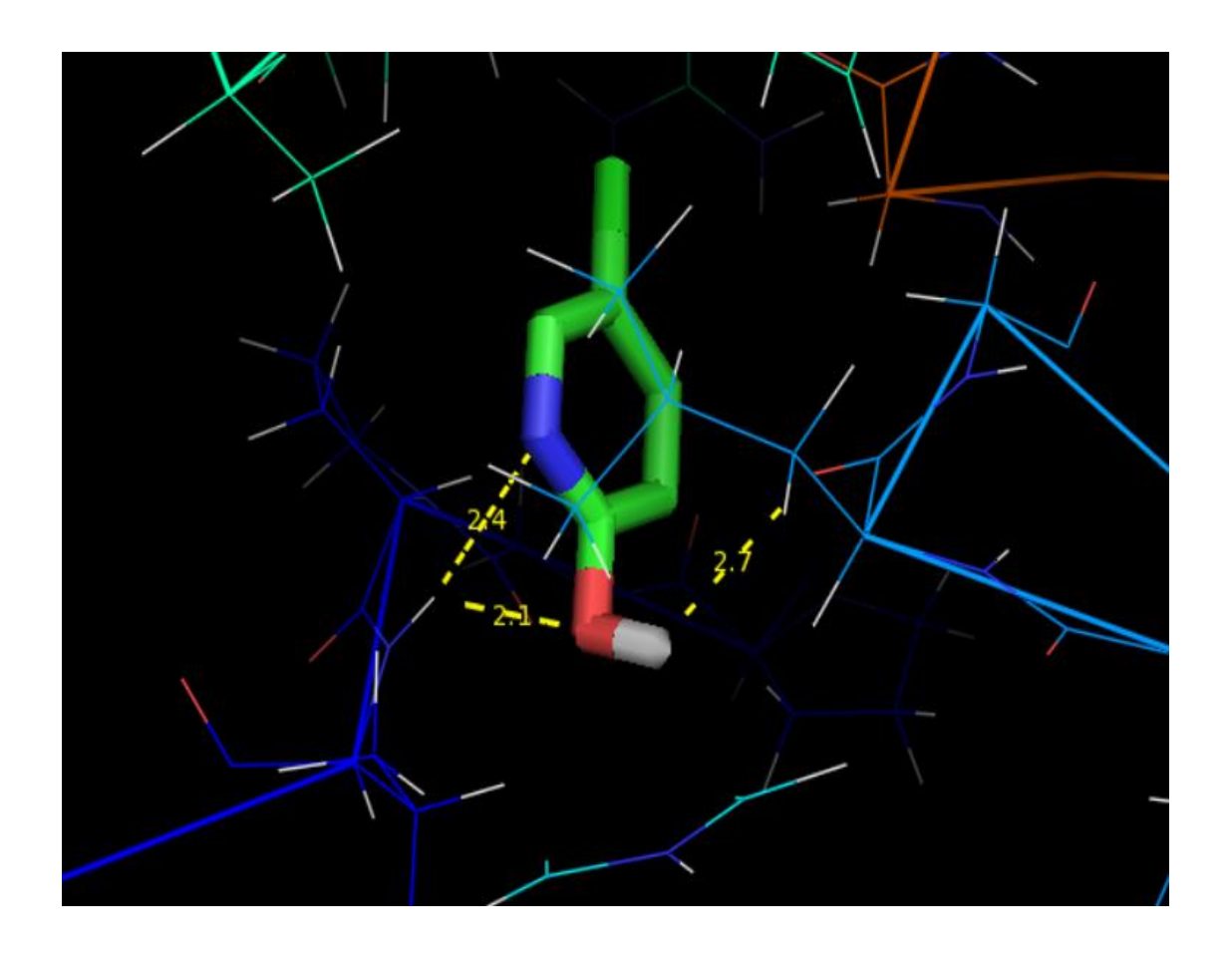


Fig 4.12 Docking and hydrogen bond interaction of 5C2HOP with 5DU3.

4.3 CONCLUSION

By exercising DFT method, the geometrical parameters, vibrational properties, Mulliken charges, FMO and UV studies of 5C2HOP in gas phase and in eco-friendly solvents (water, DMSO, ethanol and acetone) are entirely explicated in this work. The vibrational FT -IR and FT -Raman spectra of 5C2HOP are documented and reckoned vibrational wavenumbers with their PED is estimated. The theoretical findings displayed a satisfactory general concurrence with the experimental record. Molecular electrostatic potential (MEP) diagram exposed the negative and positive regions of the molecule. The frontier energy gap of the heading compound in gas phase and also in

eco-friendly solvents were calculated from the HOMO-LUMO energy values. The high electrophilicity value (3.272156) in gas phase obtained for the heading molecule depicts it to be an important class of compound. The strong delocalization of 27.08 kJ/mol is observed from $\pi(C2-C3)$ to $\pi^*(C1-N6)$ for the heading molecule. UV analysis spectra strengthen to predict the varied properties of the molecule. To compare the difference in mulliken charges in each task, the charge and multiplicity are varied. Fukui function was also analysed for the heading compound. The spots for nucleophilic and electrophilic occurrences were identified and the value of local softness was recognized to be maximum at C2 (0.056768). The two-dimensional graphical representations of ELF and LOL values were carried out and symbolised as coloured and contour maps. Drug likeness and environmental toxicity parameters were estimated for 5C2HOP. From the drug likeness parameters obtained, the heading molecule can be consented to behave as a drug. Finally, the heading compound was docked into the energetic spot of 4DM3 and 5DU3 associated with alopecia treatment and exhibiting the property of insulysin inhibitor. The molecular docking output showed the binding energy value to be -4.02 kcal/mol for both the proteins.

REFERENCES

- [1] Gilchrist T L 1997 Heterocyclic Chemistry Longman Harlow 3th ed 1-8.
- [2] Balasubramanian M, Keay J G 1996 Compr. Heterocycl Chem. II 5 245-300.
- [3] Joule J A, Mills K 2010 Heterocyclic Chemistry Wiley Blackwell, Oxford fifth ed, 645-664.
- [4] Frost C G, Williams. J.M.J 1995 Contemp. Org. Synth. 2 (2) 65-83.
- [5] Bolm, Angew C 1991 Chem. Int. Ed. Engl. 30 542.
- [6] Jones G 1996 Compr. Heterocycl. Chem. II 5 167-243.
- [7] Johnson C D 1996 Compr. Heterocycl. Chem. II 5 1-3.
- [8] Shahida R, Muthu S, Raja M, Rajmuhamed R, Narayana B, Prakash S Nayak, Sarojini B K 2017 Optik 140 1127-1142.
- [9] Wancen Xie, Tong Li, Chen Chen, Haibo Wu, Songmiao Liang, Haiqing Chang, Baicang Liu, Enrico Drioli, Qingyuan Wang, John C. Crittenden, Ind. Eng. Chem. Res. (2019) 6413–6423.
- [10] Sangeetha M, Mathammal R 2016 Journal of Molecular Structure 1117 121-134.
- [11] Pourayoubi M, Ghadimi S, Ebrahimi Valmoozi A A 2007 Acta Cryst. E63 o4631.
- [12] Karabacak M, Karaca C, Atac A, Eskici M, Karanfil A 2012 Spectrochim. Acta A 97 556-567.

- [13] Surisseau C, Marvell P 1994 J. Raman Spectrosc. 25 447-455.
- [14] Barnes A J, Majid M A, Stuckey M A, Gregory P, Stead C V 1985 Spectrochim. Acta A 629-635.
- [15] Varsanyi G 1973 Assignment for Vibrational Spectra of Seven Hundred Benzene Derivatives, Vol. 1-2, Academic Kiaclo, Budapest.
- [16] Silverstein M, Basseler G C, Morill C 1981 Spectrometric Identification of Organic compounds, Wiley. New York.
- [17] Colthup N B, Daly L H, Wiberley S E Introduction to IR spectroscopy,

 Academic Press, New York.
- [18] Varsanyi G 1974 Assignments for Vibrational Spectra of Seven Hundred Benzene Derivatives Vol. 1 Adam Hilger London.
- [19] https://www2.chemistry.msu.edu/faculty/reush/VirtTxtJml/Spectrpy/InfraRed/infrared.html.
- [20] http://www.chem.ucla.edu/-webspectra/irtable.html.
- [21] F. Weinhold, C.R. Landis, Chem. Educ. Res. Pract. 2 (2) (2001) 91–104.
- [22] H. Raissi, A.F. Jalbout, M. Yoosefian, M. Fazli, A. Nowroozi, M. Shahinin, A.De Leon, Int. J. Quantum Chem. 110 (4) (2009) 821–830.
- [23] Sevvanthi S, Muthu S, Raja M 2017 Journal of molecular structure 1149 487-498.
- [24] Jayabharathi J, Thanikachalam V, Jayamoorthy K, Perumal M V 2012 Spectrochim. Acta Mol. Biomol. Spectrosc. 97 131-136.

- [25] Rajagopalan N R, Krishnamoorthy P, Jayamoorthy K, Austeria M, Karbala 2016 Inter.J. Mod. Sci. 2(4) 219-225.
- [26] Lewis D F V, Ioannides C, Parke D V 1994 Xenobiotica 24 401-408.
- [27] G.-J. Zhao, J.-Y. Liu, L.-C. Zhou, K.-L. Han, J. Phys. Chem. B 111 (30) (2007) 8940–8945.
- [28] P. Manjusha, J.C. Prasana, S. Muthu, B.F. Rizwana, Comput. Biol. Chem. (2020) 107330.
- [29] Sakthivel S, Alagesan T, Muthu S, Christina Susan Abraham, Geetha E 2018

 Journal of Molecular Structure 1156 645-656.
- [30] A.M. Bayoumy, M. Ibrahim, A. Omar, Opt. Quantum Electron. 52 (7) (2020).
- [31] Tintu K Kuruvilla, Johanan Christian Prasana, Muthu S, Jacob George 2018

 Journal of Molecular Structure 1157 519-529.
- [32] Fathima Rizwana B, Johanan Christian Prasana, Christina Susan Abraham, Muthu S 2018 Journal of Molecular Structure 1164 447-458.
- [33] Chattaraj P K, Maiti B, Sarkar U 2003 J.phys. Chem. A 107 4973-4975.
- [34] Silvi B, Savin A 1994 Classification of chemical bonds based on topological analysis of electron localization functions, Nature 371 683–686.
- [35] Jacobsen, Heiko 2008 Localized-orbital locator (LOL) profiles of chemical bonding. Can. J. Chem. 86 695–702.
- [36] Lipinski C A, Lomlardo F, Dominy B W, Feeney P J 1997 Adv.Drug Deliv. Rev.23 (1-3) 3-25.

- [37] Lipinski C A 2004 Drug Discov. Today Technol. 1(4) 337-341.
- [38] Morris G M, Huey R, Olson A J 2008 Using AutoDock for ligand-receptor docking, Curr. Protoc. Bioinf. 24 (8.14) 1-40.
- [39] H.M. Berman, T. Battistuz, T.N. Bhat, W.F. Bluhm, P.E. Bourne, K. Burkhardt, Z. Feng, G.L. Gilliland, L. Iype, S. Jain, P. Fagan, J. Marvin, D. Padilla, V. Ravichandran, B. Schneider, N. Thanki, H. Weissig, J.D. Westbrook, C. Zardecki, The protein data bank, Acta Crystallogr. Sect. D Biol. Crystallogr. 58 (2002) 899–907.
- [40] F.B. Asif, F.L.A. Khan, S. Muthu, M. Raja, Comput. Theor. Chem. 1198 (2021)113169.
- [41] S. Muthu, S. Renuga, Spectrochim, Acta Part A Mol. Biomol. Spectrosc. 132 (2014) 313–325.

CHAPTER V

DONOR ACCEPTOR GROUPS EFFECT, POLAR PROTIC SOLVENTS INFLUENCE ON ELECTRONIC PROPERTIES AND REACTIVITY OF 2-CHLOROPYRIDINE-4-CARBOXYLIC ACID

5.1 INTRODUCTION

Taking into account the utmost challenging branches of carbon-based chemistry, heterocyclic compound chemistry is considered to be one among them. Its hypothetical ramifications, the multiplicity of its synthesis techniques, the industrial and biological relevance of heteroaromatic molecules are all fascinating. Chemists, pharmacologists, and physicists have been studying nitrogen-comprising heterocyclic organic compounds as structure splinters of numerous medications, colours, and food additives for decades in order to uncover a link concerning chemical structure and biological action [1-4]. Pyridine derivatives have engrossed noteworthy attentiveness in pharmacological, biochemistry, cosmetics and agrochemical fields [5-11]. Carboxylic acids of the pyridine series or its derivatives are recognised to have significant pharmacologic value, predominantly as B-vitamins, chemotherapeutic medicines to promote metabolism, anti-hyperlipidemic agents to lower cholesterol levels, antituberculosis drugs, and so on. [12–15]. 2-Chloropyridine-4-carboxylic acid (2CP4CA), a pyridine derivative with the chemical formula C₆H₄ClNO₂ has been picked for quantum mechanical investigation having 157.55 as its molecular weight. Literature review endorses that DFT reports of 2-Chloropyridine-4-carboxylic acid (2CP4CA) has not disclosed yet. This motivates us to conduct a theoretical analysis of 2CP4CA's skeletal, electronic, and vibrational modes. 2-Chloropyridine-4-carboxylic acid (2CP4CA) was scrutinized theoretically in gas phase and using dissimilar solvents in this study. DFT calculations are useful for the prediction and calculation of material behaviour of the caption compound. The acquired computed values of geometrical factors and vibrational frequencies are revealed here. Solvents perform a substantial role in the chemical industry's environmental performance, as well as cost, security, and wellbeing concerns. The concept of "green" solvents articulates the desire to reduce the ecological influence of solvent consumption in chemical synthesis. Usually, the solvents are categorized into three grades such as favoured, utilisable and unacceptable solvents [16]. The first two groups fall under the heading of eco-friendly solvents. These globally friendly solvents cause meagre destructiveness in regard to social wellbeing and the ecosystem, and are favoured for their longer-lasting properties. Results show that simple alcohols are environmentally preferable solvents [17]. The polar protic solvents namely H₂O, CH₃OH, C₂H₅OH and CH₃(CH₂)₂OH coming under ecofriendly solvents fitting in utilisable grouping [18] were preferably designated to examine the solvent impact of 2CP4CA. Globschemical.com provided facts on the solvents for the molecule, which revealed that it is soluble in the polar protic solvents chosen for investigation.

5.2 OUTCOMES AND DISCUSSION

5.2.1 Geometrical Factors

For 2CP4CA, the envisaged geometrical factors are exhibited in Table 5.1 and the augmented molecular configuration accompanied by the numbering scheme of atom is exposed in Fig 5.1. The heading compound has 5 C - C bonds, two C - N bonds, single C - Cl bond, three C - H bonds, single O - H bond and two C - O bonds. 1.759 Å was the longest bond length detected between carbon and chlorine atom and the least value of 0.969 Å was found between oxygen and hydrogen atom in gas phase. Carbon2-Carbon1-Nitrogen6 (124.8°) was spotted to have highest bond angle and the least bond angle was observed at C7-O8-H14 (54.9°) in gas phase.

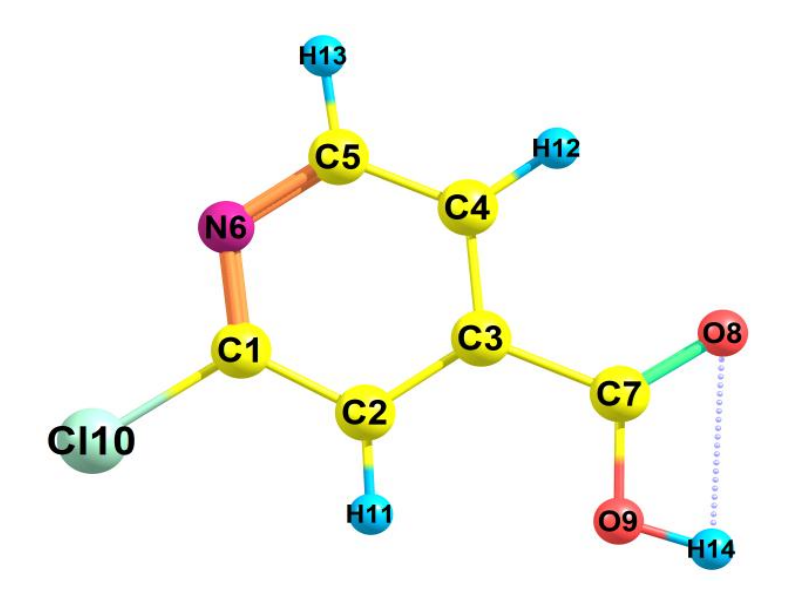


Fig 5.1 Optimized picture of 2CP4CA with atom numbering.

Table 5.1 Geometric parameters of 2CP4CA in gas phase.

PARAMETER	B3LYP/6-311++G(d,p)	PARAMETER	B3LYP/6-311++G(d,p)
BOND LENGTI		BOND ANGLE	(°)
C1-C2	1.396	C2-C1-N6	124.8
C1-N6	1.316	C2-C1-Cl10	118.4
C1-Cl10	1.759	C1-C2-C3	117.1
C2-C3	1.393	C1-C2-H11	121.3
C2-H11	1.08	N6-C1-Cl10	116.8
C3-C4	1.398	C1-N6-C5	117.5
C3-C7	1.495	C3-C2-H11	121.7
C4-C5	1.388	C2-C3-C4	119.2
C4-H12	1.082	C2-C3-C7	122.2
C5-N6	1.34	C4-C3-C7	118.6
C5-H13	1.085	C3-C4-C5	118.2
C7-O8	1.206	C3-C4-H12	120.2
C7-O9	1.352	C3-C7-O8	124.3
O9-H14	0.969	C3-C7-O9	112.7
		C5-C4-H12	121.6
		C4-C5-N6	123.3
		C4-C5-H13	120.9
		N6-C5-H13	115.9
		O8-C7-O9	123
		C7-O8-H14	54.9
		C7-O9-H14	107.3
		O9-H14-O8	74.8

5.2.2 Assignments of Vibrational bands

In order to analyse the existence of functional group in the molecule, vibrational spectroscopy is found to be an appropriate approach in organic chemistry [19]. 36 regular modes of vibrations were detected for the caption molecule comprising of 14 atoms. Theoretical estimates of FT(IR & Raman) spectra generated applying the computational approach are recorded. The documentation in Table 5.2 reveals the vibrational modes together with the assessed frequencies in different polar protic solvents coupled with PED values. PED stands for Potential Energy Distribution. The PED contribution to higher percentage confirms the stability of the compound.

The range of 1650–1100 cm⁻¹ are ventured to be favourable for vibrations of Carbon – Carbon [20]. In the existing analysis, the ascertained evaluations of stretching vibrations of C - C are sensed hypothetically between 1561 and 1066 cm⁻¹.

1400–1200 cm⁻¹ is the range noticeable for C–N stretching. [21]. The computed Carbon – Nitrogen vibrations that stretch were attained in the current analysis between 1561 and 967 cm⁻¹ with highest PED influence of 44 % at ascended wavenumber of 1237 cm⁻¹, theoretically.

In compounds with many chlorine atoms, asymmetric and symmetric stretching modes produce extremely wide bands. In aromatic chloro compounds, 850–550 cm⁻¹ is the range producing steady vibrations of C-Cl stretch. [22,23]. For the caption molecule, the vibrations are recognized theoretically at 813, 696 and 401 cm⁻¹.

C-H symmetric vibration is most common in range of 3100 –3000 cm⁻¹ [24]. Peak matching to C-H vibrations of stretch as seen in a theoretical scheme are spotted at 3108, 3089, 3049 cm⁻¹ with PED influence of 99 percent conforming to vibration at 3108 cm⁻¹.

C=O grouping stretch vibrations are expected to arise in the scope of 1680-1715 cm⁻¹ whereas, 1300-1000 cm⁻¹ is found to be scope for C–O symmetry stretch [25,26]. For 2CP4CA, the value of former stretching is premeditated at 1730 cm⁻¹ in addition to PED of 85 % theoretically. At 1312, 1107, and 1066 $^{1}/_{cm}$, the points that are comparable to C–O symmetric stretch vibrations are observed.

In maximum cases, the hydroxyl group (O - H) symmetric vibrations of stretch has been detected between 3600 and 3400 $^{1}/_{cm}$. [27]. Hydrogen bonding is prone to such O–H vibrations of stretch [28]. The existing effort reveals such vibration at 3620 cm⁻¹ with corresponding P.E.D influence of hundred percent, signifying this one to be an absolute extending vibration.

The assessments premeditated theoretically by DFT approach are exhibited in the current study. The influence of polar protic solvents on 2CP4CA vibrations was investigated [29]. There were significant changes in wavenumbers between the gas phase and polar protic solvents.

Table 5. 2 Theoretical comparison of vibrational frequency of 2CP4CA in gas and in different solvents.

		Frequency -	Gas	Fr	equency in d	lifferent sol	vents	
S.No	Scaled	Intensity- IR	Intensity- RAMAN	Water	Methanol	Ethanol	1-Propanol	Assignment
1	3620	113	140	3601.08	3601.64	3601.94	3602.20	YOH (100)
2	3108	3	53	3111.09	3111.00	3110.96	3110.90	YCH (99)
3	3089	2	97	3094.87	3094.71	3094.62	3094.54	YCH (97)
4	3049	13	119	3059.57	3059.27	3059.12	3058.98	YCH (97)
5	1730	344	72	1691.05	1692.25	1692.86	1693.42	YOC (85)
6	1561	15	30	1563.79	1563.71	1563.68	1563.64	YNC(12)+YCC (34)
7	1531	114	6	1525.19	1525.35	1525.44	1525.52	YNC (21)+YCC (33)+βCCN (13)
8	1436	37	7	1435.34	1435.39	1435.42	1435.44	YNC (11)+βHCC (12)+βHCN (40)
9	1341	79	3	1339.02	1339.08	1339.11	1339.14	YNC (12)+YCC (21)+βHCC (32)
10	1312	138	10	1310.69	1310.72	1310.74	1310.75	YOC (19)+YCC (16)+βHOC (33)+βOCO(12)
11	1258	3	1	1255.34	1255.45	1255.50	1255.54	YNC (16)+βHCC (30)+βHCN (37)
12	1237	1	7	1232.67	1232.81	1232.89	1232.96	YNC(44)+YCC (47)
13	1158	183	26	1146.88	1147.11	1147.22	1147.34	YCC (14)+βHOC (37)
14	1107	164	2	1101.44	1101.65	1101.76	1101.85	YCC (14)+YOC (13)+βHCC (21)
15	1066	97	2	1067.91	1067.82	1067.77	1067.73	YCC (18)+YOC (29)+βHCC (14)+βCCC(11)
16	1058	11	2	1052.84	1053.04	1053.14	1053.23	βCCN (34)+βHCC (40)
17	967	2	36	967.46	967.44	967.42	967.42	YNC (36)+βCCN (26)+βCNC(11)
18	962	0	0	964.20	964.17	964.16	964.14	τHCCN(30)+ τHCNC(52)+ τCCNC(16)
19	881	5	0	879.29	879.47	879.56	879.63	τHCCC(70)+ τCCCN(11)
20	848	10	0	847.87	847.95	847.99	848.03	τHCCN(46)+ τHCNC(30)+ωOCOC(11)+ωCCCC(10)

		Frequency -	Gas	Fr	equency in d	lifferent sol	vents	
S.No	Scaled	Intensity- IR	Intensity- RAMAN	Water	Methanol	Ethanol	1-Propanol	Assignment
21	813	32	2	808.66	808.78	808.84	808.90	YCC (20)+YClC (17)+βCNC (19)
22	750	60	0	745.32	745.55	745.66	745.76	τ HCCC(10)+ τ HCCN(15)+ωOCOC(61)
23	706	5	0	705.05	705.10	705.13	705.15	τ CCNC(51)+ τ CCCN(21)
24	696	30	12	690.39	690.56	690.66	690.73	YCIC (12) +βCCN (31)+βCNC (12)+βCCC (14)
25	622	61	1	618.92	619.01	619.07	619.10	βOCO (56)
26	579	78	2	570.78	571.05	571.19	571.31	τHOCC(78)
27	497	14	1	496.80	496.81	496.80	496.81	βCNC (11)+βOCC (46)+βCCC (15)
28	489	8	1	489.85	489.79	489.75	489.72	τ HOCC(14)+ τ CCNC(21)+ τ CCCN(13)+ωClCNC(33)
29	415	20	0	415.17	415.16	415.15	415.15	τHCCC(12)+ τHCNC(12)+ τCCNC(28)+ τCCCN(14)
30	401	6	7	398.08	398.17	398.21	398.25	YCIC (51) + β CCN (12)+ β CICN (13)
31	359	3	3	358.23	358.23	358.23	358.24	YCC (28) +βOCO (12)+βCCC (23)
32	299	2	3	298.30	298.32	298.33	298.34	βOCC (21)+βCCC (11)+βClCN (45)
33	184	1	1	184.23	184.19	184.17	184.15	τ CCNC(43)+ τ CCCN(17)+ ω ClCNC(19)
34	153	1	1	153.07	153.10	153.11	153.12	βOCC (12)+βCCC (50)+βClCN (18)
35	139	0	1	138.96	138.99	139.00	139.01	τCCNC(11)+ τCCCN(20)+ωClCNC(17)+ωCCCC(42)
36	50	2	0	41.76	41.94	42.03	42.11	τOCCC(91)

Υ -stretching, β- in plane bending, ω – out plane bending, τ - torsion

5.2.3 NLO Analysis

Organic constituents that are employed in signal processing, optical interconnections, and telecommunications have the nonlinear optical (NLO) feature [30]. DFT investigations are the most cost-effective and practical method of predicting the material's NLO properties. Table 5.3 reveals the scrutinized values of nonlinear parameters such as μ -dipole moment, β -first order hyperpolarizability and α -polarizability of 2CP4CA in gaseous phase and polar protic solvents. Urea is exercised regularly as a verge material for relative purposefulness [31].

The heading compound has a first order hyperpolarizability value of 1.4794 x 10^{-30} esu. This is evaluated to be larger than (7.5 times) that of the verge material in gas phase. This substantial value suggests that 2CP4CA has extensive NLO properties. The value of β for the polar protic solvents was computed to be 5.9538 x 10^{-30} (water), 5.8325 x 10^{-30} (methanol), 5.7695 x 10^{-30} (ethanol) and 5.7149 x 10^{-30} (1-propanol). The deviations emerged in the properties explores that the solvents have amplified the polarizability of 2CP4CA. Due to higher values, the heading compound possibly be exposed as a suitable NLO compound.

Table 5.3 The values of calculated dipole moment $\mu(D)$, polarizability(α) and first order hyperpolarizability(β) of 2CP4CA in different solvents.

	B3LYP/6-311++G(d,p)									
parameter	GAS	WATER	METHANOL	ETHANOL	1-PROPANOL					
μ_{x}	0.7452315	0.9996061	0.9907088	0.9860768	0.9820438					
μ_{y}	0.116896	0.1552186	0.1533667	0.1524179	0.1516002					
μ_{z}	0.0347375	0.0469922	0.0465965	0.0463902	0.0462104					
μ(D)	0.755143269	1.012676373	1.003591802	0.998864717	0.994750243					
α_{xx}	120.831785	158.798207	157.5853782	156.9516441	156.3985358					
α_{xy}	-15.3971453	-21.1175629	-20.9696874	-20.891548	-20.8228575					
α_{yy}	116.7601661	160.9580522	159.4681129	158.691908	158.0137947					
$lpha_{xz}$	2.1974466	2.6285455	2.6271433	2.6260087	2.6247969					
α_{yz}	-2.9591016	-3.8478169	-3.8325797	-3.8242136	-3.8166877					
α_{zz}	51.9086672	67.9450826	67.19931	66.8179618	66.4897015					
α (a.u)	96.5002061	129.2337806	128.084267	127.4871713	126.967344					
α (e.s.u)	1.4301 x 10 ⁻²³	1.915244 x 10 ⁻²³	1.898208 x 10 ⁻²³	1.889359 x 10 ⁻²³	1.881656 x 10 ⁻²³					
Δα (a.u)	219.7437289	290.009992	287.824275	286.6799982	285.6797851					

	B3LYP/6-311++G(d,p)									
parameter	GAS	WATER	METHANOL	ETHANOL	1-PROPANOL					
Δα (e.s.u)	3.2566 x 10 ⁻²³	4.29794 x 10 ⁻²³	4.26555 x 10 ⁻²³	4.24859 x 10 ⁻²³	4.23377 x 10 ⁻²³					
β_{xxx}	175.470493	203.5668533	205.9675523	207.0934743	208.0053315					
β_{xxy}	-34.8547024	-117.7730324	-114.453499	-112.7375639	-111.2504385					
β_{xyy}	81.6671783	235.8723017	228.5129227	224.7380871	221.4830865					
eta_{yyy}	-164.6933616	-402.4717105	-392.5686255	-387.452538	-383.0204408					
β_{zxx}	12.0833734	24.6457112	24.0421705	23.733488	23.4680262					
eta_{xyz}	-6.7755993	-20.5850697	-19.8574867	-19.4900507	-19.1767951					
eta_{zyy}	15.8246198	41.4209782	40.1895782	39.560553	39.0198649					
eta_{xzz}	-7.2429983	-12.2635488	-12.2574622	-12.2467941	-12.2335707					
eta_{yzz}	-4.0395931	-14.7703003	-14.1837039	-13.8875587	-13.634804					
β_{zzz}	5.7585163	12.7833258	12.2710126	12.0097319	11.7852621					
β _{tot} (a.u)	324.081341	689.1570357	675.1151462	667.8307243	661.5030552					
β _{tot} (e.s.u)	2.7998 x 10 ⁻³⁰	5.9538 x 10 ⁻³⁰	5.8325 x 10 ⁻³⁰	5.7695 x 10 ⁻³⁰	5.7149 x 10 ⁻³⁰					

5.2.4 Donor – Acceptor Interaction

The shift of charges and charges' delocalization owing to bonds interacting intramolecularly and intermolecularly were investigated using NBO exploration [32,33]. E(2) is accomplished as the stabilisation energy related with the $i \rightarrow j$ delocalization for each contributor-i and acceptor-j [34] and is projected to be

$$E(2) = \Delta E_{ij} = q_i (F_{ij})^2 / (\epsilon_j - \epsilon_i)$$

where the contributor orbital tenancy and the off- transverse NBO Fock matrix component are denoted as q_i and F_{ij} respectively and ε_j and ε_i denote the diagonal elements. The element's high stabilisation energy indicates the donor's greatest potential to donate to acceptors and the strength of the entire conjugative arrangement [35]. The bonding and anti-bonding of 2CP4CA with stabilization energy were scrutinised and exposed in Table 5.4. The interaction from σ (C5-H13) to σ *(C1-N6) and π (Carbon2-Carbon3) to π * (Carbon1-Nitrogen6) led to E(2) of 4.67 Kcal/mol and 24.33 Kcal/mol respectively. E(2) of 46.08 Kcal/mol owing to strong interactions caused by the change of electron concentration from LP(2) of O9 to π *(C7-O8) has been detected. Also the interaction of LP(3) of Cl10 with π *(C1-N6) with stabilization energy of 18.91 Kcal/mol has been observed. The other significant interaction involves the interaction of LP(2) of O8 with σ *(C2-C3), detected to have a low E(2) of 0.6 Kcal/mol. The assessed value of E (2) being 61.18 Kcal / mol attained for π *(Carbon2-Carbon3) to π *(Carbon4-Carbon5) was found to be the highest.

Table 5.4 Second order perturbation theory analysis of Fock matrix in NBO for 2CP4CA.

Donor	Type	ED/e(qi)	Acceptor	Type	ED/e(qi)	E(2) kcal/mol	E(j)- E(i) a.u.	F(i,j) a.u.
C 1-C 2	σ	1.98539	C 1-N 6	σ*	0.0356	1.45	1.21	0.038
C 1-N 6	σ	1.98749	C 1-C 2	σ^*	0.03634	1.67	1.34	0.042
C 1-N 6	π	1.73539	C 2-C 3	π^*	0.3144	13.2	0.32	0.059
C 1-Cl 10	σ	1.98906	C 2-C 3	σ^*	0.02149	2.14	1.27	0.047
C 2-C 3	σ	1.9733	C 1-C 2	σ^*	0.03634	2.5	1.22	0.049
C 2-C 3	π	1.66704	C 1-N 6	π^*	0.42218	24.33	0.24	0.07
C 2-H 11	σ	1.97797	C 1-C 2	σ^*	0.03634	0.57	1.03	0.022
C 3-C 4	σ	1.97282	C 2-C 3	σ^*	0.02149	3.07	1.22	0.055
C 3-C 7	σ	1.97707	C 1-C 2	σ^*	0.03634	2.22	1.18	0.046
C 4-C 5	σ	1.98096	C 3-C 4	σ^*	0.02196	3.13	1.28	0.057
C 4-C 5	π	1.66119	C 1-N 6	π^*	0.42218	16.8	0.25	0.059
C 4-H 12	σ	1.97445	C 2-C 3	σ^*	0.02149	3.53	1.05	0.054
C 5-N 6	σ	1.97636	C 1-N 6	σ^*	0.0356	0.9	1.29	0.031
C 5-H 13	σ	1.97507	C 1-N 6	σ^*	0.0356	4.67	0.98	0.06
C 7-O 8	σ	1.99498	C 2-C 3	σ^*	0.02149	1.27	1.61	0.041
C 7-O 8	π	1.98004	C 2-C 3	π^*	0.3144	4.57	0.4	0.041
C 7-O 9	σ	1.99602	C 3-C 4	σ^*	0.02196	0.95	1.49	0.034
O 9-H 14	σ	1.98477	C 3-C 7	σ^*	0.06414	5.17	1.13	0.069
N 6	LP (1)	1.91449	C 1-C 2	σ^*	0.03634	8.48	0.87	0.078
O 8	LP (1)	1.98001	C 3-C 7	σ^*	0.06414	1.99	1.08	0.042
O 8	LP (2)	1.86319	C 2-C 3	σ^*	0.02149	0.6	0.8	0.02
O 9	LP (1)	1.9778	C 7-O 8	σ^*	0.01811	6.01	1.23	0.077
O 9	LP (2)	1.81995	C 7-O 8	π^*	0.23205	46.08	0.35	0.114
Cl 10	LP (1)	1.99162	C 1-C 2	σ^*	0.03634	1.96	1.43	0.048
Cl 10	LP (2)	1.96039	C 1-C 2	σ^*	0.03634	4.07	0.82	0.052
Cl 10	LP (3)	1.89979	C 1-N 6	π^*	0.42218	18.91	0.29	0.072
C 1-N 6	π*	0.42218	C 1-Cl 10	σ^*	0.04571	0.52	0.19	0.018
C 2-C 3	π*	0.3144	C 4-C 5	π*	0.24304	61.18	0.03	0.076

5.2.5 Thermodynamical Properties

For 2CP4CA, in both gaseous phase and in chosen solvents, Entropy, Specific heat capacity and Heat content of the material were reckoned and displayed in Table 5.5 between the temperature range of 100 Kelvin and 1000 Kelvin. The thermodynamical characteristics in relation to temperature provide information on the nature of the chemical. The computed values of above-mentioned parameters for 2CP2CA were found to be 383.236 J/mol K, 135.032 J/mol K and 24.08 J/mol K at 298.15K correspondingly in gaseous phase. Amongst all the polar protic solvents, water was detected to have the highest thermodynamical values at 298.15 K. The premeditated evaluates of 2CP4CA may afford to chemical reactions in the thermochemical sector grounded on the second law of thermodynamics [36]. The connection chart linking the temperature with the thermodynamical parameters in gas phase is publicized in Fig 5.2.

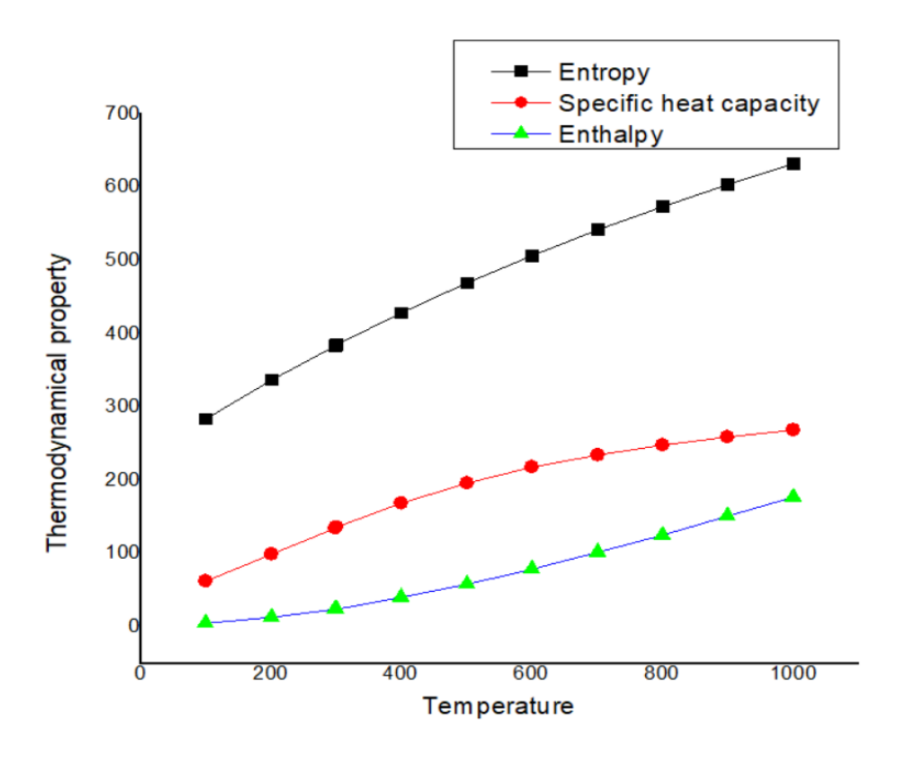


Fig 5.2 Graph representing dependence of entropy, specific heat capacity and enthalpy on temperature of 2CP4CA in gas phase.

Table 5.5 Thermodynamical parameters of 2CP4CA in different phases.

a) Ent	tropy				
T (K)	Gas	Water	Methanol	Ethanol	1-Propanol
100	282.955	284.479	284.443	284.425	284.408
200	337.048	338.704	338.664	338.644	338.626
298.15	383.236	385.015	384.971	384.949	384.928
300	384.073	385.854	385.811	385.788	385.768
400	427.81	429.701	429.654	429.629	429.607
500	468.572	470.555	470.504	470.478	470.454
600	506.334	508.39	508.336	508.309	508.284
700	541.216	543.329	543.274	543.245	543.219
800	573.456	575.613	575.556	575.527	575.501
900	603.328	605.52	605.462	605.432	605.405
1000	631.099	633.319	633.26	633.229	633.202
b) Spe	cific heat ca _l	pacity			
T (K)	Gas	Water	Methanol	Ethanol	1-Propanol
100	62.372	62.535	62.531	62.529	62.527
200	98.49	98.749	98.74	98.736	98.732
298.15	135.032	135.387	135.374	135.368	135.362
300	135.697	136.054	136.041	136.035	136.029
400	169.037	169.44	169.426	169.418	169.412
500	196.28	196.689	196.674	196.667	196.661
600	217.735	218.123	218.11	218.103	218.097
700	234.612	234.965	234.953	234.947	234.941
800	248.078	248.392	248.381	248.375	248.371
900	259.013	259.29	259.28	259.276	259.271
1000	268.037	268.28	268.272	268.268	268.264
c) Enthalpy	7				
T (K)	Gas	Water	Methanol	Ethanol	1-Propanol
100	4.596	4.638	4.637	4.637	4.637
200	12.607	12.669	12.667	12.667	12.666
298.15	24.08	24.173	24.17	24.169	24.168
300	24.33	24.424	24.421	24.42	24.419
400	39.614	39.746	39.741	39.739	39.738
500	57.932	58.104	58.099	58.096	58.094
600	78.676	78.889	78.882	78.878	78.875
700	101.326	101.576	101.568	101.564	101.56
800	125.485	125.768	125.759	125.754	125.75
900	150.858	151.17	151.16	151.155	151.15
1000	177.224	177.563	177.551	177.546	177.541

5.2.6 Electronic Analysis

The stimulation from ground state to excited state specifies the absorption of energy by an electron. UV-visible spectroscopy is used to research such transitions. The theoretical UV-Visible band of 2CP4CA is constructed utilizing TD-DFT method with IEFPCM solvation prototype for gas and polar protic solvents [37]. The transition contribution %, wavelength of absorption, oscillator potency and energy of transition accounted for dissimilar thinners are displayed in Table 5.6. The comparative UV spectra of the heading molecule in dissimilar solvents is exposed in Fig 5.3. For gas, the uppermost absorption crest was 290.967 nm with 4.26 eV as energy band gap for the transition contribution H-1->LUMO (71%), HOMO->LUMO (24%). The highest absorption peak for the polar protic solvents were found to be 313.884 nm (water), 267.987 nm (methanol), 268.126 nm(ethanol) and 268.242 nm (1-propanol) with band gap energy values of 3.95 eV(water), 4.63 eV (methanol) and 4.62 eV (ethanol and 1-propanol). Between the chosen solvent phase and the gaseous phase, the band gap energy values differ slightly.

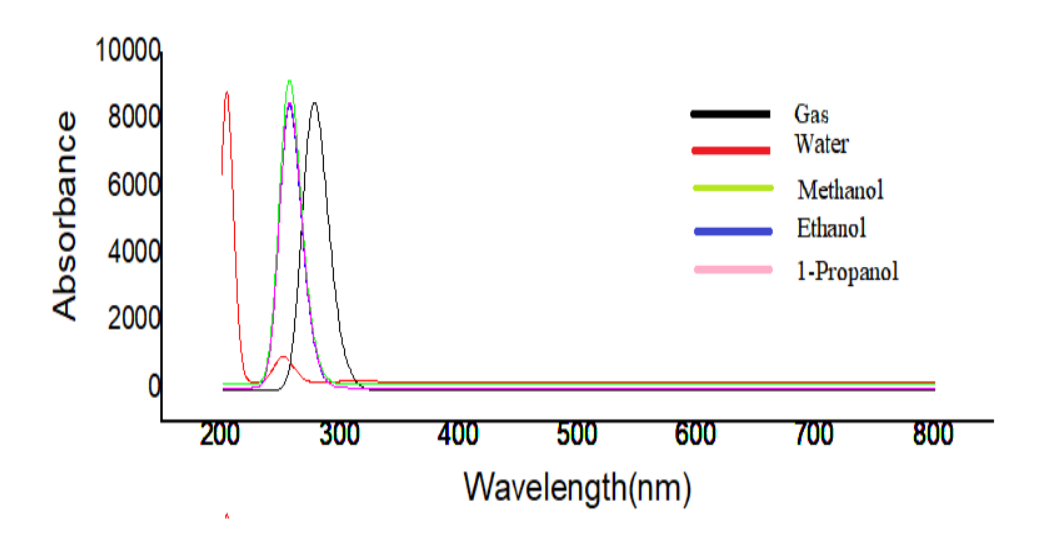


Fig 5.3 Theoretical comparative UV spectra of 2CP4CA in different solvents.

Table 5.6 Simulated UV-Vis spectrum with absorption maxima(nm), energy (cm⁻¹) and oscillator strength(f) for 2CP4CA with different solvents.

Solvents	Wavelength (nm)	Band gap (ev)	Energy (cm ⁻¹)	Osc. Strength(f)	Symmetry	Major contributions
GAS	290.9675741	4.26	34368.09077	0.01	Singlet-A	H-1->LUMO (71%), HOMO->LUMO (24%)
	278.4909996	4.45	35907.80318	0.025	Singlet-A	H-2->LUMO (57%), HOMO->LUMO (33%)
	275.8821411	4.49	36247.36259	0.036	Singlet-A	H-2->LUMO (36%), H-1->LUMO (23%), HOMO->LUMO (36%)
WATER	313.8840329	3.95	31858.89995	0.0004	Singlet-A	HOMO->LUMO (72%), HOMO->L+2 (18%)
	251.6117238	4.93	39743.77604	0.0046	Singlet-A	H-3->LUMO (66%), H-2->LUMO (23%)
	204.2775118	6.07	48953.01451	0.0516	Singlet-A	H-4->L+1 (14%), H-3->LUMO (19%), H-2->LUMO (54%)
METHANOL	267.9870161	4.63	37315.24066	0.0195	Singlet-A	H-2->LUMO (58%), H-1->LUMO (11%), HOMO->LUMO (20%)
	256.504868	4.83	38985.61488	0.0904	Singlet-A	H-3->LUMO (13%), H-2->LUMO (12%), HOMO->LUMO (63%)
	252.8071142	4.9	39555.84886	0.0168	Singlet-A	H-3->LUMO (64%), H-2->LUMO (10%)
ETHANOL	268.1261067	4.62	37295.88335	0.0199	Singlet-A	H-2->LUMO (57%), H-1->LUMO (12%), HOMO->LUMO (20%)
	256.6216687	4.83	38967.87068	0.0926	Singlet-A	H-3->LUMO (13%), H-2->LUMO (12%), HOMO->LUMO (63%)
	252.9205708	4.9	39538.10466	0.0166	Singlet-A	H-3->LUMO (65%), H-2->LUMO (10%)
1-PROPANOL	268.2421259	4.62	37279.75226	0.0202	Singlet-A	H-2->LUMO (55%), H-1->LUMO (14%), HOMO->LUMO (20%)
	256.7119966	4.83	38954.15926	0.0941	Singlet-A	H-3->LUMO (13%), H-2->LUMO (12%), HOMO->LUMO (63%)
	253.0134747	4.9	39523.58668	0.0165	Singlet-A	H-3->LUMO (65%)

5.2.7 Reactive Site Analysis

The MEP drawing exercises colour grading to indicate shape, size, and electrostatic potential [38]. MEP diagram of the heading compound at various polar protic solvents chosen is displayed in Fig 5.4 and it is evident from all, that the red colour on the oxygen atoms signifies that it has a negative potential and the blue shade on atoms of nitrogen specifies to possess positive potential. The plot of MEP for gas phase and polar protic solvents stretches out between – 6.894e-2 and 6.894e-2(gas), – 8.010e-2 and 8.010e-2(water), – 7.977e-2 and 7.977e-2 (methanol), – 7.960e-2 and 7.960e-2 (ethanol), – 7.945e-2 and 7.945e-2 (1-propanol).

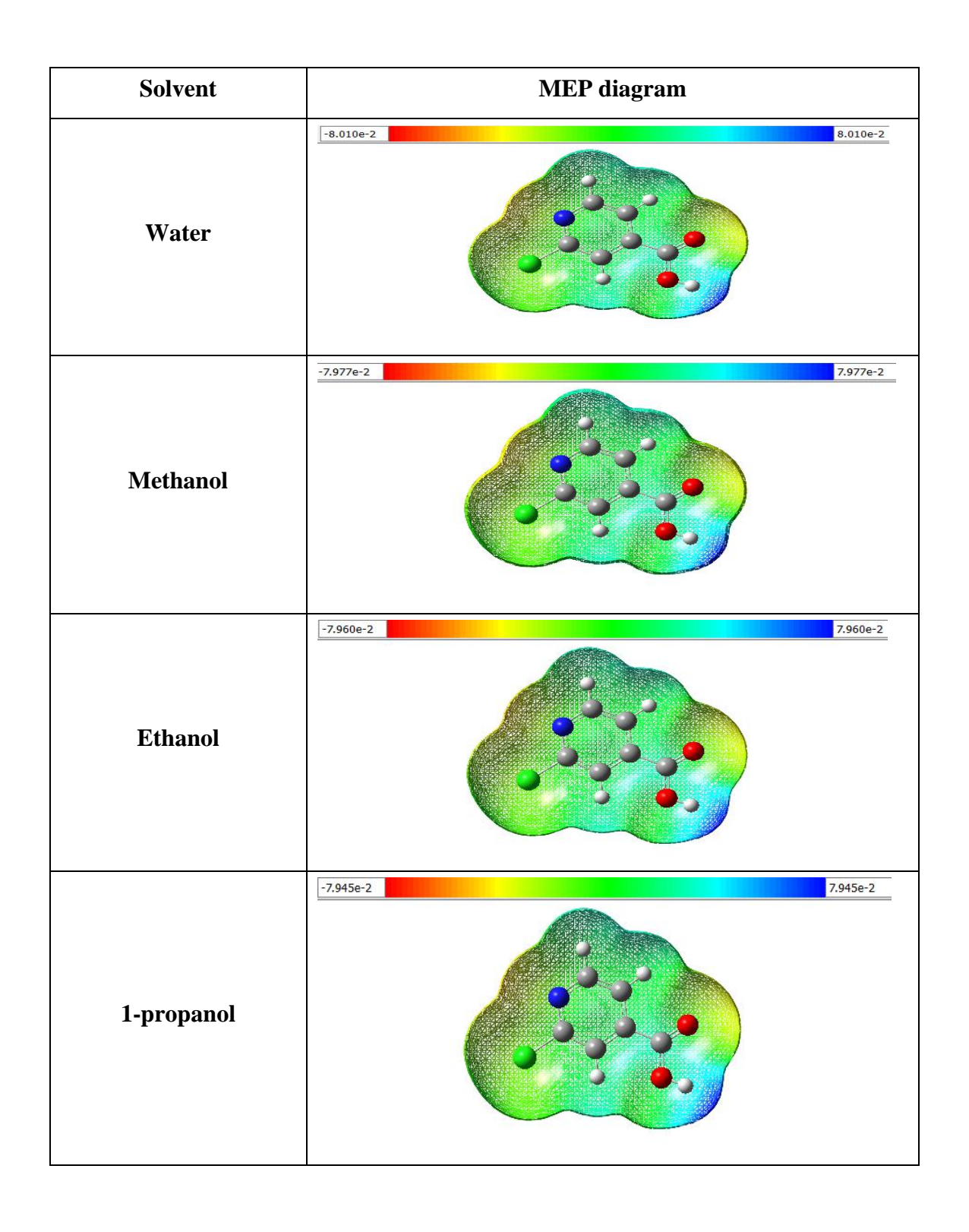


Fig 5.4 Molecular Electrostatic Potential of 2CP4CA in different solvents.

5.2.8 FMO Investigation

The FMO theory is substantial in establishing a molecule's chemical strength and chemical reactivity [39]. Calculating DFT-based reactivity descriptors is necessary for depicting the reactivity and location selectivity of diverse biomolecules [40]. Table 5.7 designates the premeditated values of universal descriptors in dissimilar solvents of 2CP4CA. Between the chosen solvents and gas phase of the molecule's HOMO&LUMO orbitals, only negligible fluctuations were noticed. In gas phase, for 2CP4CA, the premeditated values of energy gap, electronegativity, chemical hardness and softness were found to be 5.031425 eV, 5.155578, 2.5157 and 0.1987 correspondingly.

Taking into account, the molecular signifiers of the solvents, the uppermost energy gap of 5.02625 eV and chemical hardness of 2.513127 was documented for water whereas the highest value of electronegativity (5.176191) and electrophilicity index (5.33088) was obtained for 1- propanol and highest value of chemical softness (0.19897) was obtained for ethanol. Fig 5.5 depicts the expounding picture of HOMO and LUMO for 2CP4CA in gas phase. Chemical potential is the amount of energy in a system that can be used to do beneficial work [41] which is calculated as -5.15578 eV for 2CP4CA in gas phase.

Table 5.7 Calculated energy values of 2CP4CA with solvation effect.

Molecular descriptors	Gas	Water	Methnol	Ethanol	1-Propanol
HOMO(eV)	-7.67149	-7.68755	-7.68837	-7.688638	-7.68918181
LUMO(eV)	-2.64007	-2.66129	-2.66238	-2.662927	-2.66319929
Ionization potential	7.671494	7.687549	7.688365	7.6886376	7.689181812
Electron affinity	2.640069	2.661294	2.662383	2.6629272	2.663199292
Energy gap(eV)	5.031425	5.026255	5.025983	5.0257104	5.02598252
Electronegativity	5.155782	5.174422	5.175374	5.1757824	5.176190552
Chemical potential	-5.15578	-5.17442	-5.17537	-5.175782	-5.17619055
Chemical hardness	2.515712	2.513127	2.512991	2.5128552	2.51299126
Chemical softness	0.198751	0.198955	0.198966	0.1989768	0.198966072
Electrophilicity index	5.283212	5.326957	5.329206	5.3303356	5.330887747
Electronic charge	2.049432	2.058957	2.059448	2.0597217	2.059772604
Electron donating capability (w-)	8.175567	8.228309	8.231017	8.2323337	8.23310693
Electron accepting capability (w+)	3.019786	3.053887	3.055643	3.0565513	3.056916378

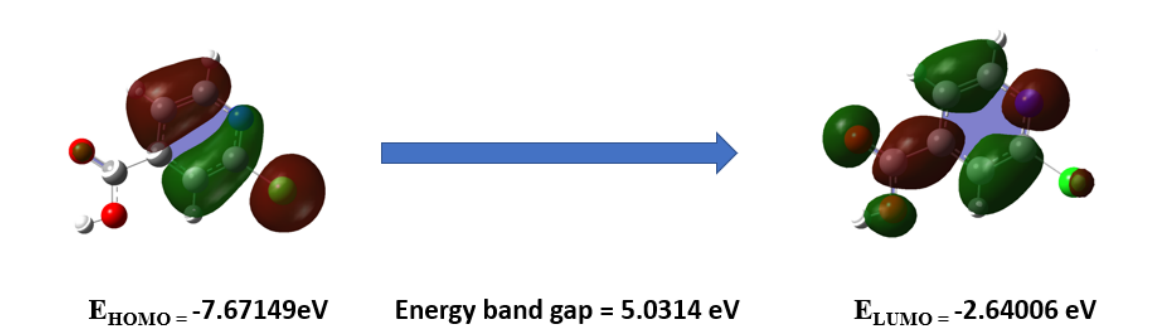


Fig 5.5 Atomic orbital HOMO - LUMO composition of the frontier molecular orbital of 2CP4CA in gas phase.

5.2.9 Molecular Reactivity and Population Analyses

For all the atomic locations of 2CP4CA, mulliken charges and local softness together with Fukui functions on the r_{th} atomic spot for free radical f_r^0 , electrophilic f_r^- , nucleophilic f_r^+ , and dual descriptor $\Delta f(r)$ are accounted. These accounted values for 2CP4CA are displayed in Table 5.8. Fig 5.6 depicts the Fukui function chart for expected charges of 2CP4CA. It is noticed that C1 is the spot for nucleophilic existence and all remaining atoms are the spots for electrophilic occurrence. The reactivity sequence for the nucleophilic case is depicted as C110 > C2 > H12 > H13 > H11 atoms and for electrophilic case as C3 > O8 > N6 > C1 > C4 > O9 > C7 > H14 > C5 atoms. The system's local softness is also linked with fukui function which was obtained to be maximum at C1(0.000506) for 2CP4CA.

The Mulliken charge spreading of 2CP4CA in polar protic solvents in addition to gas phase were assessed and listed in Table 5.9. The pictographic depiction of Mulliken charges for 2CP4CA is exhibited in Fig 5.7 which discloses that carbon atoms have a mixture of positive and negative atomic charges, whereas all the atoms of hydrogen possess positive charges in gas and chosen polar protic solvents. When compared to gas phase, the Mulliken charges of different solvents show significant differences. As well, in gas phase and in solvents chosen, Cl10 atom is spotted to carry maximum atomic charge.

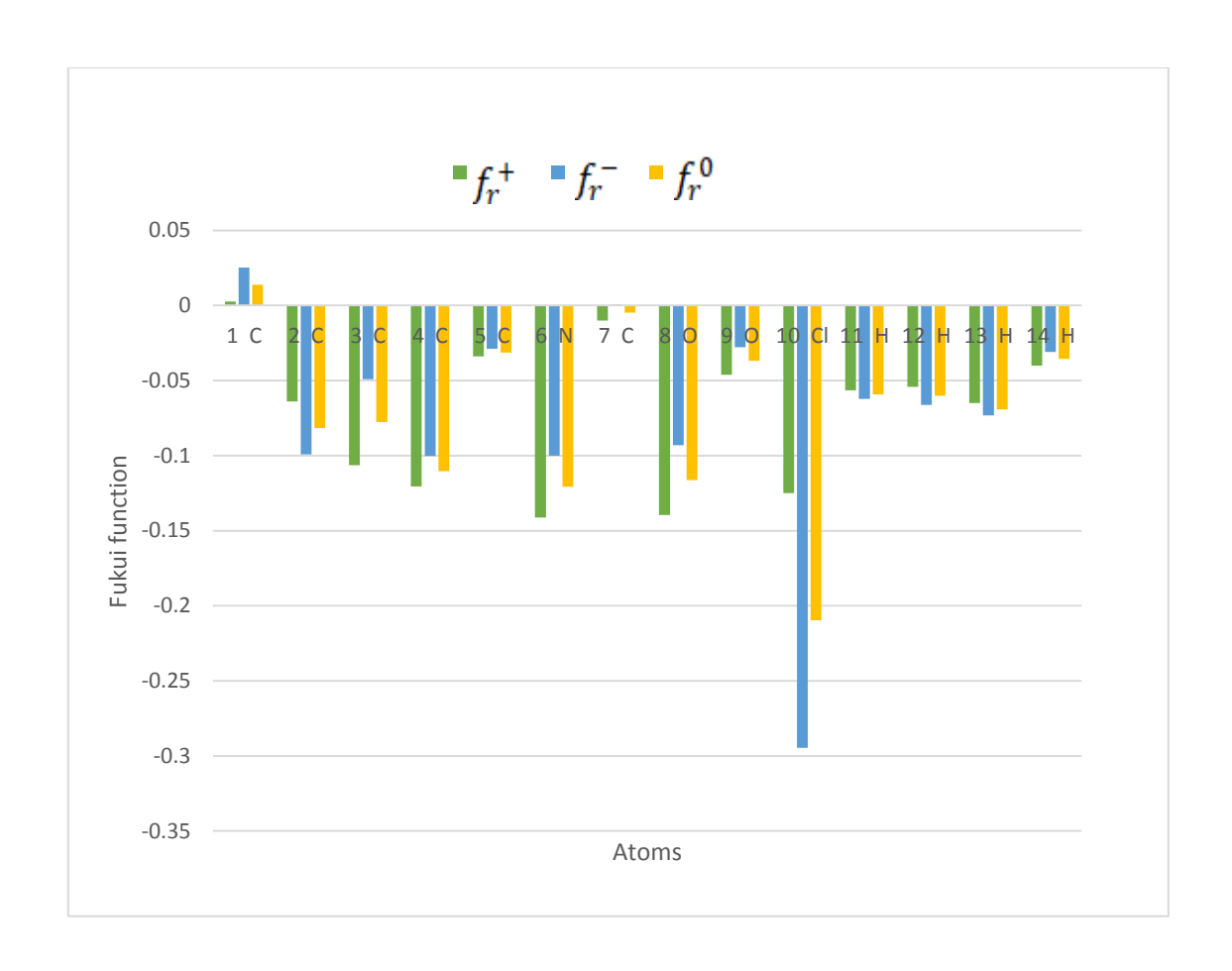


Fig 5.6 Fukui function graph for natural charges of 2CP4CA.

Table 5.8 Fukui functions, local softness and dual descriptor of 2CP4CA.

	Mulliken atomic charges			Fukui functions				local softness		
Atom	N (0,1)	N +1 (-1, 2)	N - 1 (1, 2)	f_r^+	f_r^-	f_r^{0}	Δf(r)	$s_r^+ f_r^+$	$s_r^- f_r^-$	$s_r^0 f_r^0$
1 C	-0.82467	-0.822118	-0.84977	0.002548	0.025107	0.013828	-0.02256	0.000506	0.004990	0.002748
2 C	0.319466	0.255505	0.418649	-0.06396	-0.09918	-0.08157	0.035222	-0.01271	-0.019713	-0.01621
3 C	0.123633	0.017273	0.172769	-0.10636	-0.04914	-0.07775	-0.05722	-0.02114	-0.009766	-0.01545
4 C	-0.0296	-0.150134	0.070697	-0.12054	-0.1003	-0.11042	-0.02024	-0.02396	-0.019934	-0.02195
5 C	-0.28783	-0.321788	-0.25906	-0.03396	-0.02877	-0.03137	-0.00519	-0.00675	-0.005718	-0.00623
6 N	0.083542	-0.057736	0.183606	-0.14128	-0.10006	-0.12067	-0.04121	-0.02808	-0.019888	-0.02398
7 C	-0.06265	-0.072788	-0.06315	-0.01014	0.000497	-0.00482	-0.01064	-0.00201	0.000099	-0.00096
8 O	-0.29616	-0.435718	-0.20302	-0.13955	-0.09314	-0.11635	-0.04641	-0.02774	-0.018512	-0.02312
9 O	-0.21238	-0.258472	-0.18464	-0.04609	-0.02774	-0.03692	-0.01835	-0.00916	-0.005514	-0.00734
10 Cl	0.419775	0.294857	0.714326	-0.12492	-0.29455	-0.20973	0.169633	-0.02483	-0.058542	-0.04168
11 H	0.176755	0.120313	0.239064	-0.05644	-0.06231	-0.05938	0.005867	-0.01122	-0.012384	-0.0118
12 H	0.170219	0.116034	0.23638	-0.05419	-0.06616	-0.06017	0.011976	-0.01077	-0.013150	-0.01196
13 H	0.136849	0.071814	0.210088	-0.06504	-0.07324	-0.06914	0.008204	-0.01293	-0.014556	-0.01374
14 H	0.283047	0.242958	0.314058	-0.04009	-0.03101	-0.03555	-0.00908	-0.00797	-0.006163	-0.00707

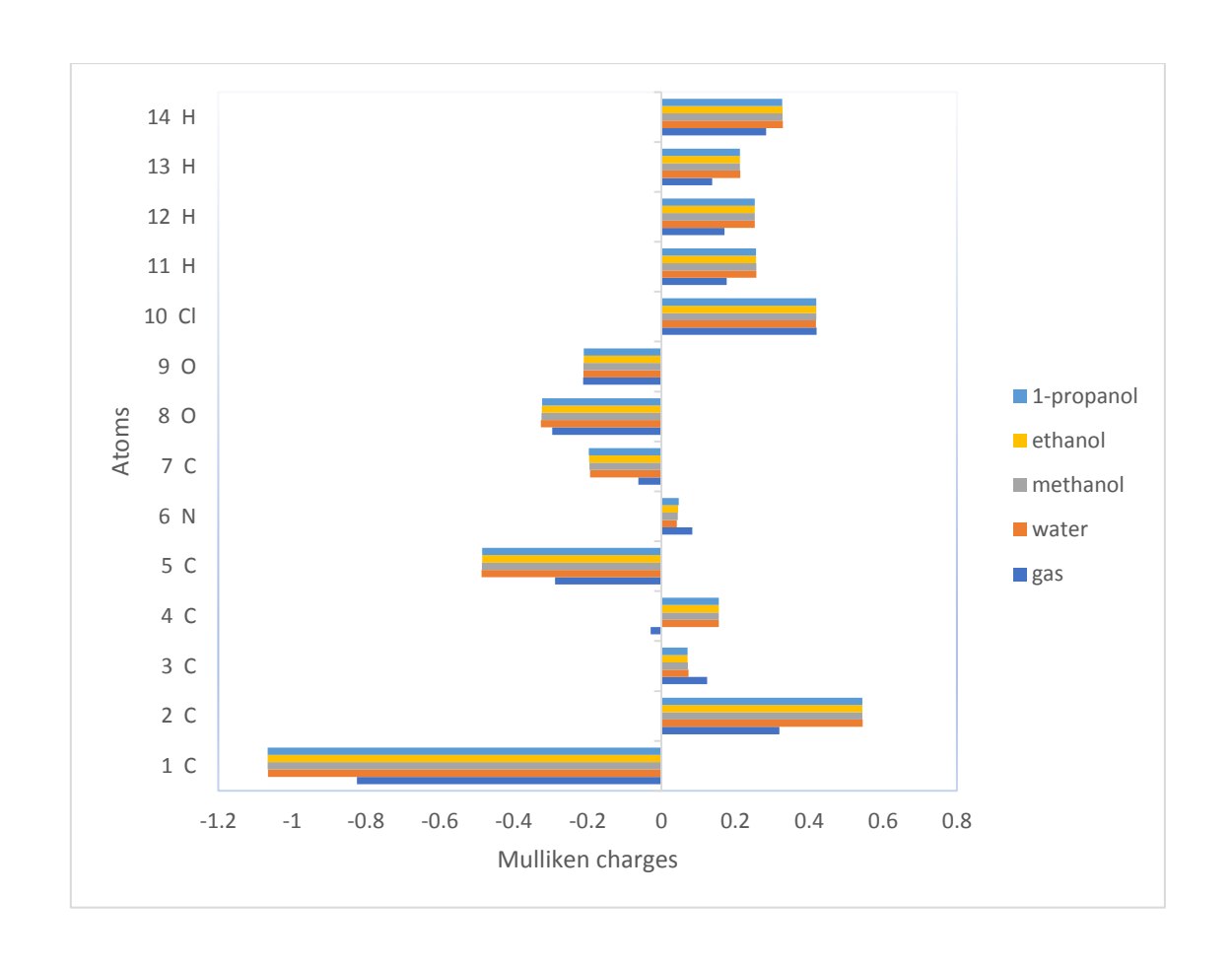


Fig 5.7 The histogram of calculated Mulliken Charges of 2CP4CA in different phases.

Table 5.9 Mulliken charge distribution of 2CP4CA in gas phase and in other solvents.

Atoms	gas	water	methanol	ethanol	1-propanol
1 C	-0.824666	-1.06586	-1.06612	-1.06625	-1.066366
2 C	0.319466	0.545149	0.544292	0.543851	0.543471
3 C	0.123633	0.07308	0.071699	0.07098	0.070355
4 C	-0.029599	0.15521	0.155044	0.154959	0.154885
5 C	-0.287827	-0.48727	-0.48619	-0.48563	-0.485148
6 N	0.083542	0.041596	0.044064	0.045349	0.04647
7 C	-0.06265	-0.19355	-0.19522	-0.19609	-0.196853
8 O	-0.296164	-0.32636	-0.32495	-0.3242	-0.323549
9 O	-0.212383	-0.2115	-0.21095	-0.21065	-0.210393
10 Cl	0.419775	0.418092	0.418794	0.419162	0.419484
11 H	0.176755	0.256983	0.256511	0.256262	0.256044
12 H	0.170219	0.252447	0.252349	0.252292	0.252239
13 H	0.136849	0.213362	0.212737	0.212407	0.212117
14 H	0.283047	0.32862	0.327931	0.327566	0.327244

5.2.10 ELF, LOL & Charge Transfer Studies

The feature of the identical spin pair density, ELF, is a widely used technique for estimating electron localization in atomic or molecular systems, whereas LOL elucidates maximum localized orbitals intersecting due to the gradients of orbitals. Fig 5.8 depicts the vector – colour filled map of ELF of 2CP4CA in gas phase. The region around the hydrogen atom is red in the current study, representing a region of maximal Pauli repulsion and the region around the chlorine and carbon atoms appear to have the least measure of Pauli repulsion, while the oxygen atoms have a mid-range value. The vector – colour filled map of LOL for 2CP4CA in gas phase is exhibited in Fig 5.9. The little blue colour circles encompassing chlorine and carbon atoms signify electron depletion between the valence and inner shells while the red colour indications adjoining hydrogen atoms with high LOL values are due covalent bonds between the atoms.

The hole-electron transition distribution interprets charge transfer of electron and the hole taking place within the compound for three excited states. Table 5.10 reveals the excitation energy (E), D index, Δr index and t index for three excited states for 2CP4CA and relating electron (green)-hole (blue) iso surface contributions is exemplified in Fig 5.10. It is evident that the D index value (centroid distance between the electron-hole) and Δr index (measure of the hole-electron transfer length) value for the first excitation state is larger which depicts that strong excitation occurs.

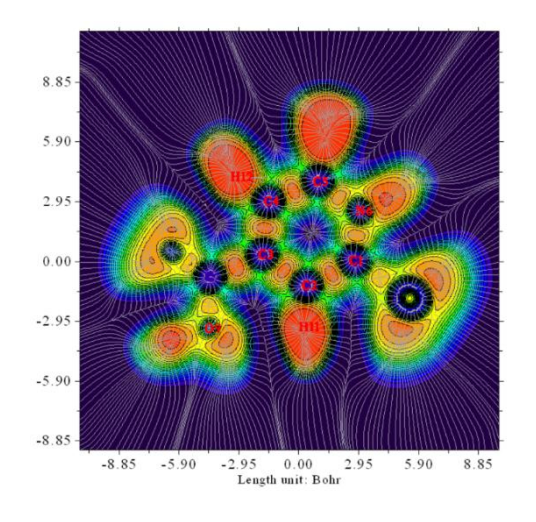


Fig 5.8 ELF, vector - colour filled map of 2CP4CA in gas phase.

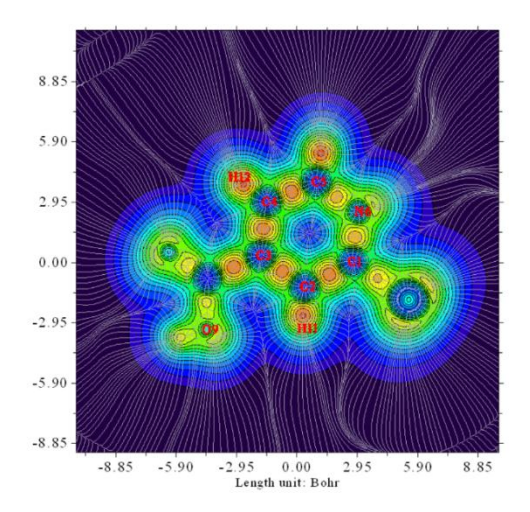


Fig 5.9 LOL, vector - colour filled map of 2CP4CA in gas phase.

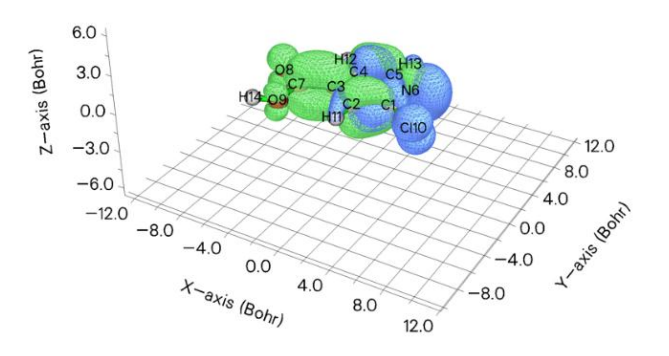


Fig 5.10 Iso surface of hole and electron distribution of 2CP4CA.

Table 5.10 Electron - hole interaction parameters of 2CP4CA.

Parameters	First excited state	Second excited state	Third excited state
Excitation energy, E (eV)	4.261	4.452	4.494
D index (A°)	2.0684	1.565	1.6963
Δr index	2.185	0.194	0.154
t index	0.739	-1.021	-1.393

5.2.11 RDG Analysis

RDG-Reduced density gradient is a standard implement for reckoning and envisioning the intense exchanges of molecule [42].

RDG (r) =
$$\frac{1}{2(3\pi r^2)^{1/3}} + \frac{[\nabla \rho(r)]}{\rho(r)^{4/3}}$$

The above formula reveals the dimensionless type of concentration gradient of electron. NCI analyses are critical components of major biological research. In the existing work, the RDG colour filled map for the heading compound in gas phase, indicated in blue, green and red blemished regions is depicted in Fig 5.11. The intensity connection in the molecular structure shows that blue colour represents higher attraction, red colour represents the ring system that causes the steric effect and the green colour signifies non-covalent interaction that might be accountable for stabilization of the heading compound.

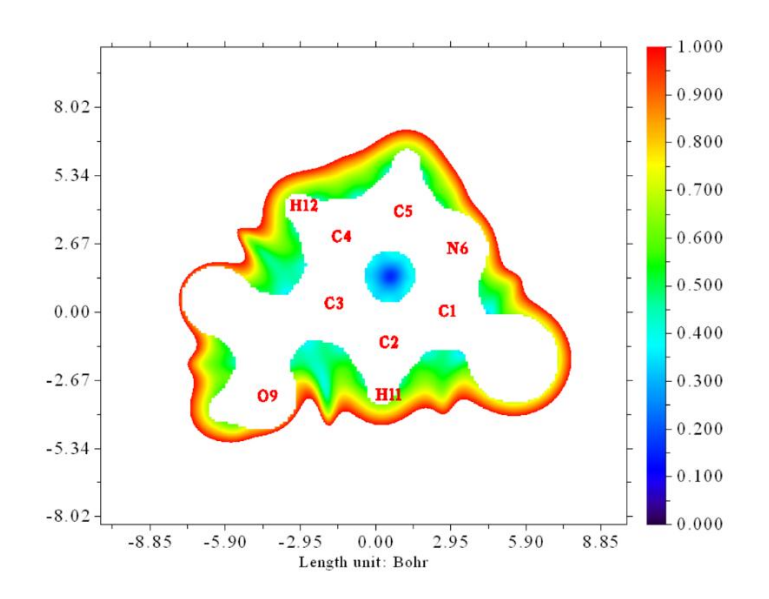


Fig 5.11 RDG-colour filled map of 2CP4CA in gas phase.

5.3 CONCLUSION

This works exclusively explicate, the geometrical factors, vibrational properties, FMO analysis, reactive sites, NLO, Mulliken charges, thermodynamical properties and UV investigations of 2CP4CA in polar protic solvents (water, methanol, ethanol and 1-propanol) and in gas phase by implementing DFT approach. The theoretical geometrical factors and experimental geometrical factors acquired from the literature swot were compared and found to be in accord. For 2CP4CA, the premeditated vibrational wavenumbers and their PED are estimated. Theoretical outcomes were mostly in agreement with the experimental information. The assessed value of first order hyperpolarizability for 2CP4CA is 1.4794×10^{-30} esu in gas phase measured to be greater than that of urea (7.5 times) indicates that 2CP4CA has extensive NLO properties. The highest stabilisation energy of 61.18 K cal / mol is spotted from π^* (Carbon2-Carbon3) to π^* (C4-C5) for the caption compound. Among all the polar protic solvents, water is detected to have the highest thermodynamical values. UV investigation spectra reinforce to forecast the differed properties of the compound. The

positive and negative regions of 2CP4CA with water showing highest potential range between -8.010e-2 to 8.010e-2 is revealed from the MEP figure. In addition, the ELF, LOL and electron-hole interaction studies were also conducted. Exploration of Mulliken charges and Fukui analysis for 2CP4CA was explicated for the heading molecule. From the molecular descriptors of the polar protic solvents, water was found to have the highest energy gap of 5.02625 eV. The polar protic solvents disclosed conspicuous variations when compared with gas phase for 2CP4CA.

REFERENCES

- [1] Y.B. Atalay, D.M.Di Toro, R.F. Carbonaro, Estimation of stability constants for metal-ligand complexes containing neutral nitrogen donor atoms with applications to natural organic matter, Geochim. Cosmochim. Acta 122 (2013) 464–477, https://doi.org/10.1016/j.gca.2013.08.030.
- [2] A.M.K. El-Dean, A.A. Abd-Ella, R. Hassanien, M.E.A. El-Sayed, Sh.A.A. Abdel Raheem, Design, synthesis, characterization, and insecticidal bioefficacy screening of some new pyridine derivatives, ACS Omega 4 (2019) 8406–8412, https://doi.org/10.1021/acsomega.9b00932.
- [3] P. Koczoń, J. Piekut, M. Borawska, R. Świsłocka, W. Lewandowski, The relationship between chemical structure and antimicrobial activity of selected nicotinates, p-iodobenzoates, picolinates and isonicotinates, Spectrochim. Acta Part A 61 (2005) 1917–1922, https://doi.org/10.1016/j.saa.2004.07.022.
- [4] S.S. Dhondge, P.N. Dahasahasra, L.J. Paliwal, V.M. Tangde, D.W. Deshmukh, Volumetric and viscometric study of thiamine hydrochloride, pyridoxine hydrochloride and sodium ascorbate at T = (275.15, 277.15 and 279.15) K in dilute aqueous solutions, J. Chem. Thermodyn. 107 (2017) 189–200, https://doi.org/10.1016/j.jct.2016.12.033.
- [5] Zheng, Q.-Z., Zhang, X.-M., Xu, Y., Cheng, K., Jiao, Q.-C., & Zhu, H.-L. Synthesis, biological evaluation, and molecular docking studies of 2-chloropyridine derivatives possessing 1,3,4-oxadiazole moiety as potential antitumor agents, Bioorganic & Medicinal Chemistry, 18(22) (2010), 7836–7841. doi:10.1016/j.bmc.2010.09.051.
- [6] K. Datta, D.K. Roy, A.K. Mukherjee, Spectroscopic and thermodynamic study of charge transfer interaction between vitamin B6 and p-chloranil in aqueous ethanol mixtures of varying composition, Spectrochim. Acta. Part A: Mol. Biomol. Spectrosc. 70 (2008) 425–429, https://doi.org/10.1016/j.saa.2007.12.024.

- [7] J.S. Loring, M. Karlsson, W.R. Fawcett, W.H. Casey, Attenuated total reflectionFourier- transform infrared and 27Al nuclear magnetic resonance investigation of speciation and complexation in aqueous Al(III)- picolinate solutions, Geochim. Cosmochim. Acta 64 (2000) 4115–4129, https://doi.org/10.1016/S0016-7037(00) 00499-3.
- [8] K. Kieć-Kononowicz, E. Szymańska, Antimycobacterial activity of 5-arylidene derivatives of hydantoin, II Farmaco. 57 (2002) 909–916, https://doi.org/10.1016/S0014-827X(02)01292-2.
- [9] W. Wang, A. Basinger, R.A. Neese, B. Shane, S.A. Myong, M. Christiansen, M.K. Hellerstein, Effect of nicotinic acid administration on hepatic very low density lipoprotein triglyceride production, Am. J. Physiol. Endocrinol. Metab. 280 (2001) 540–547, https://doi.org/10.1152/ajpendo.2001.280.3.E540.
- [10] Tyunina, E. Y., Krutova, O. N., & Lytkin, A. I, Determination of the complexation parameters of L-asparagine with some biologically active pyridine derivatives in aqueous solutions from calorimetric results. Thermochimica Acta,(2020) 178704. doi:10.1016/j.tca.2020.178704.
- [11] E. Aydemir, S. Kansiz, M. K. Gumus, N. Y. Gorobets and N. Dege, Crystal structure and Hirshfeld surface analysis of 7-ethoxy-5-methyl-2-(pyridin-3-yl)-11,12- dihydro-5,11-methano[1,2,4] triazolo[1,5-c][1,3,5] benzoxadiazocine, Acta Cryst. E74, (2018)367-370.https://doi.org/10.1107/S2056989018002621.
- [12] E.M. Gonçalves, A. Joseph, A.C.L. Conceição, M.E. Minas da Piedade, Potentiometric titration study of the temperature and ionic strength dependence of the of the acidity constants of nicotinic acid (niacin), J. Chem. Eng. Data 56 (2011) 2964–2970, https://doi.org/10.1021/je200263g.
- [13] A. Gille, E.T. Bodor, K. Ahmed, S. Offermanns, Nicotinic acid: pharmacological effects and mechanisms of action, Annu. Rev. Pharmacol. Toxicol. 48 (2008) 79–106, https://doi.org/10.1146/annurev.pharmtox.48.113006.094746.

- [14] Y. Zhang, The magic bullets and tuberculosis drug targets, Annu. Rev. Pharmacol. Toxicol. 45 (2005) 529–564, https://doi.org/10.1146/annurev.pharmtox.45. 120403.100120.
- [15] W. Lewandowski, M. Kalinowska, H. Lewandowska, The influence of metals on the electronic system of biologically important ligands. Spectroscopic study of benzoates, salicylates, nicotinates and isoorotates. Review, J. Inorg. Biochem. 99 (2005) 1407–1423, https://doi.org/10.1016/j.jinorgbio.2005.04.010.
- [16] Fergal P. Byrne, Saimeng Jin, Giulia Paggiola, Tabitha H.M. Petchey, James H. Clark, Thomas J. Farmer, Andrew J. Hunt, C. Robert McElroy, James Sherwood, Tools and techniques for solvent selection: green solvent selection guides, Sustain. Chem. Processes 4 (1) (2016), https://doi.org/10.1186/s40508-016-0051-z.
- [17] Christian Capello, Ulrich Fischer, Konrad Hungerbühler, what is a green solvent? A comprehensive framework for the environmental assessment of solvents, Green Chem. 9 (9) (2007) 927, https://doi.org/10.1039/b617536h.
- [18] Wancen Xie, Tong Li, Chen Chen, Haibo Wu, Songmiao Liang, Haiqing Chang, Baicang Liu, Enrico Drioli, Qingyuan Wang, John C. Crittenden, Using the green solvent dimethyl sulfoxide to replace traditional solvents partly and fabricating PVC/PVC–g–PEGMA blended ultrafiltration membranes with high permeability and rejection, Ind. Eng. Chem. Res. (2019) 6413–6423, doi: 10.1021/acs. iecr.9b00370.
- [19] Vimala, M., Mary, S. S., Ramalakshmi, R., & Muthu, S., Theoretical description of green solvents effect on electronic property and reactivity of Tertbutyl 4-formylpiperidine-1-carboxylate. Computational and Theoretical Chemistry, 1201 (2021). 113255. doi:10.1016/j.comptc.2021.113255.
- [20] M. Karabacak, C. Karaca, A. Atac, M. Eskici, A. Karanfil, E. Kose, Synthesis, analysis of spectroscopic and nonlinear optical properties of the novel compound: [S]-N-benzyl-1-phenyl-5-[thiophen-3-yl]-4-pentyn-2-amine, Spectrochim. Acta Part A: Mol. Biomol. Spectrosc. 97 (2012) 556–567, https://doi.org/10.1016/j. saa.2012.05.087.

- [21] Sarala, S., Geetha, S. K., Muthu, S., & Asif, F. B., Vibrational spectra and Wavefunction investigation for antidepressant drug of Amoxapine based on quantum computational studies. Chemical Data Collections, 33 (2021) 100699. doi:10.1016/j.cdc.2021.100699.
- [22] Muthu, S., Prasath, M., Isac Paulraj, E., & Arun Balaji, R., FT-IR, FT-Raman spectra and ab initio HF and DFT calculations of 7-chloro-5-(2-chlorophenyl)-3-hydroxy-2,3-dihydro-1H-1,4-benzodiazepin-2-one. Spectrochimica Acta Part A: Molecular and Biomolecular Spectroscopy, 120 (2014) 185–194. doi:10.1016/j.saa.2013.09.150.
- [23] Varsanyi G 1974 Assignments for Vibrational Spectra of Seven Hundred Benzene Derivatives Vol. 1 Adam Hilger London.
- [24] J. George, J.C. Prasana, S. Muthu, T.K. Kuruvilla, R.S. Saji, Evaluation of vibrational, electronic, reactivity and bioactivity of propafenone—a spectroscopic, DFT and molecular docking approach, Chem. Data Collect. 26 (2020) 100360, https://doi.org/10.1016/j.cdc.2020.100360.
- [25] Jeelani, A., Muthu, S., & Narayana, B., Molecular structure determination, Bioactivity score, Spectroscopic and Quantum computational studies on (E)-N'-(4-Chlorobenzylidene)-2-(napthalen-2-yloxy) acetohydrazide. Journal of Molecular Structure, 1241 (2021) 130558. doi:10.1016/j.molstruc.2021.13055.
- [26] Erdogdu, Y., Unsalan, O., Amalanathan, M., & Hubert Joe, I., Infrared and Raman spectra, vibrational assignment, NBO analysis and DFT calculations of 6-aminoflavone. Journal of Molecular Structure, 980(1-3) (2010) 24–30. doi:10.1016/j.molstruc.2010.06.032.
- [27] Bhavani, K., Renuga, S., Muthu, S., & Sankara narayanan, K., Quantum mechanical study and spectroscopic (FT-IR, FT-Raman, 13C, 1H) study, first order hyperpolarizability, NBO analysis, HOMO and LUMO analysis of 2-acetoxybenzoic acid by density functional methods. Spectrochimica Acta Part A: Molecular and Biomolecular Spectroscopy, 136 (2015) 1260–1268. doi:10.1016/j.saa.2014.10.012.

- [28] Ghalla, H., Issaoui, N., Bardak, F., & Atac, A,. Intermolecular interactions and molecular docking investigations on 4-methoxybenzaldehyde. Computational Materials Science, 149 (2018) 291–300. doi:10.1016/j.commatsci.2018.03.0.
- [29] Majid Ali, Asim Mansha, Sadia Asim, Muhammad Zahid, Muhammad Usman, Narmeen Ali, DFT study for the spectroscopic and structural analysis of p-dimethylaminoazobenzene, J. Spectrosc. 2018 (2018) 1–15, https://doi.org/10.1155/2018/9365153.
- [30] Rajeshirke, M., & Sekar, N., NLO properties of ester containing fluorescent carbazole based styryl dyes Consolidated spectroscopic and DFT approach. Optical Materials, 76 (2018) 191–209. doi:10.1016/j.optmat.2017.12.035.
- [31] Abraham, C. S., Prasana, J. C., & Muthu, S., Quantum mechanical, spectroscopic and docking studies of 2-Amino-3-bromo-5-nitropyridine by Density Functional Method. Spectrochimica Acta Part A: Molecular and Biomolecular Spectroscopy, 181 (2017) 153–163. doi:10.1016/j.saa.2017.03.045.
- [32] Weinhold F, Landis C R 2005 Valency and Bonding: a Natural Bond Orbital Donor-acceptor Perspective, Cambridge University Press, Cambridge.
- [33] Sıdır, İ., Sıdır, Y. G., Kumalar, M., & Taşal, E., Ab initio Hartree–Fock and density functional theory investigations on the conformational stability, molecular structure and vibrational spectra of 7-acetoxy-6-(2,3-dibromopropyl)-4,8-dimethylcoumarin molecule. Journal of Molecular Structure, 964(1-3) (2010)134–151. doi:10.1016/j.molstruc.2009.11.023.
- [34] Jayabharathi, J., Thanikachalam, V., Jayamoorthy, K., & Venkatesh Perumal, M., Computational studies of 1,2-disubstituted benzimidazole derivatives. Spectrochimica Acta Part A: Molecular and Biomolecular Spectroscopy, 97 (2012) 131–136. doi:10.1016/j.saa.2012.05.085.
- [35] Y.S. Priya, K.R. Rao, P. V. Chalapathi, A. Veeraiah, K.E. Srikanth, Y.S. Mary, R. Thomas, Intricate spectroscopic profiling, light harvesting studies and other quantum mechanical properties of 3-phenyl-5-isooxazolone using experimental and computational strategies, J. Mol. Struct. 1203 (2020) 127461. https://doi.org/10.1016/j.molstruc.2019.127461.

- [36] J. Ott, Juliana Boerio-Goates, Chemical thermodynamics: principles and applications, Academic Press, San Diego, 2000.
- [37] P. Manjusha, J.C. Prasana, S. Muthu, B.F. Rizwana, Spectroscopic elucidation [FTIR, FT-Raman and UV-visible] with NBO, NLO, ELF, LOL, drug likeness and molecular docking analysis on 1-[2-ethylsulfonylethyl]-2-methyl-5-nitro-imidazole: an antiprotozoal agent, Comput. Biol. Chem. (2020) 107330, https://doi.org/10.1016/j.compbiol.chem.2020.107330.
- [38] Eram Khan Shweta, Poonam Tandon, Rakesh Maurya, Padam Kumar, A theoretical study on molecular structure, chemical reactivity and molecular docking studies on dalbergin and methyldalbergin, J.Mol.Struct. 1183 (2019) 100–106, https://doi.org/10.1016/j.molstruc.2019.01.065.
- [39] Maria Julie, M., Prabhu, T., Elamuruguporchelvi, E., Asif, F. B., Muthu, S., & Irfan, A., Structural (monomer and dimer), wavefunctional, NCI analysis in aqueous phase, electronic and excited state properties in different solvent atmosphere of 3-{(E)-[(3,4-dichlorophenyl)imino]methyl} benzene-1,2-diol. Journal of Molecular Liquids, 336 (2021) 116335. doi:10.1016/j.molliq.2021.116335.
- [40] Almuqrin, A. H., Al-Otaibi, J. S., Mary, Y. S., Mary, Y. S., & Thomas, R., Structural study of letrozole and metronidazole and formation of self-assembly with graphene and fullerene with the enhancement of physical, chemical and biological activities. Journal of Biomolecular Structure and Dynamics, 1–7(2020), doi:10.1080/07391102.2020.1790420.
- [41] Al-Otaibi, J. S., Mary, Y. S., Armaković, S., & Thomas, R., Hybrid and bioactive cocrystals of pyrazinamide with hydroxybenzoic acids: Detailed study of structure, spectroscopic characteristics, other potential applications and noncovalent interactions using SAPT, Journal of Molecular Structure, (2020), 127316, doi:10.1016/j.molstruc.2019.127316.
- [42] Chaima Daghra, Noureddine Issaoui, Houda Marouani, Thierry Roisnel, Omar Al-Dossary, Journal of Molecular Structure, Volume 1247, 5 January 2022, 131311. https://doi.org/10.1016/j.molstruc.2021.131311

CHAPTER VI

EXPLORATION OF FEW POLAR PROTIC AND APROTIC LIQUIDS EFFECT ON VIBRATIONAL, ELECTRONIC INFLUENCES AND REACTIVITY USING IEFPCM SOLVATION STANDARD AND MOLECULAR DOCKING SCRUTINY OF 2FLUORO-4-IODO-5-METHYLPYRIDINE

6.1 INTRODUCTION

Pyridine has been used as a molecular framework, a solvent, a base, a ligand, and a functional group. It is particularly significant class of chemical due to its broad range of biological activities. It performs a vital role in the expansion of synthetic heterocyclic chemistry. In pharmaceutical science, such heterocyclic compounds are widely employed for a variety of purposes [1]. Many substituted pyridines are involved in bioactivities with medicinal and agricultural implications [2]. Functional pyridines are important molecules that are used in a variety of applications [3]. Pyridine along with their derivatives can be found in numerous natural items and have therapeutic uses [4]. Certain pyridine derivatives exhibit anti -bacterial, anti -microbial, pesticide, antitumor, anti -allergic, anti -fungal, analgesic or antihypertensive properties [5-7]. Amongst them are methyl - pyridine derivatives which have operative hypolipidemic effects, anti -inflammatory and anti -neoplastic activities [8]. Taking into account the innumerable significance of methyl-pyridine derivatives, 2-Fluoro-4-iodo-5methylpyridine (2FIMP) having 237.01 as molecular weight, has been preferred for quantum chemical investigation. According to a review of the literature, no vibrational scrutiny or quantum chemical investigation of 2-Fluoro-4-iodo-5-methylpyridine has been published. This inspires us to analyse the modes of vibration and electronic properties of 2FIMP, theoretically. In the existing work, 2-Fluoro-4-iodo-5methylpyridine (2FIMP) was investigated theoretically in gas phase and with dissimilar solvents. Solvents have gotten a lot of attention in the context of green chemistry [9-13]. A distinctive response in the manufacturing of an energetic medicinal constituent includes a solvent as a significant component [14]. Among the different categories of solvents, polar protic solvents (water, 2-propanol) and polar aprotic solvents (acetone, acetonitrile) has been selected to study the solvent effect of 2FIMP. These solvents are chosen as they come under the preferred and usable category in concern with health, safety and environmental aspects [15]. GSK, Pfizer and Sanofi solvent collection guides data reveal a number of inferences [16-19] about the solvents. In the existing study, NBO analysis and NLO properties of the title compound are scrutinised. Furthermore, electronic properties, topology analysis and thermodynamic properties of 2FIMP in dissimilar solvents are conferred along with the drug likeness parameters and docking reports revealing the interaction of 2FIMP with specific (pseudolysin inhibitor and complement factor D inhibitor) proteins.

6.2 OUTCOMES AND DISCUSSION

6.2.1 Geometrical Factors

In theoretical research of organic molecules, geometrical parameters play the most vital significance as it reveals the stability of the molecules [20]. The optimized geometrical parameters of 2FIMP are premeditated by DFT using B3LYP scheme and LANL2DZ set of functions. The geometrical factors in terms of bond length and bond angles are ascertained in this study, and the results are displayed in Table 6.1. The entire numbering of atoms beginning from one to 14 has been identified and the atoms are

exhibited in specific colours as in Fig 6.1. Crystal information of 2FIMP is compared with structurally associated molecule [21]. 2FIMP possess 5 C-C, 1 C-F, 1 C-I, 2 C-N and 5 C-H bonds. Among the 5 C-C bonds, C4-C7 possess highest bond length of 1.512 Å and among the five C-H bonds, C7-H12 and C7-H14 are found with highest value of 1.097 Å. C1-N6 and C5-N6 was found to have bond length of 1.324 and 1.357 Å correspondingly. 2.138 Å was the longest bond length noticed between carbon and iodine atom and a value of 1.394 Å was found between carbon and fluorine atom in gas phase. Carbon2-Carbon1-Nitrogen6 (125.5°) was observed to have highest bond angle and the least bond angle was spotted at H12-C7-H14 (107.1°) in gas phase. The experimental data are quite close to the theoretical data. Slight variations are observed in the computed values because the experimental values signified are of a compound that's analogous with the heading compound and not the precise one. Moreover, differences emerge because experimental studies are executed in the solid state, whereas theoretical reckonings are accomplished on a secluded molecule in the vaporised state.

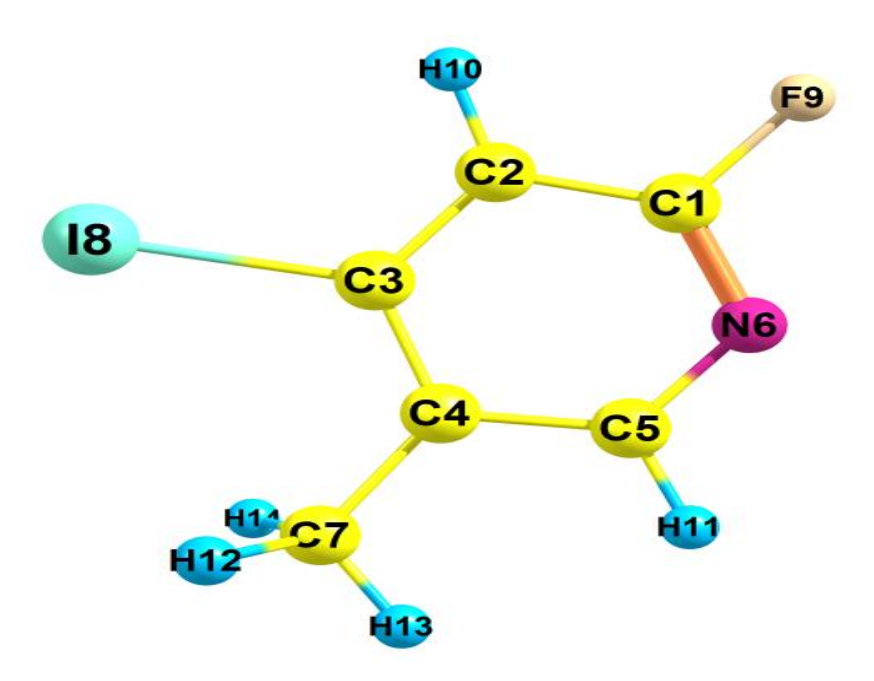


Fig 6.1 Optimized picture of 2FIMP with atom numbering.

Table 6.1 Geometric parameters of 2FIMP in gas phase at B3LYP/LANL2DZ.

PARAMETER	B3LYP/LANL2DZ	Experimental*	PARAMETER	B3LYP/LANL2DZ	Experimental*
BOND LENG	TH(Å)		BOND ANGLE (°)	
C1-C2	1.403	1.375	C2-C1-N6	125.5	125.1
C1-N6	1.324	1.307	C2-C1-F9	117.7	
C1-F9	1.394		C1-C2-C3	116.6	117.3
C2-C3	1.405	1.367	C1-C2-H10	120.4	121.3
C2-H10	1.083	0.93	N6-C1-F9	116.8	
C3-C4	1.419	1.383	C1-N6-C5	117	116.3
C3-I8	2.138		C3-C2-H10	123	120
C4-C5	1.413	1.378	C2-C3-C4	120.6	120
C4-C7	1.512	1.491	C2-C3-I8	118.3	
C5-N6	1.357	1.334	C4-C3-I8	121.1	
C5-H11	1.086	0.93	C3-C4-C5	116	116.9
C7-H12	1.097	0.97	C3-C4-C7	124	122.7
C7-H13	1.095	0.97	C5-C4-C7	120	122.7
C7-H14	1.097	0.97	C4-C5-N6	124.4	124.3
			C4-C5-H11	119.8	117.9
			C4-C7-H12	111.4	109.4
			C4-C7-H13	110.7	109.4
			C4-C7-H14	111.3	109.4
			N6-C5-H11	115.9	117.9
			H12-C7-H13	108.1	108
			H12-C7-H14	107.1	108
			H13-C7-H14	108.1	108

^{*}Ref[21]

6.2.2 Vibrational Description

2FIMP consists of 14 atoms leading to have 36 normal modes of fundamental vibrations (3N-6). Theoretical estimates generated applying the computational approach were competed with observed FT (IR & Raman) spectra procured from the

spectra source internet site [22]. After multiplying with the scaling factor 0.961, the scaled values of 2FIMP were derived from unscaled data. Table 6.2 discloses the vibrational modes together with the assessed frequencies in dissimilar polar protic and aprotic liquids chosen for study along with PED values.

The vibrations of C - C stretch are predictable to emerge in 1650–1100 1/cm range [23] whereas the C–H vibrations commonly appear in the outline region, 3100–3000 1/cm [24]. The determined evaluations of stretching vibrations of C - C are identified hypothetically between 1540 and 1206 cm⁻¹ and for C - H vibrations between 3138 and 2929 1/cm with 100% PED contribution at 3026 1/cm.

The distinctive Carbon–Nitrogen vibrations of stretch are spotted in the section 1400–1200 1/cm and merging of numerous bands are probable in this section [25]. The computed Carbon – Nitrogen vibrations that stretch were accomplished in the current investigation between 1540 and 845 cm⁻¹ with highest PED influence of 34 % at ascended wavenumber of 1520 cm⁻¹, theoretically.

A PED influence of 19 % is found for the C-F band of molecule spotted at 1170 1/cm. The ascertained evaluations of vibrations of stretch of C - I are identified hypothetically at 651,332 and 210 cm⁻¹.

The assessments premeditated by DFT approach exhibit satisfactory concurrence relating the investigational values procured from the foundation of spectra. The influence of polar protic and aprotic solvents on 2FIMA vibrations was investigated and noticeable variations in wavenumbers between the gas phase and polar protic and aprotic solvents were observed.

Table 6.2 Theoretical comparison of vibrational frequency of 2FIMP at B3LYP method with LANL2DZ basis set in gas and in different solvents.

	Expe	rimental*		Frequency - 0	Gas		Frequency i	n different solve	nts	
S.No	FT-IR	FT- RAMAN	Scaled	Intensity- IR	Intensity- RAMAN	Water	Acetone	Acetonitrile	2-Propanol	Assignment
1			3138	1	68	3140.50	3140.36	3140.45	3140.27	YCH (99)
2			3092	14	122	3104.32	3103.76	3104.07	3103.72	YCH (99)
3	3050	3055	3026	19	50	3033.18	3032.84	3033.03	3032.77	YCH (100)
4			3002	14	56	3004.84	3004.82	3004.88	3004.79	YCH (80)
5			2929	17	165	2932.10	2931.97	2932.07	2931.94	YCH (100)
6	1590	1580	1540	97	16	1533.25	1533.57	1533.38	1533.55	YNC (13)+YCC (33)+βCCN (10)
7	1520	1525	1520	139	9	1523.63	1523.53	1523.60	1523.44	YNC (34)+YCC (19)+βCCC (11)
8	1450	1460	1456	5	7	1448.80	1449.36	1449.04	1449.39	βНСН (70)
9			1452	14	12	1442.12	1442.71	1442.37	1442.77	βНСН (78)+τНССС(14)
10			1434	139	1	1428.59	1429.02	1428.78	1429.05	βHCC (22)+βHCN (30)+βCCN (17)
11	1350	1355	1400	22	12	1393.41	1393.94	1393.63	1394.00	βНСН (94)
12	1310	1300	1299	57	2	1298.00	1298.04	1298.01	1298.05	YCC (52)
13			1286	4	1	1285.11	1285.35	1285.23	1285.35	ΥNC (20)+βHCC (18)+βHCN(42)
14	1250	1255	1258	4	23	1258.32	1258.30	1258.32	1258.16	YCC (53)+YNC (24)
15	1220	1215	1206	25	15	1196.71	1197.17	1196.89	1197.17	YCC (41)+YNC (14)+YFC (16)
16			1170	29	2	1160.83	1161.63	1161.21	1161.68	YFC (19)+βHCC (36)+βCCC (11)
17		1040	1046	10	1	1045.44	1045.53	1045.47	1045.54	βHCH (22)+τHCCC(57)+ωCCCC(14)
18	1025		1003	2	3	1006.38	1006.23	1006.32	1006.21	βHCC (10)+βCCC (25)
19			990	21	4	992.75	992.79	992.77	992.78	βНСН (10)+τНССС(48)
20	900	905	910	7	0	912.04	912.08	912.06	912.08	τHCNC(78)+ τCCNC(10)
21	880	890	875	28	2	872.47	872.97	872.69	873.04	τHCCN(77)

	Exper	imental [*]	F	requency -	Gas	Fr	equency i	in different se	olvents	
S. No	FT-IR	FT- RAMAN	Scaled	Intensity- IR	Intensity- RAMAN	Water	Acetone	Acetonitrile	2-Propanol	Assignment
22			845	65	22	837.79	838.22	837.99	838.25	YNC (18)+YCC (21)+YFC(16)+βCCN (18)
23		756	727	0	4	725.90	726.05	725.96	726.07	τCCNC(53)+ τCCCN(19)
24			709	16	6	704.77	705.16	704.95	705.18	YCC (28)+YFC(19)+βCCN (32)
25	680	675	651	23	6	649.82	649.92	649.86	649.93	ΥΙC (12)+βCCN (20)+βCNC (37)+βFCN (10)
26		600	584	2	3	582.61	582.70	582.64	582.72	τCCNC(12)+ ωFCNC(30)+ωICCC(20)+ωCCCC(14)
27	510	500	481	4	8	478.78	478.87	478.82	478.88	ΥFC (10) +βCCN (20)+βFCN (31)
28	450	455	446	13	0	445.25	445.41	445.32	445.43	τHCNC(13)+ τCCCN(10)+ τCCNC(36)+ωFCNC(16)+ωICCC(15)
29			436	3	3	436.39	436.60	436.49	436.62	βCNC (10)+βCCC (29)+βFCN (14)
30		350	334	4	3	335.06	335.09	335.07	335.11	τCCCN(10)+ωFCNC(15)+ωCCCC(48)
31			332	0	3	332.84	332.92	332.86	332.92	YIC (18)+βCCC (40)+βFCN(24)
32		220	210	0	6	210.93	210.88	210.90	210.88	YIC (54)+βCCC (22)
33		170	163	1	2	164.08	163.72	163.79	163.71	βICC (77)
34			161	0	0	162.91	163.00	162.93	163.01	тHCCC(79)
35			150	1	1	150.42	150.46	150.41	150.46	τCCCN(24)+ ωFCNC(15)+ωICCC(37)+ωCCCC(10)
36			121	1	1	122.17	122.28	122.20	122.32	τ CCNC(47)+ τ CCCN(22)+ ω ICCC(12)

Υ -stretching, β- in plane bending, ω – out plane bending, τ – torsion

^{*}Ref [22]

6.2.3 Electronic Properties

The ultraviolet–visible spectroscopy is used to analyse the dynamic and static properties of the molecule in their higher state [26]. The TD/DFT has newly arisen as an influential tool for studying the standing and energetic properties of molecules in their excited states, providing for a better balance of precision and price of computation [27]. The hypothetical UV/Visible band of 2FIMP is raised utilizing TD-DFT method with IEFPCM solvation prototype for gas along with polar protic and aprotic liquids.

Table 6.3 displays the transition contribution %, absorption wavelength, oscillator potency and energy of transition for dissimilar solvents. Fig 6.2 reveals the comparative UV spectra of 2FIMP in dissimilar solvents. The highest absorption peak for the solvents chosen were found to be 261.9 nm (water), 262.2 nm (acetone), 262.03 nm (acetonitrile) and 262.25 nm (2-propanol) with band gap energy value of 4.73 eV for all the selected protic and aprotic liquids. For gas, the uppermost absorption peak was 262.57 nm with energy band gap as 4.72 eV for the transition contribution HOMO->L+1 (95%). The band gap energy values vary slightly between the chosen solvent phase and the gaseous phase.

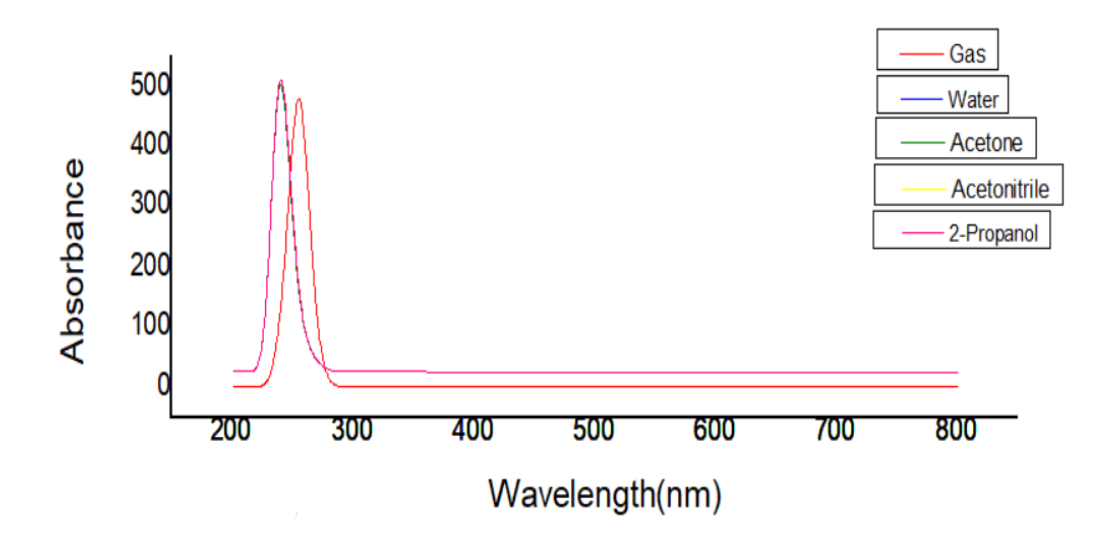


Fig 6.2 Theoretical comparative UV spectra of 2FIMP in different solvents.

Table 6.3 Theoretical electronic transition parameters of 2FIMP in gas and other solvents.

Solvents	Wavelength (nm)	Band gap (ev)	Energy (cm ⁻¹)	Osc. Strength(f)	Symmetry	Major contributions
GAS	262.5782393	4.72	38083.88703	0.0002	Singlet-A	HOMO->L+1 (95%)
	255.4742186	4.85	39142.89299	0.0061	Singlet-A	H-3->LUMO (16%), H-2->LUMO (73%)
	243.3543869	5.09	41092.33505	0.0011	Singlet-A	H-3->L+1 (45%), H-2->L+1 (37%)
WATER	261.9015484	4.73	38182.28667	0.0004	Singlet-A	HOMO->L+1 (98%)
	249.2194678	4.97	40125.27629	0.0015	Singlet-A	H-1->L+1 (99%)
	238.4861757	5.2	41931.15165	0.0081	Singlet-A	H-3->LUMO (92%)
ACETONE	262.2006366	4.73	38138.73273	0.0004	Singlet-A	HOMO->L+1 (98%)
	249.289621	4.97	40113.98453	0.0015	Singlet-A	H-1->L+1 (99%)
	239.1255241	5.18	41819.04059	0.0081	Singlet-A	H-3->LUMO (92%)
ACETONITRILE	262.0343922	4.73	38162.92936	0.0004	Singlet-A	HOMO->L+1 (98%)
	249.2495286	4.97	40120.43696	0.0015	Singlet-A	H-1->L+1 (99%)
	238.7617336	5.19	41882.75839	0.0081	Singlet-A	H-3->LUMO (92%)
2-PROPANOL	262.2560983	4.73	38130.66719	0.0004	Singlet-A	HOMO->L+1 (98%)
	249.3196988	4.97	40109.1452	0.0016	Singlet-A	H-1->L+1 (99%)
	239.1993383	5.18	41806.13572	0.0082	Singlet-A	H-3->LUMO (92%)

6.2.4 MEP Analysis

MEP mapping have been proven to be extremely useful in analysing molecular structure, electron density and its physicochemical features [28]. MEP of 2FIMP was obtained at the B3LYP/ LANL2DZ level of theory for a range of -4.695e1 to 4.692e1 eV in gas phase and has been portrayed in Fig 6.3.

The electrophilic location is shown in red, the nucleophilic site is highlighted in blue, the neutral sites are highlighted in green and light blue indicates the slightly electro deficient region. For 2FIMP, the negative regions are primarily localized on fluorine and iodine atoms and blue shade on atom of nitrogen specifies to possess positive potential.

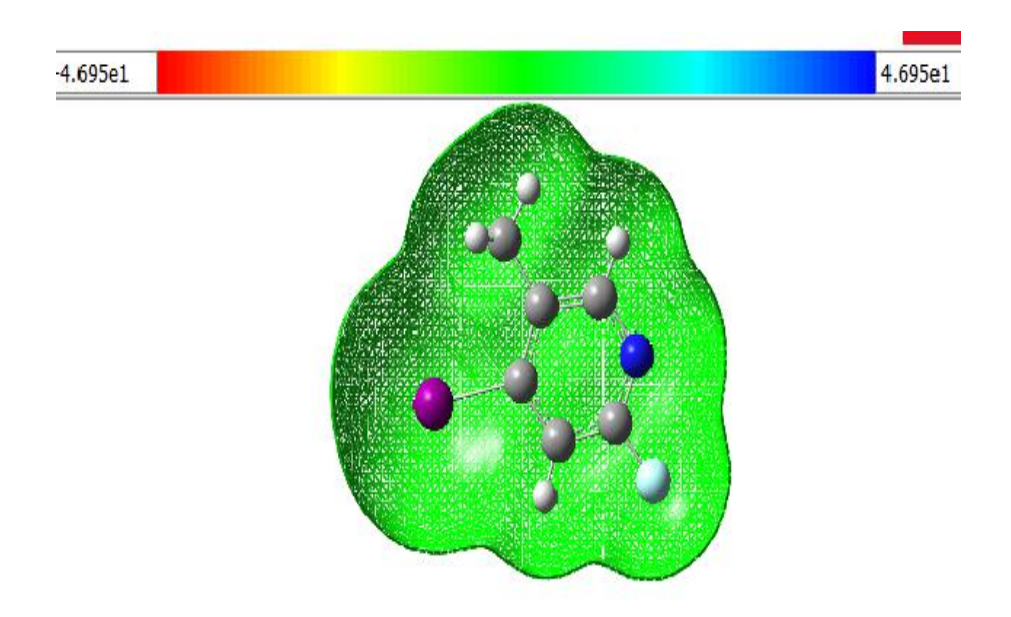


Fig 6.3 Molecular Electrostatic Potential of 2FIMP by B3LYP/LANL2DZ in gas phase.

6.2.5 NLO Investigation

In the prevailing world, NLO active materials are employed in data storage, telecommunications and optical signal processing [29]. The most cost-effective and practical approach of estimating the material's NLO properties is through DFT research. Table 6.4 discloses the analysed values of nonlinear parameters such as μ -dipole moment, β - first order hyperpolarizability and α - polarizability of 2FIMP in gaseous phase and polar protic and aprotic solvents. 2FIMP has a dipole moment and first order hyperpolarizability values of 1.3706 D and 1.1768 x 10⁻³⁰ esu respectively in gas phase which is evaluated to be larger than that of the verge material suggesting that 2FIMP has extensive NLO properties.

The value of β for the polar protic and aprotic solvents was computed to be 3.75596 x 10^{-30} (water), 3.49582 x 10^{-30} (acetone), 3.64557 x 10^{-30} (acetonitrile) and 3.4752 x 10^{-30} (2-propanol). Among the solvents chosen, water was found to have a high μ value (1.73119 D) and α value (1.65749 x 10^{-23} esu). The variations appeared in the properties explores that the solvents have amplified the polarizability of 2FIMP. Due to higher values, the caption compound conceivably be exposed as a capable NLO compound.

Table 6.4 The values of calculated dipole moment $\mu(D)$, polarizability(α) and first order hyperpolarizability(β) of 2FIMP.

			B3LYP/LAN	L2DZ		
parameter	GAS	WATER	ACETONE	ACETONITRILE	2-PROPANOL	
μ_{x}	-1.3608577	-1.7236891	-1.7022922	-1.7145027	-1.7004913	
μ_{y}	0.1630004	0.1601544	0.1614941	0.1607452	0.161601	
$\mu_{\rm z}$	0.0142481	0.0169281	0.016742	0.0168475	0.0167266	
μ(D)	1.370658899	1.731196149	1.71001736	1.722104052	1.708234563	
α_{xx}	121.994999	162.6840425	160.1930722	161.6130311	159.9840052	
α_{xy}	13.1720502	20.9995721	20.4842966	20.7774511	20.4412628	
$\alpha_{ m yy}$	97.5238286	129.0437797	127.0189121	128.171443	126.8496035	
α_{xz}	-0.4158873	-0.5596122	-0.551808	-0.5562766	-0.5511456	
α_{yz}	-0.1378331	-0.2084335	-0.2036095	-0.2063513	-0.2032076	
α_{zz}	35.9194487	43.7965693	43.1333724	43.5073706	43.07919	
α (a.u)	85.1460921	111.8414638	110.1151189	111.0972816	109.9709329	
α (e.s.u)	1.2619E-23	1.65749E-23	1.63191E-23	1.6465E-23	1.6298E-23	
Δα (a.u)	224.8328455	301.1059378	296.4887892	299.1219843	296.1008258	
Δα (e.s.u)	3.3320E-23	4.46239E-23	4.39396E-23	4.4330E-23	4.3882E-23	
β_{xxx}	5.366673	186.2641116	168.0810721	178.7014169	166.6633006	
β_{xxy}	74.6926672	209.2898274	197.7420592	204.2149593	196.7887047	
β_{xyy}	-0.9465335	67.9042651	61.0424533	64.9518595	60.4932299	
β_{yyy}	29.7759613	42.4754249	41.5624827	42.1321295	41.4950179	
β_{zxx}	0.1477393	-0.5834374	-0.369209	-0.5530077	-0.3622689	
β_{xyz}	-0.3775293	-0.8675621	-0.6693945	-0.8500699	-0.6645831	
β_{zyy}	-0.5265331	-1.2437522	-1.1007204	-1.2127454	-1.0940758	
β_{xzz}	24.690766	53.6684145	50.8093846	52.5160886	50.593583	
β_{yzz}	28.5857431	55.2044266	52.8604589	54.2062521	52.6736755	
β_{zzz}	-1.0600885	-2.1960005	-2.0866805	-2.1497814	-2.0780778	
β _{tot} (a.u)	136.2093279	434.7528721	404.6423992	421.9762255	402.260892	
β_{tot} (e.s.u)	1.1768E-30	3.75596E-30	3.49583E-30	3.6456E-30	3.47525E-30	

6.2.6 Thermodynamical Properties

The typical statistical thermodynamical parameters such as heat capacity, enthalpy and entropy for 2FIMP were calculated in gaseous phase and selected solvents phase and are recorded in Table 6.5. In gaseous phase, the computed values of abovementioned parameters for 2FIMP were found to be 131.463 J/mol K, 23.943 J/mol K

and 386.987 J/mol K at 298.15K correspondingly. Amongst the polar protic and aprotic solvents chosen for study, water and acetonitrile were detected to have the highest thermodynamical values respectively at 298.15 K. Chemical reactions in the thermochemical sector may benefit from the planned evaluations of 2FIMP, which are based on the second law of thermodynamics [30]. The linking chart of temperature with the thermodynamical parameters in gas phase is exposed in Fig 6.4.

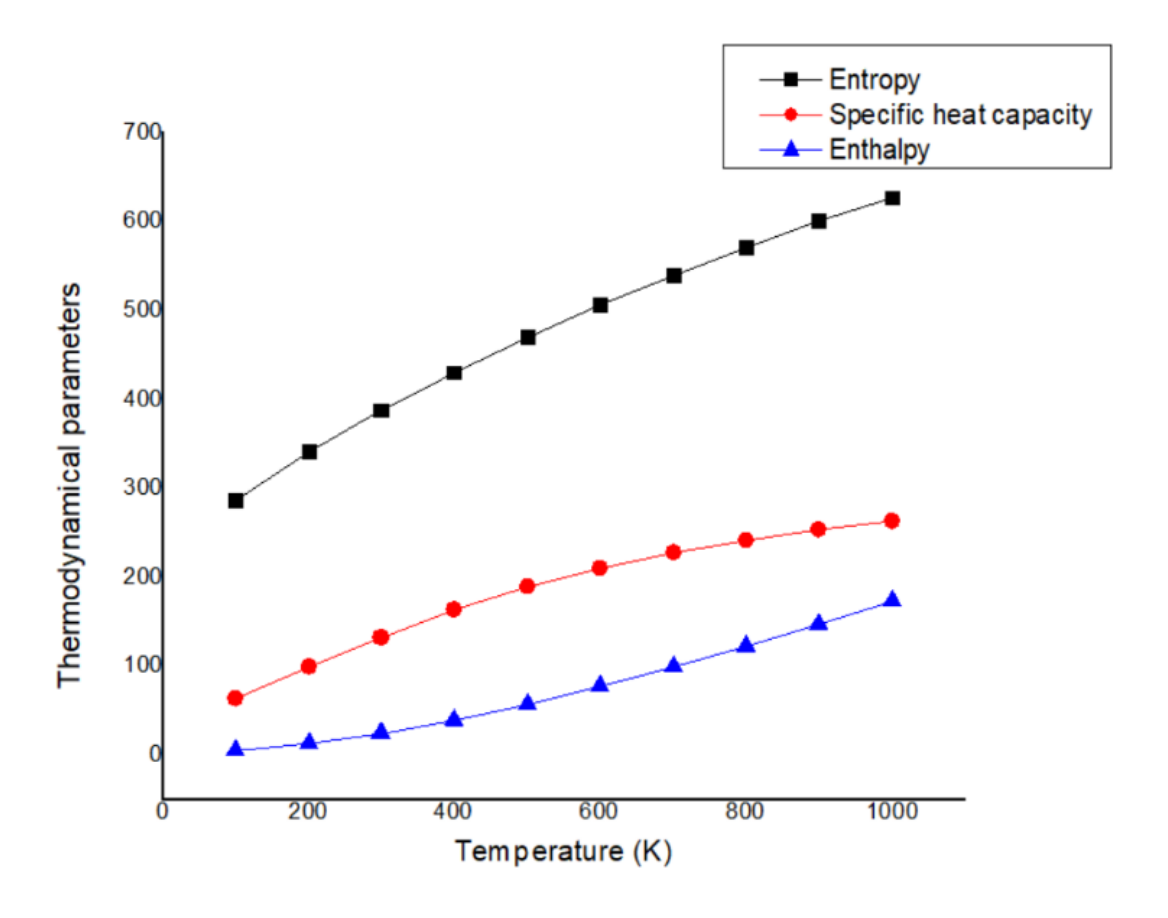


Fig 6.4 Graph representing thermodynamical parameters on temperature of 2FIMP in gas phase.

Table 6.5 Thermodynamical parameters of 2FIMP in different phases.

a) Entropy					
T (K)	Gas	Water	Acetone	Acetonitrile	2-Propanol
100	285.985	285.755	285.757	285.762	285.754
200	341.354	341.053	341.051	341.062	341.047
298.15	386.987	386.715	386.705	386.72	386.7
300	387.802	387.53	387.521	387.536	387.515
400	430.075	429.857	429.84	429.86	429.834
500	469.271	469.107	469.084	469.107	469.078
600	505.634	505.515	505.487	505.513	505.48
700	539.341	539.257	539.226	539.253	539.219
800	570.619	570.561	570.527	570.556	570.52
900	599.713	599.674	599.639	599.669	599.632
1000	626.857	626.832	626.795	626.826	626.788
b) Specific h	eat capacity				
T (K)	Gas	Water	Acetone	Acetonitrile	2-Propanol
100	63.858	63.669	63.67	63.675	63.668
200	99.086	99.09	99.076	99.086	99.074
298.15	131.463	131.602	131.579	131.593	131.577
300	132.06	132.201	132.178	132.192	132.176
400	162.678	162.901	162.874	162.89	162.872
500	188.767	189.018	188.991	189.006	188.99
600	210.002	210.244	210.219	210.233	210.218
700	227.163	227.376	227.355	227.367	227.354
800	241.164	241.344	241.325	241.336	241.325
900	252.736	252.884	252.868	252.877	252.868
1000	262.411	262.531	262.518	262.525	262.518
c) Enthalpy					
T (K)	Gas	Water	Acetone	Acetonitrile	2-Propanol
100	4.431	4.417	4.417	4.417	4.417
200	12.62	12.597	12.597	12.598	12.596
298.15	23.943	23.928	23.925	23.928	23.925
300	24.187	24.172	24.169	24.172	24.169
400	38.955	38.958	38.953	38.957	38.953
500	56.569	56.596	56.589	56.594	56.588
600	76.545	76.598	76.587	76.594	76.586
700	98.433	98.509	98.496	98.504	98.495
800	121.873	121.968	121.953	121.962	121.952
900	146.585	146.697	146.681	146.691	146.679
1000	172.357	172.482	172.464	172.475	172.463

6.2.7 FMO, NBO and topology analyses

6.2.7.1 FMO Investigation

The HOMO & LUMO are termed as FMO. The HOMO is cogently considered as a nucleophilic which is immediately related to the ionisation potential, whereas the LUMO is electrophilic, with electron accepting orbitals that are directly tied to the molecule's electron affinity [31]. Fig 6.5 portrays the HOMO-LUMO plot of 2FIMP molecule. Table 6.6 specifies the premeditated values of universal descriptors in dissimilar solvents of 2FIMP. The computed values of energy gap and electronegativity were found to be 5.75906 eV and 4.6746 respectively whereas chemical hardness and softness were found to be 2.8793 and 0.173639 correspondingly for 2FIMP in gaseous phase. Considering the polar protic and aprotic solvents chosen, the highest values of energy gap (5.68504 eV), ionisation potential (7.29515), chemical hardness (2.8425), electrophilicity index (3.4873) and lowest chemical softness (0.1759) were recorded for 2-propanol. Chemical potential is found to be -4.6746 for 2FIMP in gas phase.

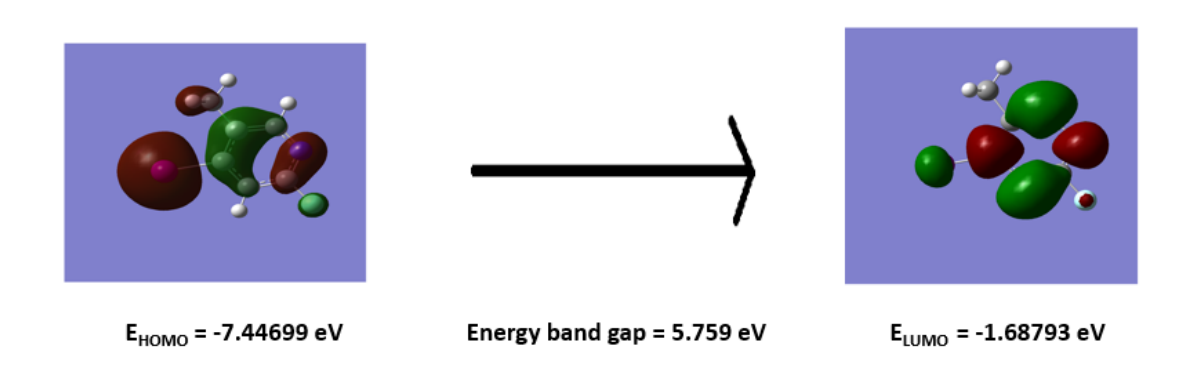


Fig 6.5 Atomic orbital HOMO - LUMO composition of the frontier molecular orbital of 2FIMP in gas phase.

Table 6.6 Calculated energy values of 2FIMP with solvation effect.

Molecular descriptors	Gas	Water	Acetone	Acetonitrile	2-Propanol
HOMO(eV)	-7.44699	-7.29026	-7.29489	-7.2921646	-7.29515784
LUMO(eV)	-1.68793	-1.60929	-1.61011	-1.6095661	-1.61011037
Ionization potential	7.44699	7.29026	7.294886	7.29216457	7.295157844
Electron affinity	1.68793	1.609294	1.61011	1.60956614	1.610110372
Energy gap(eV)	5.75906	5.680966	5.684775	5.68259843	5.685047472
Electronegativity	4.56746	4.449777	4.452498	4.45086535	4.452634108
Chemical potential	-4.56746	-4.44978	-4.4525	-4.4508654	-4.45263411
Chemical hardness	2.87953	2.840483	2.842388	2.84129921	2.842523736
Chemical softness	0.173639	0.176026	0.175908	0.17597583	0.175900026
Electrophilicity index	3.622412	3.485413	3.487339	3.4861169	3.487385215
Electronic charge	1.586182	1.566556	1.566464	1.56648949	1.566436914
Electron donating capability (w-)	6.266084	6.065362	6.068886	6.06671198	6.069017736
Electron accepting capability (w+)	1.698624	1.615585	1.616388	1.61584662	1.616383628

6.2.7.2 NBO studies

Based on the electron occupancy between the matching bonds, NBO analysis indicates the type of bonds and their hybridization [32]. Table 6.7 depicts the bonding and anti-bonding of 2FIMP along with stabilization energy. E (2) of 6.48 Kcal/mol and 25.4 Kcal/mol respectively were noted for the interaction from σ (C5-H11) to σ *(C1-N6) and π (Carbon2-Carbon3) to π * (Carbon1-Nitrogen6). Strong interactions caused by the change of electron concentration from LP(3) of F9 to π *(C1-N6) has been detected with E(2) of 25.76 Kcal/mol. The highest assessed value of E (2) being 155.5 Kcal / mol was spotted for interaction from π *(Carbon1-Nitrogen6) to π *(Carbon2-Carbon3).

Table 6.7 Second order perturbation theory analysis of Fock matrix in NBO for 2FIMP.

Donor	Type	ED/e(qi)	Acceptor	Type	ED/e(qi)	E(2) kcal/mol	E(j)- E(i) a.u.	F(i,j) a.u.
C 1-C 2	σ	1.9776	C 1-N 6	σ*	0.03554	0.76	1.17	0.027
C 1-N 6	σ	1.98614	C 1-C 2	σ^*	0.04086	1.2	1.31	0.036
C 1-N 6	π	1.72879	C 2-C 3	π^*	0.36129	15.12	0.31	0.063
C 1-F 9	σ	1.99242	C 2-C 3	σ^*	0.0221	2.04	1.55	0.05
C 2-C 3	σ	1.97933	C 1-C 2	σ^*	0.04086	1.17	1.21	0.034
C 2-C 3	π	1.71023	C 1-N 6	π^*	0.42305	25.4	0.25	0.074
C 2-H 10	σ	1.97528	C 1-N 6	σ^*	0.03554	4.5	0.97	0.059
C 3-C 4	σ	1.97473	C 2-C 3	σ^*	0.0221	1.77	1.21	0.041
C 3-I 8	σ	1.97519	C 1-C 2	σ^*	0.04086	5.44	0.99	0.066
C 4-C 5	σ	1.96416	C 3-C 4	σ^*	0.0221	4.08	1.26	0.064
C 4-C 5	π	1.65547	C 1-N 6	π^*	0.42305	17.22	0.25	0.06
C 4-C 5	π	1.65547	C 7-H 12	σ^*	0.00849	2.1	0.72	0.038
C 4-C 7	σ	1.9749	C 2-C 3	σ^*	0.0221	3.74	1.13	0.058
C 5-N 6	σ	1.97843	C 1-F 9	σ^*	0.05118	4.7	1.07	0.064
C 5-H 11	σ	1.96561	C 1-N 6	σ^*	0.03554	6.48	0.94	0.07
C 7-H 12	σ	1.97538	C 3-C 4	σ^*	0.0462	3.13	0.99	0.05
C 7-H 12	σ	1.97538	C 4-C 5	π^*	0.28207	3.8	0.54	0.043
C 7-H 13	σ	1.97538	C 3-C 4	σ^*	0.0462	3.17	0.99	0.05
C 7-H 13	σ	1.97538	C 4-C 5	π^*	0.28207	3.78	0.54	0.043
C 7-H 14	σ	1.98539	C 4-C 5	σ^*	0.03707	6.09	1.14	0.075
N 6	LP(1)	1.9138	C 1-C 2	σ^*	0.04086	9.53	0.82	0.08
I 8	LP(1)	1.99225	C 2-C 3	σ^*	0.0221	1.08	1.09	0.031
I 8	LP (2)	1.96842	C 2-C 3	σ^*	0.0221	2.72	0.76	0.041
I 8	LP (3)	1.93583	C 2-C 3	π^*	0.36129	7.81	0.26	0.044
F 9	LP (1)	1.98773	C 1-C 2	σ^*	0.04086	1.73	1.5	0.046
F 9	LP (2)	1.96488	C 1-C 2	σ^*	0.04086	6.88	0.9	0.07
F 9	LP (3)	1.90943	C 1-N 6	π^*	0.42305	25.76	0.39	0.098
C 1-N 6	π^*	0.42305	C 2-C 3	π^*	0.36129	155.5	0.02	0.085
C 2-C 3	π^*	0.36129	C 4-C 5	π^*	0.28207	49.89	0.05	0.08
C 4-C 5	π*	0.28207	C 7-H 12	σ*	0.00849	1.1	0.39	0.049

6.2.7.3 Topology studies

The research of ELF and LOL primarily explain surface or topological analysis. Figs. 6.6a and 6.6b portrays the colour filled & contour plots of ELF respectively. Figs. 6.7a and 6.7b depicts the colour stuffed and contour images of LOL correspondingly for the caption molecule in gas phase.

The red colour cloud surrounding the hydrogen atoms proves the presence of bonding & non-bonding electrons, while the presence of low electron localization values is signalled by blue colour cloud surrounding the atoms of carbon. The little blue colour circles around carbon signify electron depletion between the valence and inner shells, but the red colour suggestions next to hydrogen atoms with high LOL values represent covalent connections between the atoms.

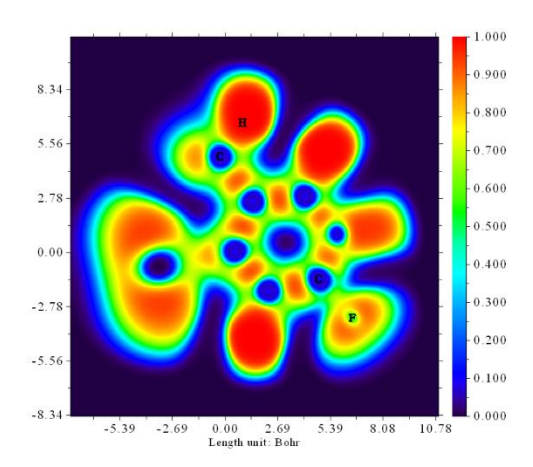


Fig 6.6a ELF - Colour filled map of 2FIMP.

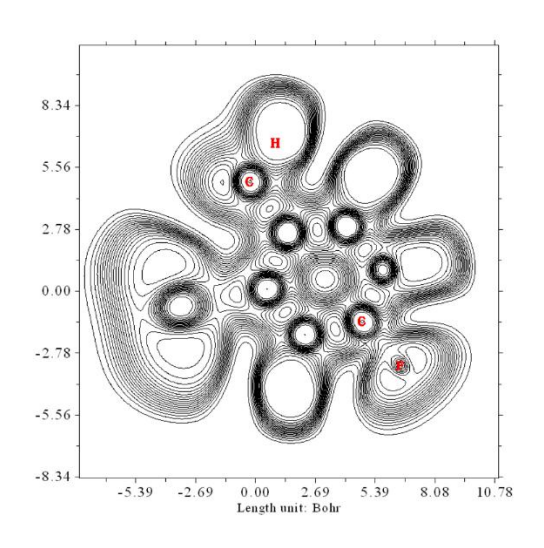


Fig 6.6b ELF - Contour map of 2FIMP.

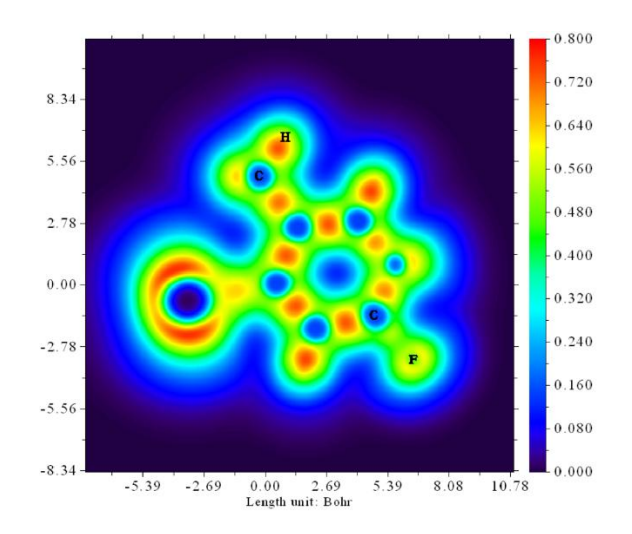


Fig 6.7a LOL - Colour filled map of 2FIMP.

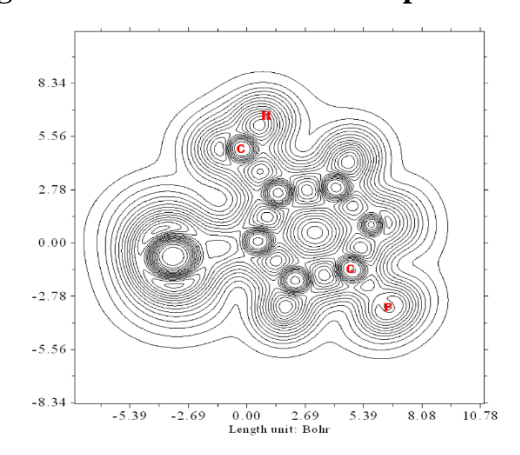


Fig 6.7b LOL - Contour map of 2FIMP.

6.2.8 Molecular reactivity and population analyses

A local reactivity descriptor, fukui function shows the preferred locations where the density of a chemical species varies as the number of electrons changes. For all the atomic locations of 2FIMP, mulliken charges and local softness together with Fukui functions are accounted and reported in Table 6.8. A positive $\Delta f(r)$ value represents nucleophilic site and negative value represents electrophilic site. For 2FIMP, C1, C4, I8, F9, H12 and H13 are nucleophilic attack sites whereas C2, C3, C5, N6, C7, H10, H11 and H14 are electrophilic attack sites. As a result, the behaviour of molecules as acceptors or donors during a reaction may be predicted. Fig 6.8 reveals the Fukui function chart for expected charges of 2FIMP.

The information regarding Mulliken atomic charges is utilised in quantum chemistry to analyse molecule orbitals [33]. Table 6.9 discloses the Mulliken charge spreading of 2FIMP in polar protic and aprotic solvents including gaseous phase. From the table it is observed that, C1, C4, 8I, H10, H11, H12, H13 atoms are positive and C2, C3, C5, C7, F9 are negative in gas and the chosen solvents phase whereas N6 carry positive atomic charge in gas phase and negative atomic charge in all the chosen solvents phase. The Mulliken charges of various solvents differ significantly when compared to those of gas phase. C4 atom is detected to carry the maximum charge in both gaseous and chosen liquids phases. Fig 6.9 exhibits the pictorial representation of Mulliken charges for 2FIMP.

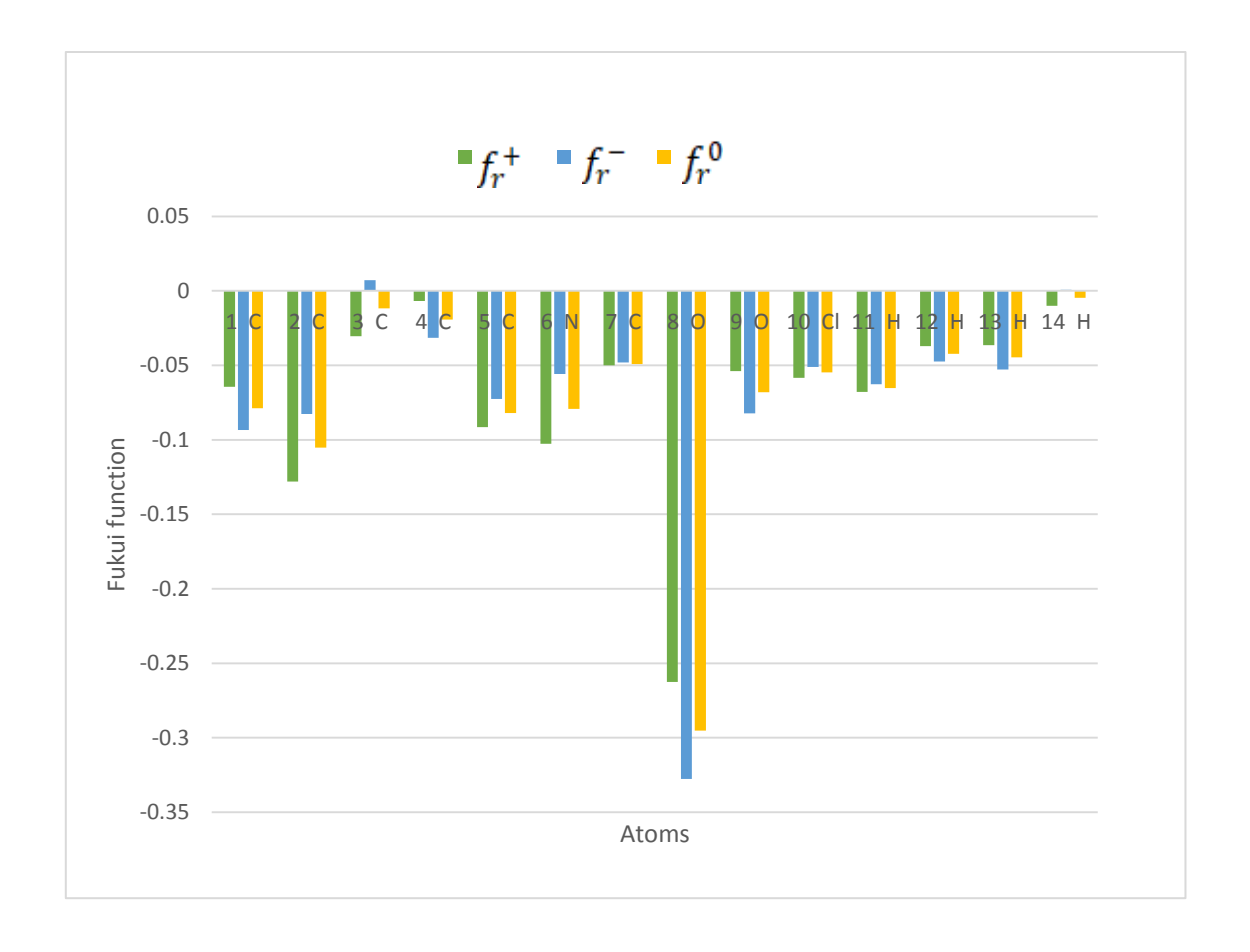


Fig 6.8 Fukui function graph for natural charges of 2FIMP.

Table 6.8 Fukui functions, local softness and dual descriptor of 2FIMP.

	Mulli	ken atomic ch	n atomic charges		Fukui fu	nctions		1	local softness		
Atom	N (0,1)	N +1 (-1, 2)	N-1 (1,2)	f_r^+	f_r^-	f_r^{0}	Δf(r)	$s_r^+ f_r^+$	$s_r^- f_r^-$	$s_r^0 f_r^0$	
1 C	0.10383	0.039511	0.197203	-0.06432	-0.09337	-0.07885	0.02905	-0.01117	-0.016213	-0.01369	
2 C	-0.26921	-0.397275	-0.1866	-0.12807	-0.08261	-0.10534	-0.04546	-0.02224	-0.014344	-0.01829	
3 C	-0.35831	-0.388809	-0.36539	-0.0305	0.007082	-0.01171	-0.03759	-0.0053	0.001230	-0.00203	
4 C	0.52616	0.519267	0.557741	-0.00689	-0.03158	-0.01924	0.024694	-0.0012	-0.005484	-0.00334	
5 C	-0.41442	-0.505821	-0.34191	-0.0914	-0.07251	-0.08196	-0.01889	-0.01587	-0.012591	-0.01423	
6 N	0.00108	-0.101571	0.056801	-0.10265	-0.05572	-0.07919	-0.04693	-0.01782	-0.009675	-0.01375	
7 C	-0.69864	-0.748621	-0.65045	-0.04998	-0.04819	-0.04909	-0.00178	-0.00868	-0.008368	-0.00852	
8 I	0.13158	-0.130977	0.459234	-0.26256	-0.32766	-0.29511	0.065101	-0.04559	-0.056894	-0.05124	
9 F	-0.16	-0.213827	-0.07783	-0.05383	-0.08217	-0.068	0.028337	-0.00935	-0.014267	-0.01181	
10 H	0.2533	0.194915	0.304309	-0.05839	-0.05101	-0.0547	-0.00738	-0.01014	-0.008857	-0.0095	
11 H	0.22946	0.16164	0.292115	-0.06782	-0.06266	-0.06524	-0.00516	-0.01178	-0.010880	-0.01133	
12 H	0.2245	0.187383	0.271876	-0.03711	-0.04738	-0.04225	0.010269	-0.00644	-0.008227	-0.00734	
13 H	0.22417	0.187731	0.277047	-0.03644	-0.05288	-0.04466	0.016446	-0.00633	-0.009182	-0.00775	
14 H	0.2065	0.196455	0.205846	-0.01005	0.000658	-0.0047	-0.01071	-0.00174	0.000114	-0.00082	

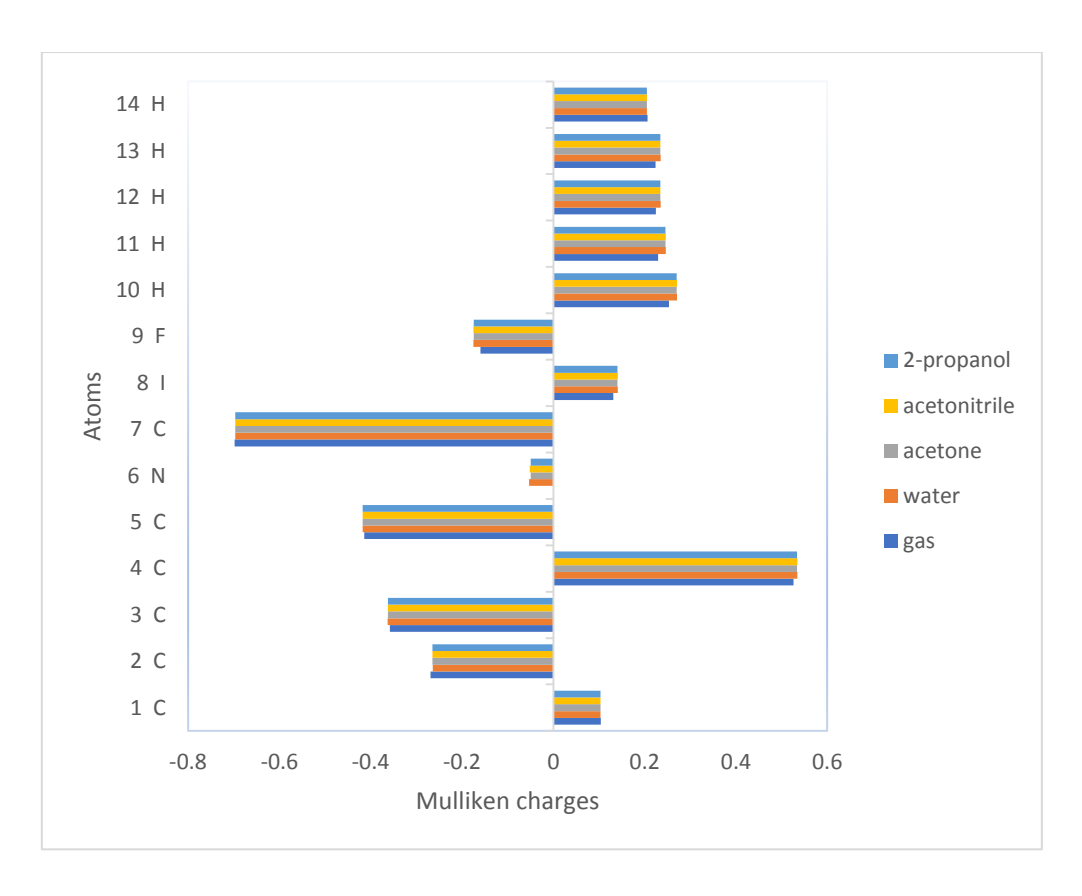


Fig 6.9 The histogram of calculated Mulliken Charges of 2FIMP in different phases.

Table 6.9 Mulliken charge distribution of 2FIMP in gas phase and in other solvents.

Atoms	gas	water	acetone	acetonitrile	2-propanol
1 C	0.103832	0.103103	0.103098	0.103101	0.103098
2 C	-0.269205	-0.26457	-0.26494	-0.26473	-0.264965
3 C	-0.358305	-0.36281	-0.36263	-0.36273	-0.36261
4 C	0.526157	0.534485	0.533902	0.534233	0.533854
5 C	-0.414421	-0.41798	-0.41785	-0.417927	-0.417843
6 N	0.001081	-0.05298	-0.04962	-0.051536	-0.049338
7 C	-0.698643	-0.69693	-0.69703	-0.696973	-0.697042
8 I	0.131578	0.141086	0.140517	0.140842	0.140469
9 F	-0.159997	-0.17551	-0.17469	-0.17516	-0.174624
10 H	0.253303	0.271187	0.270216	0.270771	0.270134
11 H	0.229456	0.246394	0.245469	0.245998	0.245391
12 H	0.224495	0.234917	0.234385	0.23469	0.23434
13 H	0.224166	0.234744	0.234197	0.23451	0.23415
14 H	0.206504	0.204864	0.204976	0.204913	0.204985

6.2.9 Drug Likeness and Molecular Docking Approach

Drug likeness can be used to assess the possibility for 2FIMP to be used as an active component in a few pharmaceutical products. The polar surface area (PSA), amount of hydrogen bond acceptors and donors, AlogP, molar refractivity and amount of rotatable bonds are the drug likeness components that have been identified in the existing work. Table 6.10 declares all the above said elements. The HBD and HBA are 1 and 0 respectively, AlogP and TPSA are found to be 2.67 and 12.89 Å² correspondingly, implying that 2FIMP can be envisioned as a drug.

Molecular docking studies assist us in determining the precise binding position of the protein and ligand [34]. The optimised structure in SMILES format of 2FIMP was utilised to estimate the activity of the molecule using PASS, an online programme [35]. The structure of the target proteins was retrieved in PDB format from RCSB. [36]. 2FIMP was docked into the operative location of proteins 2OL2 and 5DUQ associated with pseudolysin inhibitor property and complement factor D inhibitor property respectively. Ramachandran plots strengthen the steady nature of designated proteins. From the Figs. 6.10a and 6.10b, it is noticed that, for the two designated proteins, larger part of the residues and small number of residues appear within the allowable red and prohibited regions correspondingly. The favoured proteins 2OL2 and 5DUQ are structurally firm, according to the Ramachandran plot outcomes. Table 6.11 lists several data such as binding energy, assessed inhibition constant, bond distance along with reference RMSD. The orientation of binding of 2FIMP with the intended proteins 2OL2 and 5DUQ are exposed correspondingly in Fig 6.11 and Fig 6.12. Lower binding energy and intermolecular energy of -4.04 kcal/mol & -4.52 kcal/mol are detected in the ligand's interaction with the proteins 2OL2 and 5DUQ respectively whereas inhibition constant was found to be 1.09 mM and 486.12 μM for the chosen proteins correspondingly.

Table 6.10 Drug likeness parameters for 2FIMP.

Descriptor	Value
Hydrogen Bond Donor (HBD)	1
Hydrogen Bond Acceptor (HBA)	0
AlogP	2.67
Topological polar surface area (PSA)	12.89
Molar refractivity	237.01
Number of atoms	9
Number of rotatable bonds	0

2012

135
90

45
-135
-180

-135
-180

-135
-180

-135
-180

-135
-180

-135
-180

-135
-180

-135
-180

-135
-180

-135
-180

-135
-180

-135
-180

-135
-180

-135
-180

-135
-180

-135
-180

-135
-180

-135
-180

-135
-180

-135
-180

-135
-180

-135
-180

-135
-180

-135
-180

-135
-180

-135
-180

-135
-180

-135
-180

-135
-180

-135
-180

-135
-180

-135
-180

-135
-180

-135
-180

-135
-180

-135
-180

-135
-180

-135
-180

-135
-180

-135
-180

-135
-180

-135
-180

-135
-180

-135
-180

-135
-180

-135
-180

-135
-180

-135
-180

-135
-180

-135
-180

-135
-180

-180

-180

-180

-180

-180

-180

-180

-180

-180

-180

-180

-180

-180

-180

-180

-180

-180

-180

-180

-180

-180

-180

-180

-180

-180

-180

-180

-180

-180

-180

-180

-180

-180

-180

-180

-180

-180

-180

-180

-180

-180

-180

-180

-180

-180

-180

-180

-180

-180

-180

-180

-180

-180

-180

-180

-180

-180

-180

-180

-180

-180

-180

-180

-180

-180

-180

-180

-180

-180

-180

-180

-180

-180

-180

-180

-180

-180

-180

-180

-180

-180

-180

-180

-180

-180

-180

-180

-180

-180

-180

-180

-180

-180

-180

-180

-180

-180

-180

-180

-180

-180

-180

-180

-180

-180

-180

-180

-180

-180

-180

-180

-180

-180

-180

-180

-180

-180

-180

-180

-180

-180

-180

-180

-180

-180

-180

-180

-180

-180

-180

-180

-180

-180

-180

-180

-180

-180

-180

-180

-180

-180

-180

-180

-180

-180

-180

-180

-180

-180

-180

-180

-180

-180

-180

-180

-180

-180

-180

-180

-180

-180

-180

-180

-180

-180

-180

-180

-180

-180

-180

-180

-180

-180

-180

-180

-180

-180

-180

-180

-180

-180

-180

-180

-180

-180

-180

-180

-180

-180

-180

-180

-180

-180

-180

-180

-180

-180

-180

-180

-180

-180

-180

-180

-180

-180

-180

-180

-180

-180

-180

-180

-180

-180

-180

-180

-180

-180

-180

-180

-180

-180

-180

-180

-180

-180

-180

-180

Fig 6.10a Ramachandran plot of 2OL2 protein.

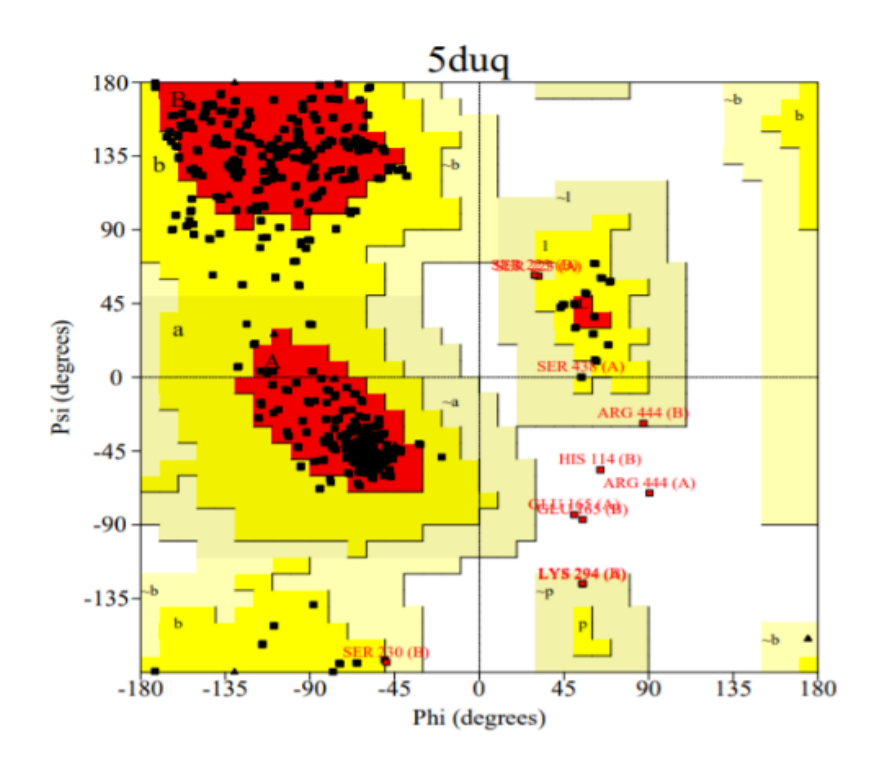


Fig 6.10b Ramachandran plot of 5DUQ protein.

Table 6.11 Docking of 2FIMP with different proteins.

Protein B	onded residues	Bond distance (Å)	Intermolecular Energy (Kcal/mol)	Inhibition Constant	Binding Energy(Kcal/mol)	Reference RMSD(Å)
2OL2	GLN294	2.1	-4.04	1.09 mM	-4.04	13.55
5DUQ	LEU 345	2.5	-4.52	486.12 μΜ	-4.52	45.37

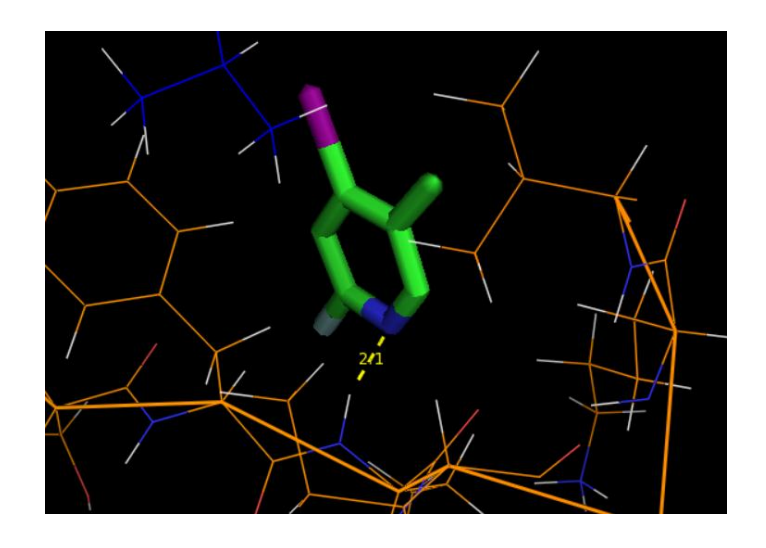


Fig 6.11 Molecular docking of active site of 2FIMP with 2OL2 protein.

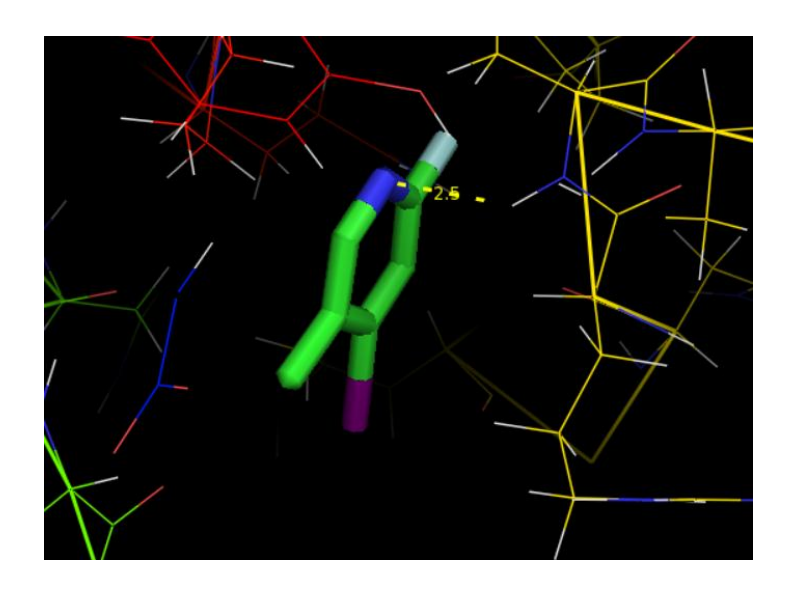


Fig 6.12 Molecular docking of active site of 2FIMP with 5DUQ protein.

6.3 CONCLUSION

DFT/B3LYP/ LANL2DZ source set was used to do vibrational analysis on 2-fluoro-4-iodo-5-methylpyridine. The geometrical parameters were premeditated, laying the groundwork for the calculation of additional parameters in this study. FMO analysis, NLO studies, Mulliken charges, UV investigations and thermodynamical properties of 2FIMP in polar protic solvents (water, 2-propanol), polar aprotic solvents (acetone, acetonitrile) and in gas phase were exclusively elucidated in this work by instigating DFT approach. The electrophilic and nucleophilic locations on the surface on the caption compound was revealed by MEP map. Dipole moment and first order hyperpolarizability values of 1.3706 D and 1.1768 x 10^{-30} esu respectively in gas phase which is evaluated to be larger than that of urea recommending that 2FIMP has wideranging NLO properties. The highest assessed value of stabilisation energy being 155.5 Kcal/mol was speckled for interaction from π^* (Carbon1-Nitrogen6) to π^* (Carbon2-Carbon3). UV investigation spectra reinforce to estimate the diverged properties of the compound. Fukui analysis and Mulliken charges were disclosed for 2FIMP. The

computed values of energy gap and electronegativity were found to be 5.75906 eV and 4.6746 respectively in gas phase and among the preferred solvents, the highest premeditated values of universal descriptors were recorded for 2-propanol with lowest chemical softness value of 0.1759. Amongst the polar protic and aprotic solvents chosen for study, water and acetonitrile were detected to have the highest thermodynamical values respectively at 298.15 K. Molecular docking studies were carried out for 2FIMP with the target proteins 2OL2 and 5DUQ associated with pseudolysin inhibitor property and complement factor D inhibitor property respectively and was recognised to be a bio-active one. Lower binding energy and intermolecular energy of -4.04 kcal / mol and -4.52 kcal / mol were detected in the ligand's interaction with the proteins 2OL2 and 5DUQ respectively.

REFERENCES

- [1] Radwan, Mohamed A.A.; Alshubramy, Maha A.; Abdel-Motaal, Marwa; Hemdan, Bahaa A.; El-Kady, Dina S. (2019). Synthesis, molecular docking and antimicrobial activity of new fused Pyrimidine and Pyridine derivatives. Bioorganic Chemistry, 103516.
- [2] Sujin P. Jose; S. Mohan (2006). Vibrational spectra and normal co-ordinate analysis of 2-aminopyridine and 2-amino picoline, 64(1), 240–245.
- [3] Pierrat, Philippe; Gros, Philippe C.; Fort, Yves (2005). Solid Phase Synthesis of Pyridine-Based Derivatives from a 2-Chloro-5-Bromopyridine Scaffold. Journal of Combinatorial Chemistry, 7(6), 879–886.
- [4] Premkumar, S.; Rekha, T.N.; Mohamed Asath, R.; Mathavan, T.; Milton Franklin Benial, A. (2016). Vibrational spectroscopic, molecular docking and density functional theory studies on 2-acetylamino-5-bromo-6-methylpyridine. European Journal of Pharmaceutical Sciences, 82, 115–125.
- [5] Cocco, M.T., C. Congiu, and V. Onnis, Synthesis and antitumour activity of 4-hydroxy-2-pyridone derivatives. European Journal of Medicinal Chemistry, 35 (2000) 545-552.
- [6] Al-Otaibi, J.S., Experimental (FT-IR and FT-Raman spectra) and Theoretical (Ab initio/HF, DFT/B3LYP) Study of 2-Amino-5-Chloropyridine and 2-Amino-6-Chloropyridine Chemistry and Materials Research 7 (2015).
- [7] M. M. Krayushkin, I. P. Sedishev, V. N. Yarovenko, I. V. Zavarzin, S. K. Kotovskaya, D. N. Kozhevnikov, Synthesis of Pyridines from 1,2,4-Triazines under High Pressure Russian Journal of Organic Chemistry, 44 (2008) 407-411.
- [8] C.Schmuck and H.Wennemers, Highlights in Bioorganic Chemistry. Weinheim: Wiley-Vch Veriag GmbH & Co. KGaA, 2004.
- [9] Pollet P, Davey EA, Ureña-Benavides EE, Eckert CA, Liotta CL (2014) Solvents for sustainable chemical processes. Green Chem 16:1034–1055.

- [10] Breeden SW, Clark JH, Macquarrie DJ, Sherwood J (2012) Green Solvents. In: Zhang W, Cue BW Jr (eds) Green techniques for organic synthesis and medicinal chemistry. Wiley, Chichester, pp 241–261.
- [11] Earle MJ, Seddon KR (2000) Ionic liquids green solvents for the future. Pure Appl Chem 72:1391–1398.
- [12] Pena-Pereira F, Kloskowski A, Namieśnik J (2015) Perspectives on the replacement of harmful organic solvents in analytical methodologies: a framework toward the implementation of a novel generation of eco-friendly alternatives. Green Chem 17:3687–3705.
- [13] Clark JH, Farmer TJ, Hunt AJ, Sherwood J (2015) Opportunities for biobased solvents created as petrochemical and fuel products transition towards renewable resources. Int J Mol Sci 16:17101–17159.
- [14] Constable DJC, Jimenez-Gonzalez C, Henderson RK (2007) Perspective on solvent use in the pharmaceutical industry. Org Process Res Dev 11:133–137.
- [15] Byrne, Fergal P.; Jin, Saimeng; Paggiola, Giulia; Petchey, Tabitha H. M.; Clark, James H.; Farmer, Thomas J.; Hunt, Andrew J.; Robert McElroy, C.; Sherwood, James (2016). Tools and techniques for solvent selection: green solvent selection guides. Sustainable Chemical Processes, 4(1), 7.
- [16] Curzons AD, Constable DC, Cunningham VL (1999) Solvent selection guide: a guide to the integration of environmental, health and safety criteria into the selection of solvents. Clean Prod Process 1:82–90.
- [17] Jiménez-González C, Curzons AD, Constable DJC, Cunningham VL (2004) Expanding GSK's solvent selection guide—application of life cycle assessment to enhance solvent selections. Clean Technol Environ Policy 7:42–50 41.
- [18] Prat D, Pardigon O, Flemming HW, Letestu S, Ducandas V, Isnard P, Guntrum E, Senac T, Ruisseau S, Cruciani P, Hosek P (2013) Sanofi's solvent selection guide: a step toward more sustainable processes. Org Process Res Dev 17:1517–1525.

- [19] Kim Alfonsi K, Colberg J, Dunn PJ, Fevig T, Jennings S, Johnson TA, Kleine HP, Knight C, Nagy MA, Perry DA, Stefaniak M (2008) Green chemistry tools to influence a medicinal chemistry and research chemistry based organisation. Green Chem 10:31–36.
- [20] S. Aayisha, T.S. Renuga Devi, S. Janani, S. Muthu, M. Raja, S. Sevvanthi, DFT, molecular docking and experimental FT-IR, FT-Raman, NMR inquisitions on "4- chloro-N-(4,5-dihydro-1H-imidazol-2-yl)-6-methoxy-2-methylpyrimidin-5-amine": alpha-2-imidazoline receptor agonist antihypertensive agent, J. Mol. Struct. 1186 (2019) 468–481.
- [21] Z.-Q. Feng, X.-L. Yang, Y.-F. Ye, H.-Q. Wang and L.-Y. Hao, 2-Chloro-5-(chloromethyl)pyridine, Acta Cryst. (2011). E67, o366.
- [22] John Wiley & Sons, Inc. SpectraBase; Spectrabase compound ID=HaPmFQ5d1C6. Available from: https://spectrabase.com/compound/HaPmFQ5d1C6 (accessed 3/25/2021).
- [23] M. Karabacak, C. Karaca, A. Atac, M. Eskici, A. Karanfil, E. Kose, Synthesis, analysis of spectroscopic and nonlinear optical properties of the novel compound: [S]-N-benzyl-1-phenyl-5-[thiophen-3-yl]-4-pentyn-2-amine, Spectrochim. Acta Part A: Mol. Biomol. Spectrosc. 97 (2012) 556–567.
- [24] K. Arulaabaranam, S. Muthu, G. Mani, S. Sevvanthi, Quantum mechanical computation, spectroscopic exploration and molecular docking analysis of 2-Bromo-4-fluoroacetanilide, J. Mol. Struct. 1220 (2020) 128639.
- [25] S. Periandy, S. Ramalingam, Experimental (FT-IR and FT-Raman) and theoretical (HF and DFT) investigation, IR intensity, Raman activity and frequency estimation analyses on 1-Bromo-4-chlorobenzene, Spectrochim. Acta 79 (2011) 920e927.
- [26] G.-J. Zhao, J.-Y. Liu, L.-C. Zhou, K.-L. Han, Site-selective photoinduced electron transfer from alcoholic solvents to the chromophore facilitated by hydrogen bonding: a new fluorescence quenching mechanism, J. Phys. Chem. B 111 (30) (2007) 8940–8945.

- [27] Chandralekha B., Hemamalini Rajagopal , S. Muthu, S. Sevvanthi, Spectroscopic (FT-IR, FT-RAMAN, NMR, UV-Vis) investigations, Computational analysis and molecular docking study of 5-bromo-2-hydroxy pyrimidine, J. Mol. Struct. 1218 (2020) 128494.
- [28] S. Muthu, J. Uma Maheswari, Sundius Tom, Quantum mechanical, spectroscopic studies (FT-IR, FT-Raman, NMR, UV) and normal coordinates analysis on 3-([2-(diaminomethyleneamino) thiazol-4-yl] methylthio)-N' sulfamoyl-propanimidamide, Spectrochim. Acta Mol. Biomol. Spectrosc. 108 (2013) 307e318.
- [29] Aarthi K V, Hemamalini Rajagopal , S. Muthu , V. Jayanthi , R. Girija , Quantum chemical calculations, spectroscopic investigation and molecular docking analysis of 4-chloro-N-methylpyridine-2- carboxamide, J. Mol. Struct. 1210 (2020) 128053.
- [30] J. Ott, Juliana Boerio-Goates, Chemical thermodynamics: principles and applications, Academic Press, San Diego, 2000.
- [31] S. Sivaprakash, S. Prakash, S. Mohan, Sujin P. Jose, Quantum chemical studies and spectroscopic investigations on 2-amino-3- methyl-5-nitropyridine by density functional theory, Heliyon 5 (2019) e02149.
- [32] F. Weinhold, C.R. Landis, E.D. Glendening, What is NBO analysis and how is it useful? Int. Rev. Phys. Chem. 35 (2016) 399–440.
- [33] A. Alsalme, T. Pooventhiran, N. Al-Zaqri, D.J. Rao, R. Thomas, Structural, physico-chemical landscapes, ground state and excited state properties in different solvent atmosphere of Avapritinib and its ultrasensitive detection using SERS/GERS on self-assembly formation with graphene quantum dots, J. Mol. Liq. (2020), 114555.
- [34] H. Pir, N. Gunay, O. Tamer, D. Avcı, Y. Atalay, Theoretical investigation of 5-(2- Acetoxyethyl)-6-methylpyrimidin-2,4-dione: conformational study, NBO and NLO analysis, molecular structure and NMR spectra, Spectrochim. Acta Part A Mol. Biomol. Spectrosc 112 (2013) 331e342.

- [35] S. Sevvanthi, S. Muthu, M. Raja, Molecular docking, vibrational spectroscopy studies of (RS)-2-(tert-Butylamino)-1-(3-chlorophenyl)propan-1-one: a potential Adrenaline uptake inhibitor, J. Mol. Struct. 1173 (2018) 251e260.
- [36] Beaula, T. J., Joe, I. H., Rastogi, V. K., Jothy, V. B. (2015). Spectral investigations, DFT computations and molecular docking studies of the antimicrobial 5-nitroisatin dimer. Che. Phy. Lett. 624: 93–101.

CHAPTER VII

SUMMARY AND CONCLUSIONS

Few pyridine derivatives were chosen for this work in order to conduct a thorough inquiry into spectroscopic, molecular structure, optical, quantum mechanical, and molecular docking studies. In the current work, the experimental and theoretical reports on the upgraded geometrical structure, electronic and vibrational features of some pyridine derivatives are presented. 2-Amino-5-chloro-3-nitropyridine, 2-Amino-3,5-dichloropyridine, 5-Chloro-2-hydroxypyridine, 2-Chloropyridine-4-carboxylic acid and 2-Fluoro-4-iodo-5-methylpyridine were the compounds preferred for investigation. FT-IR and FT-Raman spectral techniques were used to characterize the pyridine derivatives chosen and they were compared with computational (DFT) approaches. The full literature review disclosed that the selected compounds had not been evaluated for the computational analysis, thus this task was conducted.

Geometrical evaluations were performed on all of the compounds chosen using the suitable approach. The compounds' comprehensive vibrational assignments were accomplished based on the Potential Energy Distribution (PED) of the vibrational modes employing VEDA program. Theoretical and experimental findings were in agreement. For each compound, the HOMO and LUMO energy gaps were reckoned, and this energy gap exposed the presence of charge transfer within the molecule while

Molecular Electrostatic Potential (MEP) maps disclosed the qualitative evaluations of electrophilic and nucleophilic reactivity.

The molecular parameters such as Polarizability, first order Hyperpolarizability and Dipole moment of the compounds contributed from the Gaussian NLO output file were used to verify the NLO nature. The first order hyperpolarizability value for all compounds was higher than Urea, a reference molecule, which accredited the NLO feature of the compounds.

To comprehend the stability, reactivity, and bioactivity of all compounds, the chemical potential, chemical hardness & softness, electronegativity, Electrophilicity index and electron affinity of the compound were ascertained employing Frontier orbitals. The shift of charges and charges' delocalization owing to bonds interacting intramolecularly and intermolecularly were investigated using NBO exploration for all the compounds. Theoretic UV-Vis inspection of some compounds have been accomplished using TD-DFT methodology exercising IEFPCM standard in few solvents. Electron localization function (ELF) and localised orbital locator (LOL) explored chemically significant locations, topology, and inter and intra-atomic interactions.

Molecular docking studies assist us in determining the precise binding position of the protein and ligand. The optimised structure in SMILES format was utilised to estimate the activity of the molecule using PASS, an online programme. The structure of the target proteins was procured in PDB format from RCSB. Ligand-target protein interactions are significant for a wide range of bioactivities and hence the molecular

docking factors like inhibition constant, binding energy and intermolecular energy of the molecules were computed.

To summarise, this thesis presents a complete examination using quantum computational and spectroscopic approaches for the characterization and exposition of selected pyridine derivatives and also provide a framework for future academics to conduct additional research on the substances indicated and build predictive metrics and criteria. The collected results are quite beneficial in preparing for future study in research field.

LIST OF PUBLICATIONS

- S. Selvakumari, C. Venkataraju, S. Muthu, BR. Raajaraman, P. Sangeetha,
 A. Saral. Spectroscopic, quantum mechanical investigation and molecular docking study of 2-amino-5-chloro-3-nitropyridine, Materials Today:
 Proceedings, Volume 50, Part 7, 2022, Pages 2711-2719.
 https://doi.org/10.1016/j.matpr.2020.08.223
- S. Selvakumari, C. Venkataraju, S. Muthu, Ahmad Irfan, S. Sevvanthi, Fazilath Basha Asif. Spectroscopic (FT-IR, FT-Raman, UV-Visible), Quantum Mechanical Based Computational Studies and Molecular Docking Analysis of 2- Amino-3,5-dichloropyridine, Analytical Chemistry Letters, 11:6, 848-861. https://doi.org/10.1080/22297928.2021.1981440
- 3. **S. Selvakumari, C. Venkataraju, S. Muthu, Ahmad Irfan, A.Saral.** Evaluation of electronic properties in different solvents, spectroscopic exposition (FT-IR, FT-Raman), and molecular docking studies of 5-Chloro-2-hydroxypyridine insulysin inhibitor. **Journal of Molecular Liquids,** Volume 341, 1 November 2021, 117304. https://doi.org/10.1016/j.molliq.2021.117304
- 4. S. Selvakumari, C. Venkataraju, S. Muthu, Ahmad Irfan, D.Shanthi. Donor acceptor groups effect, polar protic solvents influence on electronic properties and reactivity of 2-Chloropyridine-4-carboxylic acid, Journal of the Indian Chemical Society, Volume 99, Issue 6, June 2022, 100478. https://doi.org/10.1016/j.jics.2022.100478
- 5. **S. Selvakumari, C. Venkataraju, S. Muthu.** Vibrational, electronic influences and reactivity using IEFPCM solvation standard and molecular docking scrutiny of 2-Fluoro-4-iodo-5-methylpyridine- Pseudolysin inhibitor and complement factor D inhibitor proteins, **Spectroscopy Letters** (Communicated)

LIST OF PAPERS PRESENTED

- 1. S. Selvakumari, Vibrational spectroscopic (FT-IR and FT- RAMAN), NBO, first order hyperpolarizability, HOMO-LUMO, fukui function and molecular docking analysis of 5-chloro-2-hydroxypyridine, *International Virtual Conference on Smart Advanced Material Science and Engineering Applications (IVCSAMSEA 2020)* organized by Department of Physics, KL University, Guntur, India, held during 03rd 05th December, 2020.
- 2. S. Selvakumari, Theoretical delineation of polar protic solvents influence on electronic properties and reactivity of 2-Chloropyridine-4-carboxylic acid, Virtual International Conference on Functional Materials and Its Application Aspects (ICFMAA 2021) organized by Department of Physics, Saveetha School of Engineering, SIMATS, Chennai-602105, Tamil Nadu, India, held during 29 &30, October 2021.

ELSEVIER

Contents lists available at ScienceDirect

Materials Today: Proceedings

journal homepage: www.elsevier.com/locate/matpr



Spectroscopic, quantum mechanical investigation and molecular docking study of 2-amino-5-chloro-3-nitropyridine

S. Selvakumari ^{a,*}, C. Venkataraju ^b, S. Muthu ^c, BR. Raajaraman ^d, P. Sangeetha ^a, A. Saral ^e

- ^a Department of Physics, Panimalar Institute of Technology, Chennai 600 123, Tamilnadu, India
- ^b PG and Research Department of Physics, Thiru.Vi.Ka Govt Arts College, Thiruvarur 610 003, Tamilnadu, India
- ^c Department of Physics, Arignar Anna Govt.Arts College, Cheyyar 604 407, Tamilnadu, India
- ^d Department of Applied Physics, Sri Venkateswara College of Engineering, Sriperumbudur, 602 117, Tamilnadu, India
- ^e Department of Chemistry, Panimalar Institute of Technology, Chennai 600 123, Tamilnadu, India

ARTICLE INFO

Article history: Received 30 April 2020 Received in revised form 2 August 2020 Accepted 5 August 2020 Available online 9 September 2020

Keywords: DFT FT- IR FT- RAMAN NLO HOMO -LUMO

ABSTRACT

Pyridine and its derivatives are the most important nitrogen based heterocyclic compounds which play a vital role in catalysing biological systems. In the present study, FT -IR, FT- Raman spectra of the title compound 2-Amino-5-chloro-3-nitropyridine have been recorded. Quantum mechanical analysis of the title compound have been carried out by DFT/B3LYP using 6–311++G (d, p) basis set. The vibrational frequencies obtained from the above said DFT method has been compared with the experimental spectral data recorded. The vibrational assignments of wave numbers have been calculated using the Potential Energy Distribution. The electronic properties such as HOMO -LUMO energies, energy gap, local softness, Fukui functions were determined. NBO analysis have been performed to analyse the stability of the molecule. The Molecular Electrostatic Potential and the NLO properties in terms of first order hyperpolarizability and dipole moment have also been accounted in the study. The thermodynamic parameters for different temperatures have been calculated. Molecular docking studies have been performed to investigate the biological activity of the title compound in preparation of new compounds to act as an antagonist and also to determine its binding energy.

© 2020 Elsevier Ltd. All rights reserved. Selection and peer-review under responsibility of the scientific committee of the National Conference on Material Science

1. Introduction

Pyridine is a basic heterocyclic compound with the chemical formula C_5H_5N . Pyridine derivatives are very important chemicals with remarkable biological applications [1]. It plays a key role in catalyzing both biological and chemical systems. Pyridine forms the nucleus over 7000 existing drugs in pharmaceutical industries .6Many synthetic methods has been developed for the construction of the pyridine ring and for its substitution [2] due to its applications in many pharmaceutical, agrochemical and research fields. Researches carried out on nitropyridine and its derivatives show anti-microbial, anti-fungal, anti-bacterial, pesticide, anti-allergic, antihypertensive, anti-tumour, antagonist or analgesic properties [3-5]. 2-Amino-5-chloro-3-nitropyridine(2A5 C3NP) with molecular formula $C_5H_4ClN_3O_2$ has a molecular weight of 173.56 g/mol. Direct nitration of 2-amino-5-chloropyridine gave

2-amino-5-chloro-3-nitropyridine which was reduced and further

E-mail address: selvi1977@gmail.com (S. Selvakumari).

made to undergo chemical reactions to yield various heterocyclic compounds which plays a vital role in pharmaceutical industry. The compound, 2A5C3NP is a derivative of pyridine and to our best knowledge, no quantum chemical investigations were carried out for this compound. Many problems in different areas of research could be solved by combined studies of theoretical and experimental work [6,7]. Density functional investigations and spectroscopic analysis of the title compound were carried out. Molecular docking studies were conducted to study the antagonist activity of the title compound. Geometrical structure, spectral analysis along with molecular electrostatic potential surfaces may lead to the better understanding of structural and spectral characteristics of the compound. The FT -IR and FT- Raman spectra of 2-Amino-5chloro-3-nitropyridine have been recorded. The density functional theory investigation helps in revealing molecular electronic structure. Determination of natural bond orbital using DFT method helps in investigating the redistribution of electron density in various bonding and antibonding orbitals. Vibrational spectral

^{*} Corresponding author.



Analytical Chemistry Letters



ISSN: (Print) (Online) Journal homepage: https://www.tandfonline.com/loi/tacl20

Spectroscopic (FT-IR, FT-Raman, UV-Visible), Quantum Mechanical Based Computational Studies and Molecular Docking Analysis of 2-Amino-3,5-dichloropyridine

S. Selvakumari, C. Venkataraju, S. Muthu, Ahmad Irfan, S. Sevvanthi & Fazilath Basha Asif

To cite this article: S. Selvakumari, C. Venkataraju, S. Muthu, Ahmad Irfan, S. Sevvanthi & Fazilath Basha Asif (2021) Spectroscopic (FT-IR, FT-Raman, UV-Visible), Quantum Mechanical Based Computational Studies and Molecular Docking Analysis of 2-Amino-3,5-dichloropyridine, Analytical Chemistry Letters, 11:6, 848-861, DOI: 10.1080/22297928.2021.1981440

To link to this article: https://doi.org/10.1080/22297928.2021.1981440



ELSEVIER

Contents lists available at ScienceDirect

Journal of Molecular Liquids

journal homepage: www.elsevier.com/locate/molliq



Evaluation of electronic properties in different solvents, spectroscopic exposition (FT-IR, FT-Raman), and molecular docking studies of 5-Chloro-2-hydroxypyridine - insulysin inhibitor



S. Selvakumari ^a, C. Venkataraju ^b, S. Muthu ^{c,d,*}, Ahmad Irfan ^e, A. Saral ^f

- a PG and Research Department of Physics, Thiru.Vi.Ka Govt Arts College, Thiruvarur 610 003 (Affiliated to Bharathidasan University), Tiruchirappali 24, Tamilnadu, India
- ^b PG and Research Department of Physics, Thiru.Vi.Ka Govt Arts College, Thiruvarur 610 003, Tamilnadu, India
- ^c Department of Physics, Arignar Anna Govt. Arts College, Cheyyar 604 407, Tamilnadu, India
- ^d Department of Physics, Puratchi Thalaivar Dr M.G.R Govt Arts and Science College, Uthiramerur, 603406, Tamilnadu, India
- ^e Department of Chemistry, College of Science, King Khalid University, Abha 61413, P.O. Box 9004, Saudi Arabia
- ^fDepartment of Chemistry, Panimalar Institute of Technology, Chennai-600 123, Tamilnadu, India

ARTICLE INFO

Article history: Received 23 July 2021 Revised 9 August 2021 Accepted 15 August 2021 Available online 18 August 2021

Keywords: DFT FT- IR FT- RAMAN NBO Molecular docking

ABSTRACT

In the current work, the experimental and theoretical reports on the upgraded geometrical structure, electronic and vibrational features of 5-chloro-2-hydroxypyridine are presented assigning B3LYP method with 6–311++G (d, p) basis set. The FT-IR and FT-Raman spectra of the heading compound were documented and the geometric parameters and wavenumbers were obtained and with scaled quantum mechanics, comprehensive vibrational assignments of wavenumbers using Potential Energy Distribution (PED) were evaluated. NBO studies was used to calculate the interaction energy and electron densities of donor and acceptor bonds. Various solvents were used to find HOMO-LUMO orbitals and band gap energy. Molecular Electrostatic Potential (MEP), Fukui functions, Mulliken charges, Electron Localisation Function (ELF) and Localised Orbital Locator (LOL) of the heading molecule were also inspected. Using the TD-DFT method and a number of solutions, the UV-Visible spectrum was explored. Additionally, drug likeness, environmental toxicity properties were analysed and molecular docking was accomplished so as to recognize the hydrogen bond lengths and minimum binding energy was determined.

© 2021 Elsevier B.V. All rights reserved.

1. Introduction

Heterocyclic mixtures are significant in the field of natural science and organic chemistry as they are predominant among the sorts of mixtures utilized as medications, veterinary items and agrochemicals [1]. Pyridine nucleus is present in many biologically noteworthy compounds used in drugs [2,3]. Pyridines have additionally routinely been utilized as ligands for metals in natural blend, and furthermore utilized as chiral ligands for transition metals [4,5]. Because of the biological significance of pyridine derivatives, a variety of synthetic approaches for constructing the pyridine ring and forming its derivatives have been created. [6,7]. One of the pyridine derivatives is 5-chloro-2-hydroxypyridine (5C2HOP) with molecular formula C_5H_4 CINO has molecular weight of 129.54 has been chosen here for quantum mechanical study. The

E-mail address: mutgee@gmail.com (S. Muthu).

DFT approach was used to investigate the structural parameters of the heading molecule, as these methods have become progressively popular for demonstrating molecular properties such as symmetry structures, frequencies of vibrations and intensities. [8]. The FT- IR and FT-Raman spectral investigations were performed for the heading compound by using B3LYP/6-311++G(d, p) set. In the existing study, the experimentally attained frequencies of vibrations were compared with the calculated wavenumbers. A full outline of the heading molecule's geometry, motions, and electronic attributes have also been computed. MEP, LOL, ELF, HOMO, LUMO, and Fukui functions are among the molecular characteristics that have been determined and stated. The charge transfer and intramolecular relations within the molecule were scrutinized using NBO analysis and Mulliken atomic charges were also calculated. The eco-friendly solvents namely water, DMSO, ethanol and acetone which lies in utilisable categorizing [9] were opted to report the solvent influence of 5C2HOP. Docking studies of 5C2HOP along with drug likeness and environmental toxicity properties have also been accomplished.

 $[\]ast$ Corresponding author at: Department of Physics, Arignar Anna Govt. Arts College, Cheyyar, 604 407, Tamilnadu, India.

ELSEVIER

Contents lists available at ScienceDirect

Journal of the Indian Chemical Society

journal homepage: www.journals.elsevier.com/journal-of-the-indian-chemical-society





Donor acceptor groups effect, polar protic solvents influence on electronic properties and reactivity of 2-Chloropyridine-4-carboxylic acid

S. Selvakumari ^{a,b}, C. Venkataraju ^c, S. Muthu ^{d,*}, Ahmad Irfan ^e, D. Shanthi ^f

- ^a PG and Research Department of Physics, Thiru Vi.Ka Govt Arts College, Thiruvarur, 610 003, Affiliated to Bharathidasan University, Tiruchirappali- 24, Tamilnadu, India
- ^b Department of Physics, Panimalar Institute of Technology, Chennai, 600 123, Tamilnadu, India
- ^c PG and Research Department of Physics, Thiru.Vi.Ka Govt Arts College, Thiruvarur, 610 003, Tamilnadu, India
- ^d Department of Physics, Arignar Anna Govt.Arts College, Cheyyar, 604 407, Tamilnadu, India
- ^e Department of Chemistry, College of Science, King Khalid University, Abha, 61413, P.O.Box 9004, Saudi Arabia
- f Department of Chemistry, Vel Tech Multi Tech Dr. Rangarajan Dr. Shakuntala Engineering College, Avadi, Chennai, 600 062, Tamilnadu, India

ARTICLEINFO

Keywords:

DFT

NLO

NBO

MEP

ABSTRACT

The computational reckoning of 2-Chloropyridine-4-carboxylic acid (2CP4CA) was accomplished employing DFT/B3LYP with the root set as 6–311++G(d, p). The impact of polar protic solvents which are eco-friendly solvents (water, methanol, ethanol, 1-propanol) on 2CP4CA were analysed. To examine the solvent effect, vibrational investigations and NLO reports of 2CP4CA in dissimilar solvents were executed. Geometrical properties were also established in gas phase for 2CP4CA. Exercising VEDA program, the entire vibrational assignment was accomplished. Donor-acceptor exchanges were ascertained utilizing NBO scrutiny technique. Thermodynamic properties of 2CP4CA were analysed at different temperatures. By applying TD - DFT approach, theoretic UV-Vis absorption spectrum was procured in different solvents. In order to evaluate the complete electron concentration and sensitive spots of 2CP4CA, MEP coupled with FMO analyses were employed. HOMO along with LUMO orbitals and energy band gap were acquired for 2CP4CA employing dissimilar polar protic solvents. Additionally, ELF, LOL and charge transfer studies were also executed. RDG analysis has been exercised for revealing non-covalent interactions.

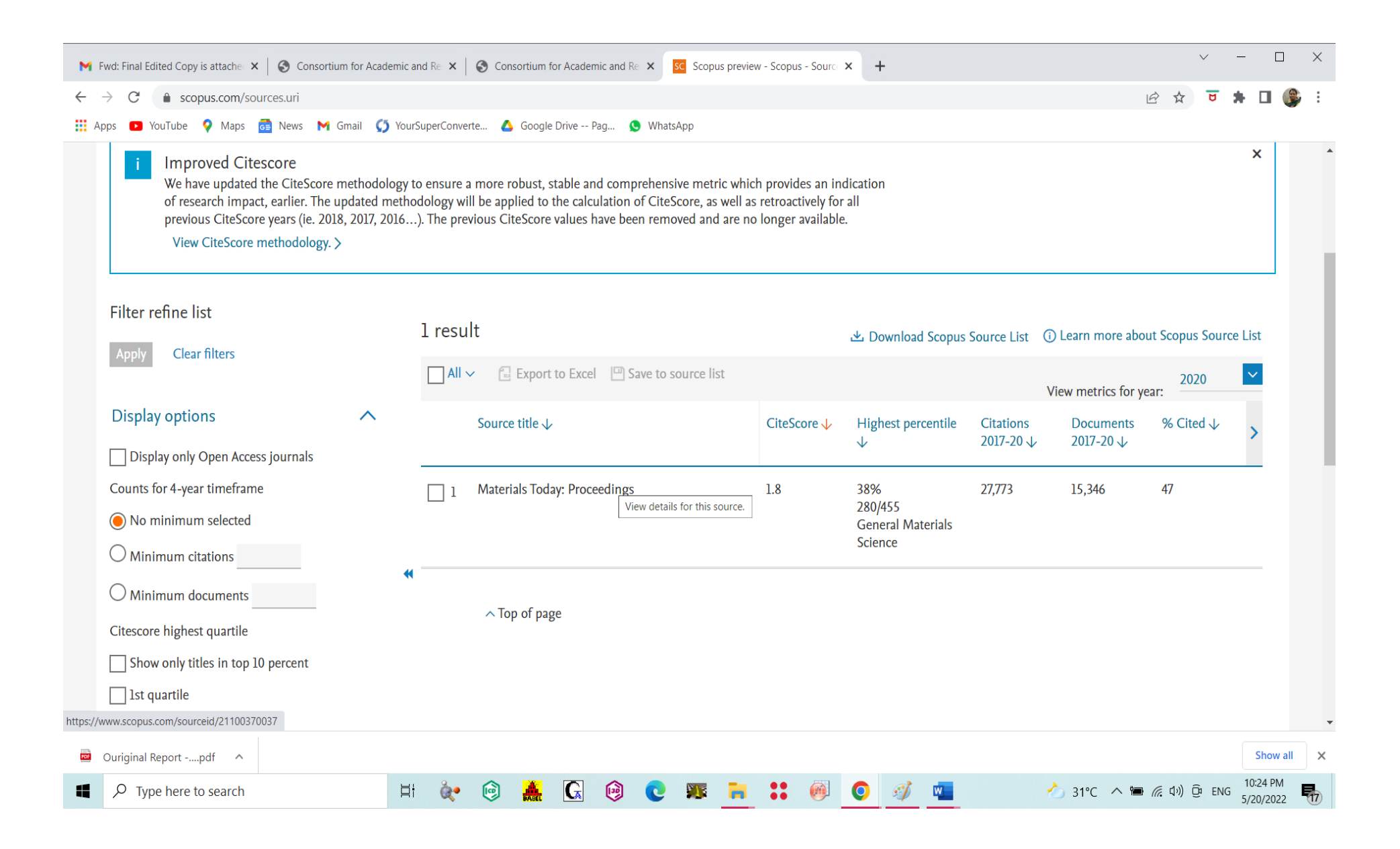
1. Introduction

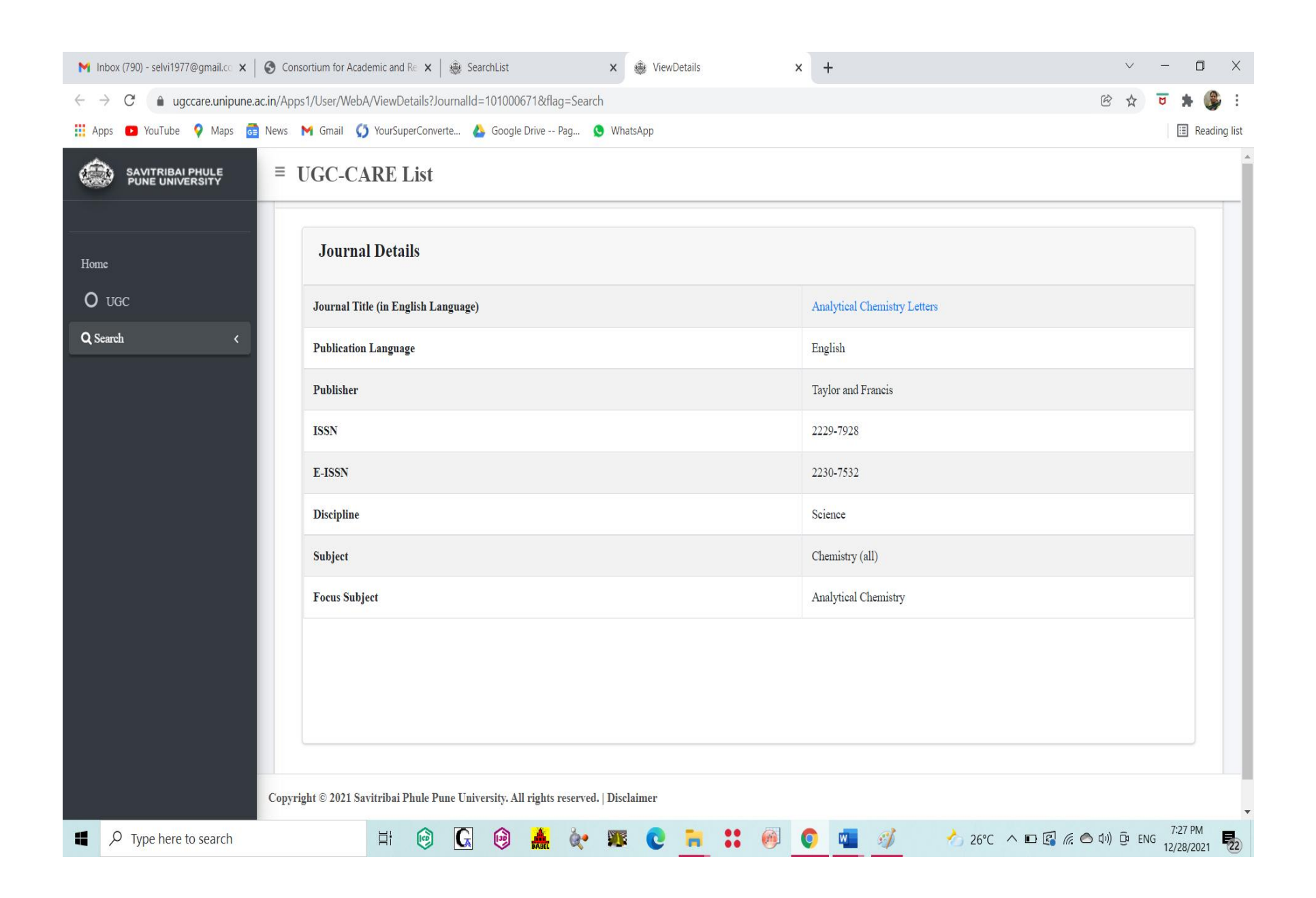
Taking into account the utmost challenging branches of carbon-based chemistry, heterocyclic compound chemistry is considered to be one among them. Its hypothetical ramifications, the multiplicity of its synthesis techniques, the industrial and biological relevance of heteroaromatic molecules are all fascinating. Chemists, pharmacologists, and physicists have been studying nitrogen-comprising heterocyclic organic compounds as structure splinters of numerous medications, colours, and food additives for decades in order to uncover a link concerning chemical structure and biological action [1–4]. Pyridine derivatives have engrossed noteworthy attentiveness in pharmacological, biochemistry, cosmetics and agrochemical fields [5–11]. Carboxylic acids of the pyridine series or its derivatives are recognized to have significant pharmacologic value, predominantly as B-vitamins, chemotherapeutic medicines to promote metabolism, anti-hyperlipidemic

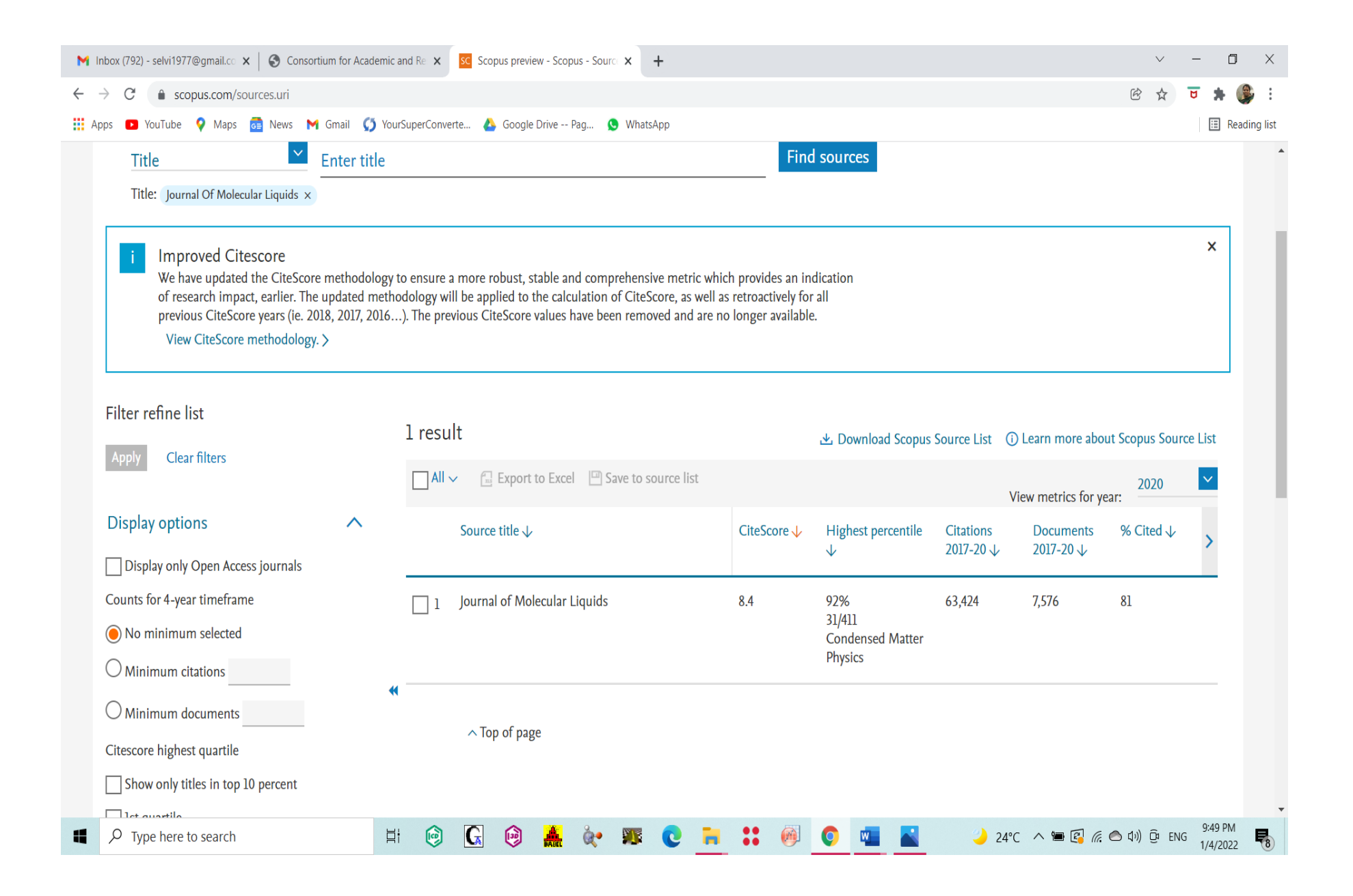
agents to lower cholesterol levels, anti-tuberculosis drugs, and so on [12–15]. 2-Chloropyridine-4-carboxylic acid (2CP4CA), a pyridine derivative with the chemical formula C₆H₄ClNO₂ has been picked for quantum mechanical investigation having 157.55 as its molecular weight. Literature review endorses that DFT reports of 2-Chloropyridine-4-carboxylic acid (2CP4CA) has not disclosed yet. This motivates us to conduct a theoretical analysis of 2CP4CA's skeletal, electronic, and vibrational modes. 2-Chloropyridine-4-carboxylic acid (2CP4CA) was scrutinized theoretically in gas phase and using dissimilar solvents in this study. DFT calculations are useful for the prediction and calculation of material behaviour of the caption compound. The acquired computed values of geometrical factors and vibrational frequencies are revealed here. Solvents perform a substantial role in the chemical industry's environmental performance, as well as cost, security, and wellbeing concerns. The concept of "green" solvents articulates the desire to reduce the ecological influence of solvent consumption in chemical synthesis.

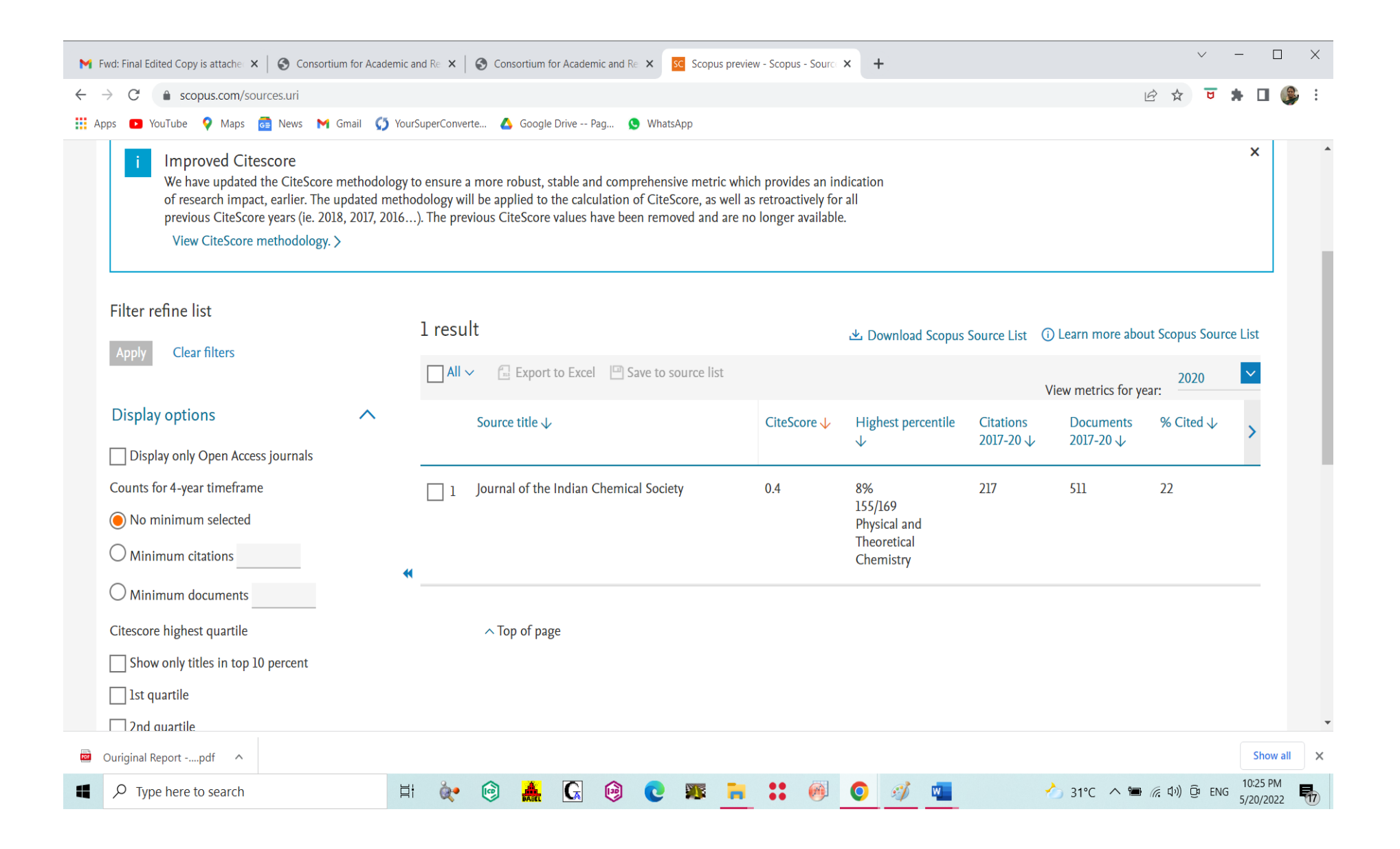
E-mail address: mutgee@gmail.com (S. Muthu).

 $^{^{\}ast}$ Corresponding author.













(NAAC Accredited 'A++' Grade University)





KONERU LAKSHMAIAH EDUCATION FOUNDATION

International Virtual Conference on Smart Advanced Material Science and Engineering Applications (IVCSAMSEA 2020)

This is to certify that Mrs. S. SELVAKUMARI, ASSISTANT PROFESSOR, Department of Physics, PANIMALAR INSTITUTE OF TECHNOLOGY, TAMILNADU, INDIA has presented the paper titled Vibrational spectroscopic (FT-IR and FT- RAMAN), NBO, first order hyperpolarizability, HOMO-LUMO, fukui function and molecular docking analysis of 5-chloro-2-hydroxypyridine (paper id: ICSM-PHY-0135) in IVCSAMSEA 2020 organized by Department of Physics, KLEF, Guntur, India, during 03rd – 05th December, 2020.

Dr. S. Shanmugan

Dr. S. Shanmuga Convener, K.L.E.F, Guntur Dr. Shaik Babu Co-Convener, K.L.E.F. Guntur

Dr. G. Sunita Sundari HOD, Dept. of Physics K.L.E.F, Guntur Prof. V. Krishna Reddy
Coordinator, FED
K.L.E.F. Guntur

Prof. A. Jagadeesh
Director, FED
K.L.E.F, Guntur

Paper Presented



SAVEETHA SCHOOL OF ENGINEERING

Approved by AICTE | IET-UK Accreditation

Certificate

of Presentation

ICFMAA-2021

This is to certify that

S.Selvakumari ,Thiru.Vi.Ka Govt Arts College, Thiruvarur

has presented a paper titled

Theoretical delineation of polar protic solvents influence on electronic properties and reactivity of 2-Chloropyridine-4-carboxylic acid

in the "VIRTUAL INTERNATIONAL CONFERENCE ON FUNCTIONAL MATERIALS AND ITS APPLICATION
ASPECTS (ICFMAA – 2021) "

on

29 &30, October 2021

Organized by

Department of Physics, Saveetha School of Engineering, SIMATS, Chennai-602105, Tamil Nadu, India

Dr.N. Kanagathara

Convener



Dr.B .Ramesh
PRINCIPAL